# EXPLORING THE STRUCTURE FUNCTION RELATION OF THE GLYCINE RECEPTOR WITH HYPEREKPLEXIA MUTATIONS

**By**

**Fatemah Safar**

Submitted for the degree of Ph.D

University College London

Neuroscience, Physiology & Pharmacology

Supervised by

Prof. Lucia G. Sivilotti

‘I confirm that the work presented in this thesis is my own. Where information has been derived from other sources, I confirm that this has been indicated in the thesis’.

Fatemah Safar

May 2018

## Abstract

The glycine receptor (GlyR) is a Cys-loop ligand-gated anion channel that mediates fast synaptic inhibition in brain and spinal cord. Heritable malfunction of glycinergic transmission in man causes hyperekplexia, a neuromotor disorder characterised by exaggerated startle responses to normal sensory stimuli. Many mutations responsible for the disease are found in GlyR subunits, where they highlight residues essential for channel activation.

I evaluated the effects of four human hyperekplexia α1 subunit mutations located in different parts of the GlyR including the extracellular domain (ECD), transmembrane domain (TM1) and transmembrane domain (TM2). Human α1 and α1β GlyR bearing the E103K, S231N, Q266H or S267N mutations in α1 were expressed in HEK293 cells. Glycine concentration-response curves obtained by whole-cell patch-clamp recordings confirmed previous reports (Bode & Lynch, 2014) that these mutations decrease the channel sensitivity to glycine, increasing its $EC_{50}$.

To understand the mechanism of action of these mutations, I performed also single-channel recordings (cell-attached, pipette potential +100 mV) at saturating glycine concentrations. This allowed measurement of the channel maximum open probability ($P_{open}$ = cluster open time / total cluster time). The mutations tested decreased the GlyR maximum $P_{open}$ to 0.37 – 0.67, cf. the wild-type value of 0.98. This reduction in maximum $P_{open}$ was clear, despite the presence of distinct gating modes (stretches of activations with different $P_{open}$) in mutant receptors. These data suggest that the human hyperekplexia mutations tested here increase glycine $EC_{50}$ by reducing gating efficacy.

To determine whether the function of the mutant GlyRs can be rescued, the intravenous anasthetic, propofol was used. Propofol (50 μM) was found to enhance responses to submaximal glycine concentrations in all heteromeric receptors (by 2.71 - 5.19-fold). However, the impaired maximum response of mutant receptors was increased by propofol only for the S231N mutant GlyR.

Residues in the ECD are likely to be vital for agonist recognition and might have influence on channel gating. This was the case with the hyperkplexia α1 E103K GlyR mutation. In order to explain that, I investigated the role of residues at the back of the binding site, in loops A and E, E103 and R131, respectively, and established that they interact, probably by forming an intersubunit salt-bridge that is crucial for channel gating of the glycine receptor. The

interruption of this interaction might explain the reason behind the effect of the E103K hyperekplexia mutation.

**Table of Contents**

## List of Tables

## List of Figures

## Abbreviations

| | |
|---|---|
| 5-$HT_3$ | 5-hydroxytrytamine type 3 receptor |
| ACh | Acetylcholine |
| AChBP | Acetylcholine binding protein |
| AChR | Acetylcholine receptor |
| ATCC | American Type Culture Collection |
| ATP | Adenosine tri-phosphate |
| BGH | Bovine growth hormone |
| cDNA | Complementary DNA |
| CMV | Cytomegalovirus |
| CNS | Central nervous system |
| Cys | Cysteine |
| DMEM | Dulbecco's modified Eagle`s medium |
| DNA | Deoxyribonucleic acid |
| ECD | Extracellular domain |
| $E_{Cl}$ | Equilibrium potential for chloride ions |
| ECM | Electron cryo-microscopy |
| eGFP | Green fluorescent protein |
| ELIC | *Erwinia chrysanthemi* ligand gated ion channel |
| $GABA_A$ | γ-aminobutyric acid |
| GLIC | *Gloeobacter violaceous* ligand-gated ion channel |
| GluCl | Glutamate-gated chloride |
| Gly | Glycine |
| GCS | Glycine cleavage system |
| GlyR | Glycine receptor |
| HEK293 | Human embryonic Kidney 293 |
| hGlyR | Human glycine receptor |
| HPLC | High Performance Liquid Chromatography |
| ICD | Intracellular domain |
| IPSC | Inhibitory postsynaptic current |
| KCC | $K^+$-$Cl^-$ co-transporter |
| LGICs | Ligand-gated ion channels |
| MNTB | Medial nucleus of the trapezoid body |

| | |
|---|---|
| nAChR | Nicotinic acetylcholine receptor |
| NMR | Nuclear magnetic resonance |
| PCR | Polymerase chain reaction |
| $P_{open}$ | Open probability |
| pre-mRNA | Precursor messenger ribonucleic acid |
| Rs | Series resistance |
| TMD | Transmembrane domain |
| XRD | X-ray diffraction |

# Chapter 1 : Introduction

## 1.1 The pentameric ligand-gated ion channel superfamily

Ligand-gated ion channels (LGICs) are membrane embedded receptors that allow ion passage through their pore, when a specific agonist binds to them. These channels mediate fast synaptic transmission, as the ionic flux changes the membrane potential of the postsynaptic cell. There are three major families of LGIC: glutamate receptors, ATP-gated channels (P2X receptors) and Cys-loop receptors. In vertebrates, the Cys-loop (or nicotinic) superfamily comprises nicotinic acetylcholine receptors (nAChR), 5-hydroxytryptamine receptors (5-$HT_3$R), γ-amino-butyric acid GABA type A receptors ($GABA_A$), glycine receptors (GlyRs) and zinc-activated channel (ZAC). The name of the superfamily (Cys-loop) is due to the presence of a disulfide bond between cysteine residues, which forms a highly conserved 13 amino acid loop within the extracellular domain (ECD). In addition to that, the nicotinic superfamily comprises also channels expressed by invertebrates, notably the glutamate-gated chloride channel (GluCl), which is activated by glutamate in nematodes such as *C. elegans*, and prokaryotic channels, such as *Erwinia chrysanthemi* ligand-gated ion channel (ELIC) and *Gloebacter violaceous* ligand-gated ion channel (GLIC). Both ELIC and GLIC are cation-selective, but GLIC is gated by low pH (i.e., protons), whereas ELIC is activated by primary amines such as cysteamine (Bocquet *et al.,* 2007; Zimmermann and Dutzler, 2011). ELIC is also activated by GABA and modulated by benzodiazepines (Spurny *et al.,* 2012). Although they are part of the nicotinic LGIC superfamily, the prokaryotic channels lack the disulfide bond and therefore have no Cys-loop in the ECD (and virtually no M3-M4 cytoplasmic domain, see below). Soluble acetylcholine binding proteins (AChBP) found in molluscs are an additional related group of proteins, which are homologous to the ECD of the channels, but do not contain a transmembrane domain (Brejc *et al.,* 2001).

All Cys-loop family members are pentamers with their subunits arranged pseudo-symmetrically around a central pore. Homomeric receptors are formed by a single subunit type and heteromeric receptors are formed by more than one subunit type. Channels can mediate either excitatory, or inhibitory, synaptic transmission as they can be selective for cations, or anions, respectively. Inhibitory channels include glycine, $GABA_A$ receptors, the excitatory channels include nicotinic, 5-$HT_3$ receptors and ZAC.

## 1.2 Glycinergic transmission

### Discovery of the transmitter

The main concepts of GlyR neurotransmission and physiological properties are based on key *in vivo* experiments conducted in the 1950s and 1960s. Based on detailed analysis of glycine distribution in the spinal cord of cats, glycine was originally proposed as an inhibitory neurotransmitter by Aprison and Werman (1965). They noticed that the highest levels of glycine are localized in the ventral horn, where the spinal inhibitory interneurons are located. Several studies document the role of glycine as an inhibitory neurotransmitter (see Bowery and Smart, 2006; Callister and Graham, 2010). Electrophysiological studies by Curtis and Watkins (1960) and Werman *et al.* (1967) demonstrated that glycine application caused a reduction of action potential firing in spinal neurons. Subsequently, an *in vivo* study showed that glycine can be synthesized by neurons (Shank and Aprison, 1970). Hopkin and Neal (1970) reported the release of glycine from isolated slices of spinal cord post stimulus application (Hopkin and Neal., 1970). Following its release, glycine it is removed by $Na^+$-dependent high-affinity transporters. All these findings lead to the acceptance of glycine as a neurotransmitter due to its fulfilling the criteria set by Werman (1966) (Werman, 1966). Moreover, it was reported that the alkaloid strychnine is the most potent antagonist of GlyR (Curtis *et al.,* 1967; Young and Snyder, 1973). Strychnine has been a valuable tool in radioligand binding studies and affinity purification of GlyRs. GlyR can be photochemically labeled by UV irradiation as $^3$H-strychnine can bind irreversibly to GlyR post UV exposure (photoaffinity labeling; Graham *et al.,* 1983).

### Role of GlyR

In the adult nervous system GlyR mediates fast inhibitory synaptic transmission (mainly in the spinal cord and brainstem). GlyR has a vital role in coordination of spinal motor reflex circuits, respiratory rhythm regulation, sensory processing and (Lynch, 2004; Dutertre *et al.,* 2012). Defects in glycinergic neurotransmission result in the neuromotor disorder hyperekplexia. GlyR also play role in controlling pain as mice lacking the α3 GlyR displayed less pain sensitization induced by peripheral inflammation or injection of spinal prostaglandin $E_{2.}$ Prostaglandin $E_2$ is a mediator of inflammatory pain sensitization. It induces chronic inflammatory pain by inhibiting and phosphorylating of α3 GlyR. (Ahmadi *et al.,* 2002; Harvey *et al.,* 2004). Strychnine poisoning affects the inhibitory function of GlyR causing

severe muscle and unregulated muscle contractions, indicating the vital role of GlyRs in motor control. In addition, sensory perception is also affected as minimal acoustic or tactile stimuli cause convulsive episodes. GlyRs are also involved in the processing of visual and auditory signals, as GlyR α3 is found at inhibitory synapses in the retina and inner ear (Dutertre *et al.,* 2012).

In embryonic neurons GlyRs (and $GABA_ARs$) are excitatory and their activation results in depolarisation of the cell membrane that triggers the activation of voltage-gated $Ca^{2+}$ channels. This excitatory action might be important for synaptogenesis as $Ca^{2+}$ influx has a role in GlyR clustering at the post-synapse (Ye, 2008). During neurodevelopment, α2 GlyR is the dominant isoform of GlyR expressed in neurons. α2 GlyRs are vital for neuronal migration and synapse formation. Patients with autism spectrum disorder have defects in the α2 GlyR encoding gene *GLRA2* (Pilorge *et al.,* 2016).

In addition, glycine has a vital excitatory role as a neurotransmitter at glutamatergic synapses. Like D-serine, it acts as an essential co-agonist of L-glutamate at N-methyl-D-aspartate receptors (NMDA receptors, a subtype of glutamate receptors). Simultaneous binding of both glycine and L-glutamate is required for the full activation of conventional $Ca^{2+}$-permeable NMDA receptors. Those receptors are composed of two glycine-binding NR1 and two glutamate-binding NR2 subunits (Johnson and Ascher, 1987; Kuryatov *et al.,* 1994; Laube *et al.,* 1997). Glycine can also exclusively activate NMDA receptors that are composed of glycine-binding subunits NR1 and NR3 and lack a glutamate-binding site (Chatterton *et al.,* 2002; Madry *et al.,* 2007).

**Key processes of glycinergic synapse**

Glycinergic neurotransmission follows the same concept of synaptic transmission (Figure 1.1; Bowery and Smart, 2006). Glycine is packed into synaptic vesicles *via* the vesicular inhibitory amino-acid transporter (VIAAT), which requires a proton concentration gradient to transport glycine (and GABA; Gasnier, 2004). In adult neurons, the arrival of action potential causes activation of the pre-synaptic voltage-gated $Ca^{2+}$ channels. $Ca^{2+}$ influx leads to fusion of the vesicles to the plasma membrane of the pre-synaptic terminal and thereby results in the release of glycine (and GABA) into the synaptic cleft. Upon the binding of glycine to the post-synaptic GlyR, conformational change allows channel opening and an influx of $Cl^-$ ions into the post-synaptic cytoplasm. The resulting hyperpolarization inhibits neuronal firing of the post-synaptic membrane. Eventually, glycinergic synaptic transmission is terminated by

glycine removal and reuptake from the synaptic cleft *via* $Na^+$-/$Cl^-$-dependent, high-affinity glycine transporters one isoform of which is expressed in glial cells (glycine transporter 1: GlyT1, Figure 1.1) and the other in glycinergic pre-synaptic terminals (glycine transporter 2: GlyT2; Zafra *et al.*, 1995; Eulenburg *et al.*, 2005; Betz *et al.*, 2006a). Glycine is then either re-packed into synaptic vesicles or degraded via the glycine cleavage system (GCS) in astroglial mitochondria.

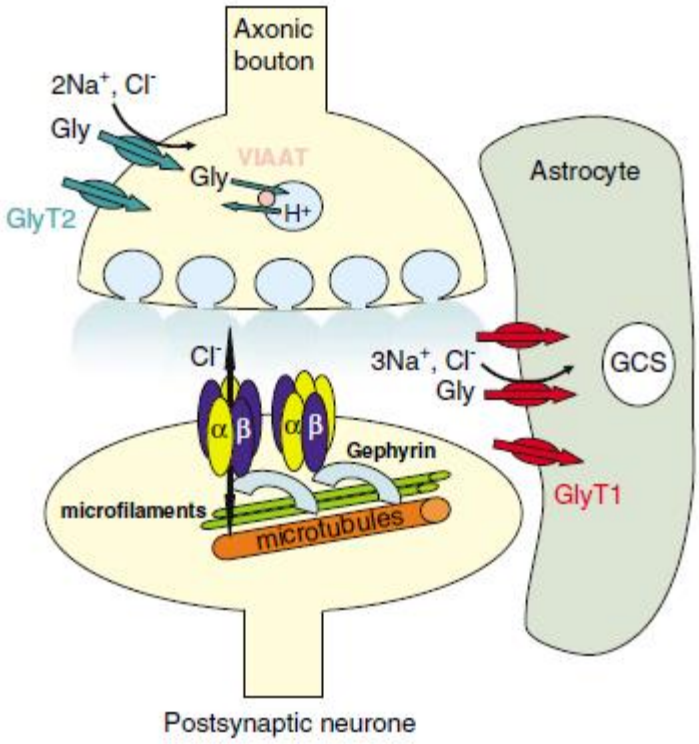


**Figure 1.1 Glycinergic transmission**
In the pre-synaptic terminal, glycine is concentrated in synaptic vesicles by the vesicular inhibitory amino-acid transporter (VIAAT). Post synaptic stimulation glycine is released in the synaptic cleft and binds to GlyR. Once glycine is dissociated from the receptor either of the glycine transporters GlyT1 (located at glial cells) or GlyT2 (located at the pre-synaptic plasma membrane) reuptake it. Glycine is then either repacked into synaptic vesicles or degraded via the glycine cleavage system (GCS). GlyRs are presented in the figure with two stoichiometries: 3α:2β and 2α:3β. The synaptic clustering of GlyRs is mediated by direct interaction of the GlyR β-subunit to the scaffolding protein gephyrin and then to the cytoskeleton. The Figure is adapted from Bowery and Smart, (2006).

## 1.3 Glycine receptors

Glycine receptors (GlyRs) are Cys-loop ion channels that mediate fast inhibitory neurotransmission in several parts of the CNS. Although the glycine receptor is found in higher brain regions including hypothalamus, nucleus accumbens, and cerebellum, the major synaptic role of glycine receptors is in the spinal cord, brain stem and retina (Lynch *et al.*, 2004). Binding of glycine to the postsynaptic glycine receptor allows permeation of chloride and bicarbonate ions and hyperpolarization, or depolarization, might result depending on the value of the equilibrium potential relative to cell resting potential. In adult neurons a low intracellular $Cl^-$ concentration (10 mM, or less) is maintained by the expression of the $K^+$-$Cl^-$ co-transporter KCC2. Given that the extracellular chloride concentration is high (approximately 110-130 mM), the equilibrium potential ($E_{Cl}$) for chloride in the adult central nervous system is hyperpolarizing with respect to the resting membrane potential (Delpy *et al.*, 2008). This means that if $E_{Cl}$ is more negative than the membrane potential, activation of GlyR will hyperpolarize the membrane and inhibit action potential generation (Lynch *et al.*, 2004). In embryonic neurons the intracellular $Cl^-$ concentration is high due to absence of the $K^+$-$Cl^-$ co-transporter KCC2. Because of that $E_{Cl}$ is depolarising and the action of GlyR is excitatory instead of inhibitory (Betz and Laube, 2006).

## 1.4 Isoforms of GlyR

The GlyR can exist as a homomer (composed by α subunits only), or as a heteromer (α subunit along with β subunit). Among GlyR subunits, there is only one β subunit isoform and 4 isoforms of α subunits (α1- α4), although the α4 gene is not functional in man. The major proteins associated with the GlyR are the 48 kD α1 subunit, 58 kD β subunit and the 93 kD gephyrin accessory protein (Graham *et al.*, 1985; Grenningloh *et al.*, 1990; Schmitt *et al.*, 1987). Gephyrin is an anchoring protein that links the TM3-TM4 of the β subunit to the cytoskeleton tubulin and F-actin providing receptor clustering and anchoring to the postsynaptic membrane (Sola *et al.*, 2004; Fritschy *et al.*, 2008). There is a 80-90% sequence identity between the α subunits, but the β subunit displays ~47% amino-acid sequence identity with the α subunits (Lynch *et al.*, 2004).

Alternative splicing produces additional α subunit isoforms. Rat α1 subunit has a $\alpha1^{ins}$ variant that includes eight additional amino-acids in the intracellular loop (Malosio *et al.,* 1991). The rat α2 subunit has two splicing variants, α2A and α2B (Kuhse *et al.,* 1990; Kuhse *et al.,* 1991). The human α3 gene has two transcripts, α3K and α3L. The α3K transcript lacks a 15 amino-acids segment in the intracellular loop (TM3-4) that is present in α3L. The rat α3 subunit has the intracellular insert (Kuhse *et al.,* 1990; Nikolic *et al.,* 1998). The β subunit has only one known form (Sola *et al.,* 2004).

Based on a UniProt search human, rat, and mouse has α1-α4 subunits and only one β subunit, although, the α4 subunit is a pseudogene in human. Between the human and rat α1 subunit there are four different amino acids and these residues are between the TM3 and TM4 domains. For the UniProt search only the high quality manually annotated and non-redundant protein sequence database "Swiss-Prot" reviewed results were included. This database combines the experimental results, computed features and the scientific conclusions.

Recombinant expression of any α GlyR subunit (other than human α4) in Human embryonic kidney (HEK 293) cells produces functional homopentameric receptors (Kuhse *et al.,* 1993). On the other hand, β subunits expressed alone cannot form functional receptors and need co-expression with α subunits to form glycine receptors. There are different views about the stoichiometry of GlyR: one favours $(\alpha1)_3(\beta)_2$ based on cross-linking experiments, electrophysiological techniques, and single molecule imaging and stepwise photobleaching techniques (Langosch *et al.,* 1988; Kuhse *et al.,* 1993; Burzomato *et al.,* 2003; Durisic *et al.,* 2012). The effects of mutating the highly conserved hydrophobic residues 9' of TM2 on the receptor sensitivity to glycine were more marked when the α subunit bore the mutation than when the mutation was inserted into β subunit. This supports $(\alpha1)_3(\beta)_2$ stoichiometry of GlyR (Burzomato *et al.,* 2003). Using another expression system, *Xenopus* oocytes, the group of Durisic *et al* used subunit counting by stepwise photobleaching. They found that GlyR stoichiometry is independent of the expression levels of individual subunits. Stepwise photobleaching of venus fluorescent protein (VFP)-tagged subunits was used to determine and count individual α1-or β-subunits within single GlyR channels and suggested a subunit ratio of $(\alpha1)_3\ (\beta)_2$. The VFP was inserted into the intracellular loop between TM3 and TM4 of human GlyR α1- and β- subunits. Even when different ratios of α: β VFP were used only receptors containing two β subunits were formed, suggesting the stoichiometry of two β subunits per heteromeric GlyR is strictly controlled (Durisic *et al*., 2012).

On the other hand, other findings support $(\alpha1)_2(\beta)_3$ with β-α-β-α-β arrangement based on expression of a tandem α1β construct and metabolic labelling analyses of recombinant GlyRs and imaging of single antibody-bound α1β GlyRs using atomic force microscopy (Grudzinska *et al.,* 2005; Yang *et al.,* 2012). Tandem subunits were constructed in which the C terminus of the α1 subunit was linked to the N terminus of the β subunit via a 7-fold alanine-glycine-serine repeat and expressed in oocytes. Expressing tandem α1- β did not produce functional receptors, unless the wild type β subunit was co-expressed. These receptors had $EC_{50}$ identical to the heteromeric α1β GlyR (Grudzinska *et al.,* 2005). Quantitation of radiolabeled methionine levels in recombinant α1 and α1β GlyRs also indicated $(\alpha1)_2(\beta)_3$ stoichiometry of heteromeric GlyR (Grudzinska *et al.,* 2005). Another study also indicated a $(\alpha1)_2(\beta)_3$ stoichiometry using atomic force microscopy technique (Yang *et al.,* 2012). FLAG and His6 epitopes were introduced into α1 and β subunits, respectively, and atomic force microscopy allowed imaging of single antibody-bound α1β receptors. Electrophysiology verified the functional expression of the α1 and β subunits with epitopes (Yang *et al.,* 2012). In either case, it is thought that three glycine molecules must bind to activate homomeric, or heteromeric, receptors fully (Beato *et al.,* 2004; Burzomato *et al.,* 2004; Lynch, 2009; Marabelli *et al.,* 2013).

## 1.5 Expression of glycine receptors in the CNS

The regional distribution and the developmental expression of GlyR in the CNS are different for the different subunits. In the CNS of rodents, glycine immunoreactivity against GlyR appears from embryonic day 12 (E12) (Chalphin and Saha, 2010). Before birth, the predominant α subunit is α2, and the expression of the β subunit is low. This was supported by analysis of mRNA and protein expression level studies (Becker *et al.,* 1988; Malosio *et al.,* 1991b; Watanabe and Akagi, 1995). The existence of α2 homomers in embryonic neuronal membranes was also suggested by functional work (Takahashi et al., 1992). The mean channel life time (single-channel properties) of embryonic (E20) receptors correspond to recombinant α2 receptors and the adult (P22) rat spinal GlyRs correspond better to α1 receptors (Takahashi et al., 1992). By the third postnatal week, expression of α2 subunits decreases, and that of α1 and β increases. In the adult, it is likely that the predominant synaptic form of the receptor is the α1β heteromer, with few exceptions (Lynch, 2009). This may be in part due to the fact that gephyrin, which is important for GlyR clustering in the

postsynaptic membrane, binds only to the β subunit of GlyR. α3 is expressed only in discrete areas of the CNS, notably the superficial dorsal horn of the spinal cord (Malosio *et al.*, 1991). GlyR containing α3 are thought to play a role in controlling pain, as mice lacking the α3 GlyR showed less pain sensitization by inflammation (Harvey *et al.*, 2004).

*In situ* hybridization data show α1 transcripts are abundant in the brainstem and spinal cord of adult rat. α1 subunits also expressed in the superior and inferior colliculi, the cerebral deep nuclei and the hypothalamus but at lower levels (Malosio *et al.*, 1991; Sato *et al.*, 1992; Garcia-Alcocer *et al.*, 2008). The β subunit is expressed in the brain from around embryonic day 14 and its expression increases in adults. The mRNA expression of β subunit is fairly high in brain regions where α subunit mRNA expression is absent (Malosio *et al.*, 1991). Considering that β subunits do not form homomers, the physiological role of this expression is not known.

GlyRs are located in the caudal part of the adult CNS, at low levels in the hippocampus, mid brain, thalamus and hypothalamus and at higher levels in the grey matter of the pons, medulla, and spinal cord. Different approaches were used to study the functional distribution of GlyR including *in vitro* autoradiography of [3H]-glycine (Bristow *et al.*, 1986) or strychnine (Young and Snyder, 1973; Zarbin *et al.*, 1981; Probst *et al.*, 1986) and immunocytochemistry studies for the GlyR anchoring protein gephyrin (Araki *et al.*, 1988; Triller *et al.*, 1985; Racca *et al.*, 1997).

The distribution of GlyR subunits is anatomically segregated across the synapse as shown in a study of rat calyx of Held synapse from the auditory brainstem. GlyRs at these pre-synaptic terminals are composed of α1 homomeric subunits (Hruskova *et al.*, 2012). Heteromeric GlyRs cluster at the postsynaptic terminal, as the β subunit interacts with gephyrin. Most of the glycinergic inhibitory transmissions are carried by heteromeric α1β GlyRs in adult CNS (Kneussel and Betz, 2000; Grudzinska *et al.*, 2005; Lynch, 2009). Homomeric GlyRs can be functional as shown in embryonic neurons (Flint *et al.*, 1998). However, the evidence for existence of homomeric GlyRs in the adult CNS is limited (Turecek and Trussell, 2001, 2002; Deleuze *et al.*, 2005).

## 1.6 Glycinergic synaptic currents

The physiological consequence of the developmental switch from α2 to α1 GlyR subunit at ~P20 in rat (Malosio *et al.,* 1991) is the change in the time course of the IPSCs. As the expression of the α1 subunit increases, the glycinergic IPSCs become faster (Ali *et al.,* 2000; Legendre and Korn, 1994; Singer *et al.,* 1998; Singer and Berger, 1999 and 2000). The time course of glycinergic IPSCs is characterised by a fast mono-exponential rising phase and a mono- or bi-exponential deactivation phase (Beato, 2008; Burzomato *et al.,* 2004; Legendre, 2001; Singer *et al.,* 1998; Singer and Berger, 1999). In the adult, the time course of glycine synaptic currents is very fast, with decay time constants between 5 and 10 ms (Singer *et al*., 1998; Burzomato *et al*., 2004). This is determined by the kinetic properties of α1β GlyR heteromers (Burzomato *et al*., 2004; Pitt *et al*., 2008). Glycine is removed from the synaptic cleft by glycine transporters with an estimated time constant of 0.3-0.9 ms (Beato *et al.,* 2008; Legendre, 2001).

The main inhibitory transmitters in the CNS are GABA and glycine. Many synapses in the spinal cord (Jonas *et al.,* 1998), brain stem (Kotak *et al.,* 1998; O'Brien *et al.,* 1999; Russier *et al.,* 2002) and cerebellum (Dumoulin *et al.,* 2001) may be mixed GABAergic-glycinergic synapses. The existence of mixed GABA-glycine synaptic terminals was shown by immunohistochemical studies (Todd *et al.,* 1996; Triller *et al.,* 1987). Mixed inhibitory interneurons in the spinal cord co-release glycine and GABA from the same vesicle (Jonas *et al.,* 1998). The deactivation of $GABA_A$ receptors is much slower than that of GlyR and this is reflected in the duration of the synaptic currents. For instance, GABA and glycine inhibitory neurotransmitters co-exist in the hypoglossal nucleus of the brainstem where most of the local cells are motoneurons. The GABAergic and glycinergic $Cl^-$ mediated synaptic transmission in the brain stem motoneurons of neonatal rats differ in terms of kinetics. GABAergic responses had slower rise and decay times than glycinergic. This applies to glycinergic sPSCs, mPSC and ePSCs (Donato and Nistri, 2000). In embryonic motoneurons the density of expressed $GABA_A$ receptors is higher than of glycine receptors (Gao and Ziskind-Conhaim 1995). With development in most spinal brainstem synapses, the transmission changes from the long-duration GABAergic inhibitory post synaptic potentials (IPSPs) to short-duration glycine IPSPs (Gao *et al.,* 2001; Baccei and Fitzgerald, 2004). In several brain regions with development the co-transmission is shifted to glycine only (Nabekura *et al.,* 2004; Awatramani *et al.,* 2005; Muller *et al.,* 2006).

A different situation occurs when GABA, co-released with glycine acts directly on glycine receptors in auditory pathways in the brainstem (Lu *et al.,* 2008). GABA is a weak partial agonist of GlyR (see below), and thus GABA co-released with glycine can act can modulate the decay of glycinergic neurotransmission (Lu *et al.,* 2008). It is shown in most of the medial nucleus of the trapezoid body (MNTB) in P16 rats that co-released GABA modifies the response of glycine receptor to glycine, speeding it. Fine-tuning of the glycinergic transmission in the mature auditory system seems to be one of the functions of co-release. GABA and glycine might work together on single receptor to enhance the temporal resolution of inhibition.

The physiological importance of GlyR mediated transmission is confirmed by the reported effects of loss of function mutations or gene deletions in man and in rodents. These are described in the introduction of the chapter three).

## 1.7 Pharmacology of GlyR

### 1.7.1 Agonists of GlyR

GlyR has several ligands that are capable of channel opening, but these have differing efficacies. The most potent agonist for GlyR is glycine, but there are other agonists that can activate the receptor (Legendre, 2001; Lynch, 2004). These include the amino acids β-alanine, L and D stereoisomers of α-alanine, sarcosine, taurine, L-serine and GABA (Schmieden and Betz, 1995). The potency of these endogenous amino acids acting on GlyRs is as follows: glycine has the highest potency, followed by β-alanine, taurine and then GABA (Lewis *et al.,* 1991; Fucile *et al.,* 1999; de Saint Jan *et al.,* 2001). Whereas glycine is a full agonist of GlyR, β-alanine, taurine and GABA are partial agonists as they have a lower efficacy than glycine (Figure 1. 2). Some GlyR ligands are listed in Table 1.1 and the most relevant GlyR agonists are described below.

**Glycine.** The simple amino acid glycine is a full agonist of GlyR, as it can keep the wild-type α1β GlyR open 96% of the time (Lape *et al.,* 2008). Glycine sensitivity is similar between α1, α2, α3 and α4 GlyR, incorporation of the β subunit alters the channel sensitivity to glycine (Lynch, 2004).

**Taurine.** Taurine can keep the wild-type α1β GlyR open only 54% of the time (Lape *et al.,* 2008). It is thought to act as a partial agonist because it has a reduced ability to induce the

conformational changes that precede channel opening (Lape *et al.,* 2008). Some reports imply that agonist efficacy is different in different expression systems. Taurine provides an example for this, as it appears to be a full agonist in α1 GlyRs expressed in mammalian cells (Rajendra *et al.,* 1995) but is less efficacious than glycine for GlyR expressed in *Xenopus* oocytes (Schmieden *et al.* 1989, 1992). Differences in the rate of agonist application and in the relative desensitisation of the peak current may underlie this phenomenon. Taurine acts as antagonist in homomeric GlyR bearing the hyperekplexia mutations α1(R271Q) and α1(R271L) (Laube *et al.,* 1995). Mutations at E53 and E57 α1 GlyR residues GlyR also change taurine into an antagonist (Absalom *et al.,* 2003).

**Sarcosine.** The endogenous amino acid sarcosine (*N*-methylglycine) acts as a GlyT1 inhibitor (Smith *et al*., 1992; Lopez-Corcuera *et al.,* 1998; Herdon *et al.,* 2001; Mallorga *et al.,* 2003) and an NMDA receptor co-agonist together with glutamate (Zhang *et al.,* 2009). Sarcosine was also found to be a GlyR agonist (Zhang *et al.,* 2009) on embryonic mouse hippocampal neurons (GlyT1 was blocked pharmacologically with the irreversible GlyT1 inhibitor N[3-(4-fluorophenyl)-3-(4-phenylphenoxy) propyl] sarcosine (NFPS) or by culturing neurons in the absence of glia upon which GlyT1 is expressed). The authors found sarcosine to be less potent than glycine ($EC_{50}$ 3.2 ± 0.7 mM vs. 57 ± 8.0 μM) and less efficacious (ca. 75%), possibly because of the extra methyl group on the N-terminus compared to glycine (Zhang *et al.,* 2009). Results from recombinantly expressed human homomeric α1 GlyR confirm that sarcosine is a partial agonist. The maximum current response of sarcosine relative to glycine reached only 80% when saturating concentrations of glycine and sarcosine were applied to the same cell of α1 GlyR using whole-cell recordings. This is further confirmed by single-channel recordings using a saturating concentration of sarcosine (Safar *et al.,* 2016).

With the sequence similarity between rat and human α1 GlyR (except for four different residues between the TM3 and TM4 regions) it is possible that agonists of human and rat α1 GlyR are similar.

### 1.7.2 Antagonist of GlyR

GlyRs have both competitive and non-competitive antagonists. The former act by competing with the agonist for the binding sites (identical, or overlapping, i.e. orthosteric sites), the latter exert their effect by binding at another site, either the ion channel pore, or an allosteric site. A wide variety of GlyR antagonists exist. A few of the more relevant GlyR antagonists are discussed below.

**Strychnine.** The inhibitory action of glycine is antagonized by the alkaloid strychnine. Strychnine is a highly potent competitive antagonist of GlyR, with a dissociation constant ($K_d$) in the range 5-15 nM for α1β GlyR (Lewis *et al,*. 1998; Alexander *et al,*. 2017). The structure of GlyR for α1 zebrafish and α3 human isoforms in complex with strychnine was solved recently (Du *et al.,* 2015; Huang *et al.,* 2015). Similar to glycine the binding site of strychnine is in the ECD. The binding sites are overlapping but not identical, because strychnine is a large, rigid molecule. The high potency and selectivity of strychnine for GlyR makes it a useful tool to discriminate between glycinergic and GABAergic synaptic currents. Strychnine interrupts GlyR function by eliminating glycinergic synaptic inhibition. This results in overexcitation of the motor system leading to muscular convulsions.

**Picrotoxin.** The plant convulsant alkaloid picrotoxin, which contains equimolar concentrations of picrotin and picrotoxinin, inhibits GlyR and it is a channel blocker (Lynch, 2004). It binds within the channel pore as indicated in the crystal structure of *C. elegans* GluCl (Hibbs and Gouaux, 2011). The inhibitory action of picrotoxin is influenced by inclusion of the β subunit of GlyR and this makes it a useful tool for discriminating between homomeric and heteromeric GlyRs. Both recombinantly expressed αβ GlyR and native GlyRs are less sensitive to picrotoxin than homomeric α GlyRs (Pribilla *et al.,* 1992). However, picrotoxin lacks specificity for GlyRs as it is also a non-competitive $GABA_A$ receptor antagonist. Whereas homomeric α1 GlyR is equally sensitive to picrotoxinin and picrotin (Lynch *et al.,* 1995), homomeric α2 GlyR shows increased sensitivity to picrotoxinin and reduced sensitivity to picrotin. Both homomeric α2 and α3 GlyR are more sensitive to block by picrotoxinin than α1 GlyR (Yang *et al.,* 2007). Heteromeric α1β GlyR is equally sensitive to picrotoxinin and picrotin and α3β is more sensitive to picrotoxinin than α1β (Yang *et al.,* 2007). This compound could therefore be used for discriminating between different isoforms of GlyR.

**Ginkgolide B.** Ginkgolide B, a component of extracts from the leaves of the *Ginkgo biloba* tree, is another chloride channel blocker (Alexander *et al.,* 2017). Glycine-induced currents in native GlyRs in isolated hippocampal neurons and of recombinantly GlyRs expressed in *Xenopus* oocytes are inhibited by Ginkgolide (Kondratskaya *et al.,* 2002, 2005). It can be used to discriminate between homomeric and heteromeric GlyRs as inclusion of the β subunit increased the sensitivity of recombinant α1β GlyRs expressed in *Xenopus* oocytes by up to 20-fold compared with that of homomeric GlyRs. It was reported that homomeric α1 GlyR is more sensitive to ginkgolide B inhibition than homomeric α2 and α3 isoforms of GlyRs using

recombinant GlyRs expressed in *Xenopus* oocytes *(*Kondratskaya *et al.,* 2005). Ginkgolide B is also selective in blocking GlyR because it is inactive at $GABA_A$ receptors (Kondratskaya *et al.,* 2005).

**RU 5135.** The convulsant steroid derivative, RU 5135 (3α-hydroxy-16-imino-5β-17-azaandrostan-11-one), is a glycine antagonist that targets all subtypes of rat GlyR (Simmonds and Turner, 1985). While strychnine is useful in discriminating between glycinergic and GABAergic synaptic currents, RU5135 lacks specificity as it is an antagonist of both glycine and $GABA_A$ receptors (Curtis and Malik, 1985).

**Other antagonists.** In addition to the above antagonists there are some inhibitors that are helpful in discriminating between different isoforms of GlyR; however, they are not selective for the GlyR. For instance, the neurosteroid pregnenolone sulphate is a more potent blocker on α1 than α2 GlyR. Co-expression of the β subunit does not affect the potency of pregnenolone sulphate at α1β but reduces the potency at α2β GlyR (Lynch, 2004; Alexander *et al.,* 2017). Moreover, the function of GlyR might be enhanced or inhibited by tropisetron (ICS 205-930), which is a 5-$HT_3$ receptor antagonist. It is more potent on α2 than on α1 GlyRs and co-expression of the β subunit increases the potency at both receptors (Lynch, 2004; Betz and Laube, 2006; Alexander *et al.,* 2017). Also, the homomeric α1 GlyR, but not the α2, is blocked by cyanotriphenylborate, an open-channel blocker (Rundstrom *et al.,* 1994).

### 1.7.3 Modulators of GlyR

Drugs that are capable of modulating GlyR function might be interesting for their potential therapeutic applications in pain alleviation and muscle relaxation (Laube *et al.,* 2002a; Lynch, 2004). A wide variety of agents can modulate the function of GlyR. While these will be further discussed in Chapter Four, a few are briefly described below.

**$Zn^{2+}$.** The divalent cation $Zn^{2+}$ has a putative physiological relevance (Smart *et al.,* 2004). In different areas of the brain such as the cortex, hippocampus and spinal cord $Zn^{2+}$ is concentrated into synaptic boutons along with GABA, glycine or glutamate (Frederickson and Danscher, 1990; Birinyi *et al,*. 2001; Brown and Dyck, 2002). It is released after neuronal stimulation in sufficient concentration (<10 μM) to modulate GlyR current (Assaf and Chung, 1984; Howell *et al.,* 1984; Xie and Smart, 1991, Miller *et al.,* 2005b).

The physiological role of $Zn^{2+}$ for proper glycinergic inhibition has been demonstrated in homozygous knock-in mice models carrying the *Glra1*(D80A) mutation. The affected mice exhibited hyperekplexia-like phenotypes such as tremors and delayed righting reflexes (a measure of how long a mouse needs to right itself after being turned on its back). This point-mutation abolished $Zn^{2+}$ potentiation of glycine-induced currents from spinal cord neuronal circuits and brainstem slices. GlyR expression levels or agonist sensitivity were not affected. This explains how a lack of $Zn^{2+}$ modulation might affect glycinergic neurotransmission *in vivo* (Hirzel *et al.,* 2006).

$Zn^{2+}$ has dual effects: at low concentrations (<10 μM) it enhances the GlyR function but at high concentrations (>10 μM) it inhibits the action of glycine. This biphasic effect is found for both native and recombinant expressed GlyRs (Harvey *et al.,* 1999; Laube *et al.,* 2000; Smart *et al.,* 2004; Miller *et al.,* 2005a; Miller *et al.,* 2005b). The molecular sites for $Zn^{2+}$ potentiation differ from those for inhibition. While $Zn^{2+}$ potentiation of glycine-activated GlyR involve α1(D80), α1(E192), α1(D194), α1(H215) residues (Lynch *et al.,* 1998; Laube *et al.,* 2000, 2002; Miller *et al.,* 2005b), its inhibition is affected by α1(H107), α1(H109), α1(T112) and α1(T133) (Harvey *et al.,* 1999; Laube *et al.,* 2000; Miller *et al.,* 2005a).
$Zn^{2+}$ potentiation of glycine response is abolished by α1(D80A)β GlyR mutation (Laube *et al.,* 2000, 2002). However, $Zn^{2+}$ modulation of response to the partial agonist taurine is maintained for the same mutation (Lynch *et al.,* 1998). This suggests either the existence of different binding sites for $Zn^{2+}$ or that the mutation only affects glycine response but not taurine.

The homomeric α1 GlyR is more sensitive to the modulation action of $Zn^{2+}$ than the α2 GlyR isoform. This difference in the sensitivity between the α1 and α2 isoforms of GlyR is maintained with the incorporation of the β subunit (Miller *et al.,* 2005a).

**Alcohol.** Alcohol is one of the most widely studied modulators of GlyR. It has been shown to enhance the function of both glycine and $GABA_A$ receptors in recombinant expression systems (Mihic *et al.,* 1997; Harris *et al.,* 2008). High alcohol concentrations of 50–200 mM are needed to observe the 40–150 % potentiation effect (Borghese *et al.,* 2012). Binding of alcohols to transmembrane binding pockets has been demonstrated in the crystal structure of GLIC (Howard *et al.,* 2011).

**Endocannabinoids.** Other allosteric GlyR modulators include endocannabinoids, which are endogenous lipid-signalling molecules that activate G-protein-coupled cannabinoid receptors

(CB1 and CB2 receptors; Piomelli, 2003). Endocannabinoids that modulate GlyR include anandamide (AEA, 10–30 μM), N-arachidonyl glycine (NA-Gly, 10 μM), and virodhamine (VIR, 10 μM; Xiong *et al.,* 2012; Yevenes & Zeilhofer, 2011).

**Ivermectin.** Ivermectin, an antiparasitic drug that is used to treat humans as well as animals, can at sub-micromolar concentrations modulate homomeric α1 and heteromeric α1β GlyRs (Shan *et al.,* 2001; Lynagh and Lynch, 2012). Its modulation effect was also observed in other electrophysiological studies (Lynagh and Lynch, 2010; Lynagh *et al.,* 2011). Ivermectin can directly activate GlyR and its activation effect is poorly reversible (Shan *et al.,* 2001; Lynagh and Lynch, 2010). The binding site for ivermectin is within the TMD as explored by the crystal structure of *C. elegans* GluCl receptor, the electron microscopy structure of zebrafish α1 GlyR and the most recent crystal structure of human α3 GlyR (Hibbs and Gouaux, 2011, Du *et al.*, 2015, Huang *et al.*, 2017).

**General anaesthetics.** In addition, several general anaesthetics such as isoflurane, enflurane, halothane, sevoflurane and propofol potentiate GlyRs (Downie *et al.,* 1996; Mascia *et al.,* 1996; Krasowski and Harrison, 1999; Yamakura *et al.,* 2001; O'Shea *et al.,* 2004; Lynagh and Laube, 2014; Nguyen *et al.*, 2009). See Chapter Four for more details on the effect of propofol.

**Table 1.1 GlyR ligands**

| Ligand | Ligand class | Reference |
|---|---|---|
| Glycine | Agonist | Bormann, (1993); Lynch *et al.* (1997); Alexander *et al*. (2017) |
| β - alanine | Agonist | Lynch *et al.* (1997); Alexander *et al.* (2017) |
| Taurine | Partial agonist | Lynch *et al.* (1997); Alexander *et al.* (2017) |
| GABA | Partial agonist | Schmieden *et al.* (1993); De Saint Jan *et al.* (2001) |
| Sarcosine | Partial agonist | Zhang *et al.* (2009) |
| strychnine | Antagonist | Vandenberg *et al.* (1992), Alexander *et al.* (2017) |
| RU5135 | Antagonist | Curtis and Malik, (1985); Simmonds and Turner, (1985); Alexander *et al.* (2017) |
| Picrotoxin | Antagonist | Alexander *et al.* (2017) |
| Picrotoxinin | Antagonist | Yang et *al.* (2007) |
| Picrotin | Antagonist | Yang et *al.* (2007) |
| Ginkgolide B | Antagonist | Kondratskaya *et al*, 2002, 2005 |
| Zinc | Allosteric modulator | Miller *et al.* (2005a); Miller *et al.* (2005b); Alexander *et al.* (2017) |
| Alcohols | Allosteric modulator | Mihic *et al.* (1997); Borghese *et al.* (2012); Alexander *et al.* (2017) |
| Anesthetics (isoflurane, enflurane, propofol etc.) | Allosteric modulator | Downie *et al.* (1996); Mascia *et al.* (1996); Krasowski and Harrison, (1999); Yamakura *et al.* (2001); O'Shea *et al.* (2004); Lynagh and Laube, (2014); Nguyen *et al.* (2009) |
| Ivermectin | Allosteric modulator | Shan *et al.* (2001); Lynagh and Lynch, (2010) |
| Endocannabinoids (anandamide) | Allosteric modulator | Xiong *et al.* (2012); Yevenes and Zeilhofer, (2011) |

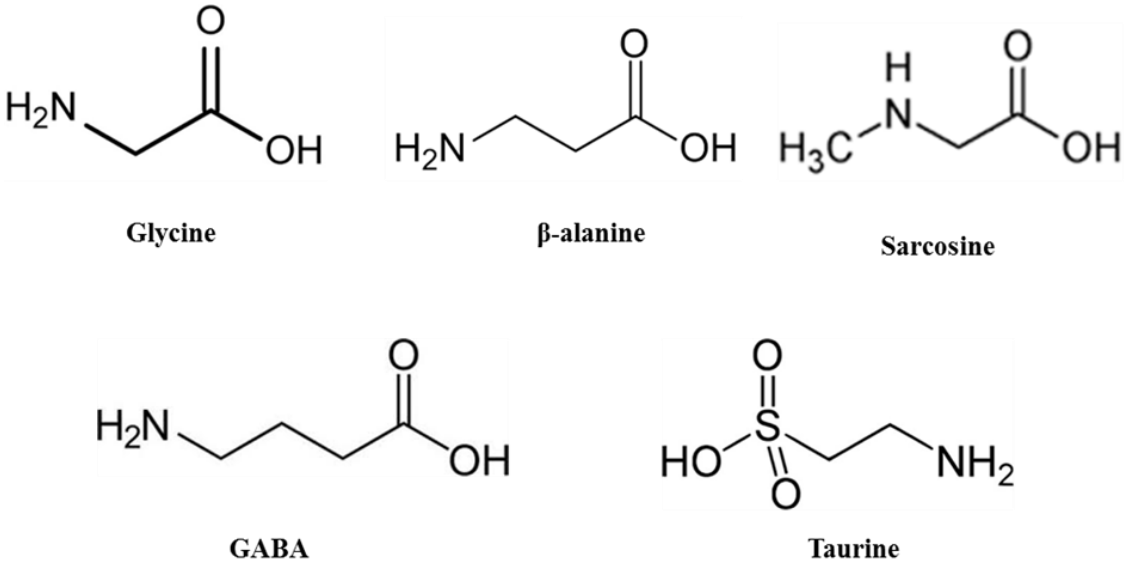


**Figure 1.2 Agonists of GlyRs.**
The chemical structure of the endogenous ligands acting on GlyRs.

## 1.8 Biophysical properties of GlyR: permeability and chloride modulation

The GlyR contains an anion conducting pore and it mainly conducts chloride ions. GlyR has been tested for anion permeability *in vitro*. The anion permeability preference of $SCN^- > NO_3^- > I^- > Br^- > Cl^- > F^-$ was found (Bormann *et al.*, 1987; Fatima-Shad and Barry, 1993; Lynch, 2004).

The time course of decay of synaptic-like GlyR currents is affected by the concentration and structure of the permeating ion. For instance, replacing chloride with another permeable anion, thiocyanate ($SCN^-$), suppressed the voltage dependence of GlyR. For α1β GlyR deactivation in $SCN^-$ was slower than in chloride (Moroni *et al.*, 2011b). For homomeric α1 GlyR, however, the deactivation in thiocyanate was faster. The nature of the permeating ion affects the voltage dependence for wild-type α1 and α1β GlyRs. Whereas currents carried by chloride slow with depolarization, currents carried by thiocyanate are insensitive. In both homomeric and heteromeric GlyRs chloride-impermeant mutants $\alpha1^{A251E}$ and $\alpha1^{R271A}$ the

voltage dependence is abolished (Moroni *et al.,* 2011b). It is possible that an interaction is needed between the activated gate and ions passing through the channel (Marchais and Marty, 1979). Two rings of positive charges, R252 and R271, are believed to attract anions before they are transported across the gate (Keramidas et al., 2004). Conductance is discussed further down.

The duration of the synaptic glycinergic inhibition is influenced by chloride concentration. It was found that increasing intracellular chloride concentration slows the decay time constant of glycinergic IPSC. This was based on agonist concentration jumps experiments as recording with high chloride concentration in the patch pipette (130 mM) slowed the current decay by three fold compared to recording with low intracellular chloride concentration (10 mM) (Pitt *et al.,* 2008). In addition, the extracellular chloride concentration also influences the time course of the synaptic-like GlyR. In symmetrical high chloride concentration (131 mM) on both sides of the membrane the decay was slower than in case of the presence of low intracellular chloride concentration (10 mM) (Moroni *et al.,* 2011b). In order to have the effect of the intracellular chloride on the time course of the inward current, anion selectivity is required. If the glycine channels are mutated to be cationic, the modulation by the intracellular chloride disappears. The presence of high or low chloride did not affect the decay of currents evoked by rapid application of glycine to $\alpha1^{A251E}$ GlyR (Moroni *et al.,* 2011b).

## 1.9 Receptor Structure

All the members of the Cys-loop family share similar topology. I will summarise the main findings general to the superfamily and discuss in more detail those that are relevant to GlyRs.

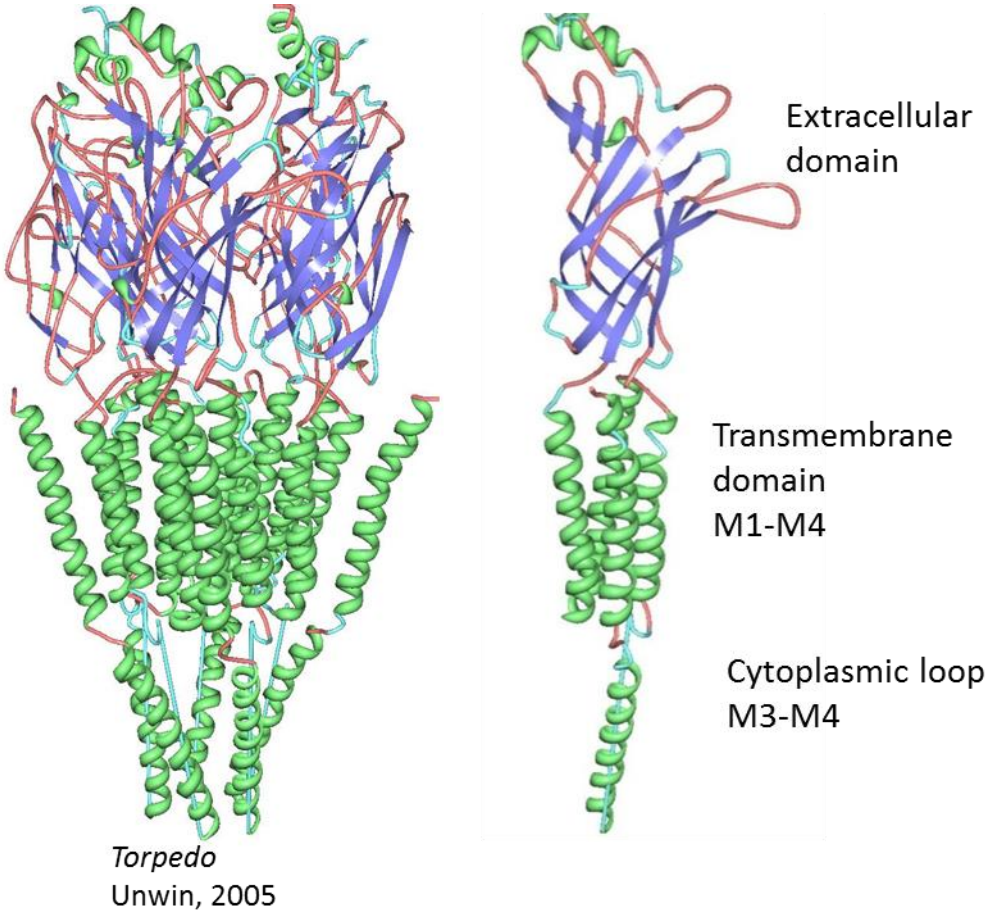


Figure 1.3 General structure of a Cys-loop receptor and constituent subunits.

Ribbon structure of the *Torpedo* nicotinic acetylcholine receptor (nAChR) (Protein Data Bank (PDB): 2BG9) showing the extracellular domain (ECD), transmembrane domain (TM) and a partial structure of the intracellular domain (ICD) (Unwin, 2005).

Each of the five subunits have a large N-terminal extracellular domain (ECD) followed by four α -helical transmembrane domains (TM1-TM4) terminating a short C-sequence. The TM1-TM4 are connected by one extracellular and two intracellular linkers. The large intracellular domain between TM3 and TM4 is mostly unstructured (Figure 1.3). The ion conducting pore is surrounded by the TM2 helices from each subunit. This central pore is lined by polar and hydrophobic residues that determine ion selectivity and constitute the channel gate. The ion channel is closed at rest. Binding of the agonist to the ECD triggers a conformational change that result in gating, or opening, of the transmembrane pore. A high resolution structure of a nicotinic ECD was first obtained for the AChBP with 2.7 A° resolution. (Brejc *et al.,* 2001). The first images of the nicotinic channel were obtained by Nigel Unwin by cryo-electron microscopy of *Torpedo* muscle-type nAChRs. Analysis of increasing image datasets led to a structure with 4 A° resolution defining the EC, the TM and partially the cytoplasmic domains (Unwin, 2005).

The increasing availability of crystal structures of other Cys-members from invertebrate and prokaryotic organisms has provided further details. These structural data all refer to homomeric channels and include the crystal structure of the prokaryotic channels ELIC from E*rwinia chrysanthemi* and GLIC from *Gloeobacter violaceus* with 3.3 A° and 3.9 - 4.35 A° resolution, respectively (Hilf and Dutzler, 2008; Bocquet *et al*., 2009; Hilf and Dutzler, 2009; Sauguet *et al.,* 2014). The crystal-structures of several eukaryotic receptors were recently solved. They include GluCl from *Caenorhabditis elegans* (3.3 A°; Hibbs and Gouaux, 2011), 5-$HT_3$ from mouse with 3.5 A° and 4.3 A° resolution, respectively (Hassaine *et al.,* 2014; Basak *et al.,* 2018), and $GABA_A$ β3 receptor from man (Miller and Aricescu, 2014). A list of the main solved structures of pLGIC is provided in Table 1.1.

For glycine receptors, the NMR structure of only the transmembrane domain of the α1 subunit is has been published (Mowrey *et al*., 2013). The structure of Lily, which is a chimeric construct produced by merging the EC domain from GLIC and the TM domain from GlyR, was solved in the locally-closed state (Moraga-Cid *et al.,* 2015). Recent electron cryo-microscopy structures of the zebrafish α1 GlyR has been solved. It provided the structure of the homopentamers GlyR in three channel conformations: an open channel conformation with glycine, a desensitized or partial open conformation with glycine/ivermectin, and a closed channel conformation with strychnine (Du *et al.,* 2015). Another study provided crystal- structure of homomeric human α3 GlyR in closed state bond with strychnine (3.0 A°; Huang *et al.,* 2015).

These recent resolved structures of GlyR provided further advancement for understanding the ion channel. The structures of GlyR supported the classic topology of Cys-loop receptors including all main parts of the subunit from the ECD to the extracellular C-terminal region (Moss and Smart *et al.,* 2001; Thompson *et al.,* 2010). Formation of functional pentameric receptor with TM2 surrounding the ion channel pore and TM4 facing towards the plasma membrane is also confirmed.

Even with the availability of the recent solved structure of several pLGICs, there are key questions needed to be determined such as the conformational coupling from ECD to ICD. Given that there are no high resolution structure of some of the pLGIC, inference have to be made from related homologues receptors despite the limited degree of homology (Figure 1.4 shows three channels). From a physiological perspective, a highly conserved structure indicates a conserved function. While these data offer the hope of a new understanding of structure-function relation in these channels, there is much controversy about what conformational state the different structures are in. This is made more difficult as most channels have been imaged only in one state, irrespective of their state of ligation. One of the best results have been obtained for GLIC, which has been imaged by X-ray crystallography in both the open and the closed conformation (and in a "locally closed" conformation of unknown significance). However, GLIC poses its own problems, as it is thought that the protonation that opens GLIC is not confined to the canonical agonist binding site (Wang *et al.,* 2012).

Molecular dynamics computational modelling may be useful to make sense of all the static structural data and yield a dynamic model of channel activation that can relate to function (daCosta and Baenziger, 2013; Yu *et al.,* 2014; Cecchini and Changeux, 2015).

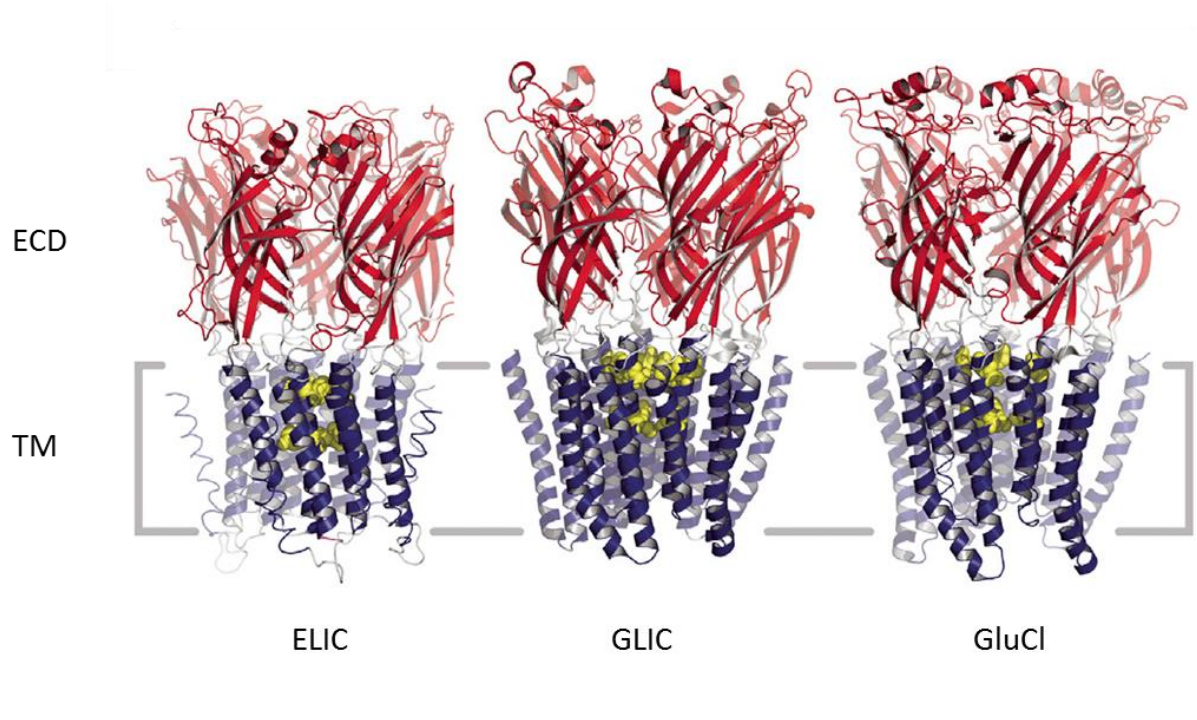


**Figure 1.4 Structure of three nicotinic superfamily LGICs.**

ELIC (left, PDB ID code 2VLO), GLIC (Middle, PDB ID code 3EAM), and GluCl (Left, PDB ID code 3RIF). The Figure is adapted from daCosta and Baenziger, (2013). ECD highlighted in red, TM highlighted in blue. Yellow spheres indicate the narrowest constrictions in the channel pore.

**Table 1.2 Main structures of pLGICs**

| Receptor | Method | Resolution (Å) | Conformation | Reference |
|---|---|---|---|---|
| AChBP | XRD | 2.7 | - | Brejc *et al.* (2001) |
| *Torpedo AChR* | ECM | 4.0 | closed channel | Unwin (2005) |
| *Torpedo AChR* | ECM | 6.2 | open/closed channel | Unwin and Fujiyoshi (2012) |
| ELIC | XRD | 3.3 | Closed channel | Hilf and Dutzler (2008) |
| GLIC | XRD | 2.9 | Open channel | Bocquet *et al.* (2009) |
| GLIC | XRD | 3.1 | Open channel | Hilf and Dutzler (2009) |
| GLIC | XRD | 4.35 | Closed channel | Sauguet *et al.* ( 2014) |
| GluCl | XRD | 3.3 | Open channel | Hibbs and Gouaux (2011) |
| GluCl | XRD | 3.6 | Closed channel | Althof *et al.*(2014) |
| 5-$HT_{3A}$ | XRD | 3.5 | Open channel | Hassaine *et al.*(2014) |
| 5-$HT_{3A}$ | ECM | 4.3 | Closed channel | Basak *et al.*(2018) |
| $GABA_A\beta_3$ | XRD | 3 | Closed channel | Miller and Aricescu (2014) |
| GlyR α1 (TMs) | NMR | - | - | Mowrey *et al.*(2013) |
| GlyR α1 | ECM | 3.9 | Open/Closed channel | Du *et al.*(2015) |
| GlyR α3 | XRD | 3.0 | Closed channel | Huang *et al.*(2015) |
| GlyR α3 | XRD | 2.6 | Open channel | Huang *et al.*(2017) |
| Chimera GLIC-GlyRα1 | XRD | 3.5 | Closed channel | Moraga-Cid *et al.*(2015) |

Summary of the main resolved structures of pLGICs. Methods used to obtain the structures are X-ray diffraction (XRD), electron cryo-microscopy (ECM), or solution nuclear magnetic resonance (NMR).

### 1.9.1 General structural features: the binding site

The ECD is formed by a highly conserved β-sandwich with an inner and an outer sheet and a total of ten β strands. The neurotransmitter binds at the interface between subunits. In a pentameric receptor there are five potential binding sites. The binding pocket consists of three regions from the "principal" or (+) side (the anticlockwise subunit, namely the A, B, and C loops and the four ''complementary'' or (-) subunits strands D, E, F, and G (Figure 1.5; Galzi & Changeux, 1995; Corringer *et al.*, 2000;Figure 1.6; Hibbs and Gouax, 2011). Although only few residues face the binding pocket directly, other nearby residues can affect binding by maintaining pocket structure, or taking part in conformational changes in this area.

Once the neurotransmitter binds to the ECD structural movements occur to allow channel opening 60 Å away. Not all the residues in the binding site are directly involved in the binding.

Structure-function studies on Cys-loop receptors such as nAChRs, $GABA_A$, and the $5\text{-}HT_3$ receptors indicate that the agonist binding occur in the N-terminal domain at interfaces between adjacent subunits (Corringer *et al.,* 2000). The identification of binding site loops was confirmed by the crystallographic data on the AChBP (Brejc *et al.,* 2001), where the principal (+) side contributes true loops, whereas the complementary (-) side contributes β strands.

AChBP lacks the transmembrane and intracellular domains but shares 15-20% sequence identity with other Cys-loop receptors (Sixma and Smit, 2003; Sixma, 2007). Despite the low homology, AChBP has been used to model the binding site as it can bind agonists, toxins and competitive antagonists (Karlin, 2002; Sixma and Smit, 2003; Ulens *et al.,* 2006).

Each AChBP subunit (Brejc *et al.,* 2001) consists of 10 β-strands, with an outer sheet formed by four strands (β4, β7, β9, and β10) and an inner sheet located towards the central formed of a six strands (β1, β2, β3, β5, β6, and β8). This structure is conserved in other receptors including α1 muscle ACh subunit (Dellisanti *et al.,* 2007), ELIC (Hilf and Dutzler, 2008), GLIC (Hilf and Dutzler, 2009) and GluCl (the most relevant for GlyR, Hibbs and Gouaux, 2011).

The ligand binding sites for homomeric and heteromeric GlyRs were investigated using electrophysiological and molecular modelling techniques (Grudzinska *et al.,* 2005). They suggested that the α-amino and α-carboxylate groups of bound glycine interact with two oppositely charged residues located on the principal and the complementary sides of all the GlyR subunits. These residues are R65 and E157 in loop D and B of the α1 subunit and the homologous residues R86 and E180 in the β subunit (Grudzinska *et al.,* 2005).

All the Cys-loop receptors contain aromatic residues that are believed to form a cation-π interaction with the ligand. The cation-π interaction in Cys-loop receptors can be provided by different aromatic side chains (Trp, Phe, or Tyr) (Beene *et al*., 2002; Lummis *et al*., 2005; Pless *et al*., 2008; Xiu *et al*., 2009; Hibbs and Gouaux, 2011). The aromatic box is formed by these aromatic side chains that are located in the three loops on the principal subunit.

Similar to all Cys-loop receptors the glycine binding site is lined with aromatic residues. There is a strong cation-π interaction of α1 F159 GlyR with glycine. This was proved by

incorporating a range of fluorinated phenylalanine derivatives by using unnatural amino acid mutagenesis (Pless *et al.,* 2008). Glycine and the partial agonists β-alanine and taurine compete for the same binding site (Schmieden *et al*., 1992; Schmieden and Betz, 1995). Weaker cation-π interactions were found with the lower efficacy agonist β-alanine and taurine than for glycine (Pless *et al.,* 2011).

A homology model of homomeric hGlyR based on GluCl from *Caenorhabditis elegans* was used to investigate the binding site for glycine and strychnine (Yu *et al.,* 2014). The model suggested the presence of a water molecule in the binding site and added to the ligand receptor interactions a glycine interaction with S129 residue in loop E. Also, the model suggested that strychnine binding induces a conformational state different from the glycine-bound or apo states, within both the ligand binding domain and the TM domain.

## 1.10 Channel activation: from the binding site to the TM domain

The picture that we have of activation is inferred by comparison of the different structures.
The most marked movement for agonist binding involves C-loop that is made up of β strands 9 and 10 and therefore connected to pre-TM1. The inward movement of the C-loop traps the agonist inside the pocket (Celie *et al*., 2004; Gao *et al*., 2005; Hansen *et al*., 2005). In the absence of agonist the C-loop is uncapped (Unwin, 2005) and it moves outwards in the presence of antagonist (Bourne *et al.,* 2005; Hansen *et al*., 2005). Similar evidence loop C changing position is also suggested by GluCl structure (Hibbs and Gouaux 2011).

The interface between the EC domain and TM domain is formed by several loops and the pre TM1 region between β10 and TM1. Thus the bottom of the ECD comprises loop 2 (between β1 and β2), the Cys-loop (loop 7), and loop 9 (between β8 and β9) (Grosman *et al*., 2000a; Rovira *et al*., 1999; Lee and Sine, 2005). A progressive isomerization begins from the neurotransmitter site high in the ECD spreading to the EC/TM domains interface and then to the TM domains.

The opening of the pore is not completely understood. It is thought to involve tilting of the TM2 helices outwards as suggested by functional mapping of the TM2 (Grosman *et al.,* 2000; Cymes and Grosman, 2005; Purohit *et al.,* 2007; Calimet *et al.,* 2013; Sauguet *et al.,* 2014a). During channel activation TM2 moves first to open the channel resulting in increasing the

channel diameter and the retraction of the TM2 towards TM1 and TM3 (Miyazawa *et al.*, 2003; Unwin, 2005).

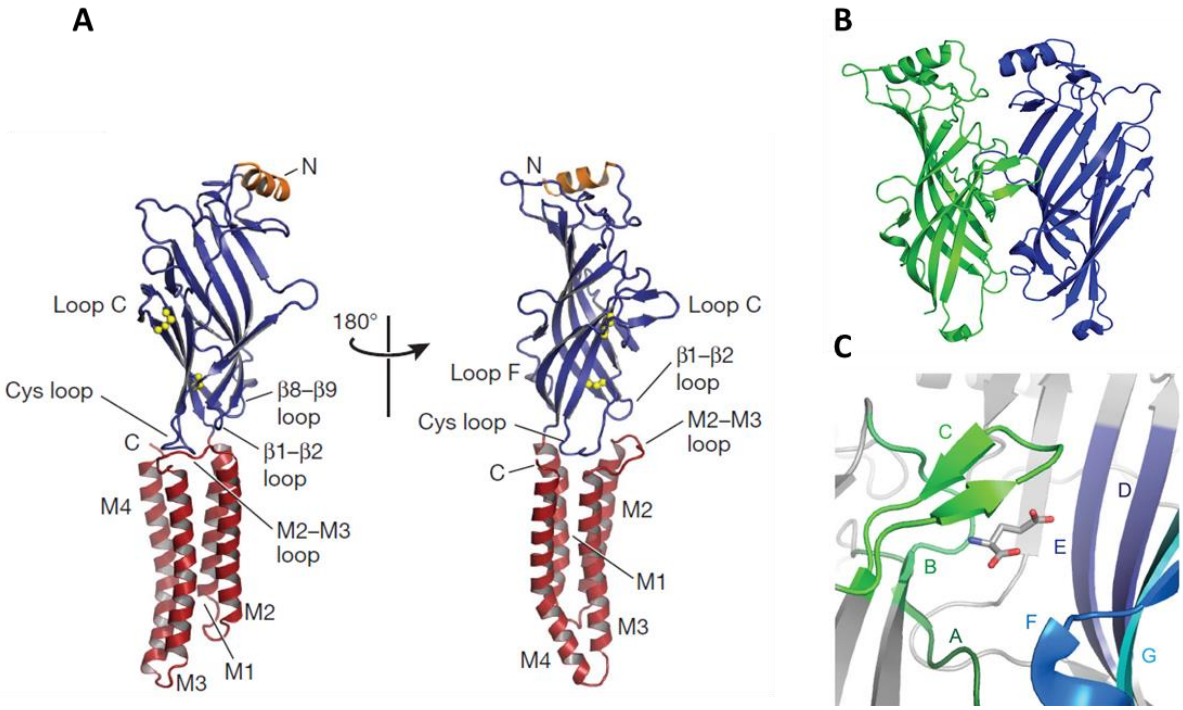


**Figure 1.5 The extracellular and transmembrane domains**

A) A single GluCl subunit viewed from two different angles (adapted from Hibbs and Gouaux, 2011). The Cys-loop and the loop C disulphide bonds are shown as spheres. B) Interface of ECD of 2 adjacent subunits. The outer β sheet of the green subunit form the principal side and the inner β sheet of the blue subunit form the complementary. C) Agonist binding site showing the principal loops (A, B, C) and the complementary strands (D,E,F,G). Images are based on the glutamate-bound *Caenorhabditis elegans* α GluCl crystal structure (Hibbs and Gouaux,2011), B and C adapted from Lynagh and Pless (2014).


**Figure 1.6 Loop alignments of different Cys-loop receptors and related proteins**

Sequence alignment based on GluCl receptor showing principal and complementary sequences adapted from Hibbs and Gouaux, (2011). GluCl α (559559), *C. elegans* GluCl β (559561), human glycine α1 (119372310), human $GABA_A$ ρ1 (194097386), human $GABA_A$ α1 (38327554), human α7 nAChR (496607), *L. stagnalis* AChBP (14285341), *A. californica* AChBP (325296909), four ACh subunits from *T. marmorata* (α, β, δ, γ: 213216, 39653645, 39653649, 39653647), human 5-$HT3_A$ (37514834), GLIC (37523766) and ELIC receptor (169791754). Red lines represent loops that form the neurotransmitter site. Grey highlighted residues are involved in disulfide bonds and yellow highlighted residues are highly conserved residues. Grey lines identify the Cys-loop.

### 1.10.1 The transmembrane domain structure

It has been known for a long time that TM2 from each subunit lines the channel pore, largely because of the effects of mutating residues within conductance and gating (Galzi *et al.,* 1992).

Charged amino-acids are located at the beginning and the end of TM1, TM3, and TM4 (Miyazawa *et al.,* 2003). TM1 is in contact with the lipid environment and with TM2. It might participate in the signal transduction from the neurotransmitter binding site in the ECD to the TM2 as several mutations in the TM1 domain produced non-functional receptors or changed $EC_{50}$ (Akabas and Karlin, 1995; Dang *et al.,* 2000; Unwin *et al.,* 2002; Miyazawa *et al.,* 2003; Lobo *et al.,* 2004; Cymes and Grosman, 2008). The lower end of the TM1 and the TM1-TM2 linker are likely to be exposed to the pore (Filippova *et al.,* 2004).

The channel gate is located in the middle of the TM2 domain (Figure 1.7; Miyazawa *et al.,* 2003, Unwin, 2005). A hydrophobic girdle is formed as a result of the interaction between the hydrophobic side chains of the 9', 10', 13', 14' residues of TM2 with the adjacent residues (e.g. 13' with 14') (Miyazawa *et al.,* 2003). It was documented that disturbance of the hydrophobic girdle by substitution of a 9' leucine residue with a hydrophilic residue (serine, S or threonine, T) tends to produce spontaneous activity as demonstrated for neuronal nicotinic receptor (Revah *et al.,* 1991) and for the muscle nicotinic receptor (Labarca *et al.,* 1995) and for the glycine receptor (Burzomato *et al.,* 2003).

The narrowest part of the open channel is at the intracellular side (-2'). Based on the NMR structure of the TM of the human glycine α1 receptor, the TM2 is formed by residues from -2' to 18' (Mowrey *et al.,* 2013). The selectivity filter was proposed to be provided in the -2 to 2 region (Imoto *et al*., 1988; Corringer *et al*., 1999; Keramidas *et al*., 2004; Hibbs and Gouaux, 2011). The estimated diameter for $GABA_A$ and GlyR pore is 5.2-6.2 Å (Bormann *et al.,* 1987; Mowrey *et al.,* 2013) and it is bigger than the estimated value for GluCl 4.6 Å (Hibbs and Gouaux, 2011). TM3 and TM4 shield TM2 from the lipid bilayer.

Another part that has a role in the conformational change is the extracellular TM2-TM3 loop. It is part of the interface between the ECD and the TMD (Lynch *et al.,* 1997). Mutations in this region disturb channel function (Rajendra *et al.,* 1994; Lape *et al.,* 2012) and cause hyperekplexia in man (Shiang *et al.,* 1993; Elmslie *et al.,* 1996).

### 1.10.2 Intracellular domain

Five amino acids form the TM1-TM2 loop of the glycine α1 receptor. This loop might be involved in the binding gating signal transduction (Lynch *et al*., 1997; Czajkowski, 2005). The intracellular domain between TM1 and TM2 is involved in zinc potentiation of GlyRs (Lynch *et al*., 1998) and in desensitisation (Saul *et al*., 1999). The main intracellular domain (ICD) is formed by the TM3-TM4 loop and is poorly conserved in sequence and length across the Cys-loop receptors (Le Novere and Changeux, 1999, 2005). Homologous receptors in bacteria have a very short heptapeptide in this position (Bocquet *et al*., 2007; Hilf and Dutzler, 2008). The ICD is involved in intracellular modulation by internal molecules and is thought to interact with kinases and phosphatases (Lynch, 2004). Such interactions can modulate receptor assembly and trafficking (Meyer *et al*., 1995; Kneussel and Betz, 2000; Kneussel and Loebrich, 2007; Melzer *et al*., 2010).

The gephyrin binding domain is located in the TM3-TM4 loop of the β subunit. These 18 amino-acid residues are required for interaction with gephyrin favouring receptor clustering and anchoring to synapses (Meyer *et al.,* 1995; Kneussel and Betz, 2000; Kneussel and Loebrich, 2007).

Unwin's data (Unwin, 2005) show that the intracellular domain is in part composed of an α-helical segment within the intracellular TM3–TM4 loop (called the membrane-associated helix, MA) which precedes TM4. The MA helices from each subunit form a pentagonal cone structure with similar size fenestrations between adjacent subunits. These openings allow ions to pass into and out of the intracellular vestibule. The maximum width of the window is suitable for sodium, or potassium ion passage in cation-selective LGICs and $Cl^-$ in anion selective channels. These fenestrations prevent passage of larger ions and provide the only pathway for the passage of ions to and from the cytoplasm. The role of the intracellular domain in conductance will be discussed below.

### 1.10.3 The pore: selectivity and conductance

It is has long been thought that in Cys loop receptors rings of charged residues in the channel pore are the main determinants of the ionic selectivity and conductance, as was shown by early work on the AChRs (Imoto *et al.,* 1988; Imoto, 1993; Konno *et al.,* 1991, reviewed in Peters *et al.,* 2010).

The -2/2 region of the channel pore has been proposed to act as charge selectivity filter in the Cys-loop receptors Figure 1.7 (Imoto *et al.,* 1988; Corringer *et al.,* 1999; Keramidas *et al.,* 2004; Hibbs and Gouaux, 2011). For anion permeation the key residues are -1' Ala and -2' Pro and for cations -1' Glu (Thompson *et al.,* 2010; Sunesen *et al.,* 2006; Hibbs and Gouaux, 2011). Thus, a cation-selective receptor such as α7 neuronal can be converted into an anion-selective receptor by mutating particular residues and *vice-versa* (Galzi *et al.,* 1992). Conversion of ion selectivity can be achieved for α homomeric GlyRs by the mutation A251E (-1') GlyR (Keramidas *et al.,* 2002).

The M1-M2 loop, which is composed of five amino acids, might have a role in ion selectivity as indicated by substituted cysteine accessibility data (Keramidas *et al*., 2000; Filippova *et al*., 2004).

TM2 domain is the major determinant of ion selectivity and conductance in the Cys-loop receptors (Cohen *et al.,* 1992a, b; Imoto *et al.,* 1991; Labarca *et al.,* 1995).

Single channel conductance of the nAChR of *Torpedo californica* is determined by three rings of negatively charged residues. These rings include the extracellular (20'), the intermediate (-1') and cytoplasmic ring (-4') (Imoto *et al.,* 1988; Langosch *et al.,* 1994; Wang *et al.,* 1999; Moorhouse *et al.,* 2002). Ion conduction and selectivity for the anion selective $GABA_A$ and GlyRs is determined by a ring of positive charge at the extracellular end of the channel (19') and at the intermediate ring (0') (Keramidas *et al.,* 2004). There are additional key residues for anion/cation selective permeability. For anion permeation these are -1' Ala and -2' Pro and for cations -1' Glu (Thompson *et al*., 2010; Sunesen *et al*., 2006; Hibbs and Gouaux, 2011) (Figure 1.7).

The ionic permeability can be switched from cationic to anionic for nAChRs and 5-$HT_3$Rs by mutating residues that are the same between nAChRs and 5-$HT_3$Rs but different from α1 GlyR and α1 $GABA_A$. This includes alteration of three residues: the point mutations V13'T and E-1'A, and proline residue insertion between G-2' and E-1' (Corringer *et al.,* 1999; Gunthorpe and Lummis 2001). The permeability of α1 GlyR can be made cationic by the analogous reverse triple mutations A-1E', T13'V, P-2'Δ (Keramidas *et al.,* 2000, 2002).

All the Cys-loop receptors have different sequence and length of the large intracellular M3-M4 loops. Prokaryotic members of the nicotinic superfamily have a very short M3-M4

domain, but in all the others the TM3-TM4 loop exceeds 70 residues, a length that was found vital for their portal-associated function (Baptista-Hon *et al.*, 2013).

Recently, regions other than the TM2 domain were found to have a role in ion conductance including the TM3-TM4 and the extracellular domain (Peters *et al.*, 2010). The TM3-TM4 can have an effect on conductance because of its shape. As shown by Unwin's data the narrow diameter fenestrations or portals between adjacent subunits (8Å in the closed *Torpedo nicotinic* ACh receptor) prevent large ion passage and facilitate cation ion transport. By this way the intracellular fenestrations contribute to the conductance is most affected of the channel (Unwin, 2005).
This was confirmed by mutations in this region (Kelley *et al.*, 2003; Peters *et al.*, 2004; Hales *et al.*, 2006; Carland *et al.*, 2009). A series of 5-HT3A/3B chimeras and 5-$HT_{3A}$ receptor mutagenesis work suggested that residues within the MA-stretch contribute to cation conductance. The cytoplasmic loop of 5-$HT_3$ receptors is partly responsible for the difference in the conductance of homomeric 5-$HT_3$A vs heteromeric 5-$HT_3$AB channels. For instance mutations of three conserved positively charged arginine residues within the MA-stretch of the human 5-HT3A subunit (R432, R436 and R440) caused a ~28 fold increase in single-channel conductance for the triple mutant (Kelley *et al.*, 2003; Peters *et al*., 2004 and 2005). This cytoplasmic region, within the MA-stretch, also contributes to regulating the single-channel conductance of α1 homomeric glycine receptors, indicating that the portals for ions accessing the channel from the cytoplasm have a similar role in cationic and anionic pLGICs (Carland *et al.*, 2009). This was suggested based on the effect of charged residues within MA stretch on channel conductance of homomeric GlyR (Carland *et al.*, 2009). Mutation of eight basic residues each to a negatively charged glutamate produced a non-functional receptor. The major influence on conductance was observed at R377, K378, K385, and K386 residues (Carland *et al.*, 2009).

ECD can also affect the conductance. A negatively charged residue in loop 5 of the ECD of the cation-permeable α1*Torpedo* nACh nicotinic receptor was found to affect ion conductance (Hansen *et al.*, 2008). Similarly, the conductance of glycine receptor is influenced by a positively charged residue (Moroni *et al.*, 2011a) in the same domain. The conductance of glycine α1 homomeric and α1β heteromeric receptor is increased by positively charged Lys residues in loop 5, a position homologous to α1 *Torpedo* Asp 97 (Moroni *et al.*, 2011a). Reversing the charge into negative Glu in the α subunit (K104E)

decreased the single-channel conductance. The effect on conductance is dependent on the subunit, as mutating β subunit (K127E) produced no effect (Moroni *et al.*, 2011a).

The type of the residues that are along the ion flow pathway from the extracellular domain to the intracellular domain passing within the TM2 pore affect the single-channel conductance. However, the main determinant of conductance of glycine receptor is the TM2 domain.

Heteromeric GlyR has lower single channel conductance and different channel kinetic than the homomeric receptor (Lynch, 2009). For GlyRs single-channel experiments have shown that heteromeric α1β GlyRs have approximately half the single-channel conductance of homomeric α1 receptors with channel amplitude of 4.7 ± 0.1 and 3.1 ±0.1 pA for homomeric and heteromeric channels at +100 mV holding potential, respectively (Burzomato *et al.*, 2003; Beato *et al.*, 2004). This difference in single-channel conductance is determined by residues within and close to the TM2 domain and this was confirmed by co-expression of α1 subunit with mutant β subunits. Mutating TM2 residues in the β subunit to corresponding residues of the α1 subunit, such as β E290Q (14 ') and β E297S (21') produced a range of conductances similar to α1 subunit conductance.

The only non-conserved residue within the TM2 domain of α1, α2, and α3 subunits of GlyR is 2' gly in α1 and ala in α2, and α3 subunit (Figure 1.7). So in order to determine the main state conductance difference of α1 vs α2/α3 homomeric GlyRs, G221 was mutated from glycine into alanine. Mutating residue G221 in this domain was shown to modify the single-channel conductance of the α1 homomeric GlyRs. The main state conductance of G221A α1 GlyR was similar to α2/α3 conductance. This indicates that the TM2 G221 residue determines the main conductance in homomeric GlyRs (Bormann *et al.*, 1993).

Depending on the recording configuration a number of different conductance levels can be observed in a patch. While recordings in the cell-attached configuration show practically only one conductance level, regardless of the receptor subtype (Beato *et al.*, 2004; Burzomato *et al.*, 2004; Beato and Sivilotti, 2007), GlyRs are found to open to different conductance levels in recordings performed using excised patches. This difference in conductance levels was shown for both recombinant (Bormann *et al.*, 1993; Beato *et al.*, 2002) and native GlyRs (Bormann *et al.*, 1987; Takahashi and Momiyama, 1991; Twyman and MacDonald, 1991).

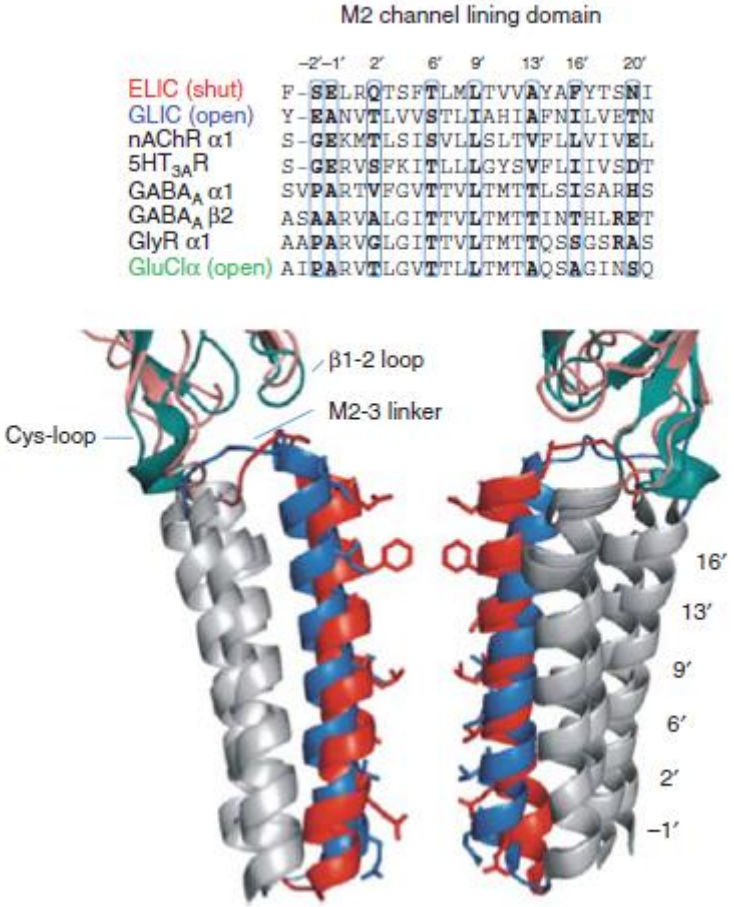


**Figure 1.7 TM2 of several Cys-loop receptors.**

Alignment of different Cys-loop receptor TM2 domains. The boxed parts indicate residues lining the channel lumen. The structural model shows the TM2 of open GLIC (green and blue) and closed ELIC (pink and red). Adapted from Smart and Paoletti (2012).

## 1.11A quantitative mechanism for the activation of GlyR

In order to activate ligand-gated ion channels must bind agonist/neurotransmitter and go through conformational changes that open the pore. These steps can be characterised quantitatively by defining activation mechanisms. Del Castillo and Katz postulated the first mechanism on frog endplate nicotinic receptor in 1957 (Scheme 1.1, R stands for receptor and A for ligand; Del Castillo and Katz, 1957). Their simple mechanism provided the first basic framework for interpreting differences in agonist efficacy. In this mechanism, the channel can exist in three different states, closed R, or AR (e.g. unliganded and liganded), or open AR*. Resting (R) closed-channel state occurs in the absence of the agonist and the other state (AR) occurs once the agonist binds but has not activated the channel. The AR* state is open. The transition rate constants names are shown near the arrows. In the del Castillo-Katz mechanism, the sensitivity of the receptor for the agonist is determined by the equilibrium dissociation constant for binding $K_A$ (ratio between k-1/k+1) and by the equilibrium constant for conformational change, *E* efficacy (ratio between β and α, β is opening, α is closing), which varies for different agonists and different receptors (Colquhoun, 1998). The $EC_{50}$ expression from del Castillo-Katz is shown in equation 2. For muscle nicotinic and glycine receptors two or three agonists must bind to open the channel with maximum efficacy reaching an opening probability of more than 95%. The expression for maximum $P_{open}$ in del Castillo-Katz mechanism is illustrated in Equation 3.

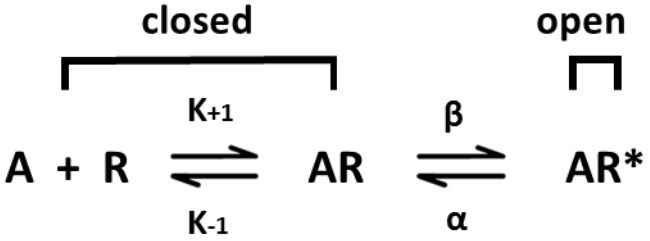


Equation 1

$$EC_{50} = \frac{K_A}{1 + E}$$

Equation 2

$$\text{Maximum } P_{open} = \frac{E}{E+1}$$ Equation 3

The del Castillo-Katz mechanism is very simple and it is now clear that its features are not sufficient fully to describe the function of Cys-loop channels. Model fitting techniques allowed detection of intermediate states following agonist binding and before channel opening. The channel is still closed in these states but its affinity has increased from the resting state (Burzomato *et al.,* 2004, Mukhtasimova *et al.,* 2009, Jadey and Auerbach, 2012). Burzomato *et al.,* 2004 postulated the flip mechanism in order to interpret the single-channel activity of heteromeric α1β GlyR (Scheme 1). In this scheme, an additional shut state was postulated before channel opening. This state is thought to represent an intermediate when the agonist is bound to the ECD, which has changed its conformational state so that the affinity for the agonist has increased, but the conformational changes have not yet reached the channel gate. The flip mechanism was postulated to explain the activation mechanism of several glycine receptor isoforms including glycine receptor α1 homomeric and heteromeric (Burzomato *et al*., 2004), α2 (Krashia *et al*., 2011), α3 (Marabelli *et al*., 2013). It was also used for describing the action of partial agonists on both glycine and muscle ACh nicotinic receptors (Lape *et al*., 2008).

Analysis with these mechanisms has proven useful to understand why a partial agonist is less effective than the full agonist. In the del Castillo-Katz mechanism, it is simply because partial agonists have small open-shut equilibrium constant *E*. In the flip model, the overall agonist efficacy depends on two parameters, the equilibrium constant for flipping (F) and the equilibrium constant for the open-shut reaction (E). The effective efficacy ($E_{eff}$) for the fully liganded receptor is

$$E_{eff} = \frac{EF}{F+1}$$ Equation 4

So the partial agonist could be partial either because it is poor at producing the initial change (flipping) (low *F*), or because it is poor at opening the channel (low *E*) or both. Analysis of the effects of glycine and taurine on the heteromeric GlyR by Lape *et al.* (2008) showed that the gating equilibrium constant (*E*) is similar for glycine (full agonist) and taurine (partial

agonist; about 50% maximum open probability). The difference is therefore in the flipping equilibrium constant (*F*). Similar results were obtained for the effects of ACh, TMA and choline on the muscle nicotinic receptor (Lape *et al.*, 2008; Lape *et al.*, 2009).

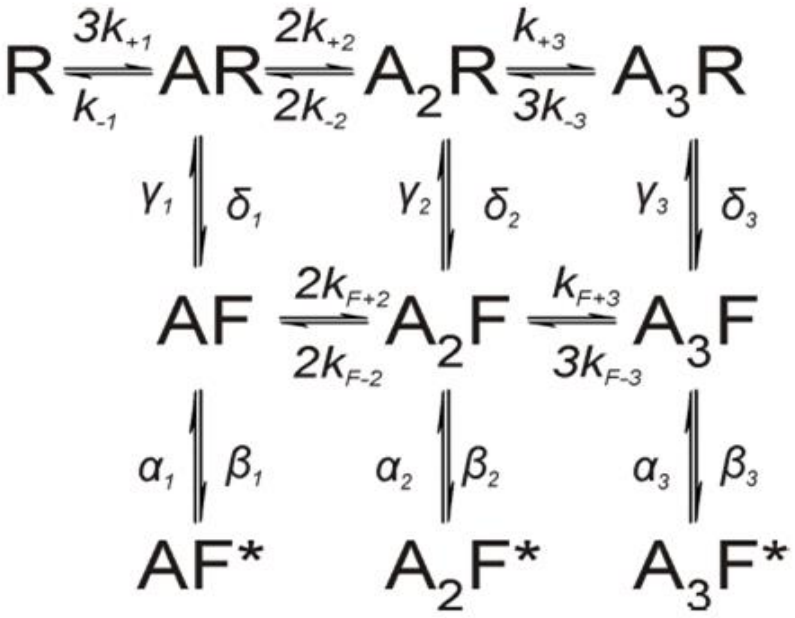


Scheme 1

**Scheme 1: "Flip" mechanism**. The single-channel activity of several glycine receptor isoforms are describes well by the Flip mechanism (Burzomato *et al.*, 2004; Lape *et al.*, 2008; Krashia *et al.*, 2011; Marabelli *et al.*, 2013; Lape *et al.*, 2008). The scheme postulates the existence of additional shut states ('flipped') in addition to the open and closed states. Flip represents a conformational change that precede channel opening (Burzomato *et al*., 2004). The scheme has 3 binding sites. An agonist molecule is presented as letter A. The number of agonist molecules that are bound to the receptor are indicated by letter A subscript. The resting closed-channel state is presented as R. The letter F denotes flip conformation in which the channel is closed but with higher binding affinity than in the rest state. F* denote open-channel state of the receptor.

## 1.12 Statement of purpose:

My work aims to expand our knowledge of the structure function relation of the GlyR. The data presented includes the study of several human hyperekplexia mutations. Whole-cell recordings and single-channel recordings were used with different agonists to understand the function of the hyperekplexia mutated residues. The knowledge obtained here can be expanded to other Cys-loop family members.

### Aim 1

Initial screening of several known human hyperekplexia mutations were conducted on both homomeric and heteromeric GlyRs by whole-cell patch-clamp to obtain macroscopic concentration-response curves for glycine. The purpose of this was to establish which of the mutations could be further studied by single channel recording. Mutants with low levels of expression or extreme loss of function, could not be further characterised. Where possible I obtained single channel measurements of the maximum open probability in the presence of saturating glycine, in order to establish which mutants impaired channel gating.

### Aim 2

When a mutation impairs gating, it is possible that allosteric modulators that enhance gating can offset the effect of the mutation and rescue the reduction of the GlyR gating function. The general anaesthetic, propofol, was selected as a modulator. Indeed we found that the reduction in glycine gating can be improved in α1(S267N)β heteromeric GlyR mutation by propofol.

### Aim 3

From an homology model based on the structure of GluCl, two residues at the back of the binding site, a negatively charged glutamate at 103 (α1 E103) position and an arginine at 131 (α1 R131) position were postulated to form a salt bridge. The effect on agonist sensitivity of of mutating these residues singly, or together, was assessed.

# Chapter 2: Methods

## 2.1 Plasmid cDNA

Human GlyR subunits α1 (UniProt accession number P23415) and β (UniProt Accession number P48167) were contained as cDNA in the vector pcDNA3.1 (Invitrogen, The Netherlands) and were kindly provided by Heinrich Betz, Frankfurt. The vector has a total size of 5.4 kb and contains the following elements (Figure 2.1, 2.2): human cytomegalovirus (CMV) promoter, T7 promoter, multiple cloning sites, bovine growth hormone (BGH) polyadenylation signal sequence, a neomycin and ampicillin resistance genes.

For the identification of transfected cells the enhanced Green Fluorescent Protein (eGFP) was expressed with the plasmid peGFP (Clontech, UK).

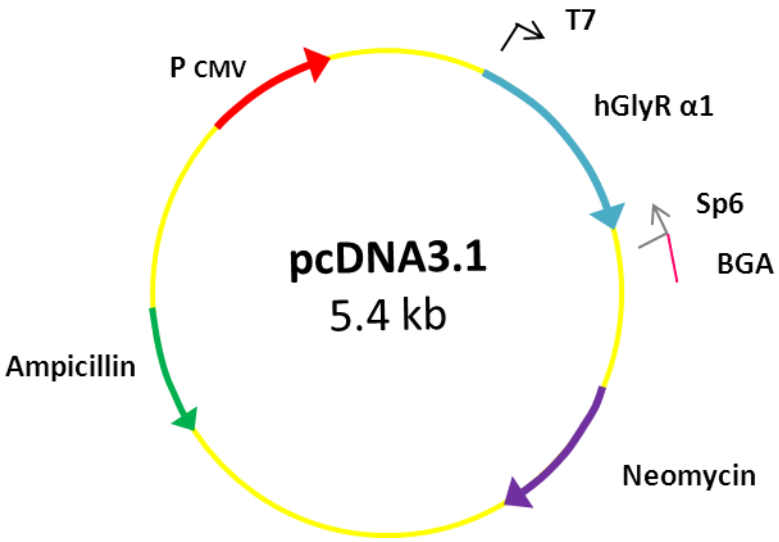


**Figure 2.1 The human glycine receptor α1 (hGlyR α1)/pcDNA3 plasmid.**
Cytomegalovirus (CMV) promotes high-level expression of the α1 receptor in the expression system (HEK293 cells). There is also the T7 promoter which is followed by multiple cloning sites in the forward, or reverse orientation, that permit insertion of the selected gene. The prokaryotic promoter Sp6 is also indicated. Ampicillin and neomycin coding sequence resistance genes are shown.

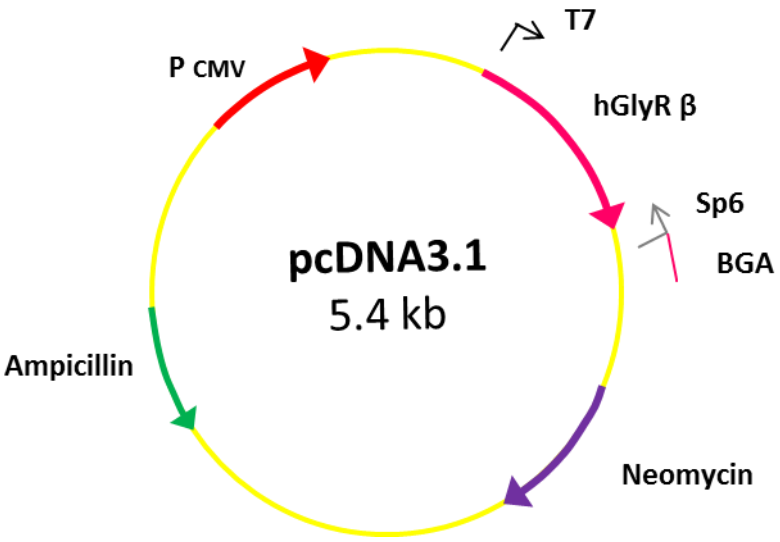


**Figure 2.2 The human glycine receptor β (hGlyR β)/pcDNA3 plasmid.**
Cytomegalovirus (CMV) promotes high-level expression of the β subunit in the expression system (HEK293 cells). There is also the T7 promoter which is followed by multiple cloning sites in the forward, or reverse, orientation that permit insertion of the selected gene. The prokaryotic promoter Sp6 is also indicated. Ampicillin and neomycin coding sequence resistance genes are shown.

## 2.2 Mutagenesis

Single point mutations were introduced into the wild-type human GlyR α1 subunit using the site-directed mutagenesis protocol (QuikChange™ Site-Directed Mutagenesis Kit, Stratagene). Vector with insert of interest and two oligonucleotides primers containing the desired mutation (see primer design) were used. The PCR reaction was divided into two steps. In first step the forward and the reverse primers were in separated PCR tubes. After five cycles of PCR run, the two reaction mixtures were combined and the PCR was continued. The PCR reaction included the following with the final concentration distilled water ($dH_2O$), 10x PCR buffer, deoxynucleoside triphosphates (dNTP; 200 µM each, DNA template (α1 GlyR vector at 100 ng), forward and reverse primers (each 0.5 µM), and *PfuTurbo*® DNA polymerase (1.25 U). The PCR amplification reaction was repeated for 30 cycles. For double mutations, one mutation was inserted first and then this was used as template for the double mutant. Temperature cycling was done using a thermocycler

(PcrExpress HYBAID). The DNA template denatured at 95°C followed by annealing of the oligonucleotide primers containing the desired mutation at 55°C. *PfuTurbo*® DNA polymerase (Stratagene) extended the primers at 68°C. This produced a mutated plasmid with staggered nicks. Parental wild-type plasmid was removed by digestion with *Dpn* I (New England Biolabs) as it is specific for methylated and hemimethylated DNA. The nicked circular vector DNA is transformed to *E.coli* where the nicks were repaired and the plasmid was amplified.

## 2.3 Primer design

Primers for site-directed mutagenesis were designed with the desired mutation in the middle and each primer was complementary to opposite strands of the vector. They were 25- 45 bases in sequence length and their melting temperature ($T_m$) was greater than, or equal to, 78ºC. Also, the primers ended with at least one C or G bases and they had a minimal GC content of 40%. The PCR primers were designed by using PrimerX web-based program: http://bioinformatics.org/primerx/. Primers were synthesized by Eurofins (Ebersberg, Germany). A list of used primers in this study is shown in Table 2.1.

**Table 2.1 Sets of primers used in this study**

| α1 GlyR Mutation | Forward primer | Reverse primer |
|---|---|---|
| R72H | GCAGCAATGGAACGACCCCC ACCTGGCCTATAATGAATACC | GGTATTCATTATAGGCCAGGTGGG GGTCGTTCCATTGCTGC |
| E103K | CCTGTTCTTTGCCAACAAGAA GGGGGCCCACTTCC | GGAAGTGGGCCCCCTTCTTGTTGGC AAAGAACAGG |
| E103R | CTGTTCTTTGCCAACCGGAAG GGGGCCCACTTC | GAAGTGGGCCCCCTTCCG GTT GGCAAAGAACAG |
| E103A | CTGTTCTTTGCCAACGCGAAG GGG GCCCACTTC | GAAGTGGGCCCCCTTCGCGTTGGC AAAGAACAG |
| R131E | GTCCTCTACAGCATCGAA ATC ACCCTGACACTG | CAGTGTCAGGGTGATTTCGAT GCT GTAGAGGAC |
| S231N | CAGATGTATATTCCCAACCTG CTCATTGTCATC | GATGACAATGAGCAGGTTGGGAAT ATACATCTG |

| | | |
|---|---|---|
| Q266H | GCTCACCATGACCACCCACAG CTCCGGCTCTCGAG | CTCGAGAGCCGGAGCTGTGGGTGG TCATGGTGAGC |
| S267N | GCTCACCATGACCACCCAGAA CTCCGGCTCTCGAGCATCTC | GAGATGCTCGAGAGCCGGAGTTCT GGGTGGTCATGGTGAGC |
| Y279C | CTGCCCAAGGTGTCCTGTGTG AAAGCCATTGAC | GTCAATGGCTTTCACACAGGACAC CTTGGGCAG |

## 2.4 Transformation of competent cells

Luria Broth (LB) agar plates were used for overnight growth of the vector with the desired mutation. They were prepared by first dissolving 10 g of LB broth base and 10 g of Agar (Invitrogen, UK) in distilled water to a final volume of one liter. The solution was then autoclaved for 20 minutes at 121 °C. Once it cooled down to a temperature that permits to hold the container by hand, an antibiotic (50 μg/ml kanamycin for peGFP plasmids or 100 μg/ml ampicillin for pcDNA3.1 plasmids) was added and the solution was poured into 100 x 15 mm petri dishes with lid (Nunclon™ Delta Surface) (~20). Plates were allowed to stand to cool down at room temperature and then stored in upside down position at 4ºC until use.

Competent *E.coli* cells were thawed on ice for 15 minutes after being stored at −80ºC. 60 μl of the competent cells were transferred into a 1.5 ml Eppendorf tube and plasmid DNA (1 ng in case of retransformation of a plasmid or about 10 μl of PCR product after mutagenesis PCR) was added and incubated on ice for 30 minutes. After heat shock (45 seconds at 42ºC), the cells were immediately transferred into ice and kept on ice for 2 minutes. Then, 900 μl of super optimal broth (S.O.C, Invitrogen) medium was added and the cells were grown shaking for one hour (300 r.p.m) at 37ºC in a thermomixer (Eppendorf, UK). Meanwhile, plates were warmed in the incubator at 37˚C. On each plate 100 μl of transformant cells were plated and incubated in the upside down position overnight at 37˚C.

The next day, one to three colonies per plate were selected, touched with Eppendorf pipette tip and allowed to grow overnight at 37ºC shaking at 220 rpm in a tube containing 2 ml (or 250 ml in case of large scale preparation) of LB medium with 100 μg/ml ampicillin. After that, purification of high yields of plasmid DNA was done by using the Miniprep kits (QIAGEN Plasmid Mini Kit) according to their respective protocols. After checking DNA

purity and concentration, a sample was sent for sequencing of the full open frame (Wolfson Institute for Biomedical Research, London UK) to make sure that only the desired mutation was introduced. Then, if the mutagenesis had worked well, large scale preparation was carried out (QIAGEN Plasmid Maxi Kit).

## 2.5 Culture and transfection of HEK293 cells

### 2.5.1 Cell culture maintenance

Human embryonic kidney 293 cells (HEK293) (American Type Culture Collection (ATCC)) were grown at 37 °C in a humidified 95 % air/5 % $CO_2$ incubator in Dulbecco's Modified Eagle Medium (DMEM) supplemented with 10 % v/v heat-inactivated fetal bovine serum, 100 U/ml penicillin G, 100 μg/ml streptomycin sulfate and 2 mM L-glutamine (all from Invitrogen). Cells were passaged every 2-3 days, up to 20 times. For this, the cells were first washed with Hank's balanced salt solution (HBSS) and then exposed to 1 ml of 0.05% (w/v) trypsin (Invitrogen) for a brief time (30-40 s) at 37°C to detach them from the flask surface. Cells were then collected in 4 ml of fresh DMEM and centrifuged for 2-4 min (1000 rpm, 157g). The supernatant was discarded and the pellet was resuspended with 1 ml of DMEM by gentle pipetting. A small volume of the cell suspension, according to the required dilution, was added to a new flask containing 5 ml growth medium.

### 2.5.2 Transfection

Cells were grown on glass coverslips coated with poly-L-lysine (Sigma-Aldrich). Coating of the coverslips (13 mm) was accomplished by incubating the coverslips for ~30 minutes with 0.01% (w/v) poly-L-lysine (Sigma-Aldrich, UK), washing with distilled water and then autoclaving for 20 minutes at 121˚C. On the day of transfection, HEK293 cells were plated onto the coverslips and placed in 35 mm culture dishes with 2 ml growth medium. The plating density for whole cell experiments was lower than for single channel recording. Expression of the ion channel of interest was achieved by transfection of HEK293 cells using the $Ca^{2+}$ -phosphate co-precipitation method (Groot-Kormelink *et al.,* 2002). In order to promote heteromeric formation of GlyR α1β, the transfection was made at a plasmid DNA ratio of 40- fold excess of β to α (Burzomato *et al.,* 2003). Enhanced green fluorescent protein (eGFP) (Clontech, UK) was used as transfection marker. A mixture of plasmids was prepared for transfection containing pcDNA3.1 with α1 or β GlyR coding sequence, pEGFP-

c1 and empty pcDNA3.1 vector. The purpose of adding empty vector is to obtain optimal level of receptor expression in each cell, while maintaining a high proportion of transfected cells. A total of 3 μg complementary DNA (cDNA) (72 μl, DNA concentration 500 ng/ μl) was used per dish (Groot-Kormelink *et al.*, 2002). In order to achieve best results, the proportion of the different plasmids within this total DNA was adjusted empirically. Details of the plasmid ratio used for optimal expression are shown in Table 2.2. $CaCl_2$ solution (340 mM in sterile water) was added to the DNA mix at a 1: 5 volume ratio. Precipitation of calcium phosphate was induced by adding an equal volume of 2x HBSS (280 mM NaCl; 2.8 mM $Na_2HPO_4$; 50 mM HEPES, pH adjusted to 7.2 with NaOH) to the DNA/$CaCl_2$ solution. The DNA mix solution was added dropwise to the petri dishes containing plated coverslips. Cells were then incubated overnight at 37°C in an 95% /air 5% $CO_2$ atmosphere. They were then washed with HBSS (to remove the precipitate) and incubated in 2 ml of DMEM. Whole-cell, or single-channel, recordings were performed at least 24 hours after the transfection.

**Table 2.2 DNA mix used for patch clamp recordings.**

| Receptor | α1 cDNA (%) | β cDNA(%) | EGFP (%) | Empty Vector (%) |
|---|---|---|---|---|
| Wild-type α1 | 5 | - | 25 | 70 |
| Wild-type α1β | 2 | 80 | 18 | 0 |
| α1(R72H) | 55 - 82 | - | 18-25 | 0 - 20 |
| α1(R72H)β | 2 - 20 | 62 - 80 | 18 | 0 |
| α1(E103K) | 55 | - | 25 | 20 |
| α1(E103K)β | 2 | 80 | 0 | 18 |
| α1(E103A) | 55 | - | 25 | 20 |
| α1(E103R) | 55 | - | 25 | 20 |
| α1(E103R/R131E) | 55 | - | 25 | 20 |
| α1(S231N) | 55 | - | 25 | 20 |
| α1(S231N)β | 2 | 80 | 18 | 0 |
| α1(Q266H) | 55 | - | 25 | 20 |
| α1(Q266H)β | 2 | 80 | 18 | 0 |
| α1(S267N) | 55 | - | 25 | 20 |
| α1(S267N)β | 2 | 80 | 18 | 0 |
| α1(Y279C) | 55 - 82 | - | 18 - 25 | 0 - 20 |
| α1(Y279C)β | 2 | 80 | 18 | 0 |

## 2.6 Whole-cell patch-clamp recording and analysis

Whole-cell patch-clamp recordings were performed to obtain macroscopic current concentration-response curves for wild type or mutant GlyRs. For the recording a coverslip with transfected cells was placed in a chamber under an inverted microscope (Axiovert 135, Zeiss, Germany). The transfected cells were identified by their expression of eGFP; this was detected by exciting the fluorophor EXFO X-cite 120 light source, X-cite ®; light with excitation 457 – 487 nm and bandpass filter 472 nm. Cells were continuously superfused with extracellular solution containing (in mM): 20 Na-gluconate, 112.7 NaCl, 2 KCl, 2 $CaCl_2$, 1.2 $MgCl_2$, 10 HEPES, 10 tetraethylammonium-Cl (TEA-Cl), and 40 glucose. The pH of the solution was adjusted to 7.4 with NaOH; the osmolarity was ~320 mOsm/L. Borosilicate glass patch pipettes (with filament; outer diameter 1.5 mm; inner diameter 0.86 mm; Harvard Apparatus) were pulled on a Flaming-Brown type puller (Sutter Instrument, model P-97) and fire-polished with a microforge just before the recording to ensure gigaohm seal formation. Pipettes had a final resistance of 3-6 MΩ when filled with intracellular solution containing (in mM): 101.1 K gluconate, 11 EGTA, 1 $CaCl_2$, 1 $MgCl_2$, 10 HEPES, 20 TEA-Cl, 2 Mg ATP and 40 sucrose. Both the intracellular and extracellular solutions were filtered before use through 0.2 $\mu$m Whatman$^{TM}$ cellulose nitrate membrane filters (GE Healthcare life sciences, Buckinghamshire, UK). The liquid junction potential was calculated to be 9 mV (Calculated using pClamp10; Molecular Devices) and no correction was done for it. Recordings were made at 19-21 °C with an Axopatch 200B amplifier (MDS Analytical Technologies, Molecular Devices, Sunnyvale, CA, USA). After achieving a strong seal, gentle suction was applied to rupture the cell membrane under the tip of the pipette. In the whole-cell configuration cells were voltage clamped at −50 mV pipette holding potential. Both series resistance (Rs) and cell membrane capacitance, Cm, were measured and were 7.26 ± 0.36 MΩ and 22.85 ± 1.42 pF, respectively. Then, series resistance compensation was applied (60-90%). Throughout the recording the Rs was monitored and if its value changed over than 25% the recording was discarded.

The drugs were applied onto the cells *via* a custom built 'U-tube' application system (Figure 2.3; Krishtal and Pidoplichko, 1980). A thick-walled borosilicate glass capillary (Drummond) was used to prepare the U-tube. First, the capillary was bent to a U-shape while holding it over a flame. At the tip of the U-tube, a hole was made by applying positive pressure to the

inside of the tube, while heating the tip near a flame. The hole was polished using a Bunsen burner, to obtain smooth edges and a final diameter of 10-30 μm.

During the experiment (see Figure 2.3), one end of the 'U-tube' was connected *via* a plastic tube to a vacuum pump, and the other end was connected to a tube immersed into a solution containing the drug. The pump was continuously sucking the drug solution into a collection jar. The cells were superfused at a rate of 2 ml/min by an independent bath perfusion system.

In order to produce drug applications, the connection between the U-tube and the vacuum pump was interrupted, so that the drug solution was forced to flow into the bath. The 'U-tube' was positioned so that the flow from the hole was directed onto the patch-clamped cell. Before the start of each experiment, the rate of onset of the agonist application (exchange rate) was tested by applying 50% diluted extracellular solution. Applying the diluted solution to the open-tip pipette, changed the liquid junction potential at the pipette tip. The rate of these changes reflects the solution exchange rate at the recording pipette tip. The 'U-tube' was discarded if the 0-100% current onset was longer than 100 ms.

Agonist was applied to the patched cells at 30-60 second time intervals. At the beginning of the experiment, the stability of the agonist response was checked by applying as a standard a saturating agonist concentration (Table 2.3) until a stable response was established. Then, different concentrations of agonist were applied in random order in order to obtain a full concentration-response curve. The standard saturating agonist concentration was applied every third response to check the stability of the responses. Recordings were discarded if there was run up, or run down, greater than 30%.

Recordings were filtered using four-pole low-pass Bessel filter of the amplifier set at 5 kHz, digitized at sampling rate of 20 kHz (Digidata 1332A, Molecular devices) and acquired on a PC (Clampex 10.2, MDS Analytical technologies). Recorded current amplitudes were measured with Clampfit 10.2 software.

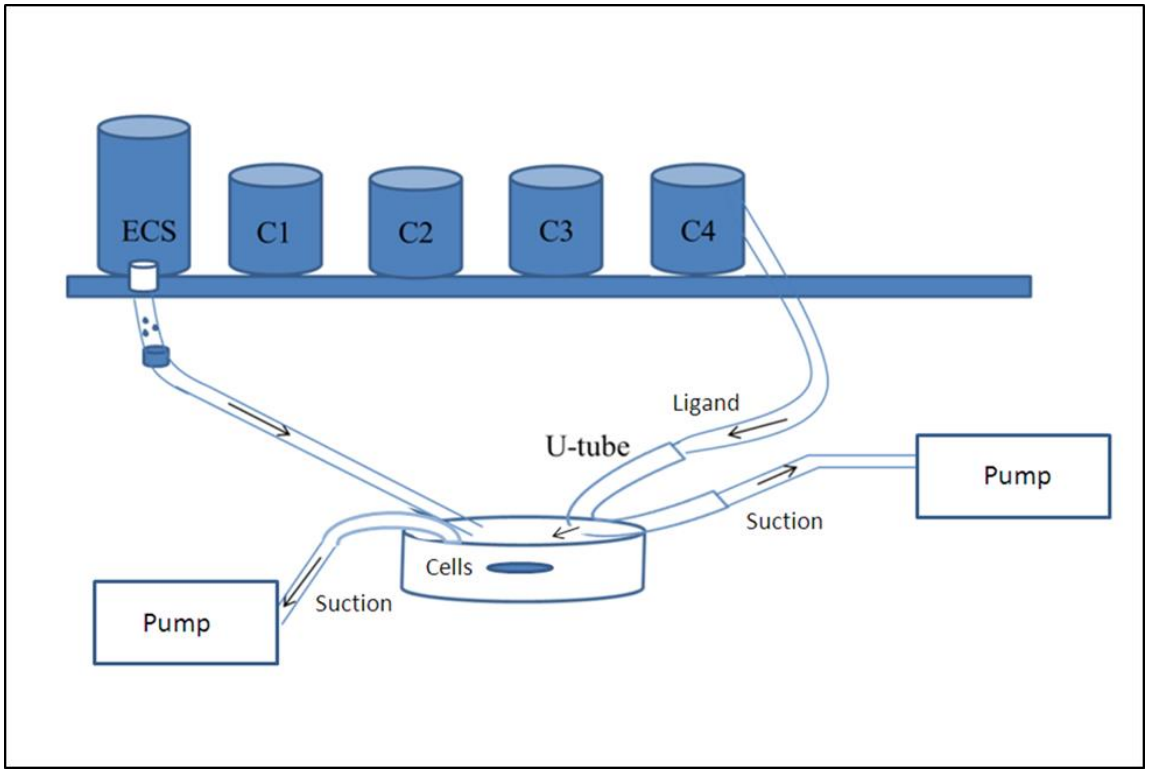


**Figure 2.3 Dual application system used for the whole-cell experiments.**
For whole-cell recordings, U-tube application of different concentrations of ligands to the cell was used (not to scale). The perfusion system consisted of three tubes. One provided continues flow of the extracellular solution to the recording chamber and other immediately sucked the solution to a waste compartment. The third was an U-tube application system and it was controlled manually. It provided continuous suction of the ligand solution but once the suction of the U-tube is switched off briefly (1-2 seconds), the solution will leak through a hole in the U-tube, applying the ligand solution onto the cells.

**Table 2.3 Standard saturating concentrations of agonists used for whole-cell experiments.**

| Receptor | Glycine (mM) | β-alanine (mM) | Sarcosine (mM) |
|---|---|---|---|
| Wild-type α1 | 10 | - | - |
| Wild-type α1β | 5, 10 | 50 | - |
| α1(R72H) | 20 | - | - |
| α1(R72H)β | 20, 100 | - | - |
| α1(E103K) | 20 | 100, 300 | 300 |
| α1(E103K)β | 50, 100 | 100, 200 | - |
| α1(E103R) | 100, 200 | - | 200 |
| α1(E103A) | 100 | - | 100 |
| α1(S231N) | 20, 50 | - | - |
| α1(S231N)β | 20, 50 | 100 | - |
| α1(Q266H) | 20, 50 | - | - |
| α1(Q266H)β | 20, 50 | - | - |
| α1(S267N) | 20, 50 | - | - |
| A1(S267N)β | 20, 50 | - | - |
| α1(E103R/R131E) | 50 | - | 300 |
| α1(Y279C) | 50 | - | - |
| A1(Y279C)β | 20 | - | - |

### 2.6.1 Concentration-response curves

For each cell, the first task in the analysis was to assess the stability of agonist responses during recording (run up/down). Cells were accepted for analysis only if there was minimal change in the amplitude of responses to a standard concentration of agonist. Typically, a saturating concentration of ligand was used as a standard. This was applied two, or three, times at the start of the recording and then every third application (see Figure 2.4). A typical concentration-response curve took approximate ten minutes length.. The cell was discarded if its response to the standard changed more than 30 % during 10 minutes from the stable standard during the experiment. Figure 2.4 shows a typical run of standard responses (in this example 20 mM glycine) in a cell expressing α1(S267N)β heteromeric GlyR.

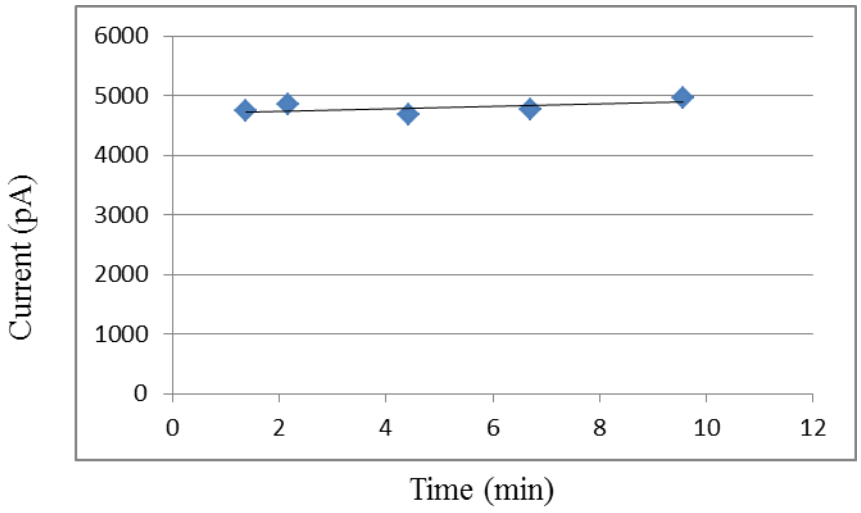


**Figure 2.4 Representative example of run up/down in the α1(S267N)β heteromeric GlyR mutation.**

The plot is showing almost stable standard glycine responses over nine minutes of recording. The dimonds are representing only the responses to the standard saturating agonist concentration (in this case 20 mM glycine). The standard was applied twice in the beginning then applied every third application of different concentrations of glycine (not shown).

After checking the stability of the current response, data from each cell was fitted separately with the Hill equation:

$$I = I_{max} \frac{[A]^{n_H}}{([A]^{n_H} + {EC_{50}}^{n_H})}$$

This is a high 'co-operativity' model. $I$ is the measured current, $I_{max}$ is the maximum current, [A] is the agonist concentration, $n_H$ is the Hill coefficient, and $EC_{50}$ is the agonist concentration needed to achieve 50% of the maximum response. The CVFIT program (http://www.ucl.ac.uk/Pharmacology/dcpr95.html) was used to estimate $I_{max}$, $EC_{50}$ and nH values. Curves were only accepted if a "poorly defined data" message does not show. This occurs when the estimates are highly correlated (> 0.9) or if the coefficient of variation (CV) is less than 33%.

The accepted concentration-response curves from each cell were normalised to their fitted maximum. Then, the normalized data sets were pooled and refitted as one set for each receptor, wild-type, or mutant. Figure 2.5 shows an example of the analysis process, in four cells expressing α1 (S231N) β GlyR. In the tables data are presented as mean (of estimates from fitting each cell) ± standard error of the mean (SEM).

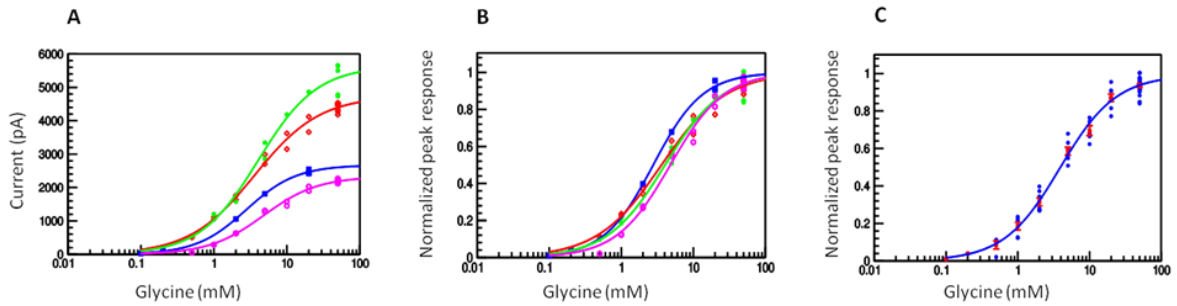


**Figure 2.5 Example of the whole-cell recording analysis using CVFIT.**

α1 (S231N) β heteromeric GlyR, $EC_{50}$ = 3.81 ± 0.42 mM, $n_H$ = 1.12 ± 0.06, $n$ = 4 for normalized, pooled data. A) Each concentration-response curve was fitted to the Hill equation. B) Normalisation of glycine gated currents to the fitted maximum in each cell. C) Pooled normalized data (error bars show ± SEM).

### 2.6.2 Propofol application

In order to determine if propofol, an intravenous anaesthetic, can rescue the function of the heteromeric GlyR hyperekplexia mutants, maximal, or submaximal ($EC_{20}$), glycine concentrations were applied *via* U-tube in the absence, or presence, of propofol. One molar stock of propofol (2, 6-diisopropylphenol) was dissolved in dimethyl sulfoxide (DMSO, both from Sigma-Aldrich). Stocks were stored at −20 °C and the desired concentrations were prepared fresh on the day of experiment. U-tube application of maximal and then submaximal glycine concentration was followed by propofol application. Two protocols of propofol application were tested. For the initial experiments propofol was co-applied *via* the U-tube with the submaximal, or maximal, glycine concentration. This method will be referred as co-application method. The other protocol was propofol pre-application in the extracellular solution for around 30 seconds followed by the co-application protocol. This method will be referred as "pre-application followed by co-application" method. The second propofol application protocol was selected when applying propofol concentrations of 50 μM. There was no glycine receptor activation during the propofol pre-application period as there was no observed change in the holding current. Peak currents were measured for the applications with, or without, propofol. Fold change [(response to glycine + propofol) / response to glycine] was calculated for each cell. Average fold change ± SEM is displayed where relevant.

## 2.7 Single-channel recording

Single-channel recordings were performed in the cell-attached configuration using an Axopatch 200B amplifier (MDS Analytical technologies, Molecular Devices, Sunnyvale, CA, USA). Borosilicate glass pipettes (thick-walled, with filament; Harvard Apparatus Ltd, USA) were pulled to a resistance of 7- 10 MΩ, when filled with the pipette solution (see below), and coated near the tip with Sylgard (Dow Corning, Midland MI, USA) to lower the noise level. Electrodes were also fire-polished before the experiment to enable the formation of giga-ohm pipette seals. Recordings were made at 19-21 C°. Pipette potential was held at +100 mV. The extracellular solution contained (in mM): 20 Na gluconate, 102.7 NaCl, 2 KCl, 2 $CaCl_2$, 1.2 $MgCl_2$, 10 HEPES, 14 glucose, 20 TEA-Cl, and 15 sucrose, pH 7.4 with NaOH and osmolarity 320 mOsmol /L. Pipette solutions were freshly prepared by adding glycine to the extracellular solution to have the required concentration (0.1-100 mM). In order to reduce contamination by ambient glycine, all solutions were prepared with high performance liquid chromatography (HPLC)-grade water (VWR international, France). Solutions were then filtered through 0.2 $\mu$m Whatman$^{TM}$ cellulose nitrate membrane filters (GE Healthcare life sciences, UK) to remove impurities that may block the electrodes. The bath level was kept as low as possible in order to maintain a high signal-to-noise ratio. After successful seal, noise level was monitored by checking the meter on the amplifier ($I_{RMS,}$ the noise is measured at 5 kHz bandwidth). The record was kept for analysis only if the patch had a noise level of 0.25 pA rms or lower.

Currents were digitised directly to a computer hard drive, using 10 kHz prefiltering (by the amplifier's 4-pole low-pass Bessel filter), a Digidata 1404A and Clampex 10.2 software (sampling rate 100 kHz, MDS Analytical Technologies, CA, USA). In order to display data off-line, currents were low-pass filtered with the Gaussian filter in Clampfit 10.2 (MDS Analytical Technologies, CA, USA) at a cut-off frequency of 3 kHz.

### 2.7.1 Single-channel analysis

#### 2.7.1.1 Amplitude measurements

Amplitudes of single -channel currents were measured in order to characterise the conductance of the channel as both mutations and subunit composition may affect it. For each selected cluster the amplitude was measured using Clampfit 10.2 (MDS Analytical Technologies, CA, USA). After 3 kHz filtering, the mean baseline was selected by placing

two cursors apart from each other just before the cluster of interest (Figure 2.6.A) in order to subtract it from the cluster signal. The cluster of interest was then selected by placing one cursor before the beginning of the cluster and another cursor at the baseline after the end of the cluster (Figure 2.6.B). All point amplitude histograms for both the baseline and the open level were established and fitted with a Gaussian. An example of the baseline and the main amplitude histogram is illustrated in (Figure 2. 6. C). The final amplitude measurement for each cluster was established by subtracting the baseline value from the open level value. Average current amplitude for each group is displayed ± SEM.

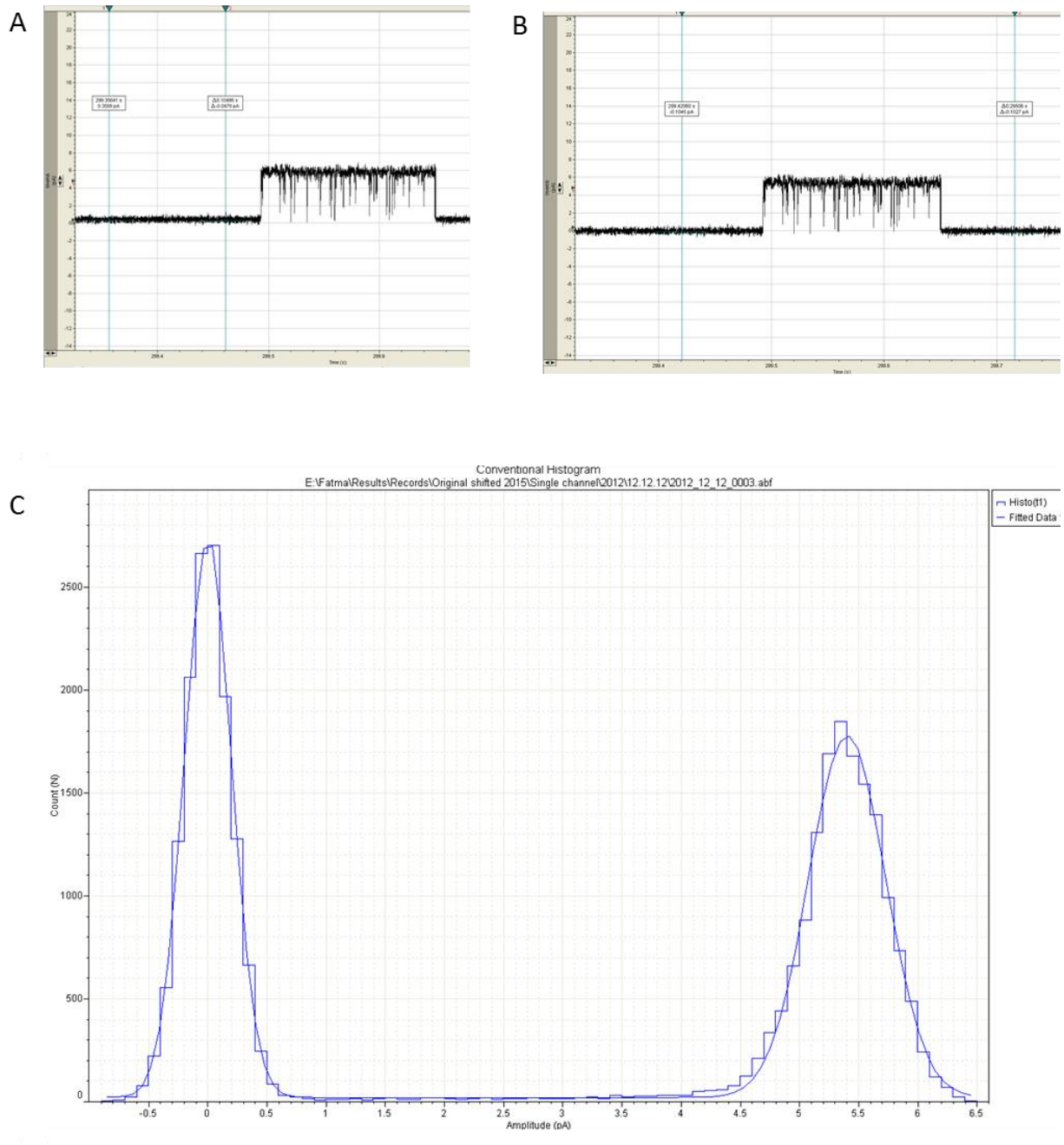


**Figure 2.6 Amplitude current measurement using Clampfit 10.2.**

A) Baseline adjustment. B) Defining area for current amplitude measurement. C) Amplitude histogram for the selected cluster.

#### 2.7.1.2 $P_{open}$ measurement

At high agonist concentration unbound shut times are at their shortest and channel openings occur in clusters separated by long closed (desensitized) intervals. If the open probability is sufficiently high (greater than 30%), clusters without double openings probably originate from the same channel ion molecule (Sivilotti, 2010). For that reason all of the single-channel recordings were conducted using saturating concentrations of the indicated agonist and were used for $P_{open}$ measurements. First, channel activity in the selected clusters was idealized by half-amplitude threshold method (Clampfit 10.2, Molecular Devices). $P_{open}$ was calculated as the ratio of cluster open time over total cluster length. Clusters longer than 10 ms were selected. The single-channel current amplitude was calculated as a difference between the full open level (at the beginning of each cluster) and the baseline (just before each cluster).

Detection and analysis of single channel data was performed by using Clampfit 10.2. In order to measure the $P_{open}$ the record was first low pass filtered at 3 kHz. Then, the cluster of interest was defined by placing one cursor at the beginning and another at its end (Figure 2.7.A). For event detection a single-channel search tool was used. The zero level cursor was placed over the baseline (closed state) and level one placed close to open channel level (Figure 2.7.B). Levels and baseline were allowed to be updated automatically. Measured events were listed in a table format (Figure 2.7.C). By selecting $P_{open}$ event analysis tool in the program the graph shows the probability of channel being open (Figure 2.7.D). Several records were used to calculate the average $P_{open}$.

A

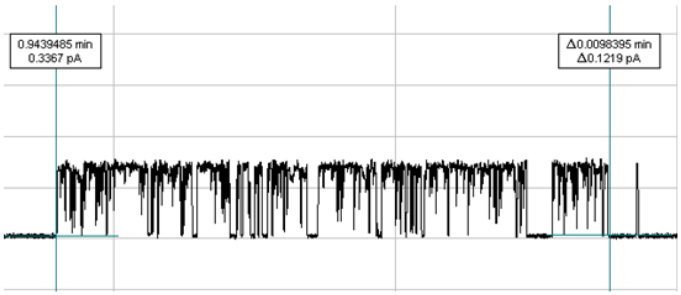


B

| | Trace | Search | Level | State | Event Start | Event End Ti | Amplitude ( | Amp S.D. (p | Dwell Time | Inst. Freq. ( | Interevent I |
|---|---|---|---|---|---|---|---|---|---|---|---|
| 5 | 1 | 1 | 1 | A | 56653.570 | 56654.789 | 6.27158 | 0.28464 | 1.21890 | 178.27855 | 5.60920 |
| 6 | 1 | 1 | 0 | A | 56654.789 | 56655.410 | 0.47678 | 0.19198 | 0.62110 | 552.91388 | 1.80860 |
| 7 | 1 | 1 | 1 | A | 56655.410 | 56656.781 | 6.56156 | 0.21591 | 1.37100 | 543.47827 | 1.84000 |
| 8 | 1 | 1 | 0 | A | 56656.781 | 56657.191 | 0.83208 | 0.04695 | 0.41030 | 501.98282 | 1.99210 |
| 9 | 1 | 1 | 1 | A | 56657.191 | 56657.641 | 6.00141 | 0.12037 | 0.44900 | 561.38776 | 1.78130 |
| 10 | 1 | 1 | 0 | AB | 56657.641 | 56657.801 | 2.81802 | 0.00000 | 0.16050 | 1163.73792 | 0.85930 |
| 11 | 1 | 1 | 1 | A | 56657.801 | 56664.578 | 5.77555 | 0.51317 | 6.77710 | 1640.68909 | 0.60950 |
| 12 | 1 | 1 | 0 | A | 56664.578 | 56665.590 | 0.17840 | 0.25849 | 1.01190 | 144.14206 | 6.93760 |
| 13 | 1 | 1 | 1 | A | 56665.590 | 56666.031 | 5.14702 | 0.04294 | 0.44120 | 128.38618 | 7.78900 |
| 14 | 1 | 1 | 0 | A | 56666.031 | 56666.488 | 0.85499 | 0.10366 | 0.45700 | 688.18390 | 1.45310 |

C

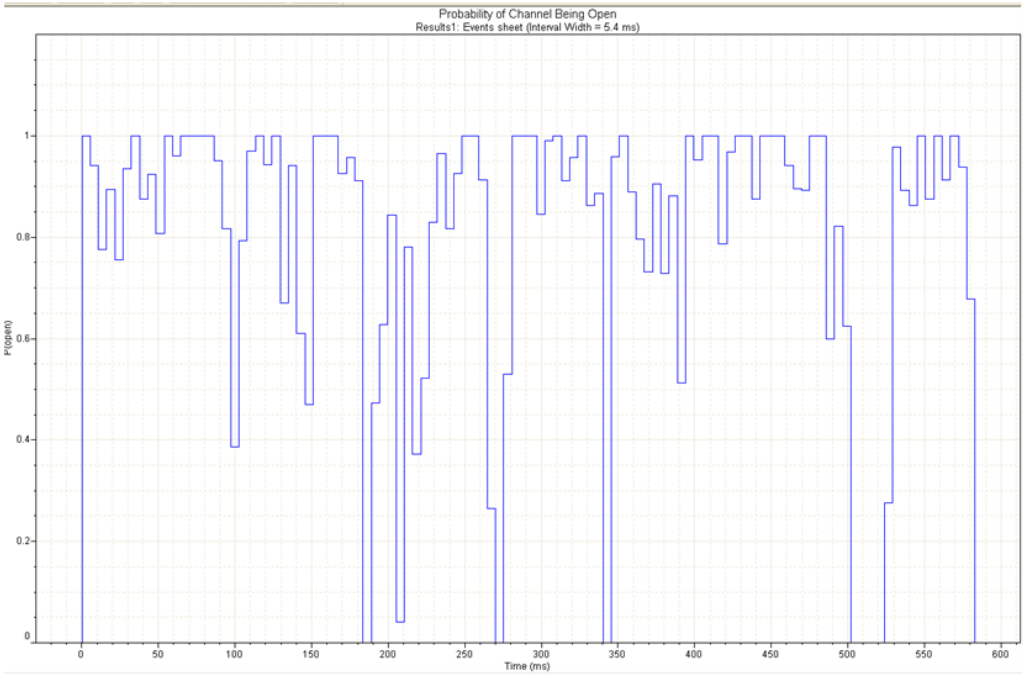


D

| Total Time (ms) | No. Events | No. Channel | P(o) | NP(o) | Interval Width (ms | Interval P(o) | Interval P(o) | Smallest Int | Largest Interval |
|---|---|---|---|---|---|---|---|---|---|
| 586.852 | 84 | 1 | 0.80446 | 0.80446 | 5.40000 | 0.80324 | 0.28240 | 0.00000 | 1.00000 |

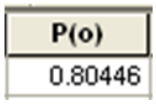


**Figure 2.7 Measurement of single-channel cluster $P_{open}$ using Clampfit 10.2.**

A) Identification of the cluster. B) Results measurements. C) Graph showing the probability of channel being open graph. D) $P_{open}$ measurement and statistics.

## 2.8 Reagents

A summary of the whole-cell and single-channel recordings solutions is givin in Table 2.4.

### 2.8.1 Whole-cell recordings experiments

Glycine, β-alanine, and sarcosine stock solutions were prepared by dissolving the desired amount into (HPLC)-grade water (VWR international, France). Stock solutions were kept at 4 °C and used within a week. The desired concentrations were prepared on the day of experiment by dissolving the stock solution in the whole-cell extracellular solution.

Propofol (2, 6-diisopropylphenol) was dissolved in DMSO. Stocks were stored at −20 °C and the desired concentrations were prepared on the day of experiment by diluting the stock solution with the whole-cell extracellular solution.

### 2.8.2 Single-channel recordings experiments

Glycine and sarcosine solutions were made by diluting the desired amount into the prepared singe-channel extracellular solution. These solutions were used on the day of experiment.

To obtain the desired propofol concentration, propofol stock was dissolved with the single-channel extracellular solution.

**Table 2.4 Solutions used for electrophysiological recordings.**

| Extracellular solution single-channel (mM) | Extracellular solution whole-cell (mM) | Intracellular solution whole-cell (mM) |
|---|---|---|
| 20 Na gluconate | 20 Na-gluconate | |
| | | 101.1 K-gluconate |
| | | 11 EGTA |
| 102.7 NaCl | 112.7 NaCl | |
| 2 KCl | 2 KCl | |
| 2 $CaCl_2$ | 2 $CaCl_2$ | 1 $CaCl_2$ |
| 1.2 $MgCl_2$ | 1.2 $MgCl_2$ | 1 $MgCl_2$ |
| 10 HEPES | 10 HEPES | 10 HEPES |
| 20 TEA-Cl | 10 TEA-Cl | 20 TEA-Cl |
| 14 glucose | 40 glucose | |
| | | 2 Mg ATP |
| 15 sucrose | | 40 sucrose |
| pH 7.4 with NaOH | pH 7.4 with NaOH | pH 7.4 with NaOH |
| osmolarity 320 mOsmol /L | osmolarity 320 mOsmol /L | osmolarity 325.2 mOsmol/L |

## 2.9 Statistics

Statistical comparisons were performed suing IBM SPSS software (IBM Analytics, USA). For single comparisons between groups unpaired t-test was used. For Chapter Four, paired t-test was used for the comparison of the measured whole-cell current before and after propofol application on the same cell. The level of significant was set to be $p < 0.05$. Data are presented as mean ± S.E.M and *n* numbers are indicated in the text.

# Chapter 3: Effects of human hyperekplexia mutations on glycine receptor single-channel activity

## 3.1 Introduction

### 3.1.1 Hyperekplexia

Hyperekplexia (OMIM # 149400) is a rare neuromotor disorder that is mainly caused by malfunction of glycinergic neurotransmission and is characterized by a non-habituating exaggerated startle response, muscle stiffness and hypertonia in response to unexpected tactile, auditory, or visual stimuli (Bakker *et al.,* 2006; Harvey *et al.,* 2008; Davies et *al.,* 2010). The startle reflex is a normal physiological reaction to unexpected stimuli and consists of an involuntary motor response including closure of the eyes, abduction of the arms, flexion of the neck, trunk, elbows, hips and knees (Dreissen *et al.,* 2012). Patients with hyperekplexia might have linguistic and cognitive defects (Thomas *et al.,* 2013). The disease was first described in 1958 in four members of a Swedish family, who suffered from sudden falls as a consequence of unexpected visual, or auditory, stimuli (Kirstein and Silfverskiold, 1958). Approximately one in 40,000 people in the United States are affected by hyperekplexia. Hyperekplexia is rare, but families with hyperekplexia have been reported from the entire world, including USA (Shiang *et al.,* 1993), Japan (Mine *et al.,* 2014), UK (Rees *et al.,* 1994), Italy (Seri *et al.,* 1997), Saudi Arabia (Seidahmed *et al.,* 2012), Oman (Al-Futaisi *et a.l,* 2012) and Taiwan (Tsai *et al.,* 2004). In addition Australian, Irish, Jordanian, Turkish and Pakistani cases were also identified (Chung *et al.,* 2010). The condition is not sex-linked i.e. autosomal and both males and females are affected by hyperekplexia. Hyperekplexia is also found in other species like cow, goat, mouse, and zebrafish (see below, Harvey *et al.,* 2008).

### 3.1.2 Genetic Causes

In most patients hyperekplexia is due to loss-of-function mutations in the key synaptic proteins involved in glycinergic neurotransmission and therefore impairment of the normal inhibitory neurotransmission (Harvey *et al.,* 2008; Thomas *et al*., 2013). Human hyperekplexia is mainly caused by missense, nonsense and frameshift mutations in the postsynaptic human glycine receptor (hGlyR) α1 gene (*GLRA1*) (Shiang, 1993; Chung *et al.,* 2010; Davis *et al.,* 2010; Bode *et al.,* 2013). Around 60 α1 hGlyR mutations have been reported to date (survey conducted in April 2018; Table 3.1). Many of the missense mutations are found in the ECD (17 mutations) followed by the TM2 (11 mutations), TM1 (7 mutations, and TM2-TM3 (6 mutations).

The disease can be inherited in either an autosomal dominant, or an autosomal recessive, pattern. Most of the hyperekplexia caused by α1 hGlyR mutations are inherited in an autosomal recessive pattern (36 vs 19). Most mutations that cause dominant hyperekplexia are found in the second transmembrane domain (TM2) and in the region between the TM2 and TM3 domain, whereas the recessive mutations are found throughout the GlyR α1 subunit (Chung *et al.,* 2010; James *et al.,* 2013). The second most common cause of hyperekplexia is mutations in the presynaptic glycine transporter-2 GlyT2 gene (*SLC6A5*) (Rees *et al.,* 2006; Harvey *et al.,* 2008; Carta *et al.,* 2012), followed by mutations in the β subunit of glycine receptor (*GLRB*) (James *et al.,* 2013; Chung *et al.,* 2013). In addition, mutations in the genes encoding the GlyR cytoskeletal anchoring protein gephyrin (Rees *et al.,* 2003) and collybistin (Harvey *et al.,* 2004) have been reported. Also, some hyperekplexia cases that are familial but do not have an identified genetic cause (*de novo*) have been reported (Seidahmed *et al.,* 2012; Thomas *et al.,* 2013).

Gain-of-function GlyR α1 mutations can also cause hyperekplexia (Chung *et al.,* 2010; Bode *et al.,* 2013; Zhou *et al.,* 2013), yet the mechanism behind this is not clear. The GlyR mutations α1(I43F), α1(W170S), α1(Q226E), α1(V280M and α1(R414H) were found to prolong the decay of IPSCs and induce spontaneous GlyR activation (Bode *et al.,* 2013; Zhang *et al.,* 2016). It is suggested that spontaneous channel opening results in increased intracellular $Cl^-$ concentration (normally low) in adult spinal motor neurons and this intracellular $Cl^-$ accumulation in turn might cause impairments of glycinergic synaptic inhibition (Zhang *et al.,* 2016).

### 3.1.3 Symptoms

The main characteristics of hyperekplexia are generalized stiffness, which appears soon after birth, exaggerated startle reflex and stiffness after the reflex. Hypertonia predominantly occurs in the trunk, or lower limbs. The hypertonia is impermanent and usually diminishes after the first years of life (1 - 5 years) (Gordon *et al.,* 1993; Bakker *et al.,* 2006; Mine *et al.,* 2014). This might suggest a compensatory mechanism by the other inhibitory receptor $GABA_A$. The syndrome produces continuous non-habituating exaggerated startle reactions in response to unexpected stimuli. For instance, tapping the bridge of the nose induces startle attacks that persist when the stimulus is repeated (Zhou *et al.,* 2002; Bakker *et al.,* 2006). During the exaggerated startle reflexes, consciousness is maintained, but afterwards

temporary generalized stiffness can lead to injuries from unprotected falls, as the arms abducted the sides cannot be used to prevent the fall. The excessive startle reflexes to unexpected stimuli persist throughout life although the severity varies from one patient to another (Zhou *et al.*, 2002; Bakker *et al.*, 2006; Thomas *et al.*, 2013).

Symptoms of this disease may appear even before birth, manifesting as increased foetal movements (Hussain *et al.*, 2012). After birth, affected neonates show hypertonia and this increases with handling and diminishes during sleep (Bakker *et al.*, 2006; Mine *et al.*, 2014). Umbilical hernia and hip dislocation are more frequent than in unaffected siblings. Muscle stiffness may start immediately after birth and decline during the first years, or appear in adult life (Gordon, 1993; Hussain *et al.*, 2012; Mine *et al.*, 2014). Another manifestation is motor delay, which is seen in the first year with subsequent catch up. Learning difficulties, developmental delay, and delayed speech acquisition are also reported (Chung *et al.*, 2010; Thomas *et al.*, 2013).

The disease is not in itself lethal, but increases the risk of sudden infant death as a result of strong muscle spasm and apnoea attacks are commonly reported (Seidahmed *et al.*, 2012; Hussain *et al.*, 2012; Thomas *et al.*, 2013; Mine *et al.*, 2014). Other consequences are injuries from unprotected falls, and these can be serious, leading to traumatic subarachnoid haemorrhage, and skull fractures (Bakker *et al.*, 2006; Thomas *et al.*, 2013; Mine *et al.*, 2014). Untreated patients can become dependent on wheelchairs due to their fear of sudden falls elicited by the exaggerated startle reflex (Zhou *et al.*, 2003).

### 3.1.4 Diagnosis

The diagnosis of hyperekplexia is mainly clinical. For early diagnosis, the most important symptoms are neonatal muscle stiffness, startle responses and a positive nose-tapping test (Bakker *et al.*, 2006; Mine *et al.*, 2014). Hyperekplexia can be confused with other disorders like epilepsy, dystonia, or cerebral palsy. In a study of a cohort of 17 Japanese hyperekplexia patients aged from neonates to 45 years only seven patients were diagnosed with hyperekplexia in their first year of life, even though all the patients had hyperekplexia symptoms. The remaining patients were misdiagnosed for a period reaching up to 45 years of age (Mine *et al.*, 2014).

No abnormalities are detected with standard blood, urine, or cerebrospinal fluid tests, or imaging studies such as computer-aided tomography (CT) and magnetic resonance imaging

(MRI), or on physiological examinations like electroencephalography (EEG) (Bakker *et al.*, 2006).

### 3.1.5 Treatment of manifestations

Based on case reports, or open studies, the symptoms of the disease can be effectively alleviated in humans by the administration of the benzodiazepine clonazepam, which improves stiffness by enhancing γ-aminobutyric acid (GABA) - gated chloride channel function. Patients treated with clonazepam (0.1-0.2 mg/kg/day) had reduced muscle stiffness and/or reduced startle responses (Zhou *et al.*, 2002; Bakker *et al.*, 2006; Thomas *et al.*, 2013). Clonazepam has adverse effects such as sleepiness and light headedness in some cases. Alternative medications including valproate, clobazam and levetiracetam are effective in some cases (Bakker *et al.*, 2006; Hussain *et al.*, 2012; Mine *et al.*, 2014).

In addition to that, life-threatening hypertonia may be acutely reduced by the Vigevano manoeuvre (forced flexion of the head and limbs toward the trunk, (Vigevano *et al*., 1989).

### 3.1.6 Animal models

Hyperekplexia phenotypes are also found in rodents. Analogous to genetic defects in hGlyR, recessively inherited mutations in the *Glra*1 gene and the *Glrb gene* were found to cause hyperekplexia in mice. Four mouse models with mutations in the α1 subunit of GlyR have been identified: *spasmodic (spd), oscillator (spd$^{ot}$), Cincinnati*, and *Nmf11*. One model in the β subunit of GlyR, *spastic (spa)* was described (Buckwalter *et al.*, 1994; Kingsmore *et al.*, 1994; Mulhardt *et al.*, 1994; Ryan *et al.*, 1994; Holland *et al.*, 2006; Traka *et al.*, 2006). All of these strains arose from spontaneous mutations, except the *Nmf11* was chemically induced by ENU (*N*-ethyl-*N*-nitrosourea), which is a chemical supermutagen used to induce point mutations through the mouse genome (Balling, 2001). Both the *Nmf11*mouse and *spasmodic* mouse, carry a missense mutation at the N-terminus of the α1GlyR, N46K and A52S, respectively (Ryan *et al.*, 1994; Traka *et al.*, 2006). In the *oscillator* model a null mutation (P327X) in the α1 subunit of GlyR leads incomplete α1 subunits, without the TM3-TM4 loop and the TM4 domain (Kling *et al.*, 1997). The *Cincinnati* mouse also harbours a null mutation in α1, F159X (Holland *et al.*, 2006). Truncated *oscillator* and *Cincinnati* α1 subunits cannot assemble into functional receptors.

The only spontaneous mouse mutant in GlyR β subunit is the *spastic* mouse mutant, where an insertion of the LINE-1 element within intron 6 of *Glrb* gene leads to a reduction in the β mRNA levels and impairs the normal expression of the GlyR complex (Kingsmore *et al.*, 1994).

The mouse models have similar phenotypes to human hyperekplexia, including the exaggerated startle reflex, increased tremor, and muscle rigidity (Zhou *et al.*, 2002). As indicated earlier, human patients with hyperekplexia exhibit symptoms postnataly, or even *in utero*. In contrast to human patients, mouse models show symptoms later, usually by the second postnatal week or even, in the case of *spasmodic*, in the third postnatal week. Except for the *spasmodic* mouse, all mice homozygous for the *oscillator*, *spastic*, *Cincinnati*, and *Nmf11* trait die about three weeks after birth. This is in contrast with, human patients with *GLRA1* null mutations, who do survive. This suggests that compensatory mechanisms may be more effective in humans than in mice (Tsai *et al.*, 2004; Becker *et al.*, 2006).

In addition to naturally arising mutations, transgenic mouse models of hyperekplexia have been generated to evaluate the physiological effects of specific mutations *in vivo* (Becker *et al.*, 2000; Becker *et al.*, 2002). Knock-in of the tgR271Q GlyR α1 mutation produced hyperekplexia phenotypes such as exaggerated startle responses to visual, or tactile, stimuli (Becker *et al.*, 2002). In another study, transgenic expression of rat wild-type GlyR β subunit in *spastic* mouse reduced the hyperekplexia symptoms completely (Hartenstein *et al.*, 1996).

**Table 3.1 Hyperekplexia mutations in the α1 subunit of the hGlyR.**

| Mutation | Type | Mode of inheritance | Position | Notes | References |
|---|---|---|---|---|---|
| del Ex1-7 | deletion | recessive | n.a | | Brune *et al.* (1996); Bode *et al.* (2013) |
| del Ex4-7 | deletion | recessive | n.a | compound heterozygous with R65L | Chung *et al.* (2010) |
| I43F | missence | *de novo* | ECD | | Horváth *et al.* (2014); Zhang *et al.* (2016) |
| R65L | missense | recessive | ECD | compound heterozygous with ΔEx4-7 | Chung *et al.* (2010) |
| R65W | missense | recessive | ECD | compound heterozygous with P230S | Chung *et al.* (2010) |
| W68C | missense | recessive | ECD | compound heterozygous with R316X | Tsai *et al.* (2004); Schaefer *et al.* (2015) |
| D70N | missense | recessive | ECD | compound heterozygous with W407R | Schaefer *et al.* (2015) |
| R72fsX47 | deletion | recessive | ECD | | Rees *et al.* (2001) |
| R72H | missense | recessive | ECD | | Coto *et al.* (2005); Schaefer *et al.* (2015) |
| R72C | missense | recessive | ECD | | Bode *et al.* |

| | | | | | |
|---|---|---|---|---|---|
| | | | | | (2013) |
| E103K | missense | recessive | ECD | compound heterozygous with L184fs21X | Chung *et al.* (2010); Thomas *et al.* (2013) |
| Y128C | missense | dominant | ECD | | Chung *et al.* (2010) |
| K132fsRX15 | deletion | recessive | ECD | | Zoons *et al.* (2012) |
| C138S | missense | recessive | ECD | compound heterozygous with D148fsX16 | Chan *et al.* (2012) |
| M147V | missense | recessive | ECD | | Rees *et al.* (2001); Thomas *et al.* (2013) |
| D148fsX16 | deletion | recessive | ECD | compound heterozygous with C138S | Chan *et al.* (2012) |
| G160R | missense | dominant | ECD | | Schaefer *et al.* (2015) |
| T162M | missense | recessive | ECD | | Schaefer *et al.* (2015) |
| D165G | missense | recessive | ECD | | Chung *et al.* (2010); Thomas *et al.* (2013) |
| W170S | missense | recessive | ECD | | Al-Futaisi *et al.* (2012); Zhou *et al.* (2013); Zhang *et al.* (2016) |
| L184fs21X | deletion | recessive | ECD | compound | Chung *et al.* |

| | | | | | |
|---|---|---|---|---|---|
| | | | | heterozygous with E103K | (2010) |
| T190M | missense | recessive | ECD | compound heterozygous with D424N | Yang *et al.* (2017) |
| Y197X | nonsense | recessive | ECD | compound heterozygous with Y202X | Chung *et al.* (2010) |
| Y202X | nonsense | recessive | ECD | compound heterozygous with Y197X | Rees *et al.* (2001); Thomas *et al.* (2013) |
| R218Q | missense | *de novo* | ECD | compound heterozygous with S296X | Miraglia *et al.* (2003); Castaldo *et al.* (2004) |
| R218W | missense | recessive | ECD | | Bode *et al.* (2013) |
| Q226E | missense | dominant | TM1 | | Bode *et al.* (2013); Scott *et al.* (2015); Zhang *et al.* (2016) |
| Y228C | missense | recessive | TM1 | | Forsyth *et al.* (2007) |
| P230S | missense | recessive | TM1 | compound heterozygous with R65W | Bode *et al.* (2013) |
| S231R | missense | recessive | TM1 | | Humeny *et al.* (2002); Villmann *et al.* (2009) |
| S231N | missense | recessive | TM1 | compound | Chung *et al.* |

| | | | | | |
|---|---|---|---|---|---|
| | | | | heterozygous with S296X | (2010); Thomas *et al.* (2013) |
| W239C | missense | dominant | TM1 | | Gilbert *et al.* (2004) |
| I244N | missense | recessive | TM1 | | Rees *et al.* (1994); Lynch *et al.* (1997); Villmann *et al.* (2009) |
| P250T | missense | dominant | TM1-TM2 loop | | Saul *et al.* (1999) |
| R252H | missense | recessive | TM2 (0') | compound heterozygous with R392H | Vergouwe *et al.* (1999); Rea *et al* (2002); Villmann *et al.* (2009) |
| R252C | missense | recessive | TM2 (0') | | Chung *et al.* (2010); Thomas *et al.* (2013) |
| G254D | missense | recessive | TM2 (2') | | Chung *et al.* (2010); Thomas *et al.* (2013) |
| V260M | missense | dominant | TM2 (8') | | del Giudice *et al.* (2001); Castaldo *et al.* (2004) |
| T265I | missense | dominant | TM2 (13') | | Chung *et al.* (2010) |

| | | | | | |
|---|---|---|---|---|---|
| Q266H | missense | dominant | TM2 (14') | | Milani *et al.* (1996); Moorhouse *et al.* (1999), Castaldo *et al.* (2004) |
| S267N | missense | dominant | TM2 (15') | | Becker *et al.* (2008) |
| S270T | missense | recessive | TM2 (18') | | Lapunzina *et al.* (2003) |
| R271L | missense | dominant | TM2 (19') | | Shiang *et al.* (1993); Langosch *et al.* (1994); Lynch *et al.* (1997); Rees *et al.* (2001); Kwok *et al.* (2001) |
| R271Q | missense | dominant | TM2 (19') | | Shiang *et al.* (1993), Langosch *et al.* (1994); Rees *et al.* (1994); Lynch *et al.* (1997); Kwok *et al.* (2001); Thomas *et al.* (2013); Mine *et al.* (2014); Scott *et al*. |

| | | | | | |
|---|---|---|---|---|---|
| | | | | | (2015) |
| R271P | missense | dominant | TM2 (19') | | Gregory *et al.* (2008) |
| R271X | nonsense | dominant | TM2 (19') | | Lee *et al.* (2013) |
| A272P | missense | dominant | TM2-TM3 loop | | Mine *et al.* (2015) |
| K276E | missense | dominant | TM2-TM3 loop | | Elmslie *et al.* (1996), Seri *et al.* (1997); Lewis *et al.* (1998); Doria *et al.* (2007); Lape *et al.* (2012); Mine *et al.* (2014); Scott *et al.* (2015) |
| K276Q | missense | *de novo* | TM2-TM3 loop | | Kang *et al.* (2008) |
| Y279C | missense | dominant | TM2-TM3 loop | | Shiang *et al.* (1995); Lynch *et al.* (1997); Kwok *et al.* (2001); Thomas *et al.* (2013) |
| Y279S | missense | dominant | TM2-TM3 loop | | Poon *et al.* (2006) |
| V280M | missense | dominant | TM2-TM3 loop | | Bode *et al.* (2013); Zhang *et al.* |

| | | | | | |
|---|---|---|---|---|---|
| | | | | | (2016) |
| L291P | missense | recessive | TM3 | compound heterozygous with D388A | Bode *et al.* (2013); Thomas *et al.* 2013 |
| S296X | nonsense | recessive | TM3 | compound heterozygous with S231N and R218Q | Bellini *et al.* (2007); Chung *et al.* (2010); Bode *et al.* (2013) |
| R316X | nonsense | recessive | TM3-TM4 loop | compound heterozygous with W68C | Tsai *et al.* (2004); Schaefer *et al.* (2015) |
| G342S | missense | recessive | TM3-TM4 loop | | Jungbluth *et al.* (2000); Rees *et al.* (2001); Chung *et al.* (2010) |
| E375X | nonsense | recessive | TM3-TM4 loop | | Bode *et al.* (2013) |
| A384P | missense | recessive | TM3-TM4 loop | compound heterozygous with R392H | Mine *et al.* (2014); Wang *et al.* 2018 |
| D388A | missense | recessive | TM3-TM4 loop | compound heterozygous with L291P | Bode *et al.* (2013) |
| R392H | missense | recessive | TM4 | compound heterozygous with R252H/ compound | Vergouwe *et al.* (1999); Rea *et al.* (2002); |

| | | | | | |
|---|---|---|---|---|---|
| | | | | homozygous | Villmann *et al.* (2009); Chung *et al.* (2010) |
| W407R | missense | recessive | TM4 | compound heterozygous with D70N | Schaefer *et al.* (2015) |
| R414H | missense | dominant | TM4 | | Bode *et al.* (2013); Zhang *et al*. (2016) |
| D424N | missense | recessive | TM4 | compound heterozygous with T190M | Yang *et al.* (2017) |

## 3.2 Results

Human hyperekplexia is caused by the malfunction of glycinergic synaptic transmission, most commonly because of mutations in the GlyRα1 subunit. As in other channelopathies, every disease causing mutation identifies a residue that is essential for the function of the channel, and thus is worth investigating (Bode and Lynch, 2014). For instance, thorough kinetic analysis of the α1 (K276E) mutation has allowed our lab to identify the crucial role of the M2-M3 domain in signal transduction in GlyRs (Lewis *et al.*, 1998; Lape *et al.*, 2012).

The first level of this investigation is to characterise the main effects of known human hyperekplexia mutations by electrophysiological recording. This means, for example establishing glycine and/or partial agonist concentration-response curves, and measuring the single channel conductance and maximum open probability of mutant channels.

The aim of my work was to perform an initial screening of several known human hyperekplexia mutations to understand their effect on both homomeric and heteromeric glycine receptors. It was very important to begin with this step as single channel kinetic analysis can be performed only in receptor variants with favourable properties. Six human hyperekplexia mutations in the α1 subunit R72H, E103K, S231N, Q266H, S267N and Y279C were selected for screening. In choosing these mutations, we tried to sample different channel domains and to avoid extreme loss of function mutations, which we know could not be analysed as such with single channel kinetics.

### 3.2.1 Expression of the wild-type human homomeric and heteromeric GlyR in HEK293 cells

The first set of experiments is obviously to characterise wild type α1 and α1β receptors. Previous work of my lab was carried out on the rat subunit (Beato *et al.*, 2002; Burzomato *et al.*, 2003; Lape *et al.*, 2012).

Sequence alignment of human *versus* rat α1 glycine receptor shows 98.5% identity and the alignment of the β subunit from these two species shows 97.2% identity. Indeed the human α1 subunit differs from the rat subunit only in 7 amino acid residues and the human β subunit differs from rat in 14 amino acids residues. While the receptors obviously perform the same function in the two species, it cannot be taken for granted that these sequence differences are unimportant. We therefore thought it essential to establish channel properties of the wild-

type human glycine receptor in order to be able to compare them with those of the human hyperekplexia mutant channels.

In order to compare the effect of different GlyR mutations on glycine channel sensitivity, I obtained glycine concentration-response curves for the wild-type receptors first for both homomeric α1 and heteromeric α1β human GlyR. Representative responses to different concentrations of glycine to wild-type α1, or α1β, receptors in cells voltage-clamped at −50 mV in asymmetrical chloride are shown in Figure 3.1 and 3.2, respectively. For the homomeric GlyR, I applied a range of different concentrations of glycine between 0.025 and 10 mM by a U-tube. The traces show that as glycine concentration increases, the risetime of the response speeds up and the amplitude of the inward current increases until it reaches saturation below 10 mM. Desensitization was clearly starting from 0.2 mM glycine concentration (*e.g.* approximately $EC_{30}$).

Whole-cell peak current amplitudes were measured, plotted and fitted with the Hill equation (see Methods 2.6.1). The fitted concentration-response curve for homomeric GlyRs is shown in Figure 3.1. Fits with the Hill equation gave estimates of $EC_{50}$ of 0.25 ± 0.03 mM and a Hill slope of 1.87 ± 0.37 ($n$ = 6). Similar results were obtained for heteromeric GlyRs, expressed with a cDNA α:β ratio of 1:40 (Burzomato *et al.*, 2003). As the concentration of glycine was increased faster activation was observed for the heteromeric GlyR. The lowest concentration for which clear desensitisation was observed was 0.1 mM, *i.e.* approximately $EC_{60}$ as shown in the sample trace in Figure 3.2. The $EC_{50}$ of the human heteromeric GlyR was 0.10 ± 0.03 mM and a Hill slope 1.48 ± 0.09 ($n$ = 6).

These values should be compared with those obtained with an identical technique for rat homomeric and heteromeric GlyRs. These have similar $EC_{50}$ values: the $EC_{50}$ of wild-type rat α1 was 0.08 ± 0.01 mM and of α1β = 0.09 ± 0.004 mM, and Hill slope of 3.3 ± 0.2 and 2.0 ± 0.2, respectively (Beato *et al.*, 2002; Burzomato *et al.*, 2003).

The human wild type GlyR homomers have a significant higher $EC_{50}$ than heteromers. It is not clear why coexpression with the β subunit should reduce the potency of glycine in human ($p < 0.01$), but not in rat receptors.

The Hill coefficient values were not significantly different for homomeric *versus* heteromeric GlyRs (1.87 ± 0.37 and 1.48 ± 0.09, $p > 0.05$), but note the large scatter of the homomeric

data. It is worth noting that both homomeric and heteromeric channels are thought to be maximally activated when three glycine molecules are bound.

The expression level, judging from the maximum current recorded, was comparable (10.34 ± 2.47 *vs* 4.43 ± 1.83 nA, for α1 and α1β respectively, $p > 0.05$).

### 3.2.2 Single-channel recordings of homomeric and heteromeric wild-type GlyR

Single channel recordings of homomeric or heteromeric wild-type human GlyR expressed in HEK293 cells were obtained in cell-attached configuration (pipette potential +100 mV).

Activation of homomeric channels with saturating glycine concentration (10 mM) is illustrated Figure 3.3. Clear clusters of openings of channels between long silent channel periods were observed. The channel closures are more likely to be desensitised intervals, a finding that was reported previously (Beato *et al.*, 2004). The maximum $P_{open}$ value was obtained for each individual cluster as the ratio between the total cluster open time and total cluster duration (see Methods). Human GlyR α1 opened with average maximum $P_{open}$ of 0.99 ± 0.002 ($n$ = 30 clusters from 4 records), a value similar to the homomeric rat GlyR with $P_{open}$ of 0.96 ± 0.3, $n$ = 45 clusters from 5 records (Beato *et al.*, 2004). Average amplitude of human homomeric GlyR was 5.77 ± 0.06 pA ($n$ = 30 clusters from 4 records) slightly higher than average amplitude of rat homomeric receptors recorded previously in our lab 4.7 ± 0.1 pA ($n$ = 26) (Beato *et al*., 2004).

Activation of wild-type α1β glycine channels with saturating concentration of glycine (1 mM) resulted in long clusters of channel openings. A sample trace of a single channel record is shown in Figure 3.4. Average $P_{open}$ of 0.98 ± 0.01 ($n$ = 29 clusters from 6 patches) was measured. This value is very similar to the one reported previously in our lab for the rat heteromeric GlyR with average maximum $P_{open}$ of 0.97 ± 0.0007, $n$ = 91 clusters from 4 patches (Burzomato *et al.*, 2004). The long clusters were separated by long sojourns in desensitized intervals. The average current amplitude for the heteromeric wild-type receptors was 3.07 ± 0.06 pA, $n$ = 29 clusters from 6 records, similar average current amplitude of 3.1± 0.1 pA has been reported for the heteromeric rat GlyRs (Burzomato *et al.*, 2004).

### 3.2.3 Conclusion human wild-type GlyR

Human wild-type heteromeric GlyR has a lower $EC_{50}$ than the homomeric GlyR. However, both homomeric and heteromeric GlyRs open with very high $P_{open}$ when activated by saturating concentration of glycine (0.99 ± 0.002, 0.98 ± 0.01, respectively). Their single channel current amplitudes are different 5.77 ± 0.06 pA cf 3.07 ± 0.06 pA.

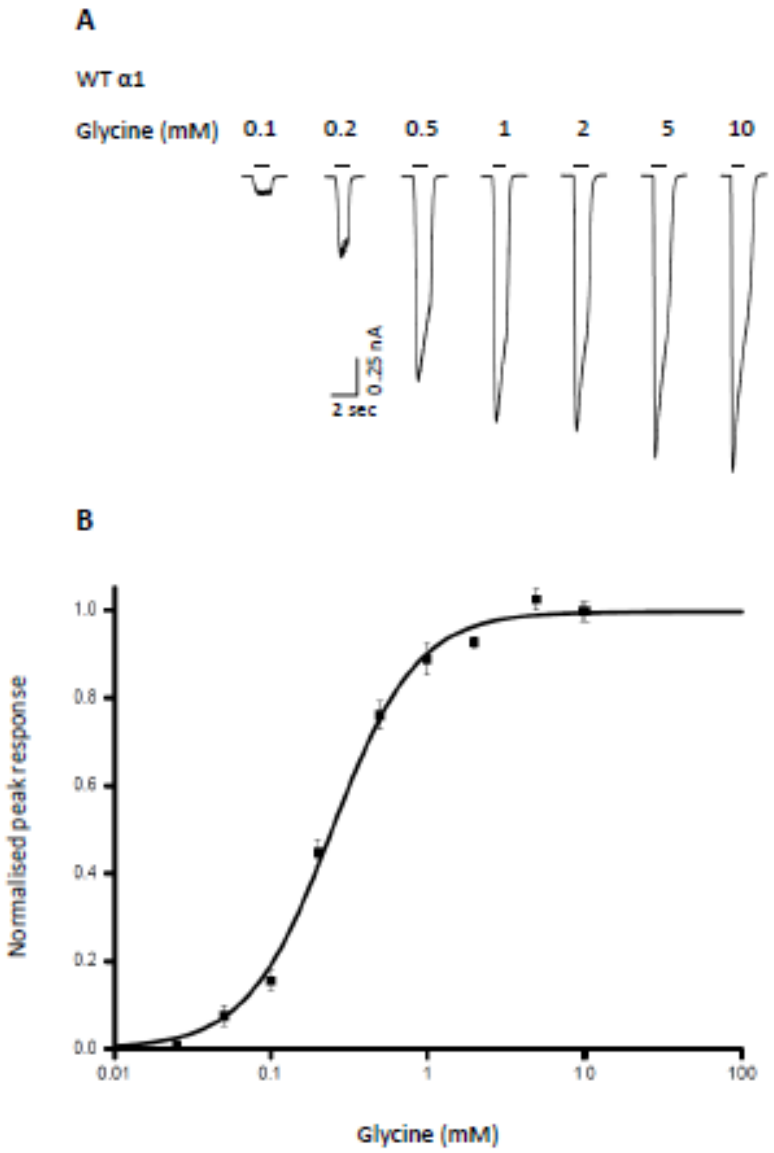


**Figure 3.1 Sensitivity of the human wild-type α1 GlyRs to glycine.**

A) Representative whole cell current traces evoked by U-tube application of 0.1, 0.2, 0.5, 1, 2, 5, and 10 mM glycine (black bars) to the recombinant HEK293 cells expressing wild-type α1 GlyR. Cells were held at – 50 mV. B) Average glycine concentration-response curve obtained from α1 wild-type GlyR. The solid curve is a fit to the Hill equation. $EC_{50}$ = 0.25 ± 0.03 mM, $n_H$ = 1.87 ± 0.37, $I_{max}$ = 10.34 ± 2.47 nA, $n$ = 6 cells. Error bars indicate mean ± SEM.

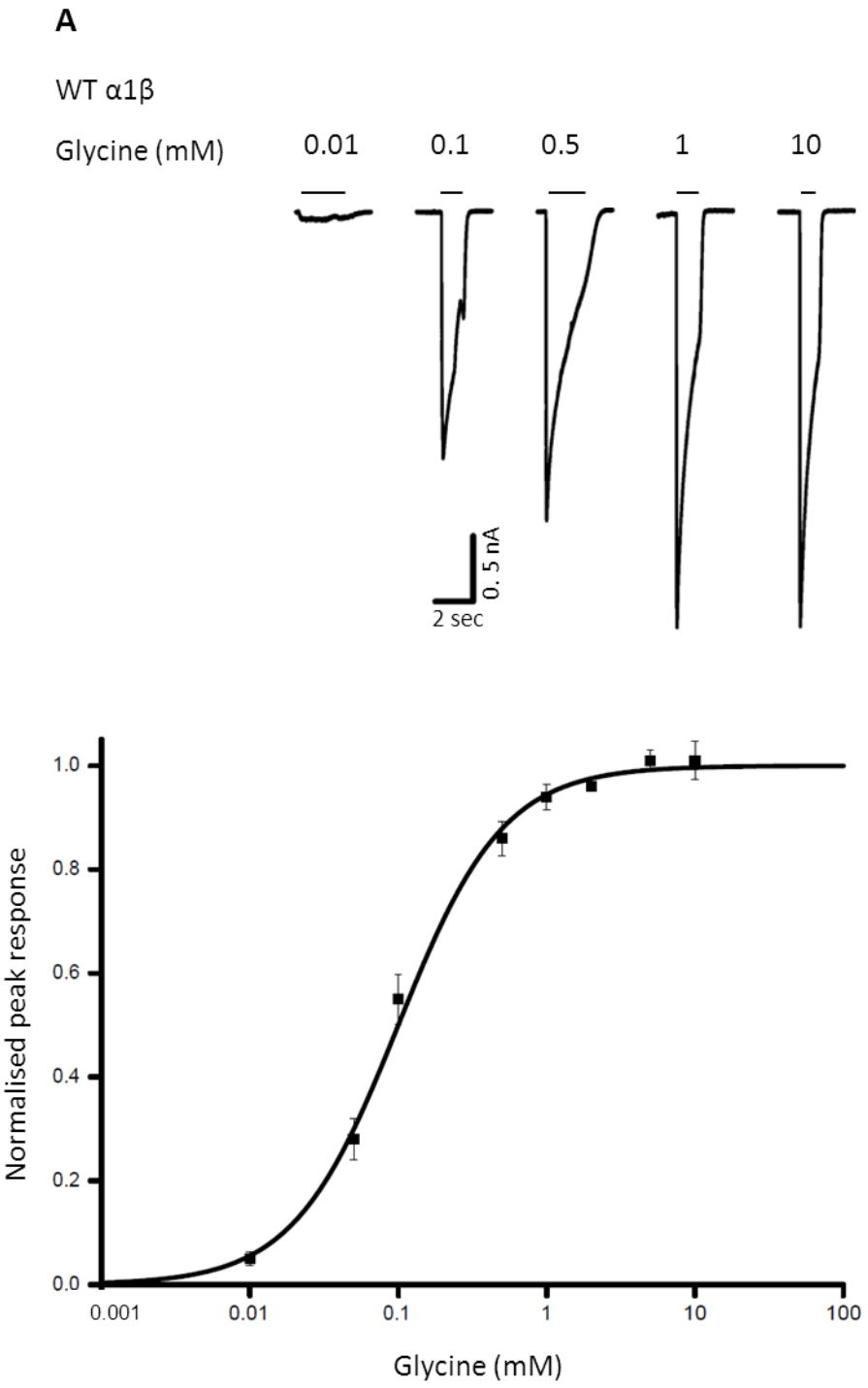


**Figure 3.2 Glycine concentration-response curve of the human wild-type α1β GlyR.**

A) Sample whole-cell glycine activated current traces evoked by U-tube application of different concentrations to recombinant HEK293 cells expressing wild-type α1β GlyR (at –50 mV). Respective concentrations of glycine are shown in mM. B) Average glycine concentration-response curves obtained from wild-type α1β GlyR. Solid curve is a fit to the Hill equation. $EC_{50}$ = 0.10 ± 0.03 mM, $n_H$ = 1.48 ± 0.09, $I_{max}$ = 4.43 ± 1.08, $n$ = 6 cells. Error bars indicate mean ± SEM.

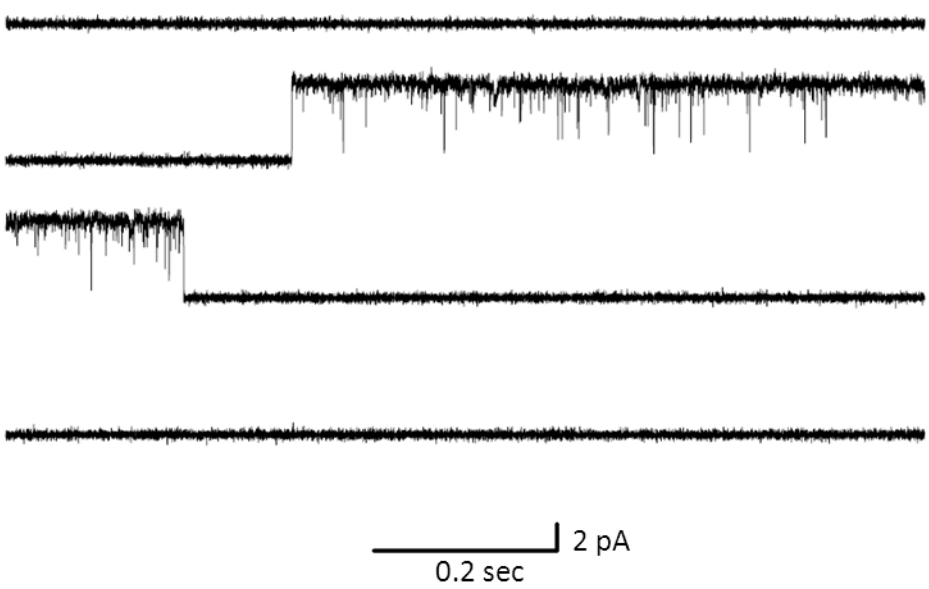


**Figure 3.3 Example of single channel activity of the human wild-type α1 GlyR in response to saturating concentration of glycine (10 mM).**

Openings of the channels were recorded in the cell attached configuration at a holding potential of + 100). There is clear clustering of the openings between long desensitised closures. Homomeric glycine channels open with average maximum $P_{open}$ of 0.99 ± 0.002 and average amplitude of 5.77 ± 0.06 pA, $n$ = 30. Channel open upward. (3 kHz low pass filtered for display).

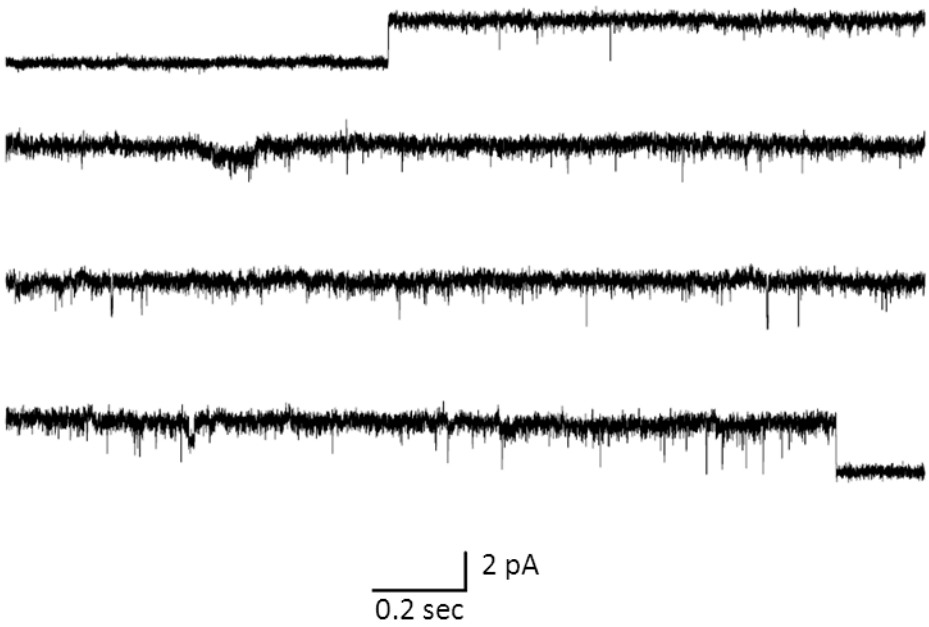


**Figure 3.4 Activation of human wild-type α1β GlyR by saturating glycine concentration.** Sample cell-attached single channel trace with one cluster opening is shown (pipette potential +100 mV). The average maximum $P_{open}$ = 0.98 ± 0.01 and the average amplitude = 3.07 ± 0.06 pA, $n$ = 29. Channel opening is upwards (3 kHz low pass filtered for display).

### 3.2.4 Choice of the human hyperekplexia mutations to characterise

There are more than 30 human hyperekplexia mutations published for the α1 subunit of the glycine receptor (Bode and Lynch, 2014). With this huge number, screening is vital to exclude channel mutants with severe, or complete loss, of function. Several human hyperekplexia mutations were selected for characterization in both homomeric and heteromeric glycine receptors. The selection of the mutations aimed to include residues in different regions of the GlyR α1 subunit, namely parts of the ECD, TM1, TM2 and the TM1-TM2 loop. Also, those mutations have different modes of inheritance and both recessive and dominant forms were included. Figure 3.5 shows a homology model of a single subunit of GlyR and the location of the selected human hyperekplexia mutations.

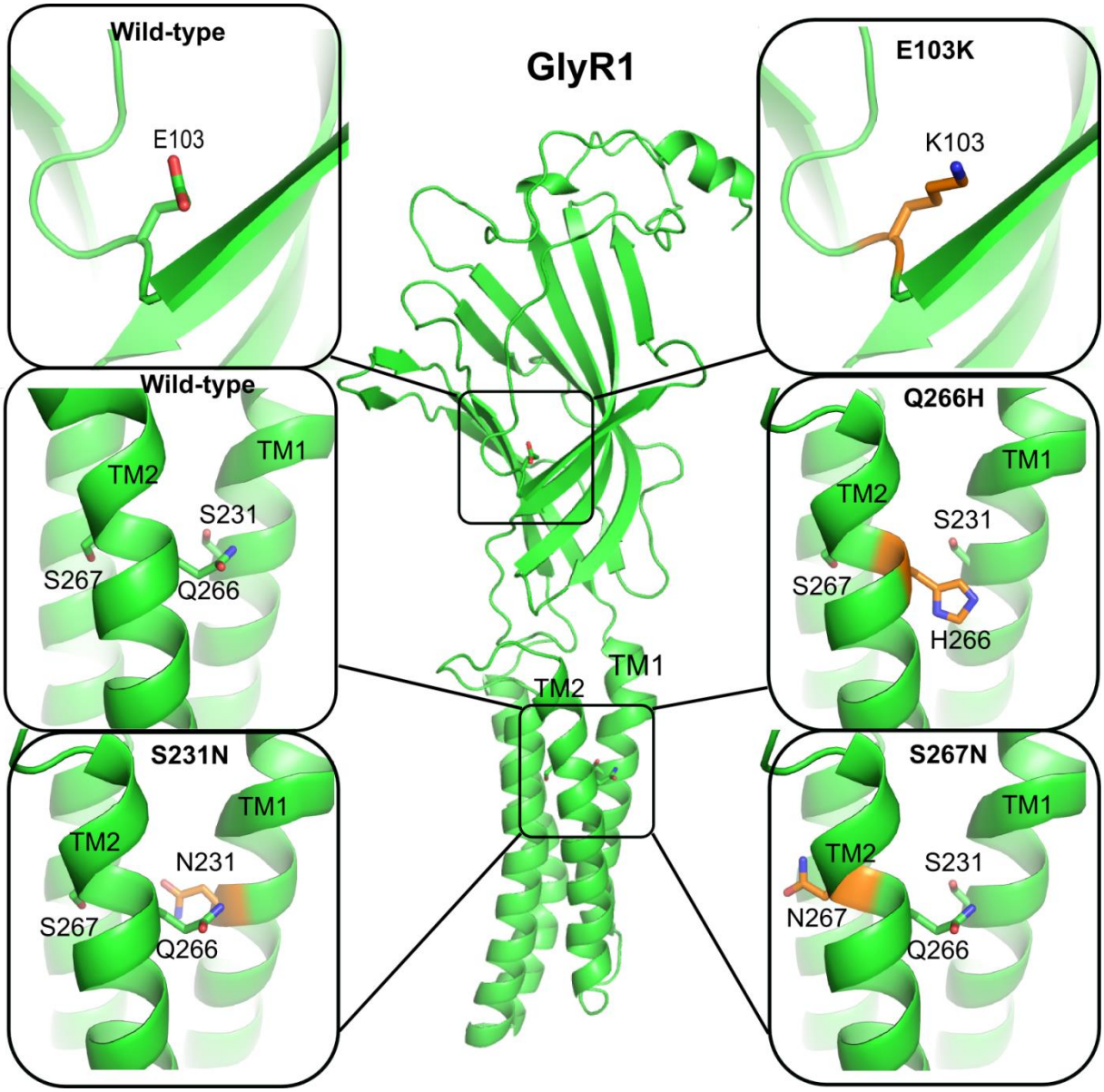


**Figure 3.5 A homology model for the α1 subunit of the glycine receptor.**

The model is presented as a side view from the inside of the channel pore towards the periphery of the receptor. The TM2 line the inner pore. The locations of the tested human hyperekplexia GlyR mutations are indicated. The middle part represents the overall view of a single GlyR α1 subunit with the extracellular domain and the transmembrane domain. This homology model is based on *C.elegans* GluCl channel (PBD ID 3WI5) and was provided by collaborators from Oxford University (Biggin and Yu, see Yu *et al.*, 2014). The mutations are highlighted in orange.

### 3.2.5 The effect of the human hyperekplexia mutations on glycine receptor sensitivity and efficacy

### 3.2.6 ECD or binding site domain: the E103K mutation

#### 3.2.6.1 Location

E103 is in loop A on the principal side of the agonist binding site, in the cleft between two adjacent subunits see Figure 3.5 (a full description of the interaction of this GlyR mutation with other residues will follow in Chapter five).

Glycine receptor α1 E103 is conserved in many subunits from different receptors and species (Figure 3.6). It is conserved in the human glycine receptor subunits α2, α3, α4, and β. It is also conserved in the bovine glycine receptor α1 and β subunits. Glycine receptor α1 subunit of *Danio rerio* (zebrafish) has the same amino acid. Furthermore, rat glycine receptor subunits α1, α2, α3, and β have a conserved glutamic acid in the indicated position. All the subunits (α1, α2, α3, α4, and β) of the mouse glycine receptor have a conserved amino acid in the region of interest. Both GluCl receptor α and β subunits from *Caenorhabditis elegans* have a conserved glutamic acid in the indicated position. *Drosophila melanogaster* (fruit fly) and *Haemonchus contortus* (Barber pole worm) GluCl channel α and β subunit, respectively, includes the conserved amino acid of interest.

#### 3.2.6.2 Reported hyperekplexia case

The E103K mutation was first reported to cause hyperekplexia in human by Chung *et al.* (2010). The index case, a Caucasian male patient did not have a family history of hyperekplexia as his parents were asymptomatic. He had stiffness and non-habituating startle response. The patient responded positively to clonazepam. DNA sequencing screening of the *GLRA1* identified the maternal hemizygous recessive missense E103K mutation in the N-terminal of GlyR α1. The patient happened to be a compound heterozygote, having inherited this mutation with the paternal frameshift mutation L184fs21X. This deletion produces a premature stop codon at amino acid position 205 (Chung *et al.*, 2010). The lack of symptoms in the mother suggests that this mutation is relatively mild and receptors containing wild-type and mutant subunits would function reasonably well.

Although when the deletion L184fs21X GlyR mutation was expressed in HEK293 cells as homomeric, or heteromeric with the β subunit, the GlyR channels were not functional. Co-expression with the E103K mutation resulted in higher level of functional channels expression. Also, the number of the functional GlyRs of the homomeric, or heteromeric, GlyR E103K mutation alone was similar to the corresponding wild-type. Since the frameshift mutation produced a non-functional allele, it is predicted that the patient's functional α1 GlyR *in vivo* contained only mutant α1 E103K subunits (Chung *et al.,* 2010).

Whole cell analysis of the homomeric α1 (E103K) or heteromeric α1 (E103K) β GlyR expressed in HEK293 cells indicated a 26, 33 fold change in glycine $EC_{50}$, respectively (Chung *et al.,* 2010). A slight disruption of the glycine binding site was predicted by structural modelling of the α1(E103K) GlyR mutant on the *Torpedo* $\alpha_1\beta\gamma\alpha_2\varepsilon$ nicotinic ACh receptor (nAChR) (Chung *et al.,* 2010).

As there are only few published functional data for the Cys-loop receptors with mutations in this position, I checked whether there were reports of other GlyR mutations in nearby residues of loop A. Cysteine, alanine, or lysine substitution of the 102, 103, or 104 residues in the GlyR α1 are shown in Table 3.2 and will be discussed further in the following paragraphs.

#### 3.2.6.3 GlyR mutations in the proximity of E103K

**N102A, N102C**

The N102 residue is important for GlyR function: an alanine scan of GlyR α1 loop A residues showed that N102A GlyRs had higher $EC_{50}$ for glycine, β-alanine and taurine (44, 32 and 14 fold greater, respectively) without a change in strychnine sensitivity (Table 3.2) (Vafa *et al.,* 1999). This finding was supported by another study, where the N102C α1 GlyR mutation was examined (Han *et al.,* 2001). The latter study reported an even greater loss of agonist sensitivity, for both glycine and taurine, by 142 and 346 fold respectively (for ease of comparison these published results are summarised in Table 3.2). The same paper reported also a significant decrease in taurine maximum response relative to glycine (from 1.03 to 0.29)

**E103C, E103A**

E103C GlyR α1expressed in HEK293 cells shifts glycine sensitivity by 44 fold from 19 to 850 μM. It also shifts taurine $EC_{50}$ by 35 fold from 120 to 4200 μM, with a slight reduction of taurine relative efficacy from 1 to 0.9 (Table 3.2) (Han *et al*., 2001). However, E103A did not produce a significant reduction of the glycine $EC_{50}$ (0.7 fold change; Table 3.2) (Vafa *et al*., 1999).

**K104A, K104C**

While α1(K104A) GlyR causes a slight decrease of the glycine sensitivity by 1.7 fold when expressed in HEK293 cells (Vafa *et al.*, 1999), the same mutation was found to increase glycine sensitivity by 0.75 fold when expressed in oocytes (Schmieden *et al.*, 1999). In the same study, this α1(K104A) GlyR mutation was found to enhance the potency of several partial agonists including taurine and β-aminoisobutyric acid and to increase the relative efficacy of taurine (see Table 3.2).

On the other hand, α1(K104C) GlyR expressed in HEK293 cells reduced both glycine and taurine $EC_{50}$ by 0.38 and 0.31 fold, respectively. No significant change in taurine relative efficacy was detected (Table 3.2) (Han *et al.*, 2001).

### 3.2.6.4 Whole-cell recordings of α1(E103K)

Different amounts of plasmid were used to have suffiecient expression of α1(E103K) mutant GlyR in HEK293 cells. The E103K GlyR barely expressed in HEK293 cells when 5 % of DNA was used so in order to study this receptor the DNA percentage of the α1(E103K) GlyR was increased from 5 to 55% (see Methods). Sample traces of glycine responses recorded from homomeric E103K GlyRs are shown in Figure 3.7.A. Higher agonist concentrations were needed to evoke current responses than in wild-type channels. As in wild-type, the risetime of the current response became faster with higher glycine concentrations, up to the maximum concentration of 20 mM glycine, where the glycine response was saturated. The glycine $EC_{50}$ was significantly decreased by 2.8 fold from its wild-type value of 0.25 ± 0.03 ($n$ = 6) to 0.71 ± 0.11 mM ($n$ = 3; $p < 0.001$, unpaired t-test). Hill slope was comparable with those of wild-type GlyR of 1.87 ± 0.37 ($n$ = 6) vs 1.32 ± 0.07 for α1(E103K) ($n$ = 3; $p > 0.05$, unpaired t-test). The maximal current was decreased insignificantly from 10.34 ± 2.47 nA for wild-type ($n$ = 6) to 2.73 ± 1.41 nA for α1(E103K) GlyRs ($n$ = 3, $p > 0.05$) (Figure 3.7.B, Table 3.3).

### 3.2.7 Whole-cell recordings of α1(E103K)β

Co-expression of the human wild-type GlyRβ with the α1E103K GlyR mutant at an α:β cDNA ratio of 1:40 resulted in functional GlyR with enough glycine current to proceed with whole-cell recordings. The average maximum glycine current elicited was similar to the one obtained with wild-type GlyRs: 4.43 ± 1.08 nA (WT, $n$ = 6) and 3.62 ± 0.89 nA (α1(E103K)β, $n$ = 6; $p$ > 0.05, unpaired t-test ). As shown in (Figure 3.8), 1 mM of glycine elicited currents with approximately an $EC_{10}$ and a very high concentration of 100 mM glycine was needed to produce a saturating response. Glycine gated currents showed desensitization with the all of the tested glycine concentrations starting at 1 mM glycine until 100 mM glycine (Figure 3.8.A). The α1(E103K)β GlyR mutation caused a significant ~ 70 fold increase of the glycine $EC_{50}$ with a value of 7.27 ± 0.58 mM, $n$ = 6 (cf.. for wild-type heteromeric GlyR = 0.10 ± 0.03 mM, $n$ = 6; $p$ < 0.001, unpaired t-test). The Hill slope was similar for wild-type and the mutant GlyR 1.48 ± 0.09 vs 1.22 ± 0.08 ($n$ = 6 for both; $p$ > 0.05, unpaired t-test; Figure 3.8.B, Table 3.4).

### 3.2.8 Single-channel recordings of homomeric and heteromeric GlyR bearing the E103K α1 mutation

Single-channel recordings of the homomeric E103K GlyR were obtained in the cell-attached configuration (pipette potential +100 mV) in the presence of 50 mM glycine, a concentration that was found to be saturating in whole cell recordings (see Figure 3.7). Mutant channels opened in clusters, separated by long desensitised periods. The clusters had a significantly reduced maximum $P_{open}$ from 0.99 ± 0.002 to 0.71 ± 0.09 ($n$ = 30, 13, respectively, $p$ < 0.01, unpaired t-test). Measurements of approximate $P_{open}$ were carried for each cluster; however, for some clusters it was difficult to judge whether two subsequent channel openings are from one or two channels (see upper trace Figure 3.9). For the illustrated example $P_{open}$ of 0.40 was selected instead of two openings with 0.78 and 0.68 $P_{open}$. For the second cluster shut time intervals (0.004 – 0.06 seconds) in addition to the apparent short open times contributed to the reduced $P_{open}$ ~ 0.8 seconds. The labelled apparent shut times are approximately measured by Clampfit 10 (Figure 3.9, last trace).

The single-channel current amplitude was estimated for each cluster separately using all point histograms and also was checked visually (see Methods). The main amplitude of mutant

receptor single channel currents was 5.22 ± 0.11 pA very similar to the one measured for wild type receptor (cf. 5.77 ± 0.06, $n$ = 13, 30 clusters, respectively, Figure 3.9). However, in the single-channel record from mutant receptor it was observed that the mutant receptor can open to a lower conductance level, an example of which is indicated with the arrow in the Figure 3.9. This sublevel is measured by the all point amplitude histogram as separate peak with amplitude of 4.6 pA. As seen in the indicated figure there seems to be a transition from one level to another 20% lower level. It is also observed that the open channel noise level is much higher than closed channel. This might be due to many very short channel closings which are not resolved.

These results were consistent with different patches tried on different days. It is worth mentioning that for single channel recordings I tested on the same day a wild-type GlyR to make sure that the transfection went well. For HEK293 cells expressing mutant homomeric GlyRs only 2 records out of 21 patches were suitable for analysis. The expression level of this mutation was poor as 55% of DNA was needed to have transfected cells compared to 2 % in wild-type GlyRs.

Similar results were obtained for single-channel recordings of heteromeric GlyR with saturating glycine concentration (50 mM, Figure 3.10). The average maximum $P_{open}$ was reduced without change in the current amplitude. As indicated earlier, measurement of current amplitude and $P_{open}$ was done for each cluster separately. Possible heterogeneity of activity was observed with the openings within the cluster (Figure 3.10). The average approximate $P_{open}$ is 0.67 ± 0.06 ($n$ = 5) a value that significantly lower of the corresponding wild-type with a $P_{open}$ of 0.98 ± 0.01 ($n$ = 29; $p$ < 0.01, unpaired t-test). The current amplitude was similar to that of the corresponding wild-type 3.10 ± 0.16 pA vs 3.07 ± 0.06 ($n$ = 5, 29, respectively). Note that there was no clear stable open level as seen in wild-type. These results were consistent among different patches tested on different days using HEK293 cells. Out of twenty records, only four were suitable for analysis. Please note that on the same day of recording HEK293 cells expressing wild-type were used as a control to make sure there is no artefact and to exclude transfection error.

#### 3.2.8.1 Conclusion- the E103K GlyR mutants.

This hyperekplexia mutation causes a decrease in the potency of the agonist glycine, and this effect is much more pronounced in the heteromeric channel (2.8 cf ~70-fold change in $EC_{50}$). This decrease is associated with a significsnt reduction in the maximum $P_{open}$ recorded in the

cell-attached configuration, from 0.99 ± 0.002 to 0.73 ± 0.07 and 0.98 ± 0.01 to 0.67 ± 0.06 homomeric, heteromeric E103K GlyR, respectively.

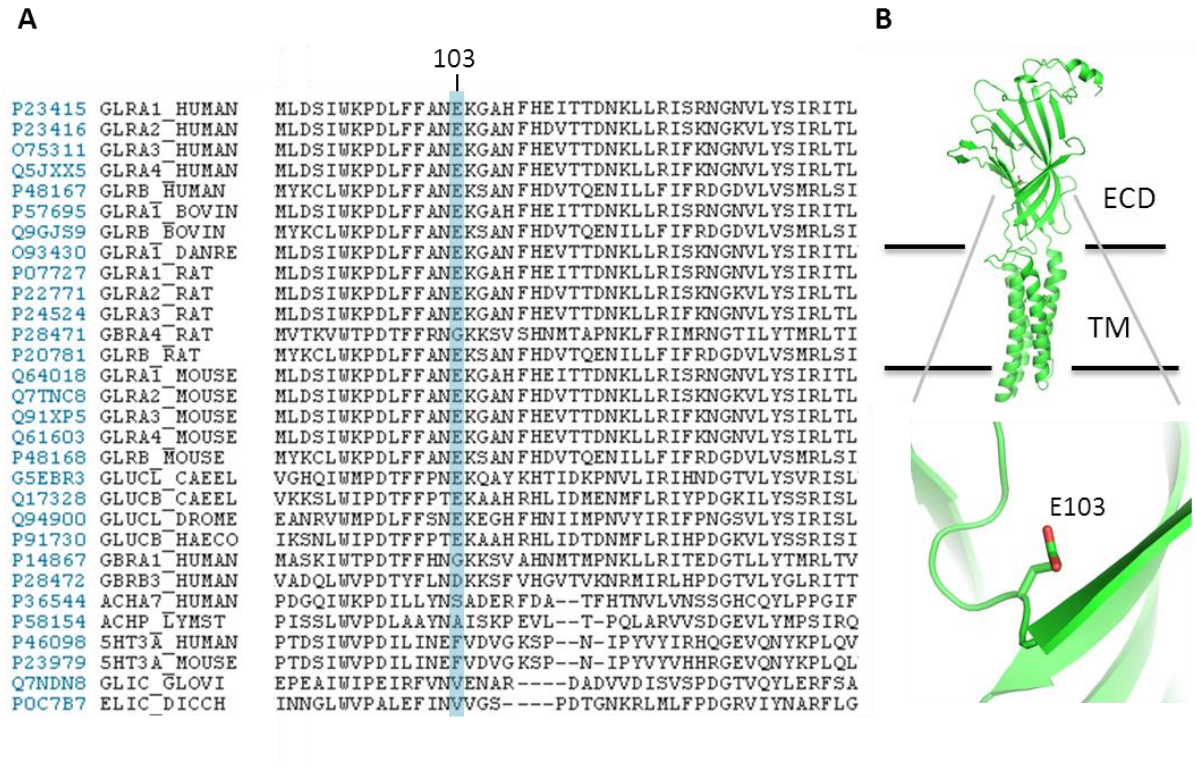


**Figure 3.6 Partial sequence alignment of GlyR with other pLGICs and proteins.**

A) The E103 human hyperekplexia mutation residue in the ECD of the GlyR α1 is highlighted in blue along with the aligned residues in other receptors. Glutamate is conserved in 21 receptors (see text). Uniprot accession numbers are indicated at the left side for each receptor, human glycine α1 (P23415), human glycine α2 (P23416), human glycine α3 (O75311), human glycine α4 (Q5JXX5), human glycine β (P48167), bovine glycine α1 (P57695), bovine glycine β (Q9GJS9), zebrafish glycine α1 (O93430), rat glycine α1 (P07727), rat glycine α2 (P22771), rat glycine α3 (P24524), rat glycine α4 (P28471), rat glycine β (P20781), mouse glycine α1(Q64018), mouse glycine α2 (Q7TNC8), mouse glycine α3 (Q91XP5), mouse glycine α4 (Q61603), mouse glycine β (P48168), *C. elegans* GluCl α (G5EBR3), *C. elegans* GluCl β (Q17328), *D. melanogaster* GluCl α (Q94900), *H. contortus* GluCl β (P91730), human $GABA_A$ α1(P14867), human $GABA_A$ β3 (P28472), human α7 nAChR (P36544), *L. stagnalis* AChBP (P58154), human 5-HT3A (P46098), mouse 5-HT3A (P23979), GLIC (Q7NDN8), and ELIC (P0C7B7). B) Homology model for GlyR α1 subunit based on *C.elegans* GluCl channel showing one GlyR subunit and the location of the indicated residue (see Yu *et al.*, 2014).

**Table 3.2 Literature review of the sensitivity of the human α1 GlyR to N102X, E103X, or K104X mutations, where X = 'other'**

| GlyR Mutation | $EC_{50}$ Glycine (fold change) | $EC_{50}$ β-alanine (fold change) | $EC_{50}$ Taurine (fold change) | $I_{Tau}/I_{maxGly}$ | Expression System | References |
|---|---|---|---|---|---|---|
| α1(N102A) | 44 | 32 | 14 | - | HEK293 | Vafa *et al.*(1999) |
| α1(N102C) | 142 | - | 346 | 0.29 ± 0.02 WT:1.03 ±0.06 | HEK293 | Han *et al.* (2001) |
| α1(E103K) | 26 | - | - | - | HEK293 | Chung *et al.* (2010) |
| α1(E103C) | 44 | - | 35 | 0.90 ± 0.07 WT: 1.03 ± 0.06 | HEK293 | Han *et al.* (2001) |
| α1(E103A) | 0.7 | - | - | - | HEK293 | Vafa *et al.* (1999) |
| α1(K104C) | 0.38 | - | 0.31 | 0.95 ± 0.08 WT: 1.03 ± 0.06 | HEK293 | Han *et al.* (2001) |
| α1(K104A) | 1.7 | - | - | - | HEK293 | Vafa *et al.* (1999) |
| α1(K104A) | 0.75 | 0.40 | 0.56 | 73.2 ± 1.7 WT: 31.9 ± 2.8 | Oocytes | Schmieden *et al.* (1999) |

Fold change = increase from WT to mutant. $I_{Tau}$ = current in response to taurine. $I_{maxGly}$ = current in response to saturating concentration of glycine.

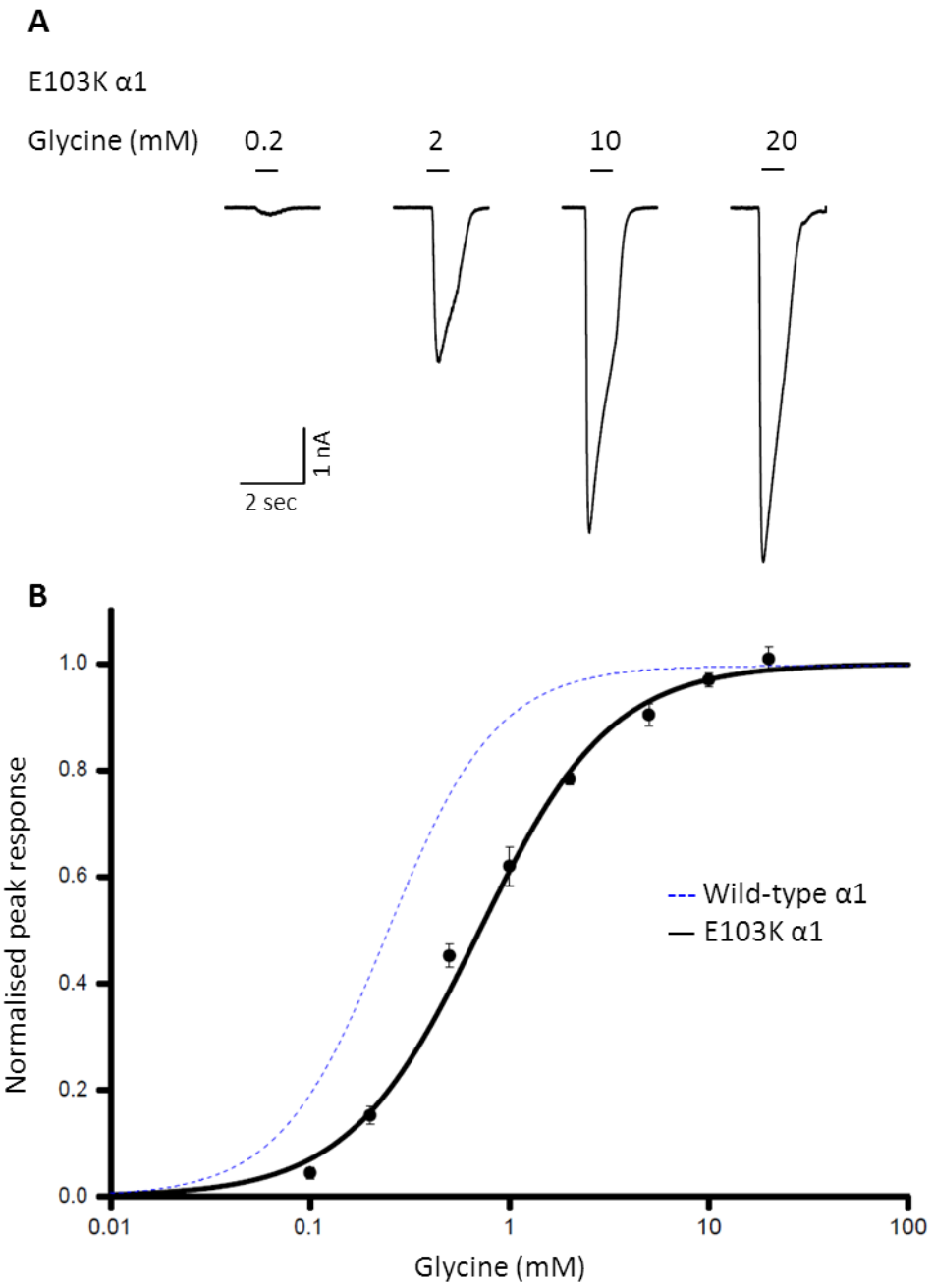


**Figure 3.7 Human α1(E103K) mutant GlyR expressed in HEK293 cells has a reduced sensitivity to glycine.**

A) Example whole-cell current traces showing inward chloride current responses to the indicated glycine concentrations in mM (holding potential = –50 mV). Bars above the traces show the application of glycine. B) Average glycine concentration-response curve for the homomeric E103K GlyR is shifted to the right by ~ 3 fold. The curve is a fit to the Hill equation with $EC_{50}$ = 0.71 ± 0.11 mM, $n_H$ = 1.32 ± 0.07, $I_{max}$ = 1.32 ± 0.07, $n$ = 3. Error bars represent SEM.

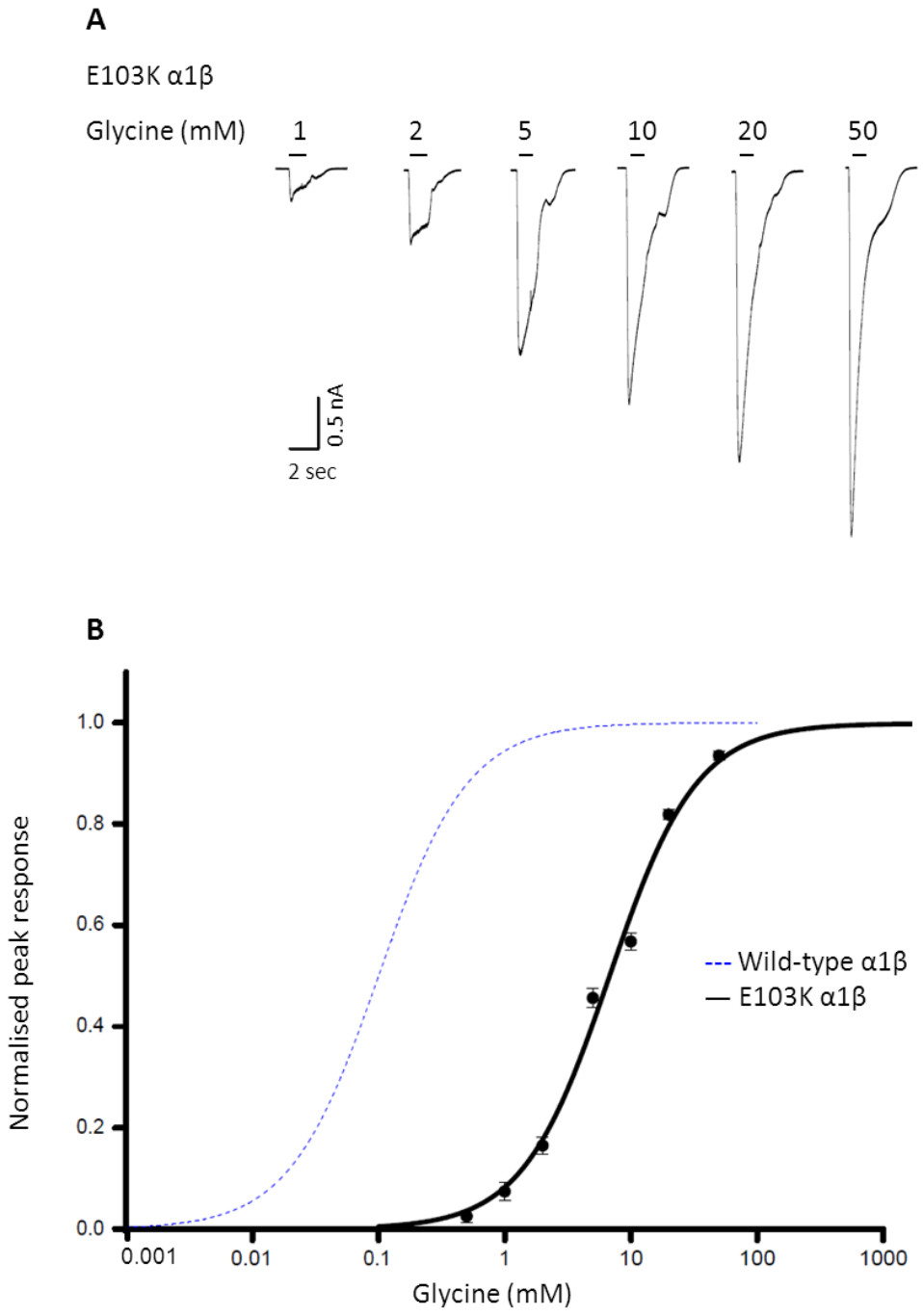


**Figure 3.8 The α1(E103K) mutation reduces the sensitivity to glycine of the human α1β GlyR.**

A) Representative whole cell traces showing inward currents elicited by U-tube application of glycine to HEK293 cells expressing α1(E103K)β human hyperekplexia receptor. The lines over the tracing refer to application of glycine (in mM). Cells were held at –50 mV. B) Average glycine concentration-response curve fitted with the Hill equation $EC_{50}$ = 7.27 ± 0.58 mM, $n_H$ = 1.22 ± 0.08, $I_{max}$ = 3.62 ± 0.89 nA, $n$ = 6 cells. Error bars represent SEM.

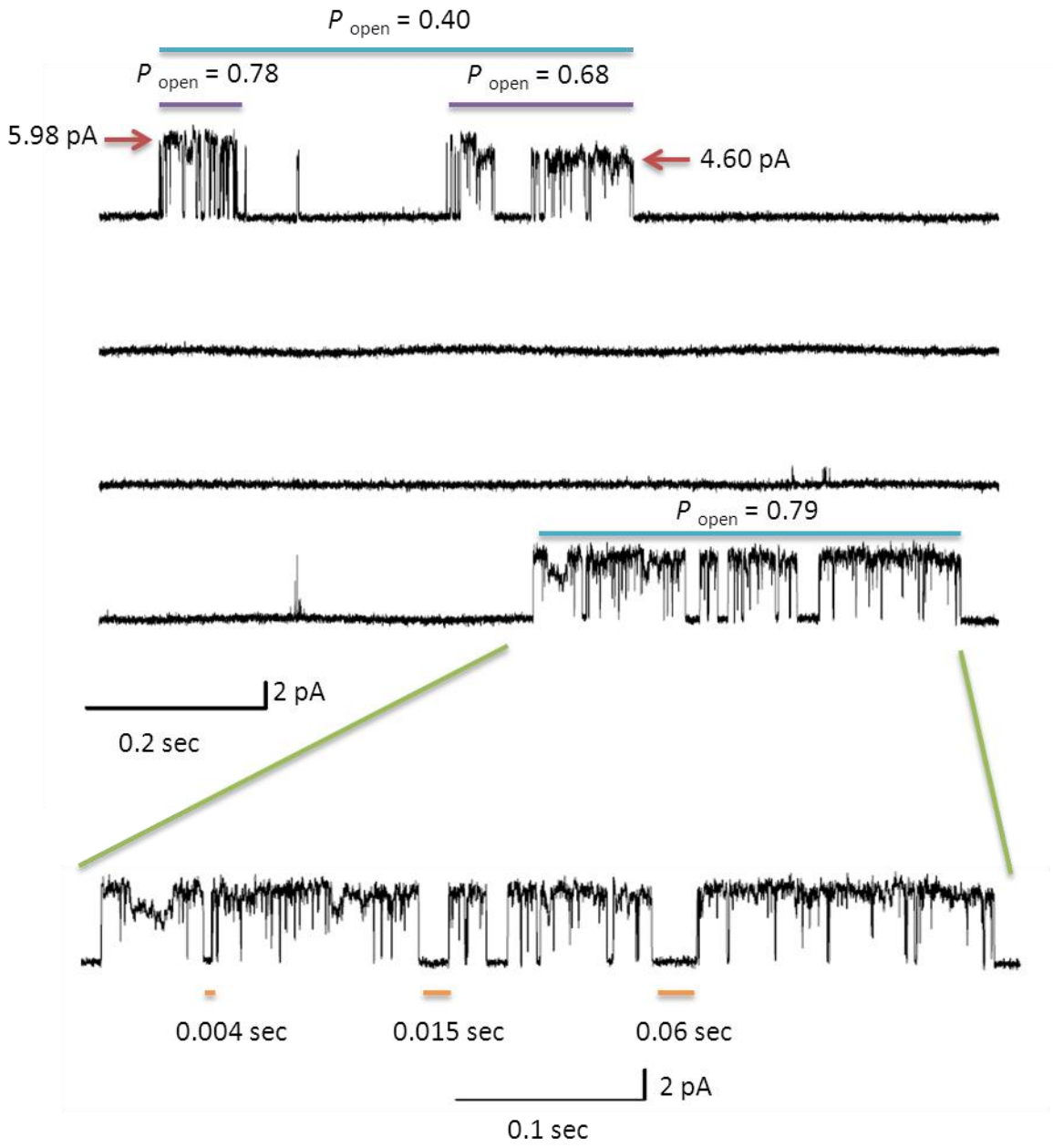


**Figure 3.9 α1(E103K) GlyR mutation reduces maximum $P_{open}$ in response to 50 mM glycine, a saturating concentration of agonist for this receptor.**

These single-channel traces (cell-attached, pipette potential + 100 mV) show that the mutant receptor opens in clusters, but at lower maximum open probability. Average maximum $P_{open}$ = 0.73 ± 0.07, average amplitude = 5.24 ±1.4 pA, $n$ = 13 clusters. Note the relative unstable opening level and existence of possible sublevels.

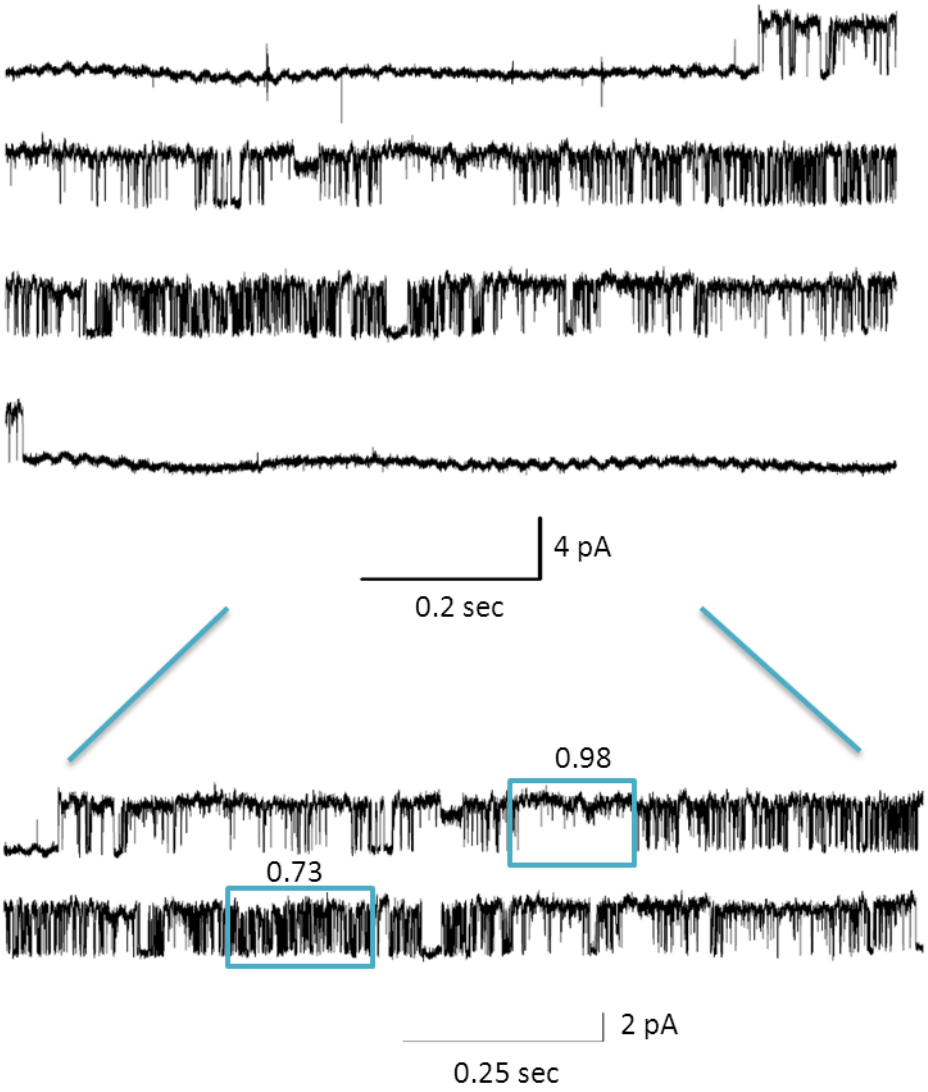


**Figure 3.10 The human hyperekplexia α1(E103K)β GlyR mutation decreases maximum open probability in response to a saturating concentration of glycine.**

Cell-attached single channel traces recorded with saturating glycine concentration of 50 mM (pipette potential +100 mV, 3 kHz low pass filtered) show a profound disruption of the open state by the mutation. Average maximum $P_{open}$ = 0.67 ± 0.06, average amplitude = 3.10 ± 0.16 pA, $n$ = 5 clusters. Expansion of the trace in the lower panel shows presence of different gating modes within the cluster.

## 3.2.9 TM1 domain: the S231N mutation

### 3.2.9.1 Location

The S231 residue is located in TM1 close to the extracellular side (Figure 3.5). Serine in this position is conserved in twenty two pLGICs. It is conserved in all of the human GlyR α subunits (α1, α2, α3, and α4). It is also conserved in bovine and *Danio rerio* (zebrafish) α1 subunit of GlyR. Rat α1, α2, and α3 GlyR subunits have conserved serine in the indicated position. Residues equivalent to S231 GlyR α1 are conserved in mouse α1, α2, α3, and α4 GlyRs. GluCl receptor α subunit from *Caenorhabditis elegans* has a conserved serine in the highlighted position. The amino acid of interest is also conserved in the human $GABA_A$ receptor α1, α2, α3, δ, ε, and π subunits. Sequence alignment of both mouse and human 5-$HT3_A$ receptors shows a conserved residue equivalent to S231 GlyRα1 (Figure 3.11).

The homology model obtained from the GluCl structure by our collaborators at Oxford University, Biggin and Yu, showed that the side chain of S231 may interact with the facing TM2 Q226 residue (Figure 3.5), offering a possible explanation for loss of function produced by the hyperekplexia S231N mutation. As S231 and Q266 are very near to each other, a steric effects of the bigger N side chain could conceivably be disruptive the transmembrane domain and channel gating. The molecular modelling suggests that the wild-type residues S231 and the Q266 may interact by a H-bond. Note that Q266H is also a startle disease mutation (Milani *et al.*, 1996; Moorhouse *et al.*, 1999).

### 3.2.9.2 Hyperekplexia phenotype

The S231N hyperekplexia GlyR mutation was first identified in a white Australian male patient with no family history of hyperekplexia. He had startle symptoms but responded well to clonazepam treatment. In this patient, the S231N missense mutation was found to be co-inherited with the nonsense mutation S296X in TM3. The patient also had an asymptomatic sibling who carried the nonsense S296X mutation alone. Expression of the S296X nonsense mutation in HEK293 cells failed to produce functional channels, whereas both homomeric and heteromeric S231N GlyRs produced functional channels when expressed in HEK293 cells. Glycine sensitivity was markedly decreased, as the glycine $EC_{50}$ shifted by 13 fold for the S231N α1GlyR (from 20 to 262 μM) and 16 fold for heteromeric receptors (from 23 to 383 μM); no change of the Hill slope was reported. The expression level of the mutant S231N GlyR was not affected as the number of cells expressing homomeric, or heteromeric,

S231N GlyRs were similar to the corresponding wild-type cells. This was tested by live cell imaging where quantification of HEK293 cells expression receptor of interest co-transfected with YFP enabled comparing the fluorescence intensity between different groups (Chung *et al.,* 2010). There is no reported data regarding the influence of the S231N GlyR mutation on the relative maximal currents. The same study hypothesized that the S231N mutation was the only functional hemizygous allele of the α1GlyR *in vivo* as neither, homomeric nor heteromeric, S296X GlyR was functional. This was predicted because S296X is a nonsense mutation. The same study predicted that based on homology modelling of *Torpedo* $\alpha_1\beta\gamma\alpha_2\varepsilon$ nicotinic ACh receptor (nAChR) this mutation may produce some alteration in the transmembrane domain, (See Figure S3. A in Chung *et al.,* 2010).

#### 3.2.9.3 Review of the literature reporting other mutations in the same residue:

**S231R**

S231R is another recessive homozygous hyperekplexia mutation found in a 6 years old boy of Iranian origin. Neither of his consanguineous parents displayed symptoms of hyperekplexia, nor his 8 years sister. Symptoms of hyperekplexia, like generalised jerks, were noticed in the patient since the third day after birth. Other symptoms of hyperekplexia, such as sudden falls caused by startle reaction, exaggerated head retraction, and increased muscle tone were also identified. Although treatment with clonazepam improved the patient's condition, the patient was also deemed to have mild mental retardation and impairment in social behaviour. Immunoblotting and whole-cell recordings from HEK293 cells transfected with S231R α1 GlyR revealed reduced recptor expression and reduced channel function as glycine maximal current was reduced (Humeny *et al.,* 2002). Another study (Villman *et al.,* 2009) confirmed that recombinant expression of homomeric, or heteromeric, α1 GlyR S231R resulted in reduced glycine-evoked whole-cell maximal current associated with reduced cell membrane integration. So for the S231R mutation it is more likely that insufficient plasma membrane insertion has more effect on the reduced glycinergic inhibition than improper channel binding, or gating, by glycine.

**S231A**

Another study evaluated the effect of alanine replacement of S231 in α1 GlyR and found that surface expression was unaffected when evaluated using [$^{35}$S] methionine-protein labelling method (Haeger *et al.*, 2010).

### 3.2.10 Whole-cell recordings from human homomeric GlyR bearing the α1(S231N) hyperekplexia mutation

To further characterize the α1(S231N) hyperekplexia mutation and determine if it has an effect on glycine efficacy as well as $EC_{50}$, whole-cell experiments were conducted. Example whole-cell traces are shown in Figure 3.12. The mutation produced a significant decrease in glycine potency, with an increase in glycine $EC_{50}$ of about four fold from 0.25 ± 0.03 to 1.16 ± 0.13 mM ($n$ = 6, 4, respectively; $p < 0.01$, unpaired t-test; Table 3.3). The average Hill slope slope was comparable with that of wild-type GlyR 1.87 ± 0.37 (WT, $n$ = 6), 1.11 ± 0.06 (α1(S231N), $n$ = 4; $p > 0.05$, unpaired t-test, Table 3.3). The maximum current was less than wild-type 10.34 ± 2.47 vs 2.05 ± 0.50 ($p < 0.05$, unpaired t-test; Table 3.3). The time course of the responses did not seem to be in any way different from those recorded from wild-type GlyR, but saturation was reached at about 20 mM. Desensitisation was observed in responses to glycine concentrations greater than 0.2 mM, approximately $EC_{10.}$

### 3.2.11 Whole-cell recordings from human heteromeric GlyR expressing the α1(S231N) hyperekplexia mutation

I next evaluated the effect of co-expression of the GlyR β subunit together with α1 S231N (α1: β ratio 1:40). Whole-cell recordings of the α1(S231N)β GlyRs showed a much greater reduction in glycine sensitivity than in homomeric channels bearing the same mutation. Glycine $EC_{50}$ significantly increased by ~ 40 fold, from 0.10 ± 0.03 mM (wild-type) to 3.81 ± 0.42 mM (α1(S231N)β, $n$ = 6, 4, respectively; $p < 0.01$, unpaired t-test; Figure 3.13, Table 3.4). Desensitization was noticeable at glycine concentrations equal to or greater than 1 mM ($EC_{20}$) and achieving maximum current response required a glycine concentration of 50 mM (Figure 3.13.A). The average Hill slope for α1(S231N)β was less than the corresponding wild-type, 1.12 ± 0.06 vs. 1.48 ± 0.09 ($n$ = 4, 6, respectively; $p < 0.05$, unpaired t-test; Table 3.4). The expression level was sufficient to allow us to obtain recordings with average

maximal response of 3.84 ± 0.80 nA ($n$ = 4) compared to 4.43 ± 1.08 nA ($n$ = 6) for wild-type heteromeric GlyR ($p$ = > 0.05, unpaired t-test; Table 3.4).

Single-channel recordings of the homomeric channels were not tested as both homomeric and heteromeric wild-type GlyRs have similar maximal $P_{open}$. Also, the E103 α1 and α1β GlyR showed comparable glycine maximal $P_{open}$. I decided to record from the heteromeric receptors as they represent the native form of synaptic GlyRs.

### 3.2.12 Single-channel recordings of α1(S231N)β hGlyR

Single channel recordings were done in the cell-attached configuration using a saturating glycine concentration of 100 mM. As sample single channel trace is illustrated in Figure 3.14. The trace clearly shows how the S231N α1 mutation profoundly changed the function of the heteromeric GlyR. Measurements of maximal $P_{open}$ were done for each cluster separately and the maximum $P_{open}$ was estimated as cluster open time/total cluster time (see Methods). The average maximum glycine $P_{open}$ was found to be significantly reduced by the mutation, to 0.38 ± 0.06 ($n$ = 16 clusters, 3 patches; $p$ < 0.0001, unpaired t-test), cf 0.98 ± 0.01 ($n$ = 29 clusters, 6 patches) in wild-type (Table 3.5).

Different modes of openings were obvious within each cluster from three records. This phenomenon was not detected in wild-type heteromeric GlyR activated by saturating concentrations of glycine (Figure 3.4). An attempt to measure the different modes of openings within the cluster is illustrated in Figure 3.14. Different parts of the cluster that seem to have similar mode of opening were first selected visually. The beginning and the end of the area of interest was defined by using Clampfit 10.2 (see Methods) and $P_{open}$ was measured for the selected part. It seems there are three modes of opening within the cluster (in this cluster) with approximate maximum $P_{open}$ of 0.1, 0.4, and 0.8. All of these modes within the cluster contributed to a cluster approximate maximum $P_{open}$ of 0.57. The current amplitude was less than the corresponding wild-type GlyR with 2.01 ± 0.05 for α1(S231N)β ($n$ = 29 clusters, 6 patches) and 3.07 ± 0.06 pA for (WT, $n$ = 16 clusters, 3 patches; $p$ < 0.001, unpaired t-test; Table 3.5). The overall finding clearly indicates that the human hyperekplexia α1(S231N)β GlyR mutation impairs channel gating.

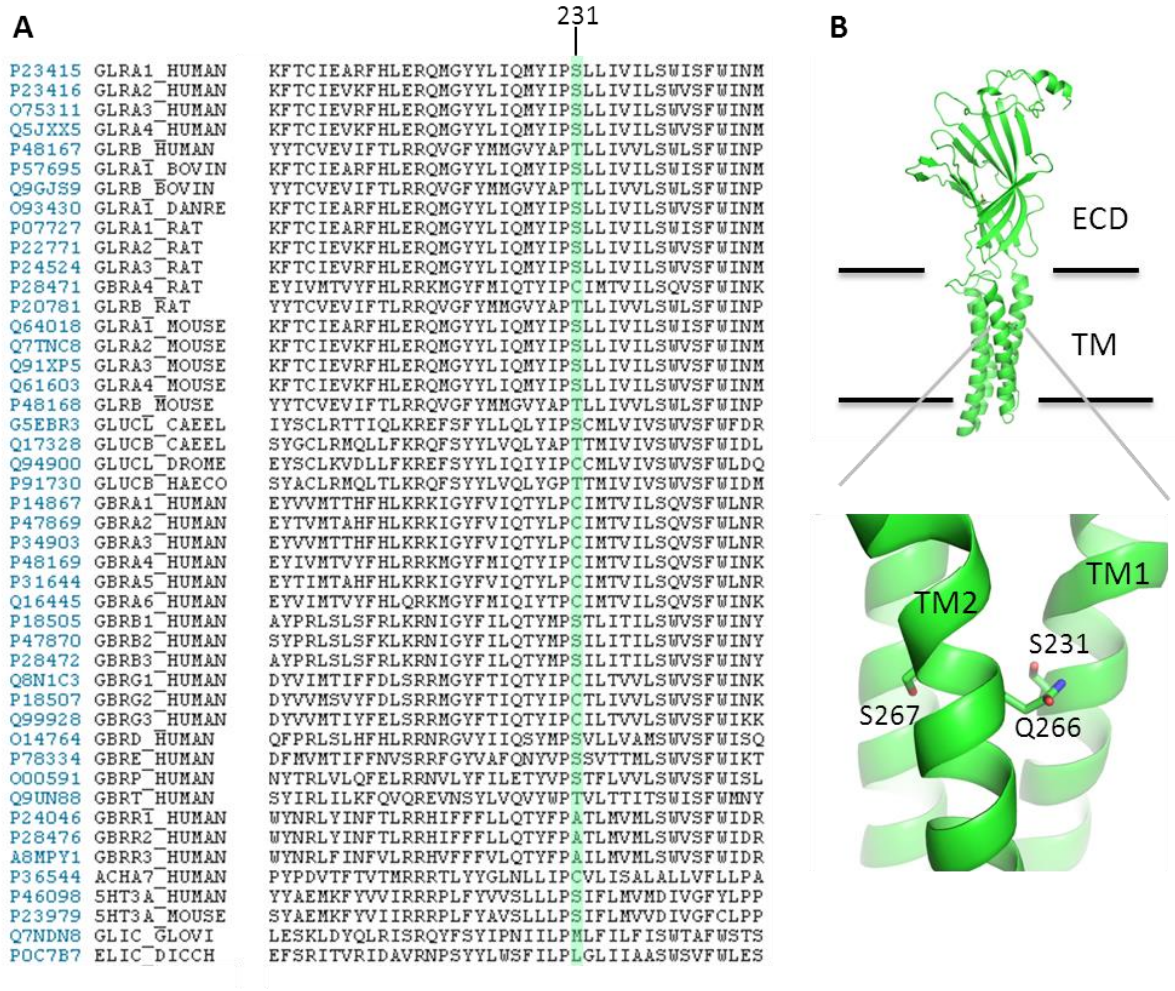


**Figure 3.11 Partial sequence alignment of TM1 S231 GlyR with a selection of related pLGICs.**

A) Equivalent residues to the selected human α1 GlyR hyperekplexia mutation S231 are highlighted in green. Serine in this location is conserved in twenty two receptors. Uniprot accession numbers are indicated: human glycine α1 (P23415), human glycine α2 (P23416), human glycine α3 (O75311), human glycine α4 (Q5JXX5), human glycine β (P48167), bovine glycine α1 (P57695), bovine glycine β (Q9GJS9), zebrafish glycine α1 (O93430), rat glycine α1 (P07727), rat glycine α2 (P22771), rat glycine α3 (P24524), rat glycine α4 (P28471), rat glycine β (P20781), mouse glycine α1(Q64018), mouse glycine α2 (Q7TNC8), mouse glycine α3 (Q91XP5), mouse glycine α4 (Q61603), mouse glycine β (P48168), *C. elegans* GluCl α (G5EBR3), *C. elegans* GluCl β (Q17328), *D. melanogaster* GluCl α (Q94900), *H. contortus* GluCl β (P91730), human $GABA_A$ α1 (P14867), human $GABA_A$ α2 (P47869), human $GABA_A$ α3 (P34903), human $GABA_A$ α4 (P48169), human $GABA_A$ α5 (P31644), human $GABA_A$ α6 (Q16445), human $GABA_A$ β1 (P18505), human $GABA_A$ β2 (P47870), human $GABA_A$ β3 (P28472), human $GABA_A$ γ1 (Q8N1C3), human $GABA_A$ γ2 (P18507), human $GABA_A$ γ3 (Q99928), human $GABA_A$ δ (O14764), human $GABA_A$ ε (P78334), human $GABA_A$ π (O00591), human $GABA_A$ θ (Q9UN88), human $GABA_A$ ρ1 (P24046), human $GABA_A$ ρ2 (P28476), human $GABA_A$ ρ3 (A8MPY1), human α7 nAChR (P36544), human 5-HT3A (P46098), mouse 5-HT3A(P23979), GLIC (Q7NDN8), and ELIC (P0C7B7). B) Homology model based on C.elegans GluCl channel showing the location of the S231 residue in one subunit of GlyR α1 (see Yu *et al.*, 2014).

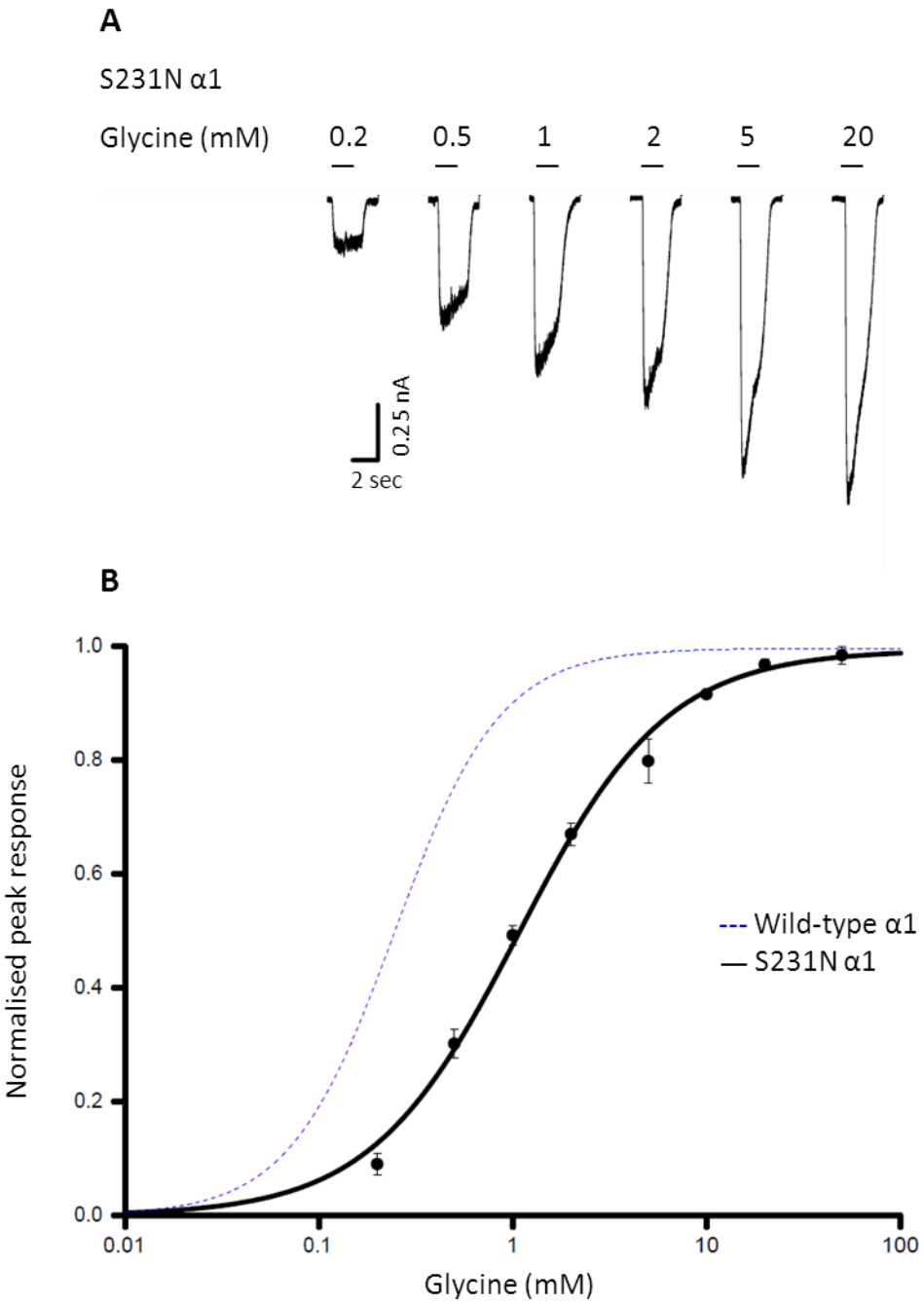


**Figure 3.12 Human α1(S231N) hyperekplexia mutation impaired the sensitivity of the homomeric hGlyR to glycine.**

A) Whole-cell current responses from HEK293 cells expressing human α1(S231N) GlyR. Glycine-evoked currents recorded at –50 mV. Glycine concentrations in mM are indicated above the traces; the bars show the duration of each application. B) Glycine concentration-response curve (normalized to their maximal response) is shifted to the right by the mutation, with $EC_{50}$ value of 1.16 ± 0.13 mM, $n$ = 4. Data points in this figure represent mean values fitted to the Hill equation. $n_H$ = 1.11 ± 0.06, $I_{max}$ = 2.05 ± 0.50 nA, $n$ = 4 cells. Error bars indicate SEM.

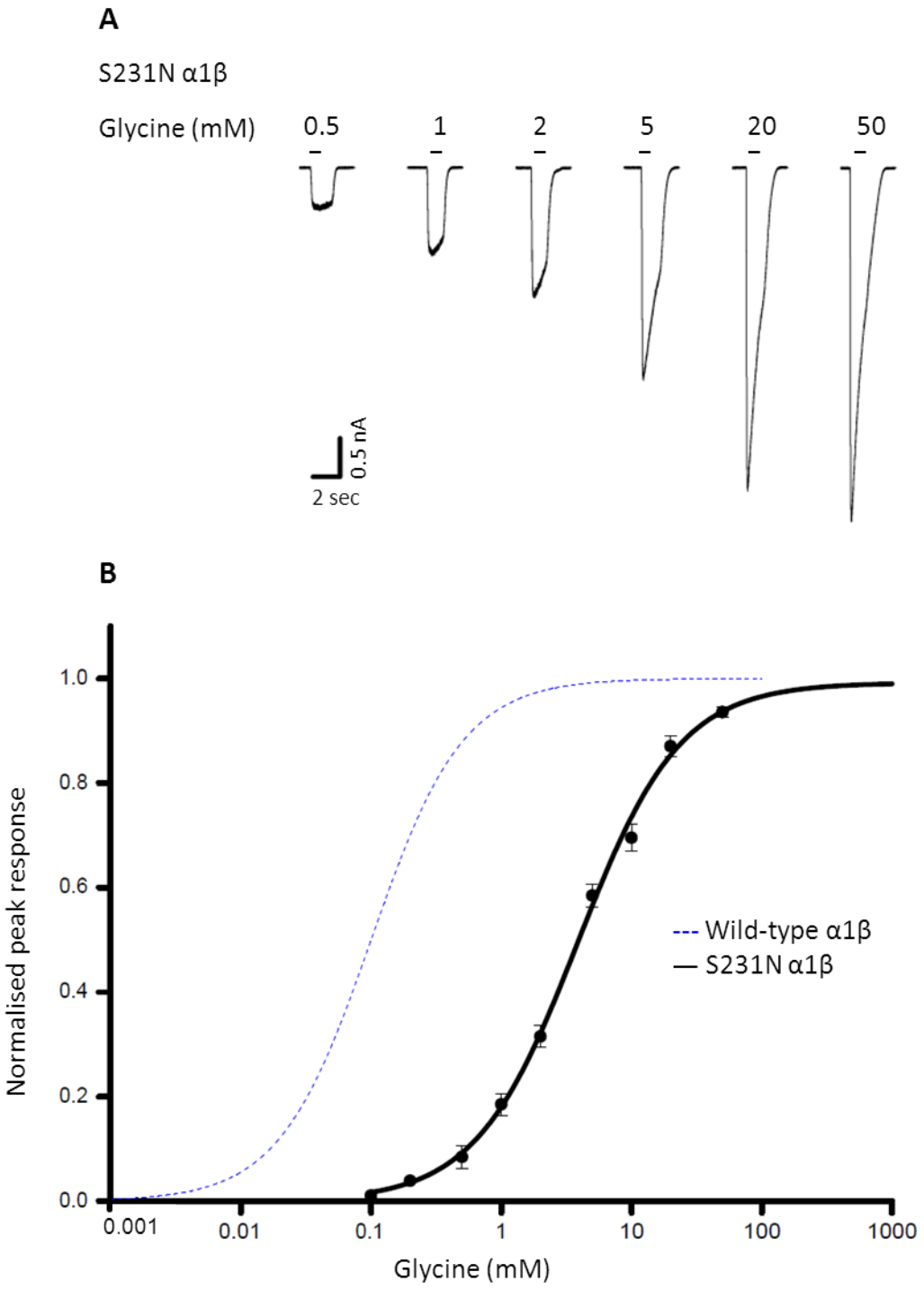


**Figure 3.13 The human heteromeric hyperekplexia α1(S231N)β GlyR mutation reduces the channel sensitivity to glycine.**

A) Whole-cell current responses from HEK293 cells expressing human α1(S231N)β GlyR. Glycine-evoked currents recorded at −50 mV. Glycine concentrations in mM are indicated above the traces; the bars show the duration of each application. B) Glycine concentration-response curve (normalized to their maximal response) is shifted to the right by the mutation, with $EC_{50}$ value of 3.81 ± 0.42 mM, $n$ = 4. Data points in this figure represent mean values fitted to the Hill equation. $n_H$ = 1.12 ± 0.06, $I_{max}$ = 3.84 ± 0.80 nA, $n$ = 4 cells. Error bars indicate SEM.

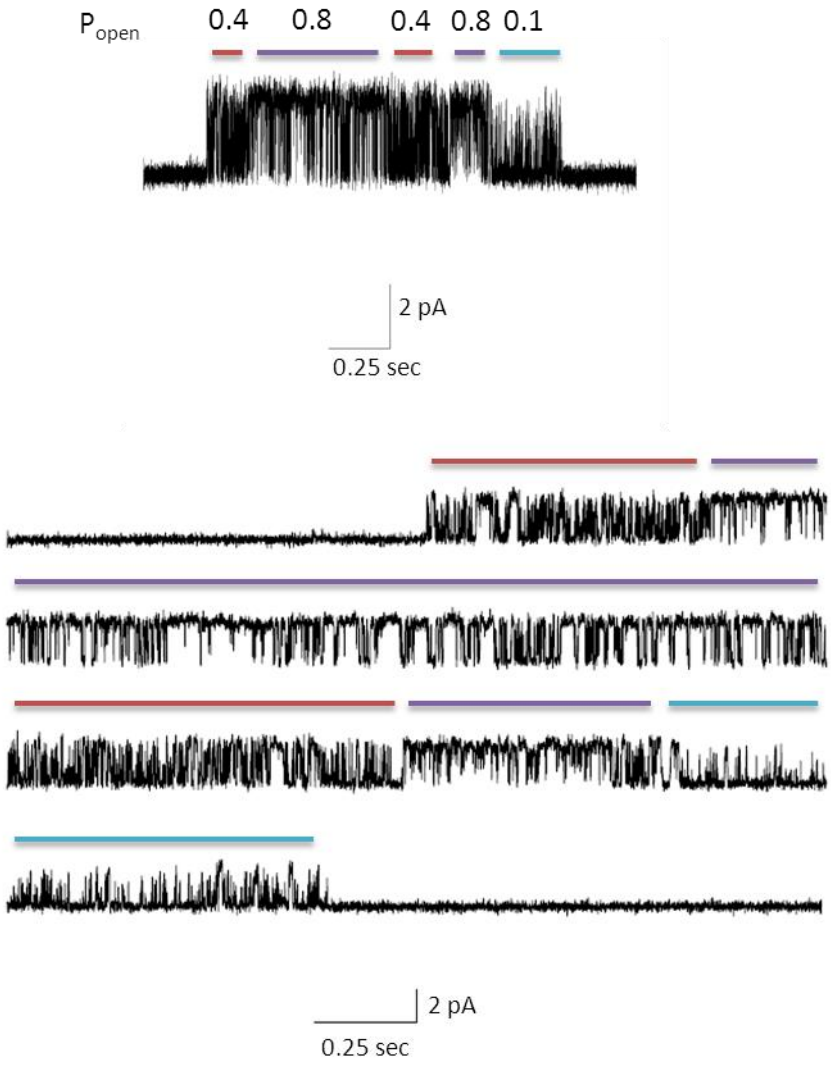


**Figure 3.14 The α1(S231N)β mutation decreases the maximum $P_{open}$ of heteromeric GlyR in response to saturating concentration of glycine.**

Mutant GlyRs show different modes within a cluster. Representative single channel cell-attached trace recorded at pipette potential +100 mV. Average maximal $P_{open}$ was reduced to 0.38 ± 0.06 in mutant GlyR ($n$ = 16). Expanded view of the cluster is shown in the lower panel. Lines with different colours above the trace indicating different modes of $P_{open}$ within the cluster (purple: 0.8, red: 0.4, blue: 0.1). Average amplitude = 2.01 ± 0.05 pA.

## 3.2.13 The Q266H mutation (14'TM2)

### 3.2.13.1 Location

The Q266 residue is part of the TM2 domain, which lines the channel pore (Figure 3.15). An alignment of the TM2 sequences (with the 14' residue highlighted) of the human GlyR α1 subunit with glycine receptor subunits from other species and with related pLGICs (obtained from Swiss-Prot, June, 2015) is shown in the same figure. There are 15 conserved glutamine residues homologous to the 266 glutamine located in 14' TM2 in the human GlyR α1 subunit. These include human, rat and mouse α1, α2, α3, and α4, and bovine α1, whereas β subunits (in man, rat, mouse and cattle) have glutamate. Glutamine is conserved also in GlyR subunits of other species like α Z1 of *Danio rerio* (Zebrafish) and in GluCl α of both *Caenorhabditis elegans* and *Drosophila melanogaster* (fruit fly).

The human hyperekplexia mutation Q266H induces a positive charge in the pore region which in theory might have beneficial effect for $Cl^-$ ion flow through the transmembrane pore. As indicated previously in this Chapter the Q266 residue might interact with the TM1 S231 residue (Figure 3.5).

### 3.2.13.2 Reported hyperekplexia family case

Milani et al reported an Italian family with hyperekplexia caused by the α1(Q266H) GlyR mutation (Milani *et al.,* 1996). The phenotype varied from one patient to another, but clearly became more severe with the third generation. Thus, in the family studied, no signs of hyperekplexia were observed in the adults of the first generation although the mutation was found in two members. This might be due to the disappearance of the symptoms in adulthood. All of the mutation carrier patients in the second and third generations had an exaggerated startle response. Hypertonia was found in one member of the second generation and in two members of the third generation. Apnoea attacks following myoclonic fits led to the death of a 45 days age infant, highlighting the severity of the symptoms in the third generation (Milani *et al.,* 1996).

### 3.2.13.3 Review of the literature reporting mutations in the same residue

**Q266H**

Glycine and taurine potency was found to be reduced by 6 fold in human homomeric α1 Q266H GlyR expressed in HEK293 cells compared to WT GlyR (Moorhouse *et al.,* 1999).

This mutation was also reported to reduce the sensitivity to glycine by 5 fold in another study using HEK293 cells (Castaldo *et al.,* 2004). In the same study the whole-cell efficacy of β-alanine, or taurine, relative to glycine was reduced compared to wild-type GlyRs ($I_{\beta\text{-alanine}}/I_{\text{Glyine}}$ from 0.95 to 0.70, $I_{\text{Taurine}}/I_{\text{Glycine}}$ from 0.90 to 0.50).

Plasma membrane expression level of Q266H α1 GlyR in HEK293 cells was not affected as shown by western blot experiments for total lysates or streptavidin-purified biotinylated plasma membrane proteins. This indicated that the shift of the agonist sensitivity is due to modified channel function and not to alteration of insertion of the α1 Q266H subunit into the plasma membrane (Castaldo *et al.,* 2004).

It is likely that the Q266H α1 GlyR mutation changed efficacy by decreasing the open probability at high and low glycine concentrations (Moorhouse *et al*., 1999). Single channel recordings of α1 Q266H GlyR in outside-out patches showed that the mean channel open time was shorter in mutant receptors than wild-type at different glycine concentrations (wild-type: 1 - 50 µM; mutant 50 - 250 µM). The mean open time was calculated from individual time constants and their relative contributions. The single-channel conductance was similar between wild-type and Q266H glycine receptors. Although the ability of the channel to open with glycine was reduced, the displacement of strychnine binding by glycine was not affected (Moorhouse *et al*., 1999).

This mutation was also reported to make the receptor less sensitive to zinc potentiation and more sensitive to zinc inhibition (Moorhouse *et al*., 1999). This will be explained further in the fourth Chapter

**Q266I**

Glycine sensitivity was reduced by nearly two fold in human homomeric α1(Q266I) GlyR expressed in HEK293 cells. In heteromeric Q266I GlyR the reduction in glycine sensitivity was somewhat smaller, less than two fold (Xiong *et al.,* 2014). A reduction in glycine sensitivity was reported for the homomeric Q266I GlyR expressed in oocytes (Borghese *et al.,* 2012). The same paper reported that ethanol (50 - 200 mM) enhancement of glycine submaximal current ($EC_5$) was almost absent in oocytes expressing α1 Q266I GlyR. A reduced enhancement effect was also found for the following allosteric enhancers: 73 mM propanol, 11 mM butanol, 2.9 mM pentanol, and 0.57 mM hexanol. However, zinc modulation of glycine response was not changed (Borghese *et al.,* 2012).

Furthermore, increased channel open time and decreased conductance was observed in outside-out single-channel recordings of HEK293 cells expressing α1(Q266I)β GlyR. These data were obtained using 10 μM glycine and compared with the results obtained with 3 μM glycine in wild type channels (Borghese *et al.,* 2012). Note that these results contrast with those of Moorhouse *et al.,* 1999).

Homozygous Q266I knock-in mice displayed muscle tremor and motor control impairment. These mice usually died within three weeks (Borghese *et al.,* 2012). Heterozygous α1 GlyR Q266I mice, however, survived and displayed increased startle response to sound stimuli (a hyperekplexia phenotype) (Blendnov *et al.,* 2012; Borghese *et al.,* 2012; Xiong *et al.,* 2014).

### 3.2.14 Whole-cell recordings from human homomeric GlyR bearing the α1(Q266H) hyperekplexia mutation

Whole-cell concentration-response curves to glycine from HEK 293 cells expressing α1(Q266H) GlyR were obtained. Sample current responses to glycine are illustrated in Figure 3.16.A. The risetime of the currents appeared to be faster with higher glycine concentrations and desensitization become clear at 0.5 mM ($EC_{40}$). The channel sensitivity to (0.1 – 50 mM) glycine was reduced significantly, as glycine $EC_{50}$ was increased by 2.7 fold from 0.25 ± 0.03 (wild-type) to 0.68 ± 0.17 mM (α1(Q266H)) GlyR, $n$ = 6, 4, respectively ($p < 0.01$, unpaired t-test; Figure 3.16.B; Table 3.3). The Hill slope obtained was comparable with corresponding exhibited from wild-type GlyR 1.87 ± 0.37 (WT, $n$ = 6) and 1.38 ± 0.40 (α1(Q266H), $n$ = 4; $p > 0.05$, unpaired t-test). The maximum currents were 10.34 ± 2.47 nA for the wild-type ($n$ = 6) and 5.27 ± 2.68 nA for α1(Q266H) GlyRs ($n$ = 4; $p > 0.05$, unpaired t-test, Table 3.3). In order to have sufficient expression of the Q266H GlyR in HEK293 cells, more plasmid was used than of wild-type GlyR (see Methods).

### 3.2.15 Whole-cell recordings from human heteromeric GlyR expressing the α1(Q266H)β hyperekplexia mutation

I investigated the effect of co-expression of the wild-type GlyR β subunit together with α1 Q266H (α1: β ratio 1:40). Whole-cell concentration-response curves from HEK 293 cells expressing heteromeric GlyR were obtained (Figure 3.17). Glycine-gated currents showed

desensitization with glycine concentrations of 0.5 mM ($EC_{30}$) and above. Also, the risetime of the glycine current response was faster with increasing glycine concentration. A significant reduction in the channel sensitivity to glycine was observed in α1(Q266H)β GlyR, with glycine $EC_{50}$ shifted from 0.10 ± 0.02 mM to 1.16 ± 0.19 mM for wild-type, Q266H GlyR respectively ($n$ = 6, 5, respectively; $p < 0.001$, unpaired t-test, Table 3.4). Thus the effect of the mutation was much larger in heteromeric GlyR, with a 10-11-fold decrease in glycine potency.

The average maximal response to glycine for α1(Q266H)β GlyR was 9.07 ± 1.16 nA compared to average maximal response in wild-type 4.43 ± 1.08 ($n$ = 5, 6, respectively, $p >$ 0.05, unpaired t-test). The Hill slope was similar for wild-type and the mutant GlyR with 1.48 ± 0.09 vs 1.35 ± 0.10 ($n$ = 6, 5, respectively, $p > 0.05$, unpaired t-test; Table 3.4).

### 3.2.16 Single-channel recordings of heteromeric α1(Q266H)β GlyR

Single-channel currents in cell-attached configuration were investigated for the α1(Q266H)β GlyR using a saturating glycine concentration of 50 mM (Figure 3.18). Activation of the heteromeric Q266H glycine channels was detectable. However, reduced channel openings were observed, without obvious cluster type opening. After the short openings, the channel tended to desensitize.

The lack of obvious clusters made it very difficult to estimate open probability with any degree of certainty. In the illustrated example, these were the only openings that were detected in the patch. If we assume that the whole trace came from one channel, $P_{open}$ could be measured from the first channel opening to the last opening as it was considered as one channel. In comparison to wild-type GlyRs, the average maximum $P_{open}$ of human α1(Q266H)β GlyR was reduced significantly from 0.98 ± 0.01 ( $n$ = 20 apparent clusters from 6 records) to 0.61 ± 0.06 ($n$ = 29 clusters from 6 records; $p < 0.001$, unpaired t-test; Table 3.5). The average current amplitude of the mutant GlyR was 3.06 ± 0.08 pA ($n$ = 20 apparent cluster from 6 records) similar to the average current amplitude of wild-type receptors 3.07 ± 0.06 pA ($n$ = 29 clusters from 6 records; $p > 0.05$, unpaired t-test; Table 3.5). The trace in the indicated figure shows that the Q266H mutation reduced the channel open probability. This effect suggests that the α1(Q266H)β mutation impaired the channel gating.

**Conclusion- the Q266H GlyR mutants.** This hyperekplexia mutation caused a significant reduction of the glycine potency and the effect is more marked in the heteromeric α1(Q266H)β GlyR (2.7 cf ~ 12 fold change). This reduction is related to a significant reduction in the maximum open probability recorded in the cell-attached configuration from 0.98 ± 0.01 to 0.61 ± 0.06.

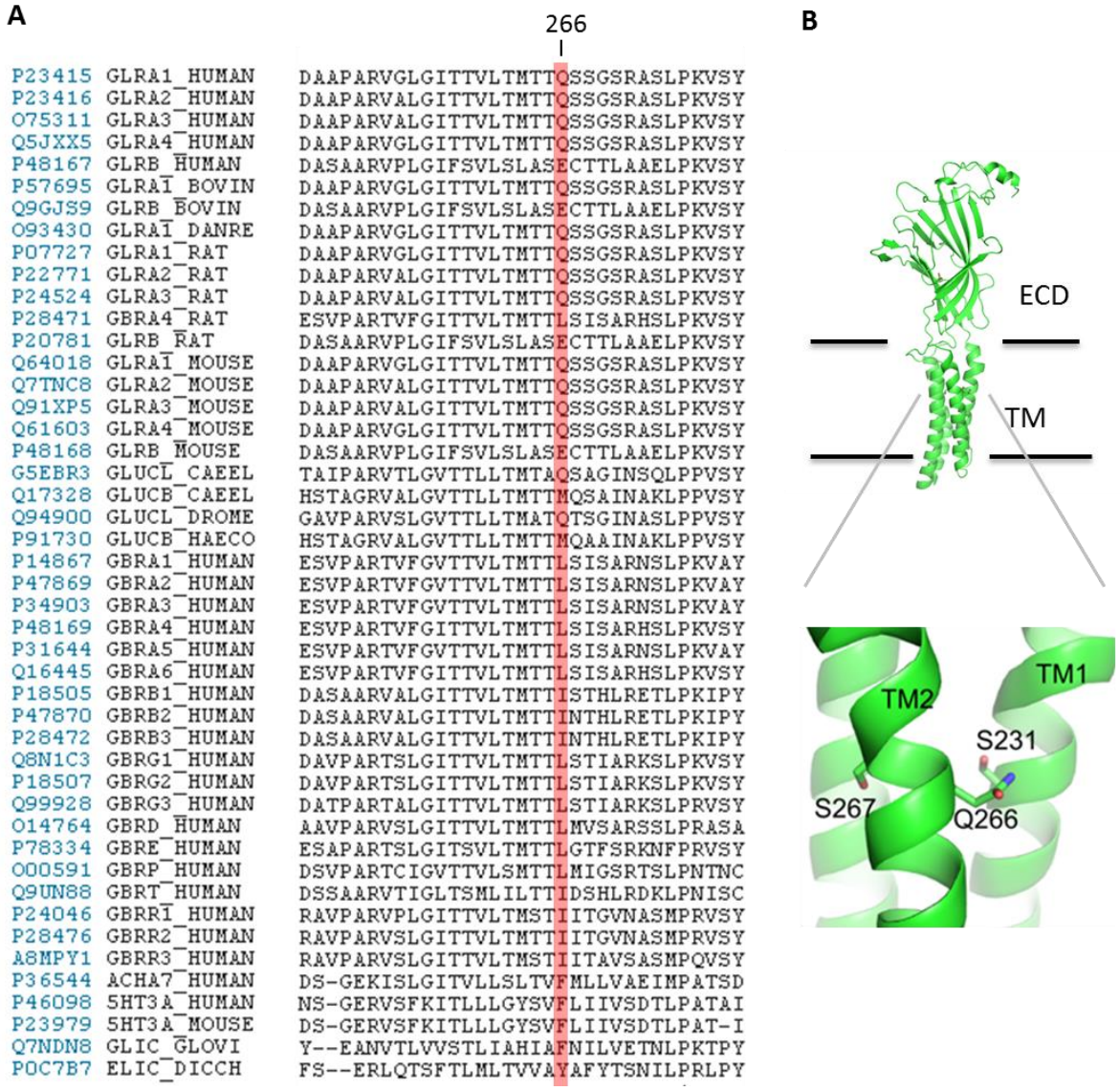


**Figure 3.15 Partial sequence alignment of TM2 Q266 GlyR with a selection of related pLGICs.**

A) Equivalent residues to the selected human α1 GlyR hyperekplexia mutation Q266 are highlighted in red. Glutamine in this location is conserved in fifteen subunits. Uniprot accession numbers are indicated: human glycine α1 (P23415), human glycine α2 (P23416), human glycine α3 (O75311), human glycine α4 (Q5JXX5), human glycine β (P48167), bovine glycine α1 (P57695), bovine glycine β (Q9GJS9), zebrafish glycine α1 (O93430), rat glycine α1 (P07727), rat glycine α2 (P22771), rat glycine α3 (P24524), rat glycine α4 (P28471), rat glycine β (P20781), mouse glycine α1(Q64018), mouse glycine α2 (Q7TNC8), mouse glycine α3 (Q91XP5), mouse glycine α4 (Q61603), mouse glycine β (P48168), *C.*

*elegans* GluCl α (G5EBR3), *C. elegans* GluCl β (Q17328), *D. melanogaster* GluCl α (Q94900), *H. contortus* GluCl β (P91730), human $GABA_A$ α1 (P14867), human $GABA_A$ α2 (P47869), human $GABA_A$ α3 (P34903), human $GABA_A$ α4 (P48169), human $GABA_A$ α5 (P31644), human $GABA_A$ α6 (Q16445), human $GABA_A$ β1 (P18505), human $GABA_A$ β2 (P47870), human $GABA_A$ β3 (P28472), human $GABA_A$ γ1 (Q8N1C3), human $GABA_A$ γ2 (P18507), human $GABA_A$ γ3 (Q99928), human $GABA_A$ δ (O14764), human $GABA_A$ ε (P78334), human $GABA_A$ π (O00591), human $GABA_A$ θ (Q9UN88), human $GABA_A$ ρ1 (P24046), human $GABA_A$ ρ2 (P28476), human $GABA_A$ ρ3 (A8MPY1), human α7 nAChR (P36544), human 5-HT3A (P46098), mouse 5-HT3A(P23979), GLIC (Q7NDN8), and ELIC (P0C7B7). B) Homology model based on *C.elegans* GluCl channel showing the location of the Q266 residue in one subunit of GlyR α1 (see Yu *et al*., 2014).

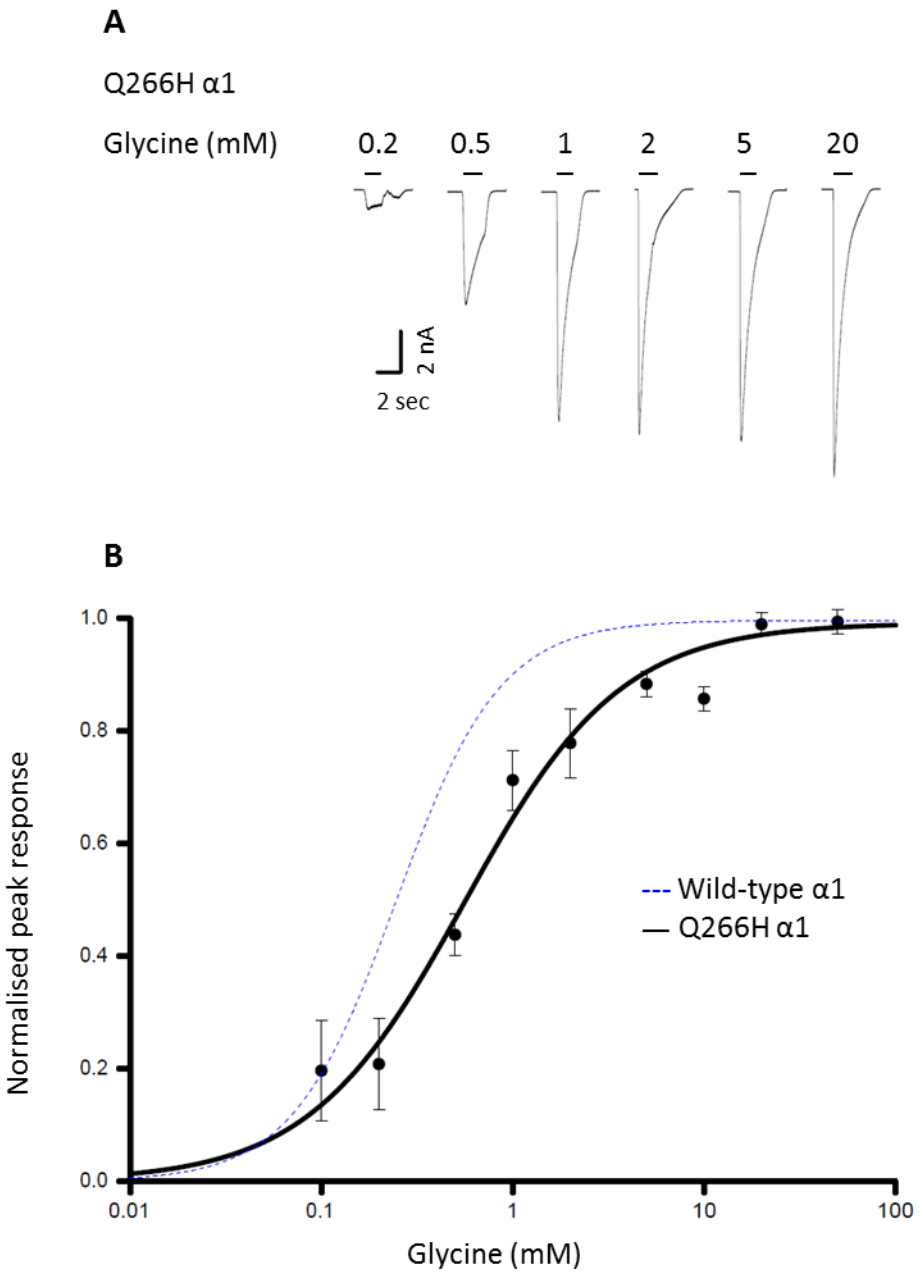


**Figure 3.16 sensitivity of the human α1(Q266H) GlyRs to glycine.**

(A) Representative whole-cell current traces evoked by U-tube application of glycine (black bars) to HEK293 cells expressing recombinant α1(Q266H) GlyRs. Glycine concentrations in mM are indicated above the traces. Cells were held at – 50 mV. B) Average glycine concentration-response curve obtained from α1(Q266H) GlyRs is shifted to the right by the mutation, with $EC_{50}$ value of 0.68 ± 0.17 mM. The solid line is a fit to the Hill equation. $n_H$ = 1.38 ± 0.40, $I_{max}$ = 5.27 ± 2.68 nA, $n$ = 4 cells. Error bars indicate ± SEM.

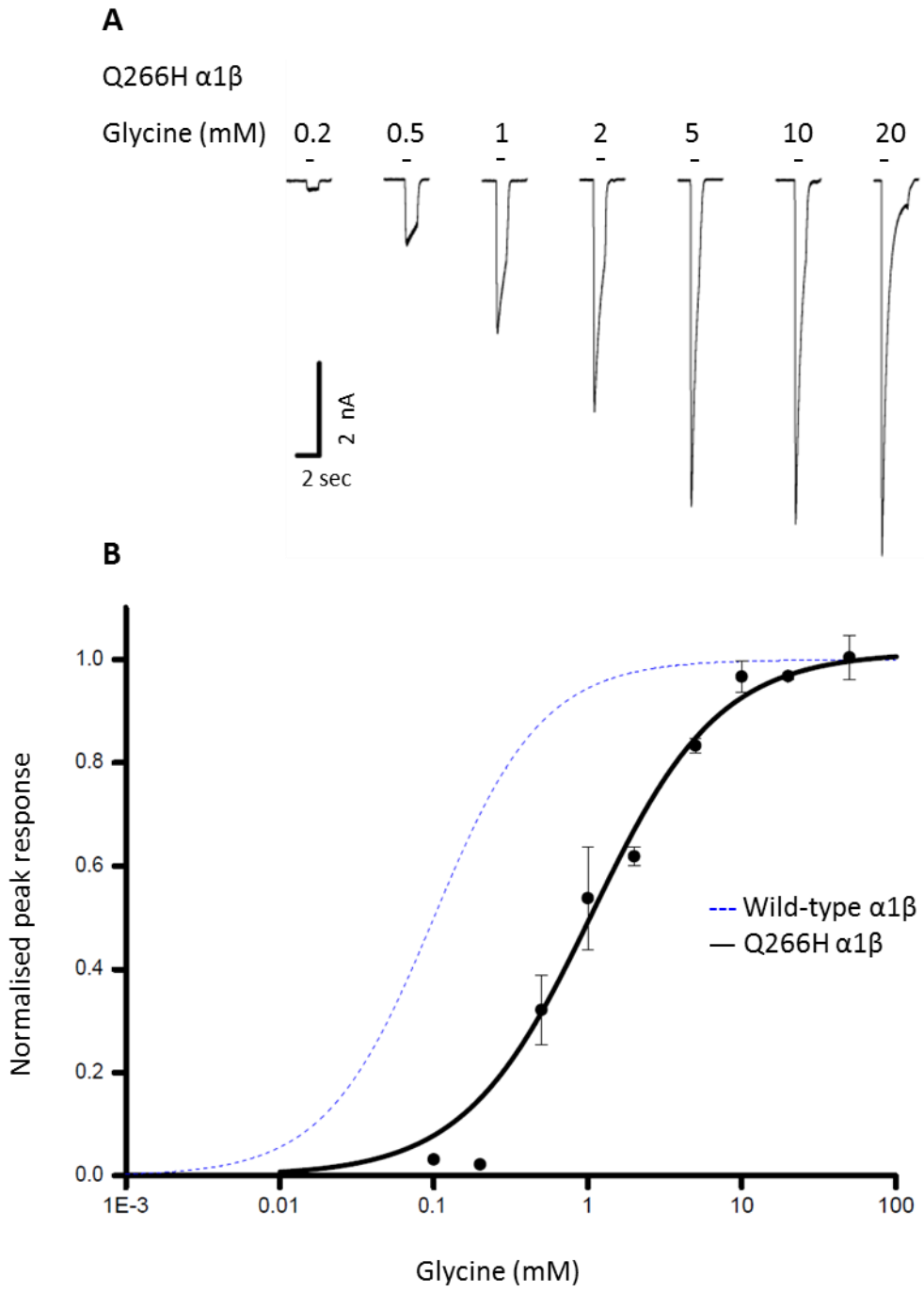


**Figure 3.17 Glycine concentration-response curve of the human α1(Q266H)β GlyR.**
A) Sample whole-cell glycine current traces evoked by U-tube application of different concentrations to HEK293 cells expressing α1(Q266H)β GlyR (at – 50 mV). Concentrations of glycine are shown in mM. B) Average glycine concentration-response curves obtained from α1(Q266H)β GlyR is shifted to the right by ~12 fold, with $EC_{50}$ value of 1.16 ± 0.19 mM. Solid lines are fits to the Hill equation. $n_H$ = 1.35 ± 0.10, $I_{max}$ = 9.07 ± 1.16 nA, $n$ = 5 cells. Error bars indicate ± SEM.

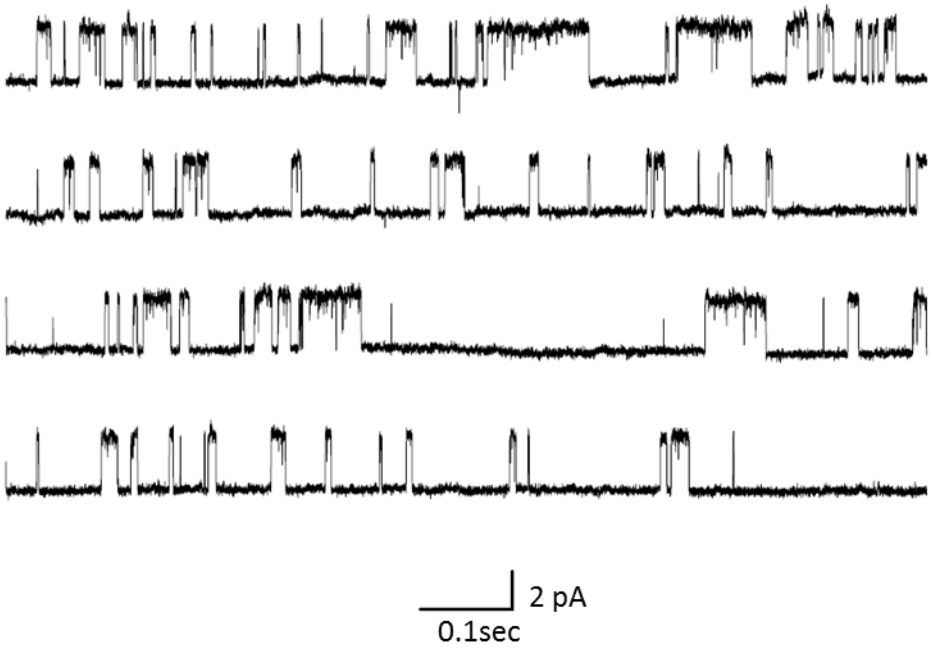


**Figure 3.18 α1(Q266H)β GlyR mutation reduced the maximum $P_{open}$ in response to saturating concentration of glycine (50 mM).**

The single-channel traces (cell-attached, pipette potential + 100 mV) show that the mutant receptor opens at lower maximum open probability. The average maximum $P_{open}$ = 0.61 ± 0.06, average amplitude = 3.06 ± 0.08 pA, $n$ = 20 apparent clusters.

## 3.2.17 The (15') S267N mutation

### 3.2.17.1 Location

The S267 residue is located in the 15' position of the α1 GlyR TM2 domain (Figure 3.5). The serine residue is similar to the asparagine (present in the mutant) in that both are uncharged. However asparagine has a larger side chain that can affect vital interactions in the channel pore. Serine in the 15' is conserved in twenty five pLGICs reviewed by Swiss-Prot (Figure 3.19). It is conserved in all of the human GlyR alpha subunits α1, α2, α3, and α4. Bovine GlyR α1 and *Danio rerio* (zebrafish) GlyRαZ1 have a conserved residue in this location. Residues equivalent to S267 GlyR α1 are conserved in rat α1, α2, α3, and α4 GlyRs. Mouse α1, α2, α3, and α4 GlyR subunits have a conserved serine in the indicated position. The amino acid of interest is also conserved in the GluCl α of *Caenorhabditis elegans* and in some, but not all human $GABA_A$ receptor subunits (α1, α2, α3, α4, α5, α6, β1, γ1, γ2, and γ3 subunits do have a S in 15'TM2)

### 3.2.17.2 Reported hyperekplexia case

A study conducted by Becker *et al.,* (2008) reported a case of hyperekplexia due to S267N substitution of 15' TM2 in a father and his son. A five weeks old patient was diagnosed with hyperekplexia as he had severe muscular hypertonia and hyperreflexia shortly after birth. With neurophysiological testing, acoustic stimuli resulted in the child startle response that affected the muscles of the head, neck and upper arms. The father reportedly had showed symptoms of hyperekplexia with later onset, but the mother was normal. The patient's father had no symptoms of acoustic startle response in adulthood, but he displayed exaggerated reflexes. For both the father and the son epilepsy was excluded on the basis of EEG recordings. The patients were found to have a point mutation in the 267 residue of the GlyR shift from serine to asparagine. The cell membrane expression of GlyR with the S267N mutation was similar to wild-type as investigated by immunobloting. However, the electrophysiological recordings of α1 S267N GlyR expressed in HEK293 cells showed a 17 fold increase in glycine $EC_{50}$. In the same study heteromeric-heterozygous GlyR expressed at 1:1:8 (α1WT/α1S267N/β), had a glycine sensitivity decreased by 5.5 fold. In homomeric S267N GlyR, the efficacy of β-alanine and taurine relative to glycine was reduced by 17% and 2%, respectively. Furthermore, this 15' GlyR mutation abolished ethanol modulation of the mutant channel (Becker *et al.,* 2008).

#### 3.2.17.3 Other mutations in the same residue in GlyR

**S267I**

Testing different chimeric receptor constructs of GlyR α1 and $GABA_A$ ρ1 receptors expressed in *Xenopus* oocytes led to the finding of TM2 and TM3 residues important for alcohol and volatile anesthetic modulation (Mihic *et al.,* 1997). The S267 residue in GlyR was found to be necessary for the ethanol modulation, as the S267I mutation resulted in loss of the enhancement by 200 mM ethanol. The potentiation of glycine submaximal responses by the volatile anaesthetic enflurane (1 mM) was reduced in the α1(S267I) GlyR (Mihic *et al.,* 1997).

**S267Y**

In the same Mihic *et al*., (1997) study, the effect of enflurane was investigated on other mutations in the same position. α1(S267Y) GlyR was found to be resistant to the enhancing effect of 1 mM enflurane.

**S267Q**

S267Q is not a natural occurring hyperekplexia mutation. Transgenic mice with α1(S267Q) GlyR mutation were produced by the Blendnov group (Findlay *et al.,* 2002).

Electrophysiological recordings in *Xenopus* oocytes expressing α1(S267Q) GlyR showed that this mutation had no effect on the glycine $EC_{50}$, in homomeric GlyR, however, with β subunit insertion there was a reduction in glycine potency by 5 fold (Findlay *et al.,* 2003). Another study using the HEK293 expression system obtained completely different results, the S267Q mutation was found to increase glycine $EC_{50}$ by nearly 3 fold for the homomeric receptors and to have no effect in heteromeric GlyR (Xiong *et al.,* 2014).

The same study examined whether the mutation has an effect on channel gating by outside-out single-channel recordings of HEK293 cells transfected with α1(S267Q) GlyR (Findlay *et al.,* 2003). The recordings showed brief openings with very unstable opening current amplitude. Also, a lack of burst like structure of openings was noticed. The records were interpreted only visually and the $P_{open}$ was not measured (Findlay *et al.,* 2003).

*In vivo* assessment of the heterozygous knock-in mice bearing the α1(S267Q) mutation revealed an increased acoustic startle response (Findlay *et al.,* 2003). The exaggerated startle

behaviour of the heterozygous α1(S267Q) mutant mice was observed also in another study (Xiong *et al.,* 2014). The homozygous knock-in mice bearing the α1(S267Q) GlyR mutation displayed seizures and survived for only 20 days after birth (Findlay *et al.,* 2003).

Protein levels of GlyR α1 subunits for the heterozygous S267Q knock-in mice were assessed by immunoblotting and [$^3$H] strychnine binding. The expression of alpha subunits of GlyR in the brain stem and spinal cord was not changed by the mutation (Findlay *et al.,* 2003).

#### 3.2.17.4 Homologous residue in $GABA_A$ receptor subunits

The role of $GABA_A$ receptor residues homologous to S267 GlyR was evaluated for the effect of ethanol and general anesthetics. Ethanol modulation of $GABA_A$ receptor α and β subunits was investigated. Ethanol enhancement of GABA evoked submaximal responses was reduced in α1(S270I)β1 and α2(S270I)β1, α1β1(S265I), and α1β3(N265I) $GABA_A$ receptors expressed in *Xenopus* oocytes (Mihic *et al.,*, 1997). The modulation effect of the volatile anesthetic enflurane was also decreased in homologous $GABA_A$ α1(S270I)β1, α2(S270I)β1, and α1β1(S265I) receptors (Mihic *et al.,* 1997).

Another study investigated by whole-cell recording the modulatory effect of the volatile anesthetics sevoflurane, desflurane and isoflurane on $GABA_A$ receptors bearing mutations in this position. The apparent GABA affinity for α1(S270W)β2γ2s, α1β2(N265W)γ2s, and α2(S270I)β3γ2s $GABA_A$ receptors expressed in HEK293 cells was reduced by 8, 2, 3 fold respectively. The α1(S270W)β2γ2s, α2(S270I)β3γ2s, $GABA_A$ receptors were found to be completely resistant to the potentiating effect of clinically relevant concentration of the anaesthetics (on responses to GABA $EC_{20}$), and α1β2(N265W)γ2s showed a reduced response. This led the Authors to propose that the S270 residue of the α1 and α2 $GABA_A$ receptor subunits is essential for the action of the volatile anesthetics sevoflurane, desflurane and isoflurane (Nishikawa *et al.,* 2003).

### 3.2.18 Whole-cell recordings from human homomeric GlyR bearing the α1(S267N) hyperekplexia mutation

The literature suggests that the S267 residue is important for the GlyR and $GABA_A$ normal function. To examine the effect of the α1(S267N) GlyR mutation on the glycine potency, a concentration-response curve was obtained. Inward currents induced by glycine (0.5 to 50 mM) were recorded. Representative recordings of the glycine-induced currents are shown in Figure 3.20.A. Desensitization was observed at 1 mM glycine (~ $EC_{10}$). Decreased glycine potency was obvious as glycine $EC_{50}$ shifted by around 18 fold, from 0.25 ± 0.03 in wild-type to 4.41 ± 0.36 in S267N ($n$ = 6 for both; $p < 0.001$, unpaired t test; Figure 3.20.B; Table 3.2). Hill slope was not changed (1.71 ± 0.12; $n$ = 6; $p > 0.05$, unpaired t-test, Table 3.2) and the average $I_{max}$ was not significantly diffent from corresponding wild-type 6.41 ± 2.07 nA ($n$ = 6; $p > 0.05$; Table 3.2).

### 3.2.19 Whole-cell recordings from human heteromeric GlyR bearing the α1(S267N) hyperekplexia mutation

The effect of co-expression of wild-type β GlyR with α1(S267N) was examined. Current responses elicited by glycine applied at 1 - 50 mM are shown in Figure 3.21.A. Desensitization was observed from 1 mM (~ $EC_{10}$). The α1(S267N)β mutation reduced the GlyR sensitivity to glycine. Glycine $EC_{50}$ was increased significantly by 35 fold from 0.10 ± 0.03 mM to 3.52 ± 0.46 ($n$ = 6, 5, respectively; $p < 0.01$, unpaired t test; Table 3.3). Wild-type and α1(S267N)β GlyR displayed comparable Hill slope: 1.48 ± 0.09 (wild-type; $n$ = 6) and 1.54 ± 0.17 (α1(S267N)β; $n$ = 5; $p > 0.05$, unpaired t-test). The average $I_{max}$ was 3.93 ± 1.03 nA, similar to values in wild-type receptors 1.48 ± 0.09 nA ($n$ = 5, 6, respectively; $p >$ 0.05, unpaired t test; Table 3.4).

### 3.2.20 Single-channel recordings of S267N GlyR

Single-channel recordings of homomeric α1(S267N) GlyR were obtained in the cell-attached configuration using a saturating concentration of glycine (50 mM; Figure 3.22). It was impossible to analyze the records obtained from single-channel recordings of the homomeric S267N GlyR. Figure 3.22 shows the best recording that I could obtain, which is clearly uninterpretable. All of the 10 recorded patches showed similar activity, although obtained on different days and different transfections. While the traces may appear to be poor quality

recordings, due to poor seals, this was not the case, and recordings from wild-type GlyRs obtained on the same day were normal and of good quality.

Single-channel recordings of the heteromeric α1(S267N)β GlyR were obtained in the cell-attached configuration using saturating concentration of glycine (50 mM; Figure 3.23). It seems that β subunit insertion has slightly improved the single-channel activity compared to homomeric α1(S267N) GlyRs. Even so, throughout the records there was a mixture of brief and long openings which suggests a profound disruption of the channel behaviour. Measurement of $P_{open}$ was conducted when the openings looked similar to the cluster outlined by the *blue* box in the figure. The average approximate $P_{open}$ was reduced significantly from 0.98 ± 0.01 ($n$ = 29 clusters obtained from 6 records) to 0.37 ± 0.06 ($n$ = 6 clusters obtained from 3 records; $p < 0.001$, unpaired t-test; Table 3.5). The current amplitude was similar to wild-type 3.09 ± 0.24 pA vs 3.07 ± 0.06 pA ($p > 0.05$, unpaired t-test; Table 3.5).

**Conclusion- the S267N GlyR mutants.** This 15' hyperekplexia mutation caused a marked reduction in glycine potency. This effect is more noticeable in the heteromeric channel (18 cf ~ 35 fold change). The reduction in the potency is associated with a disturbance of channel gating. The maximum open probability recorded in the cell-attached configuration was measured for the heteromeric α1(S267N)β GlyR and indicated a significant reduction in channel gating.

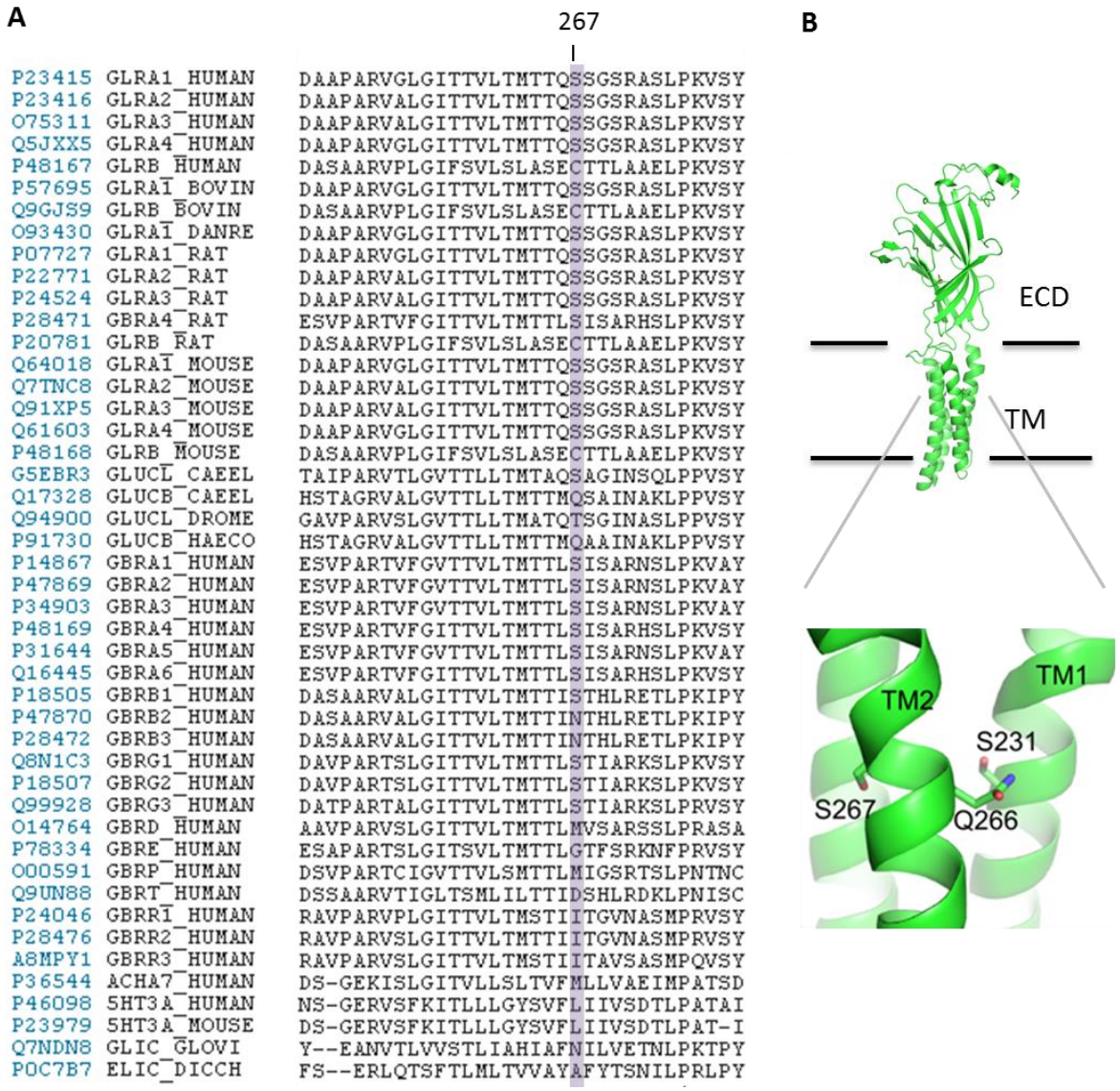


**Figure 3.19 Partial sequence alignment of TM2 S267 GlyR with a selection of related pLGICs.**

A) Equivalent residues to the selected human α1 GlyR hyperekplexia mutation S267 are highlighted in purple. Serine in this location is conserved in twenty five receptors. Uniprot accession numbers are indicated: human glycine α1 (P23415), human glycine α2 (P23416), human glycine α3 (O75311), human glycine α4 (Q5JXX5), human glycine β (P48167), bovine glycine α1 (P57695), bovine glycine β (Q9GJS9), zebrafish glycine α1 (O93430), rat glycine α1 (P07727), rat glycine α2 (P22771), rat glycine α3 (P24524), rat glycine α4 (P28471), rat glycine β (P20781), mouse glycine α1(Q64018), mouse glycine α2 (Q7TNC8), mouse glycine α3 (Q91XP5), mouse glycine α4 (Q61603), mouse glycine β (P48168), *C. elegance* GluCl α (G5EBR3), *C. elegans* GluCl β (Q17328), *D. melanogaster* GluCl α (Q94900), *H. contortus* GluCl β (P91730), human $GABA_A$ α1 (P14867), human $GABA_A$ α2

(P47869), human $GABA_A$ α3 (P34903), human $GABA_A$ α4 (P48169), human $GABA_A$ α5 (P31644), human $GABA_A$ α6 (Q16445), human $GABA_A$ β1 (P18505), human $GABA_A$ β2 (P47870), human $GABA_A$ β3 (P28472), human $GABA_A$ γ1 (Q8N1C3), human $GABA_A$ γ2 (P18507), human $GABA_A$ γ3 (Q99928), human $GABA_A$ δ (O14764), human $GABA_A$ ε (P78334), human $GABA_A$ π (O00591), human $GABA_A$ θ (Q9UN88), human $GABA_A$ ρ1 (P24046), human $GABA_A$ ρ2 (P28476), human $GABA_A$ ρ3 (A8MPY1), human α7 nAChR (P36544), human 5-HT3A (P46098), mouse 5-HT3A (P23979), GLIC (Q7NDN8), and ELIC (P0C7B7). B) Homology model based on *C.elegans* GluCl channel showing the location of the S267 residue in one subunit of GlyR α1 (see Yu *et al*., 2014).

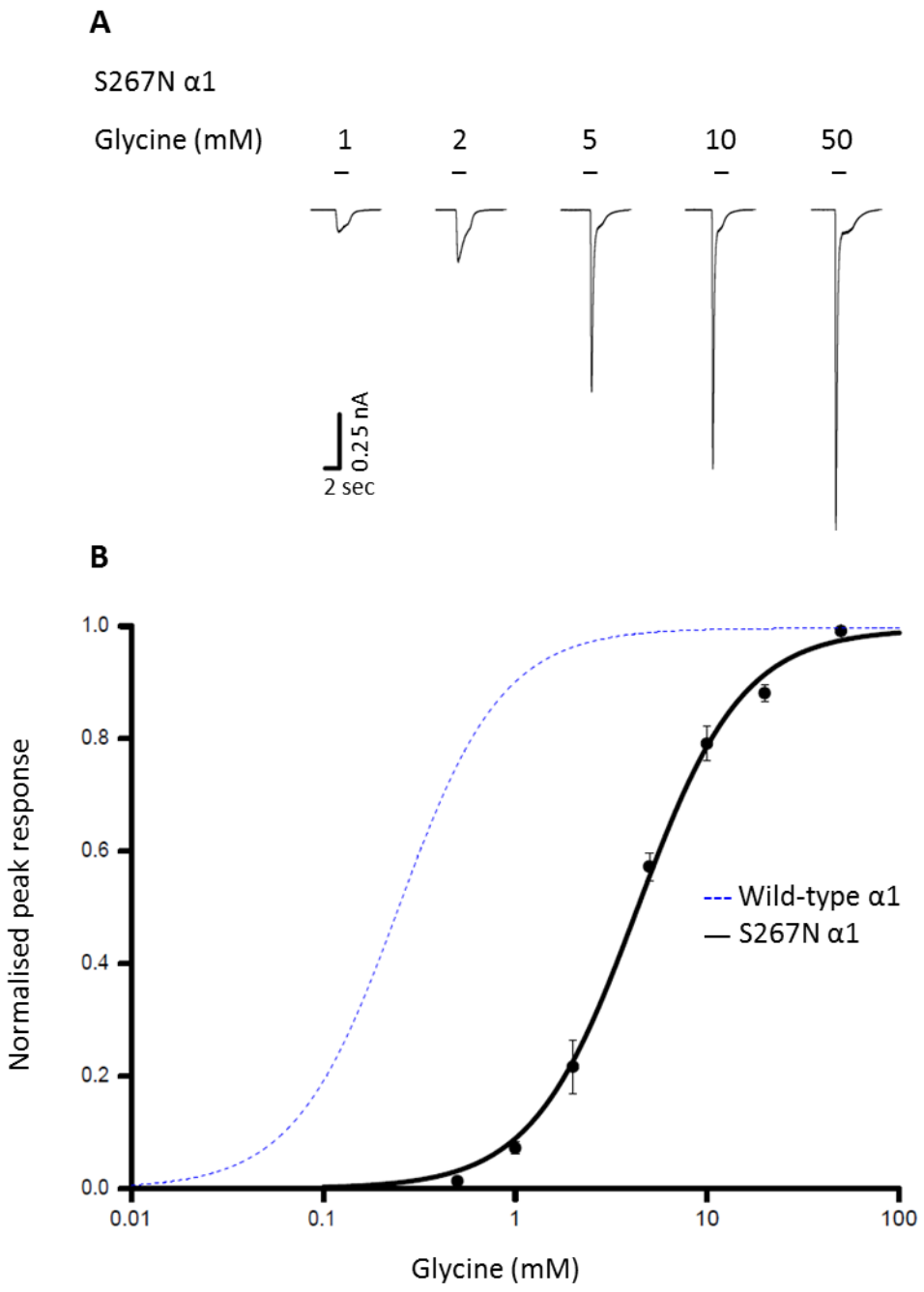


**Figure 3.20 The human homomeric hyperekplexia S267N GlyR mutation reduces the channel sensitivity to glycine.**

A) Whole-cell current responses from HEK293 cells expressing human S267N α1 GlyR. Glycine-evoked currents recorded at –50 mV. Glycine concentrations in mM are indicated above the traces; the bars show the duration of the application. B) Glycine concentration-response curve (normalized to their maximal response) is shifted to the right by ~18 fold, with $EC_{50}$ value of 4.41 ± 0.63 mM. Data points in this figure represent mean values fitted to the Hill equation. $n_H$ = 1.71 ± 0.12, $I_{max}$ = 6.41 ± 2.07 nA, $n$ = 6 cells. Error bars indicate SEM (shown only when larger than the symbol).

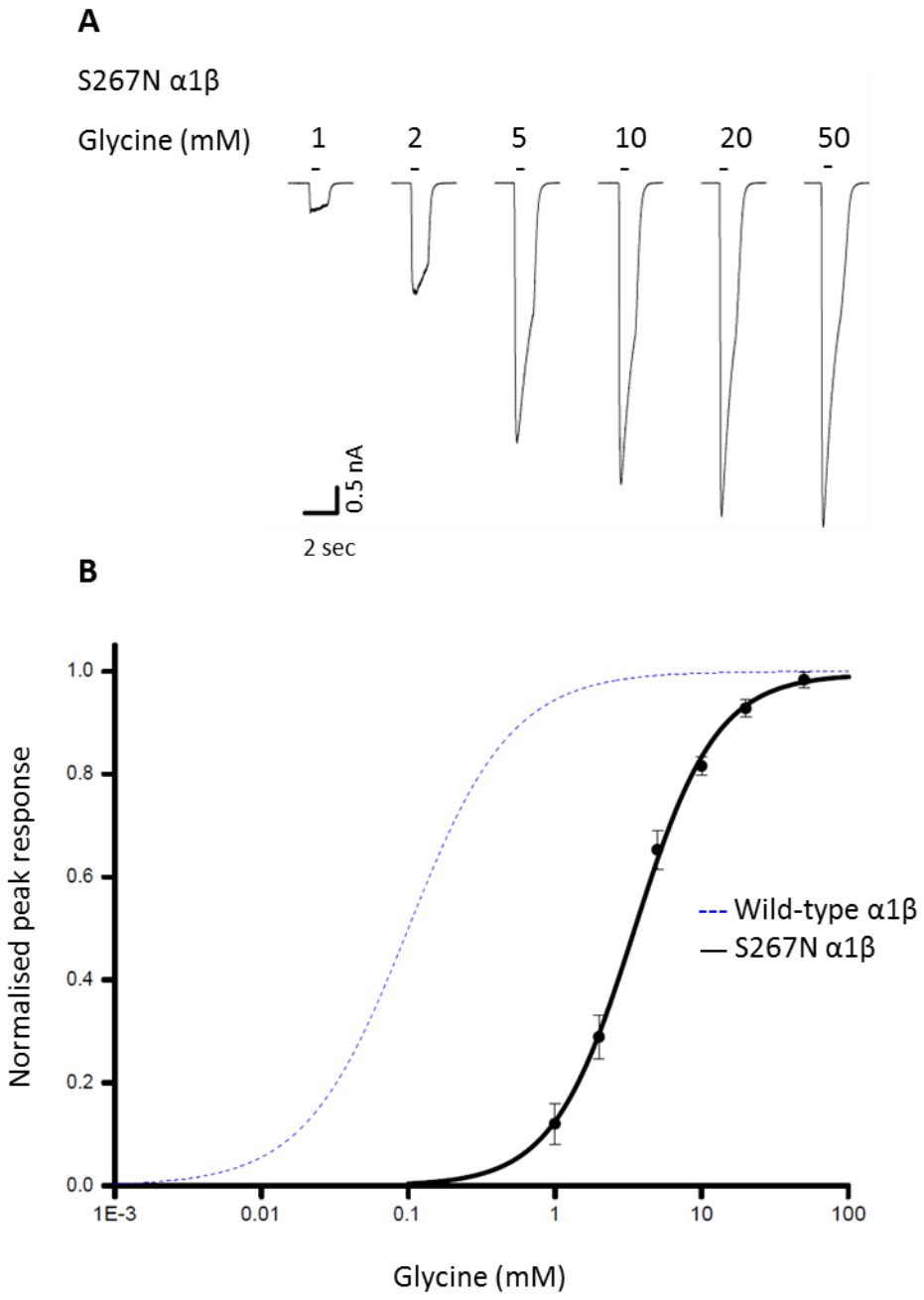


**Figure 3.21 Human α1(S267N)β mutant GlyR expressed in HEK293 cells have a reduced sensitivity to glycine.**

A) Example whole-cell traces showing inward chloride current responses to the indicated glycine concentrations in mM. Glycine-evoked currents recorded at −50 mV. Bars above the traces show the duration of glycine application glycine. B) Average glycine concentration-response curve for the heteromeric α1(S267N)β GlyR is shifted to the right by ~35 fold, with $EC_{50}$ value of 3.52 ± 0.46 mM. The curve is a fit to the Hill equation. $n_H$ = 1.54 ± 0.17, $I_{max}$ = 3.93 ± 1.03 nA, $n$ = 5 cells. Error bars represent SEM (shown only when larger than the symbol).

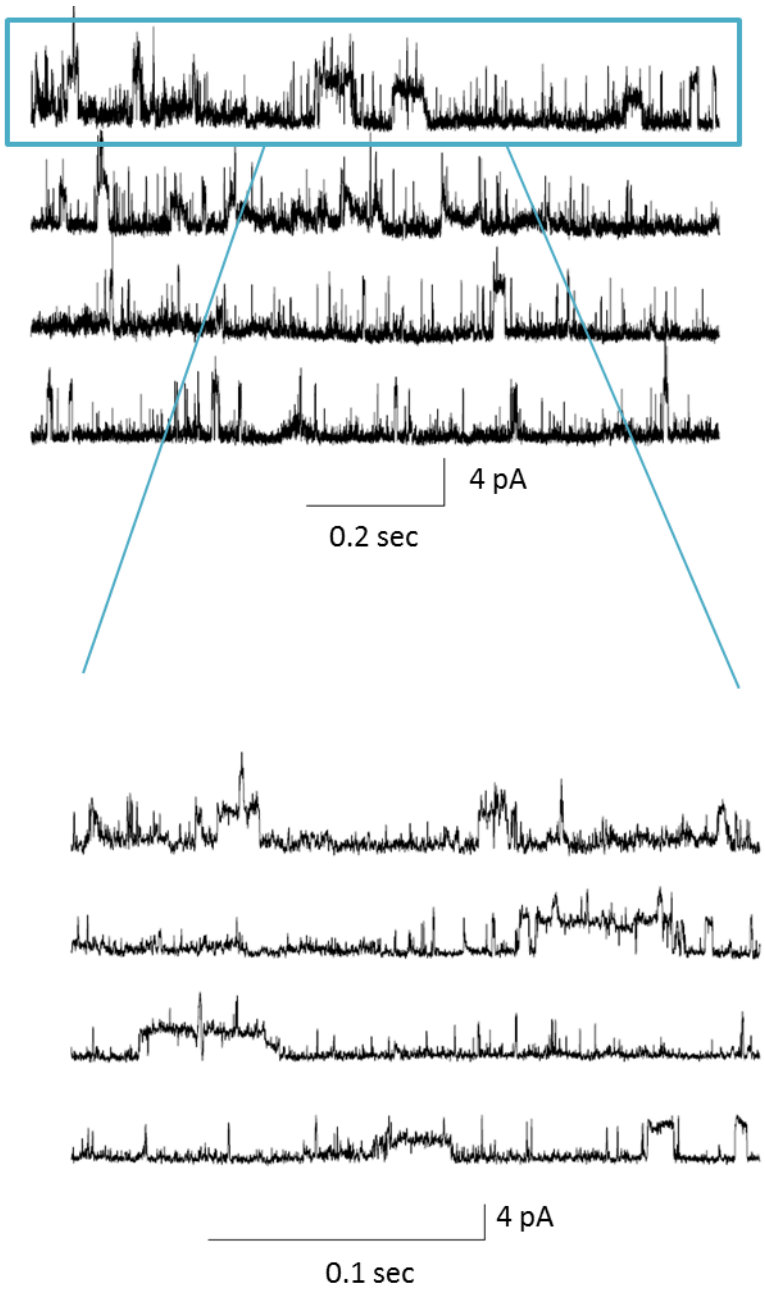


**Figure 3.22 Example of single channel activity of the α1 (S267N) GlyR in response to saturating concentration of glycine (50 mM).**

Openings of the channels were recorded in the cell-attached configuration at a holding potential of + 100. There is no clear clustering of the openings. Measurement of $P_{open}$ is not possible. Channel openings upward. (3 kHz filtered for display).

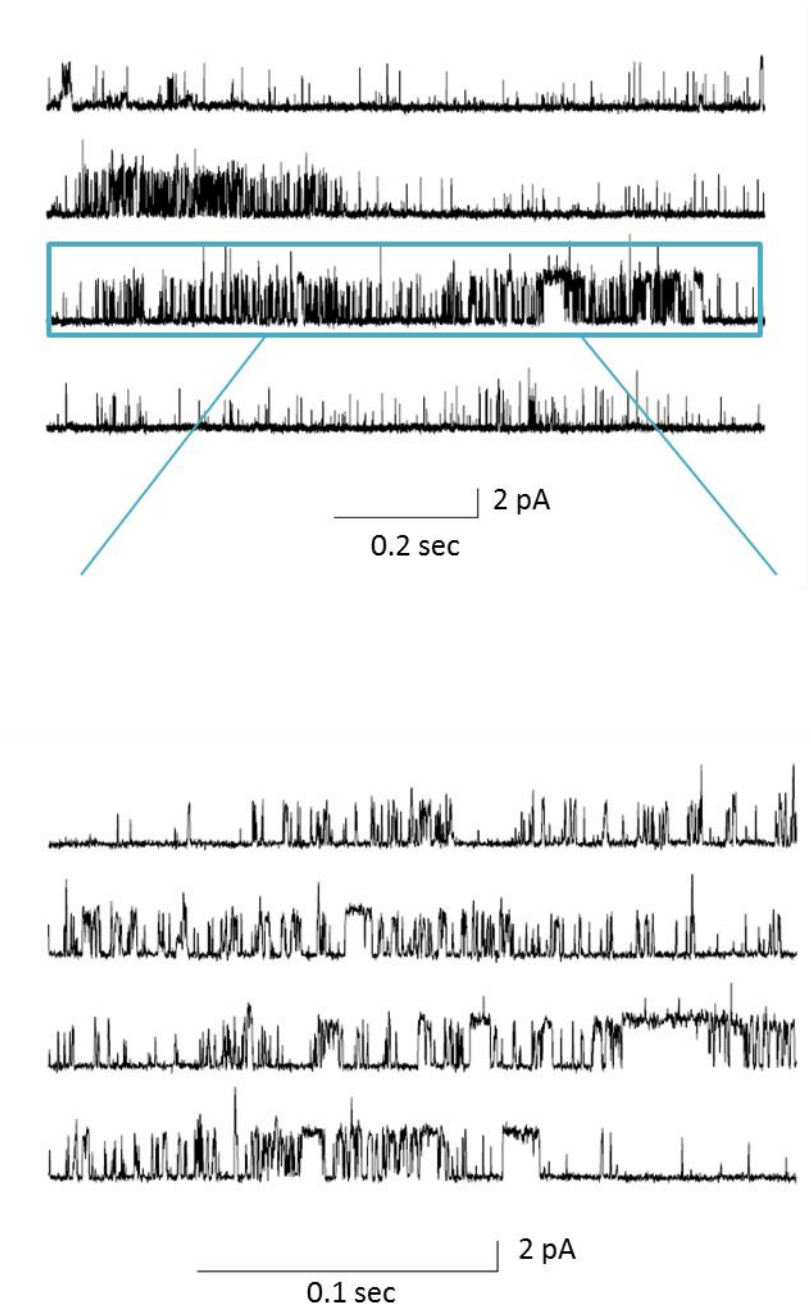


**Figure 3.23 The S267N mutation decreases the maximum $P_{open}$ of heteromeric GlyR in response to saturating concentration of glycine (50 mM).**

Representative single channel cell-attached trace recorded at pipette potential +100 mV. Average maximal $P_{open}$ was reduced to 0.37 ± 0.06 in mutant GlyR ($n$ = 6). Expanded view of the cluster is shown in the lower panel.

**Table 3.3 Functional properties of the selected human homomeric hyperekplexia mutant GlyR.**

| Receptor | Glycine $EC_{50}$ (mM) | $EC_{50}$ Fold change | *I* max (nA) | $n_H$ | *n* |
|---|---|---|---|---|---|
| α1WT | 0.25 ± 0.03 | - | 10.34 ± 2.47 | 1.87 ± 0.37 | 6 |
| α1(E103K) | 0.71 ± 0.11# | 2.84 | 2.73 ± 1.41 | 1.32 ± 0.07 | 3 |
| α1(S231N) | 1.16 ± 0.13 ‡ | 4.64 | 2.05 ± 0.50 * | 1.11 ± 0.06 | 4 |
| α1(Q266H) | 0.68 ± 0.17 ‡ | 2.7 | 5.27 ± 2.68 | 1.38 ± 0.40 | 4 |
| α1(S267N) | 4.41 ± 0.36 # | 17.64 | 6.41 ± 2.07 | 1.71 ± 0.12 | 6 |

Data are expressed as mean ± SEM, statistically different from WT α1 GlyR (* $p < 0.05$, ‡ $p < 0.01$, # $p < 0.001$) unpaired *t*-test.

**Table 3.4 Functional properties of the selected human heteromeric hyperekplexia mutant GlyR.**

| Receptor | Glycine $EC_{50}$ (mM) | $EC_{50}$ Fold change | *I* max (nA) | $n_H$ | *n* |
|---|---|---|---|---|---|
| α1β WT | 0.10 ± 0.03 | - | 4.43 ± 1.08 | 1.48 ± 0.09 | 6 |
| α1(E103K)β | 7.27 ± 0.58 # | 72.7 | 3.62 ± 0.89 | 1.22 ± 0.08 | 6 |
| α1(S231N)β | 3.81 ± 0.42 ‡ | 38.1 | 3.84 ± 0.80 | 1.12 ± 0.06 * | 4 |
| α1(Q266H)β | 1.16 ± 0.19 # | 11.6 | 9.07 ± 1.16 | 1.35 ± 0.10 | 5 |
| α1(S267N)β | 3.52 ± 0.46 ‡ | 35.2 | 3.93 ± 1.03 | 1.54 ± 0.17 | 5 |

Data are expressed as mean ± SEM, statistically different from WT α1β GlyR (* $p < 0.05$, ‡ $p < 0.01$, # $p < 0.001$) unpaired *t*-test.

**Table 3.5 Single-channel properties of the selected human hyperekplexia mutations and wild-type GlyRs using saturating glycine concentration**

| Receptor | Maximum $P_{open}$ | Amplitude (pA) | [Glycine] mM | *n* Clusters | *n* Records |
|---|---|---|---|---|---|
| α1WT | 0.99 ± 0.002 | 5.77 ± 0.06 | 10 | 30 | 4 |
| α1β WT | 0.98 ± 0.01 | 3.07 ± 0.06 | 1 | 29 | 6 |
| α1(E103K) | 0.73 ± 0.07 ‡ | 5.24 ± 0.12 | 50 | 13 | 3 |
| α1(E103K)β | 0.67 ± 0.06 ‡ | 3.10 ± 0.16 | 50 | 5 | 3 |
| α1(S231N) | - | - | - | - | - |
| α1(S231N)β | 0.38 ± 0.06 # | 2.01 ± 0.05 # | 100 | 16 | 3 |
| α1(Q266H) | - | - | - | - | - |
| α1(Q266H)β | 0.61 ± 0.06 # | 3.06 ± 0.08 | 50 | 20 | 6 |
| α1(S267N) | - | - | - | - | - |
| α1(S267N)β | 0.37 ± 0.06 # | 3.09 ± 0.24 | 50 | 6 | 3 |

Data are expressed as mean ± SEM, statistically different from WT α1 GlyR (* $p < 0.05$, ‡ $p < 0.01$, # $p < 0.001$) unpaired *t*-test.

### 3.2.21 Human hyperekplexia mutations that were excluded from the study

Most of the homomeric, or heteromeric, glycine mutant receptors that I studied here responded to glycine with macroscopic currents that were large enough to allow further, single channel investigations. The exceptions were GlyRs bearing the R72H or the Y279C mutation in the α1 subunit (Coto *et al.*, 2005; Shiang *et al.*, 1995; Lynch *et al.*, 1997).

R72H is an autosomal recessive mutation. The residue is located in loop D of the ECD. There was no electrophysiology work done on it at the time that I was conducting the experiments. R72H homomeric GlyRs showed no detectable response to 10 or 20 mM glycine (even when 55% or 82% of α1 cDNA was used). A recent study (Schaefer *et al.*, 2015) reported that no response to glycine was detected in whole-cell recordings from homomeric R72H expressed in HEK293 cells. Using an immunocytochemical technique, they observed a reduction in the whole-cell protein expression of α1 GlyR and a huge reduction of cell surface expression of R72H. The receptor failed to reach the cell surface and was retained in the endoplasmic reticulum, indicating a trafficking defect (Schaefer *et al.*, 2015).

Schaefer *et al*. (2015) investigated only homomeric receptors. For the heteromeric GlyR bearing the R27H mutation, I observed a response to glycine although it was small. For instance U-tube application of 20 mM glycine to HEK293 bearing α1(R72H)β GlyR (α1: β ratio 1:40) elicited currents of about 80 pA ($n$ = 3 cells). Also, when a α1: β ratio of 1: 3 was used, the response was small (60 pA) to 100 mM glycine ($n$ = 1 cell). Thus, it was impossible to include this mutation in the detailed single channel kinetic characterization study.

Expression of homomeric GlyRs bearing the dominant Y279C hyperekplexia mutation (TM2-TM3 loop) did not produce a detectable response to 20 mM glycine ($n$ = 3). This is maybe due to the huge maximum current reduction that was reported (Lynch *et al.*, 1997). However, small currents (about 600 pA in response to 50 mM) were recorded in heteromeric GlyRs, suggesting that expression of the β subunit might partially rescue the channel activation, or expression ($n$ = 2). Since the responses were too small for proper kinetic characterisation of the mutant, no further work was carried out for these mutants.

## 3.3 Discussion

There are many α1GlyR missense mutations related to hyperekplexia. Characterizing their functional consequences might help us in expanding our knowledge about the structure function relation of GlyRs.

What do we know about how hyperekplexia mutations affect the activation mechanism of GlyRs? The most solid way to establish this is to characterise the activation mechanism of the mutant channel by single channel kinetics. This is not an easy task, as witnessed by the fact that this has been achieved only for the heteromeric K267E GlyRs (Lape *et al.,* 2012). It was shown that the TM2-TM3 K276E human hyperekplexia mutation impaired the channel gating by slowing down access to the several intermediate shut states that occur before the channel opens. The open channel probability of the heteromeric α1(K276E)β GlyR at 100 mM glycine was reduced from 96% in wild-type to 45% (Lape *et al.,* 2012).

A less complete single channel characterisation was carried out on another human hyperekplexia mutation, Q266H, by Moorhouse *et al.* (1999). This study proposed that this mutation affected channel gating, because they detected a significant reduction in the channel open time. Whereas the mean open time for the wild-type receptors in response to low glycine concentrations was 4.75 ± 0.86 ms, it was reduced to 0.98 ± 0.12 ms for the homomeric Q266H GlyRs. The response to a saturating glycine concentration was not reported (Moorhouse *et al.,* 1999). In both cases K267E and Q266H, channel impairment was accompanied by changes in glycine sensitivity.

The initial aim of my Thesis was to screen mutations and identify one that was suitable for a full kinetic characterisation, but this aim was found not to be realistic in the time available, as many of the mutant receptors were found to be hard to characterise at the single channel level because of heterogeneity and lack of clustering.

Nevertheless, by measuring where possible glycine maximum open probability I found that many of the mutations were likely to act by causing impairments in gating.

This makes sense, because what matters for pathological impairment in human disease is the effect of mutations on glycinergic synaptic transmission. It is estimated that in the synaptic cleft glycine reaches relatively high concentrations (2.2-3.5 mM, Beato *et al.,* 2008). Thus glycinergic IPSCs would be expected to be relatively robust to changes in GlyR binding

affinity. Note also that the most important receptor type to examine is the heteromeric GlyR, which is the subtype found at adult glycinergic synapses. In addition to that, it is to be expected that the most accurate *in vitro* reproduction of hyperekplexia GlyR would be with recessive mutations, as with dominant mutations *in vivo* receptors would contain a mixture of WT and mutant subunits.

I will review briefly my findings below.

The E103K, S231N, Q266H, and S267N human hyperekplexia mutations are in positions that are conserved in many pLGICs. Measuring the $P_{open}$ of the single-channel activity gave a reasonable explanation behind the altered glycine sensitivity.

*E103K*. The residue E103 is located in the ECD at loop A of the principal subunit. In the E103K GlyR mutant the glycine $EC_{50}$ is shifted by 2.8 and ~70 fold for α1 and α1β, respectively (Table 3.3; Table 3.4). The incorporation of wild-type β subunit with α1 E103K was expected to reduce the observed impairment of the glycine $EC_{50}$ but it did not.

A change in glycine sensitivity was also reported for other non-hyperekplexia mutations in this location, e.g. E103A and E103C (Han *et al.*, 2001; Vafa *et al.*, 1999; Table 3.2). Also, glycine sensitivity was affected by mutating nearby residues like N102A, N102C, K104C, and K104A (Han *et al.*, 2001; Vafa *et al.*, 1999; Schmieden *et al*; 1999; Table 3.2). Single-channel recordings in the cell-attached configuration of GlyR bearing E103K showed a significant reduction of maximum channel $P_{open}$ (Table 3.5). The reduction in the $P_{open}$ was similar for the homomeric and heteromeric channels, from 0.99 ± 0.002 to 0.73 ± 0.07 and 0.98 ± 0.01 to 0.67 ± 0.06, respectively. So this residue might have an effect on gating although it is in the extracellular domain. Further discussion regarding this location will follow in Chapter five.

*S231N*. This residue is located in the TM1 domain. The hyperekplexia mutation leads to a shift in the glycine $EC_{50}$ whether expressed in homomeric, or heteromeric, GlyRs. Interestingly, the effect of the S231N mutation was much greater in heteromeric channels, with a reduction in glycine sensitivity of 38 fold cf.~ 5 fold for homomers response (Table 3.3; Table 3.4). This supports earlier findings obtained by whole-cell recordings from HEK293 cells bearing α1 (S231N), or α1 (S231N) β GlyR mutations (Chung *et al.*, 2010). Glycine maximal current was reduced for another hyperekplexia mutation in the same region

α1 S231R GlyR (Humeny *et al.,* 2002) and resulted from deficient plasma membrane insertion (Villman *et al.,* 2009).

It was recently reported that another GlyR TM1 α1 subunit mutation, Q226E, induces spontaneous channel opening, probably by changing an electrostatic attraction to the TM2 R271 (Bode *et al.,* 2013). As a result of the attraction the top part with the TM2 domain is tilted toward the TM1 domain away from the channel pore. So even though the mutation is in the TM1 domain, it can have an effect on channel gating. In this particular case, there might be an interaction between the side-chain of Q266 and S231. S231N can introduce some steric effect to the local region. This might affect the interactions between the TM1 and TM2 domains affecting channel gating.

I showed here that the channel gating is affected by the TM1 domain S231N. The single-channel recordings of α1β GlyR showed that the average maximum glycine $P_{open}$ was reduced from 0.98 ± 0.01 in wild-type to 0.38 ± 0.06 (Table 3.5). This reduction in maximum $P_{open}$ was accompanied by heterogeneity in the channel openings where variable modes were noticed. Different modes within the cluster were seen in most, or all, clusters and absent from wild-type recordings. We do not know what causes the gating modes. We have no explanation for that, but now we can speculate that this residue has a role in maintaining homogeneous modes of openings. We also show that this residue can have an impact on channel gating. Taking into consideration that this residue is conserved in 22 pLGIC might point to the importance of this residue. To date at this locus there are two human hyperekplexia mutations (S231N and S231R) and both are recessive (Table 3.1).

*Q266H*. Q266H is a human hyperekplexia mutation affecting the 14' residue at TM2 domain of the α1 subunit. Given that is part of the pore-lining domain, close to the presumed channel gate, it is possible that the presumed charge change with the replacement of glutamine to histidine may affect channel gating. I showed that glycine potency is reduced by this mutation by ~ 3 fold for homomeric and ~ 12 fold for heteromeric receptors (Table 3.3; Table 3.4). Previous studies had indicated that α1 Q266H reduced glycine sensitivity by 5 fold (Castaldo *et al.,* 2004) and 6 fold (Moorhouse *et al.,* 1999). Glycine potency was reduced by another mutation in the same location, α1 Q266I GlyR which also affected sensitivity to alcohols (Borghese *et al.,* 2012; Xiong *et al.,* 2014).

In the introduction to this Chapter I have described the conflicting reports on the effect of this mutation on channel open times (Moorhouse *et al.,* 1999 and Borghese *et al.,* 2012) in

homomeric and heteromeric mutant GlyRs. What seems most important to me is my measurement of a reduced maximum $P_{open}$ for the heteromeric Q266H (from 0.98 ± 0.01 to 0.61 ± 0.06 (Table 3.5).

A hypothesis for the mechanism of the functional effect of the Q266H mutation was put forward by a high-resolution NMR structure study of α1 human GlyR TM2 in isolation (Tang *et al.,* 2002). The study indicated that the side chains of Q14' narrow the channel pore during the movement of the TM2 from open to closed state. In case of the presence of an anion near the positive side chains of histidine (in case of Q266H) the channel tended to favour the closed channel state. While the NMR study indicated that the side chains of the Q266 are exposed to channel lumen, the mutagenesis study indicated it is not (Moorhouse *et al.,* 1999; Tang *et al.,* 2002).

*S267N*. The S267N human hyperekplexia mutation alters a highly conserved residue located at the 15' of the pore lining TM2 domain of the α1 subunit. This residue was found to be vital for ethanol and general anesthetic modulation (Mihic *et al.,* 1997; Lobo *et al.,* 2005). It appears that this residue is vital for GlyR function, as homozygous S267Q knock-in mice died within three weeks after birth and heterozygous mice survived with a markedly increased acoustic startle response (Findely *et al.,* 2003).

I found that glycine potency was reduced significantly for both the α1 (S267N) and α1 (S267N) β GlyRs (Table 3.3; Table 3.4). This supports the previous findings (Becker *et al.,* 2008). The reduced glycine sensitivity was more marked for the heteromeric receptors than the homomeric receptors (35 fold vs 18 fold).

Single-channel recordings of the homomeric S267N mutant with a saturating glycine concentration showed a high frequency of brief individual openings and proper clustering of the openings was missing. This unfortunately made the records not useful for $P_{open}$ analysis. Nonetheless, the profound disturbance in channel opening supports the hypothesis that the mutation impairs channel gating. A shortening of channel opening was reported for a different mutation in the same residue (α1 S267Q GlyR, Findely *et al.,* 2003). Whereas the gating was severely impaired in case of the homomeric receptor, the heteromeric S267N receptors were somewhat less impaired. This can be explained by the fact that the homomeric receptors have the mutation in all of the five subunits in the pentamer, but in the heteromeric receptor there are at least two wild-type β subunits which may improve the response. Partial

rescue of the channel function was previously observed for the heteromeric K276E hyperekplexia mutant (Lape *et al.*, 2012).

The α1(S267N)β GlyR when saturated by 50 mM glycine reached less than half (0.37 vs 0.98; Table 3.5) the $P_{open}$ of the wild-type GlyR, so the reduction of the maximum $P_{open}$ was still marked. So both of the TM2 domain mutations 14' Q266H and 15' S267N which are described here affect glycine potency and channel gating. What about other human hyperekplexia mutations next to those mutations? Do they affect glycine potency, efficacy or both? There are many reported dominant human hyperekplexia mutations affecting the TM2 domain. Mutation of 13' T265I reduced glycine $EC_{50}$ by 15, 33 fold for homomeric, heteromeric receptors, respectively (Chung *et al.,* 2010). The effect of this pore-forming TM2 domain on single-channel $P_{open}$ was not reported. The functional effect of the 16' hyperekplexia mutation is not determined (Lapunzina *et al*. 2003).

The pattern of single-channel activation of the E103K, S231N, Q266H, and S267N human hyperekplexia mutations using saturating glycine concentration was different from the previously examined wild-type glycine receptors rat α1, α1β (Beato *et al.,* 2004; Burzomato *et al.,* 2004) or the wild-type receptor in this study. Also it differed from the murine hyperekplexia heteromeric α1 (A52S) β and from the human hyperekplexia heteromeric K276E GlyR (Plested *et al.,* 2007; Lape *et al.,* 2012). The presence of different modes within the cluster in case of α1(S231N)β, absence of the cluster pattern in α1(S267N) are good examples of how changing single amino acid can disrupt the normal channel behaviour.

## Conclusion

I showed that E103K, S231N, Q266H, and S267N human hyperekplexia mutations within the α1 subunit changed glycine potency. The change in glycine sensitivity was more marked in the heteromeric than in the homomeric receptors. These hyperekplexia mutations affected the channel gating by reducing the maximum $P_{open}$ (Table 3.5). Notice that two mutations reduced the maximum $P_{open}$ to above 50% and the other two to less than 50%. This study shows that there are residues in addition to the pore lining elements can contribute to channel gating including the ECD E103 and TM1 domain S231 residues. The next step was to determine whether the glycine response of the heteromeric mutant GlyRs can be rescued using GlyR modulators.

# Chapter 4: The effect of propofol on human hyperekplexia mutant α1β GlyR

## 4.1 Introduction

### 4.1.1 Modulators of GlyRs

A number of allosteric modulators of the GlyRs have been identified. These include avermectins (e.g. ivermectin), cannabinoids (e.g. anandamide), neuroactive steroids (e.g. alphaxalone and minaxalone), volatile general anaesthetics (e.g. isoflurane and enflurane), intravenous general anaesthetics (e.g. propofol), tropeines (e.g. tropisetron), bivalent cations (zinc), glutamate, and alcohols (e.g. ethanol and trichloroethanol). The binding site of the modulator can be either to the glycine binding site or to an allosteric site (Lynch, 2004; Yevenes and Zeilhofer, 2011).

### 4.1.2 Propofol

Since the mid of the 19$^{th}$ century general anaesthetics have been in use in clinical practice. In addition to loss of consciousness these drugs can introduce amnesia, analgesia and muscle relaxation. It is believed that most of the general anaesthetics produce their modulatory actions by either binding or modulating the response of pLGICs, however, the precise mechanism governing their action is not clear (Franks and Lieb, 1994, Chau *et al.,* 2010). Currently used inhaled general anaesthetics include nitrous oxide ($N_2O$), sevoflurane, isoflurane, desflurane, and xenon. The intravenous general anaesthetics include propofol, ketamine, methohexital, etomidate, and thiopental (Garcia *et al.,* 2010, Chau *et al.,* 2010).

Propofol (2-6 diisopropylphenol) was first introduced in the 1980s. In man the estimated clinical concentration of propofol not bound to plasma proteins during total intravenous anaesthesia is in the sub micro molar range (0.5 to 1.1 µM) (Pistis *et al.,* 1997, Franks *et al.,* 2008, Garcia *et al.,* 2010). Although propofol is used extensively in clinical anaesthesia, its mechanism of action on the CNS is still not well understood with regards to the exact areas of the CNS responsible for the effect of propofol on consciousness. A review of functional imaging studies suggests that in human brain the frontal and parietal lobes, thalamus, hypothalamus, posterior cingulate cortex and pons areas are associated with the anesthetic effects of propofol (Song and Yu, 2014). It is generally accepted that propofol acts by increasing GABA-mediated inhibitory neurotransmission in the CNS. Propofol has two opposing effects on pLGICs. While it potentiates the anion selective channels i.e. $GABA_A$

and glycine receptors (Zeller *et al.*, 2008, Nguyen *et al.*, 2009), it inhibits the cation-selective $5HT_3$Rs (Rüsch *et al.*, 2007), and the nAChRs (Flood *et al.*, 2007). It also inhibits GluCl (Lynagh and Laube, 2014) and GLIC (Ghosh *et al.*, 2013, Sauguet *et al.*, 2013).

### 4.1.3 Propofol action on $GABA_A$ receptors

Propofol is well known for its ability to enhance $GABA_A$ receptor activity as a PAM and high concentrations of propofol can directly activate $GABA_A$ receptors. This was supported by various studies performed using different native, or expression, systems:

In murine cultured spinal neurons propofol (1.7-16.8 μM) reversibly enhanced $GABA_A$ receptor activity measured as whole-cell submaximal (100 μM) GABA-activated currents (Hales and Lambert, 1991).

The effect of propofol on $GABA_A$ $\alpha_1\beta_1$ $\gamma_{2L}$ receptors expressed in oocytes was evaluated by Pistis *et al*. (1997). Whole-cell currents elicited by GABA at $EC_{10}$ were potentiated by propofol (0.03-10 μM). The observed potentiation was nearly equal to the maximum current produced from GABA at saturating concentration. Direct activation of $GABA_A$ receptors by propofol (10-300 μM) was also observed in the absence of GABA (Pistis *et al.*, 1997). In addition, the positive allosteric modulation of 0.3 – 60 μM propofol was tested on oocytes expressong wild-type $GABA_A$ $\alpha_6\beta_3$ $\gamma_{2L}$ receptors (Belelli *et al.*, 1999). Propofol was found to enhance $EC_{10}$ GABA evoked current to achieve 180 ± 26 % of the GABA maximum response. Propofol (10-300 μM) in the absence of GABA induced currents reaching up to 41 ± 4% of the GABA $I_{max}$ (Belelli *et al.*, 1999).

The effect of propofol on agonist efficacy was tested by whole-cell recordings from HEK293 cells expressing $\alpha_1\beta_1\gamma_{2S}$ $GABA_A$ receptors (O'Shea *et al.*, 2000). The efficacy of the partial agonist piperidine-4-sulphonic acid (P4S) was increased by propofol. Propofol (2 μM) was effective in potentiating the response to submaximal P4S concentration and no direct receptor activation was found at this low concentration. The relative efficacy of P4S was increased from 0.65 ± 0.03 to 0.86 ± 0.02 in the presence of propofol. This might indicate an effect of propofol on channel gating (O'Shea *et al.*, 2000).

### 4.1.4 Propofol action on GlyRs

While propofol is well known for its action on the $GABA_A$ receptor, it also enhances the function of the glycine receptor. The ability of propofol to potentiate wild-type glycine receptor currents was tested in several electrophysiology studies (Table 4.1).

Propofol (5μM) potentiation of glycine $EC_2$ current was around 120% as evaluated by whole-cell recordings from *Xenopus* oocytes expressing human wild-type α1 GlyR (Mascia *et al.*, 1996). The potentiation effect of propofol was reversible. Similar results were found for the homomeric α2 GlyRs (Mascia *et al.*, 1996).

The positive allosteric modulation of glycine receptors by propofol was tested in another study, also in *Xenopus* oocytes. Glycine ($EC_{10}$) evoked currents were potentiated by 100 μM propofol to reach 85 ± 5% of the of the glycine $I_{max}$ in α1GlyR. In heteromeric α1β GlyR, glycine ($EC_{10}$) activated currents were potentiated to 98 ± 6% of the glycine $I_{max}$ by 300 μM propofol. The effect of propofol potentiation was similar in the homomeric and heteromeric GlyRs expressing wild-type channels (Pistis *et al.*, 1997). Also, it was reported that 100 μM – 1mM propofol in the absence of glycine activated both the homomeric and heteromeric GlyRs resulting in small currents of 12 ± 6%, 8 ± 2% of the glycine $I_{max}$. Propofol induced currents were inhibited by the glycine antagonist strychnine and potentiated by zinc (Pistis *et al.*, 1997).

In another study also in oocytes expressing wild-type homomeric GlyRs, lower propofol concentrations were tested (1-100 μM). The response to glycine $EC_{10}$ was potentiated by propofol 100 μM to reach 85 ± 5 % of the glycine maximum current (Belelli *et al.*, 1999). Similarly, by the allosteric action of propofol was tested on oocytes bearing wild-type homomeric GlyRs O'Shea *et al.* (2004). Propofol (1 μM) potentiated submaximal glycine currents, but the maximum potentiation was found with 0.5 mM propofol. However, at saturating glycine concentration no potentiation effect was found when propofol was co-applied with glycine to the wild-type α1 GlyRs. The glycine, β-alanine, and taurine $EC_{50}$ values were reduced by 10, 23, and 32 fold, respectively, in response to 0.5 mM propofol co-application. Also, the same study indicated that during the pre-application of 0.5 mM propofol no direct activation occured. The maximal response of wild-type α1GlyR to the partial agonists β-alanine and taurine was potentiated by 0.5 mM propofol to about the maximum response of glycine (O'Shea *et al.*, 2004).

HEK293 cells expressing wild-type α1 and α1β GlyRs were tested for propofol modulation. Co-application of propofol (3-300 μM) with glycine $EC_{20}$ potentiated the glycine-gated currents up to 100 ± 5 % $I_{max}$ (Ahrens *et al.,* 2008). The same study reported the ability of 100 μM propofol to directly activate the GlyRs in the absence of glycine. This effect was observed for both the homomeric and heteromeric receptors (Ahrens *et al.,* 2008). The effect of propofol modulation on HEK293 cells expressing wild-type α1GlyRs was evaluated in another study. Co-application of glycine $EC_{10}$ with 30 μM propofol potentiated the glycine gated current by ~350 % (Moraga-Cid *et al.,* 2011).

The modulatory effect of propofol on wild-type homomeric GlyRs expressed in oocytes was also reported recently (Lynagh and Laube, 2014). Co-application of glycine $EC_{20}$ with variable propofol concentrations (0.01 - 3 mM) potentiated the recorded current. The maximum potentiation was 3 fold when 3 mM propofol was co-applied with glycine $EC_{20}$ (Lynagh and Laube, 2014).

Similar effects were also described in native systems. Propofol (0.84 – 16.8 μM) potentiated glycine (100 μM) activated currents recorded from murine cultured spinal neurons (Hales and Lambert, 1991). Subsaturating glycine (30μM) evoked currents recorded from spinal dorsal horn neurons were potentiated by propofol (5 μM) by 1.82 ± 0.20 fold (Dong *et al.,* 2002). In addition, Nguyen and his group found that propofol positively modulated GlyRs in rat cultured neurons (Nguyen *et al.,* 2009). Propofol (10 - 100 μM) was found to potentiate glycine-gated currents in neurons isolated from the rat posterior hypothalamus. Application of a subsaturating concentration of glycine (10 μM) in the presence of 30 μM propofol enhanced glycine current by 385.6 ± 128.9 %. Propofol was also found to induce chloride currents in the absence of glycine. The study further reported behavioural effect of propofol as it induced a hypnotic state in rats marked by the loss of the righting reflex (Nguyen *et al.,* 2009), which indicates the involvement of GlyRs.

In summary, all of the above studies had indicated that propofol was found to potentiate glycine response at wild-type GlyRs (Table 4.1). The relevant anasthetic concentration of propofol (1 μM) produced enhancement of the glycine submaximal response at different recombinant expressing systems (Mascia *et al.,* 1996; Belelli *et al.,* 1999; O'Shea *et al.,* 2004; Moraga-Cid *et al.,* 2011). Using a higher propofol concentration of 300 μM produced enhancement of glycine submaximal response that reached up to 100% of the glycine $I_{max}$. Direct activation by propofol in the absence of glycine was observed when 100 μM propofol

was applied to either, homomeric or heteromeric, GlyRs (Pistis *et al.,* 1997, Ahrens *et al.,* 2008). This effect was either not observed or tested in other studies (Mascia *et al.,* 1996; Belelli *et al.,* 1999; O'Shea *et al.,* 2004; Moraga-Cid *et al.,* 2011; Lynagh and Laube, 2014).

#### 4.1.4.1 Specificity of propofol action

The sensitivity to propofol was similar between wild-type α1 GlyRs and α1β GlyRs (Pistis *et al.,* 1997; Ahrens *et al.,* 2008). Also, it was reported that both homomeric α1 and α2 GlyRs have a similar sensitivity to propofol (Mascia *et al.,* 1996). There are no other reported studies regarding propofol subunit specificity.

### 4.1.5 Sites of propofol action

Attempts to identify the propofol binding site have been conducted by mutagenesis, photolabelling studies and with the help of homology modelling. Mutagenesis studies enabled defining of approximate sites for propofol interaction. Mutations were introduced into different parts of the pLGICs. If mutating particular residues within the receptor resulted in impairment, or abolished, the modulating effect of propofol, these residues were considered to be essential for propofol action. As is the case for agonists, this may mean that the residues are in the propofol binding site, or that the residues are important in transducing its effects. A distinction between the two possibilities may be helped by structural information and photolabelling studies.

### 4.1.6 Putative propofol binding sites; $GABA_A$ receptor

The binding site for propofol in $GABA_A$ receptors is not well defined. Many studies have been conducted to identify the possible binding sites of propofol.

In $GABA_A$ receptors several mutagenesis studies have determined that the transmembrane domains are involved in modulation by propofol (Garcia *et al.,* 2010). These include TM2 and TM3 (Belelli *et al.,* 1999; Krasowski *et al.,* 2001; Bali and Akbas 2004), and possibly TM4 (Richardson *et al.,* 2007). It was further reported that $GABA_A$ receptor α, β, and γ subunits are all involved in modulation by propofol (Garcia *et al.,* 2010).

Photolabeling with *ortho*-propofol (a photoreactive propofol analogue) has shown that the propofol binding site in the $GABA_A$ receptor is near to the extracellular ends of the TM1 and TM2 domains. A hydrophobic cleft between the TM1 and TM2 domains was identified close to H267 (17'). This study also reported the involvement of the β subunit of $GABA_A$ receptors

in propofol binding (Yip *et al.,* 2013). Another photolabeling study identified propofol binding sites in $GABA_A$ receptors. It found that propofol binds to the inter-subunit sites ($\beta^+ \alpha^-$, $\alpha^+ \beta^-$, and $\beta^+ \beta^-$ ) in the TM domains of the α1β3 $GABA_A$ receptor but not in the intra-subunit binding pocket (Jayakar *et al.,* 2014).

A homology modeling study of the $GABA_A$ homomeric β3 receptor based on the structures of GluCl and GLIC supported these findings (Franks, 2015). Two possible propofol binding sites were predicted: one was postulated to be in a hydrophobic pocket between the TM1 and TM2 domains of an individual subunit and with some interaction with the TM2 domain of the adjacent subunit. The other was predicted to be in a hydrophobic cavity between TM2 domains from adjacent subunits with some interaction with residues in TM1 of one of the subunits. Both of the predicted binding sites were adjacent to residue H267 (17') (Franks, 2015).

A recent functional study tested the involvement of the predicted inter-subunit cavity in propofol action (Eaton *et al.,* 2015). The study suggested involvement of residues within the inter-subunit cavity in propofol allosteric modulation by testing the effect of propofol on *Xenopus* oocytes expressing $GABA_A$ β3 and α1β3 receptors. $GABA_A$ β3 residues which were suggested to be involved in propofol activation are Y143, F221, Q224, and T266 in TM2 (Eaton *et al.,* 2015).

## 4.1.7 Putative propofol binding sites; GlyR receptor

A number of studies have suggested that propofol is a positive allosteric modulator of GlyR. Several studies have been conducted to determine propofol binding sites in GlyRs. The amino acid residues that are involved in the effects produced by propofol were identified by functional experiments performed on GlyR α1 mutants. These sites include the GlyR α1 subunit transmembrane and intracellular domains.

### 4.1.7.1 Transmembrane domain

The binding site for other allosteric modulators of GlyR is generally thought to be within the TM domain. This is supported by studies evaluating the allosteric effects of alcohols and general anaesthetics on chimeric constructs that indicated that I229 in M1, S267 in TM2, and A288 in M3 of the α1GlyR participate in the allosteric modulation (Mihic *et al.,* 1997, Lobo *et al.,* 2005). In contrast to the many studies have been conducted to determine the action of propofol on $GABA_A$ receptors, our knowledge of propofol interaction with the GlyR is poor.

GlyR residues that may contribute to propofol-binding sites were identified by analyses of the functional properties of S267 mutant homomeric and heteromeric GlyRs expressed in HEK293 cells. Mutating the TM2 domain 15' into S267I, or S267M, reduced the enhancement effect of propofol from 100 ± 5 % $I_{max}$ to 63 ± 3% in S267I and 71 ± 9% in S267M α1 GlyRs. In the heteromeric GlyRs propofol enhancement was reduced from 90 ± 4% $I_{max}$ to 71 ± 9%, 68 ± 11% in S267I and S267M, respectively (Ahrens *et al.*, 2008).

Propofol markedly restored the function of the R271K and the R271Q GlyR loss-of-function, startle disease mutants by enhancing apparent glycine affinity and efficacy (O'Shea *et al.*, 2004). However, this TM2 19' residue is apparently not involved in the propofol binding site as indicated by Lynagh *et al*. who studied the influence of propofol on cysteine substitution on R271 and the adjacent Q226 residues (Lynagh *et al.*, 2013).

A recent study identified a possible propofol binding site by mutating residues in GlyR and GluCl as propofol has opposite effects on these receptors (Lynagh and Laube, 2014). Residues which were suspected to be essential for propofol modulation were tested by whole-cell patch clamp recordings of oocytes expressing homomeric GlyR, or GluCl, channels. Mutating the TM2 18' residue of the GluCl converted the propofol inhibition of the glutamate-gated current to enhancement. Mutation of the corresponding residue in GlyR α1 S270I markedly increased the propofol enhancement of the glycine submaximal current (Lynagh and Laube, 2014). Accordingly the 18' residue might participate to the propofol binding site, or to the transduction of the effects of propofol.

Propofol enhancement was also tested by using a chimera with GLIC in the extracellular domain, α1GlyR in the transmembrane domain, and GLIC in the short cytoplasmic loop. Propofol is known to have opposite effects on GlyR and GLIC as it potentiates α1GlyR and inhibits GLIC (Duret *et al*., 2011). The chimera was activated by protons and potentiated by propofol. Whole-cell recordings from oocytes bearing the $GLIC_{EC}$-$\alpha1GlyR_{TM}$ chimera determined up to 10 fold propofol enhancement of the current elicited by $EC_{30}$ proton concentration. Even without the GlyR cytoplasmic loop and different extracellular domain, potentiation of propofol was found in the study indicating the importance of transmembrane domains as major binding sites for propofol (Duret *et al*., 2011).

As indicated earlier propofol has an inhibitory effect on GLIC, however, it is worth to mention some related studies with the presence of the x-ray crystal structure of pLGIC bound to propofol. An atomic resolution structure of GLIC bound with propofol indicated a propofol

binding site in the upper part of the transmembrane domain (Nury *et al.*, 2011). Two general anasthetic cavities were suggested to be involved in the allosteric modulation, one located intra-subunit at the middle of the TM domains in each subunit and the other inter-subunit (Nury *et al.*, 2011). The crystal structure of GLIC in the presence, or absence, of propofol supported the involvement of an inter-subunit cavity in propofol modulation (Sauguet *et al.*, 2013). Propofol allosteric modulation of GLIC was examined by Ghosh *et al.* (2013). Propofol binding was found to contribute to the structural rearrangements of the inter-subunit and intra-subunit cavities in the transmembrane domain and modified the local environment adjacent to these subunits (Ghosh *et al.*, 2013).

#### 4.1.7.2 Intracellular domain

Other regions of the GlyR might be involved in the modulatory effect of propofol as well. It has been demonstrated that a mutation in the intracellular loop of α1GlyR resulted in a decrease of the propofol effect when compared to the potentiation produced in the wild-type GlyR (Moraga-Cid *et al.*, 2011). Using the alanine replacement method on the intracellular loop (E326-A384), whole-cell recordings of HEK293 cell expressing mutant GlyRs identified residue F380 as essential for propofol modulation: The F380A GlyR α1 mutation markedly reduced propofol potentiation. However, the sensitivity to other modulators, like alcohols, trichloroethanol, etomidate, and isoflurane was maintained. Mutation of a conserved residue (α1 F385A) of a homologous position in the TM3-TM4 loop in $GABA_A$ α1β2 receptor had similar effects. These results support the involvement of the intracellular domain in propofol sensitivity (Moraga-Cid *et al.*, 2011).

The specific residues of GlyR which are responsible for propofol action remain to be clearly elucidated.

**Table 4.1 Wild-type GlyR tested for the modulatory effect of propofol.**

| Receptor | Expression system | Effective propofol concentrations (μM) | Glycine concentration | Maximum Potentiation effect | Direct activation by propofol | Reference |
|---|---|---|---|---|---|---|
| GlyR α1 | Oocytes | 1 - 5 | $EC_2$ | Up to 120% | Not indicated | Mascia *et al.* (1996) |
| GlyR α1 | Oocytes | 10 - 300 | $EC_{10}$ | 85 ± 5% of $I_{max}$ | Yes with 100 μM | Pistis *et al.* (1997) |
| GlyR α1β | Oocytes | 10 - 300 | $EC_{10}$ | 98 ± 6% of $I_{max}$ | Yes with 100 μM | |
| GlyR α1 | Oocytes | 1 - 100 | $EC_{10}$ | 85 ± 5 % of $I_{max}$ | Not indicated | Belelli *et al.* (1999) |
| GlyR α1 | Oocytes | 1 - 500 | Submaximal, $I_{max}$ | No potentiation with $I_{max,}$ Potentiation with submaximal concentration | No with 0.5 mM | O'Shea *et al.* (2004) |
| GlyR α1 | Oocytes | 10 - 3000 | $EC_{20}$ | Up to 3 fold | Not indicated | Lynagh and Laube (2014) |
| GlyR α1 | HEK293 | 3 - 300 | $EC_{20}$ | 100 ± 5 % of $I_{max}$ | Yes with 100 μM | Ahrens *et al.* (2008) |
| GlyR α1β | HEK293 | 3 - 300 | $EC_{20}$ | 90 ± 4 % of $I_{max}$ | Yes with 100 μM | |
| GlyR α1 | HEK293 | 1 - 100 | $EC_{10}$ | 100-700 % | Not indicated | Moraga-Cid *et al.* (2011) |

## 4.2 Results

### 4.2.1 The effect of propofol on human hyperekplexia mutant α1β GlyR

As the effects of propofol on wild-type receptors indicate that it facilitates gating at submaximal glycine concentrations, it would seem reasonable that if could produce some degree of functional rescue if gating is impaired by a hyperekplexia mutation. Indeed, propofol was reported to potentiate the reduced macroscopic glycine maximal response ($I_{max}$) of some hyperekplexia GlyR α1 mutations, such as TM2-TM3 R271Q, or R271L (O'Shea *et al.,* 2004). Note that propofol does not increase equilibrium responses to maximum concentrations of glycine in wild-type receptors (O'Shea *et al.*, 2004).

I tested the ability of propofol to enhance the function of the hyperekplexia E103K, S231N, Q266H, and S267N GlyRs mutants. Different concentrations of propofol (0.1 – 50 μM) were first tested, in order to determine the best concentration to use for the experiments (Figure 4.1). A Glycine submaximal concentration of 30 μM ($EC_{20}$) was selected for the experiments. For the primary experiments propofol was co-applied with glycine (see Methods) and the potentiation of the glycine submaximal current measured. For wild-type α1β GlyR the average increase in glycine $EC_{20}$ response induced by 0.1 μM, 1 μM, 10 μM, and 50 μM propofol were 1.55 ± 0.08, 1.51 ± 0.08, 2.11 ± 0.07, and 6.29 ± 2.13 fold ($n$ = 4, 4, 3, 2, respectively). A propofol concentration of 10 μM was selected as the concentration of choice for the first experiments as it seems to be effective.

After selecting propofol concentration, the next step was to test whether this concentration can potentiate the glycine maximal response. Co-application of glycine submaximal concentration of 30 μM with 10 μM propofol was repeated in these experiments (Figure 4.2.A). Figure 4.2 shows glycine $EC_{20}$ induced current of 0.67 nA, and propofol co-application doubled the response to around 1.40 nA. Potentiation of glycine submaximal response was observed with average fold change of 2.04 ± 0.13 ($n$ = 4 cells; $p < 0.01$, paired t-test; Figure 4.2.C).

On the other hand, co-application of propofol (10 μM) with a glycine maximal concentration (10mM) did not potentiate the glycine response (Figure 4.2.B). The recorded current for the illustrated example was 6.90 nA before propofol application and 6.25 nA with propofol application. The average fold change was barely reduced 0.87 ± 0.06 but reached significant

($n$ = 3; $p$ < 0.05, paired t-test, Figure 4.2.C). So the application of 10 μM propofol enhanced glycine $I_{20}$ response but not the maximal response.

After the application protocol was established, I started with the E103K mutation.

**A**

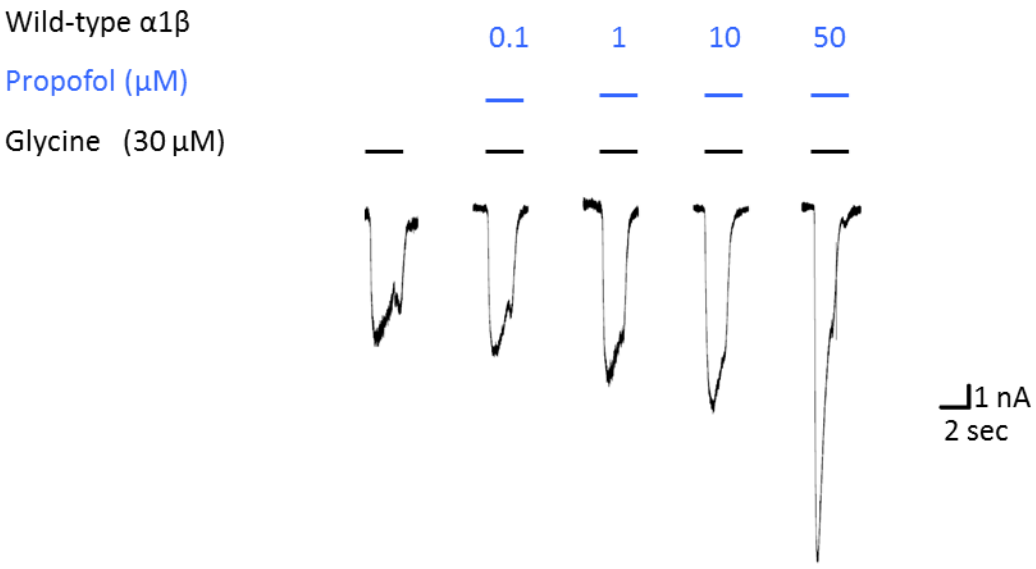


**B**

| Propofol concentration (μM) | Fold change | *n* |
|---|---|---|
| 0.1 | 1.55 ± 0.08 | 4 |
| 1 | 1.51 ± 0.08 | 4 |
| 10 | 2.11 ± 0.07 | 3 |
| 50 | 4.16 , 8.41 | 2 |

Fold change = Response to ligand + propofol / Response to ligand

**Figure 4.1 Concentration-dependence of propofol modulation of $EC_{20}$ glycine-gated currents in HEK293 cells expressing human wild-type α1β GlyRs.**

A) Sample whole-cell current traces evoked by U-tube application of submaximal glycine concentration in the presence or absence of propofol (at – 50 mV). The solid bars above the current traces indicate the time of application with black and blue bars corresponding to application of glycine and propofol, respectively. B) Summary of the results ± SEM.

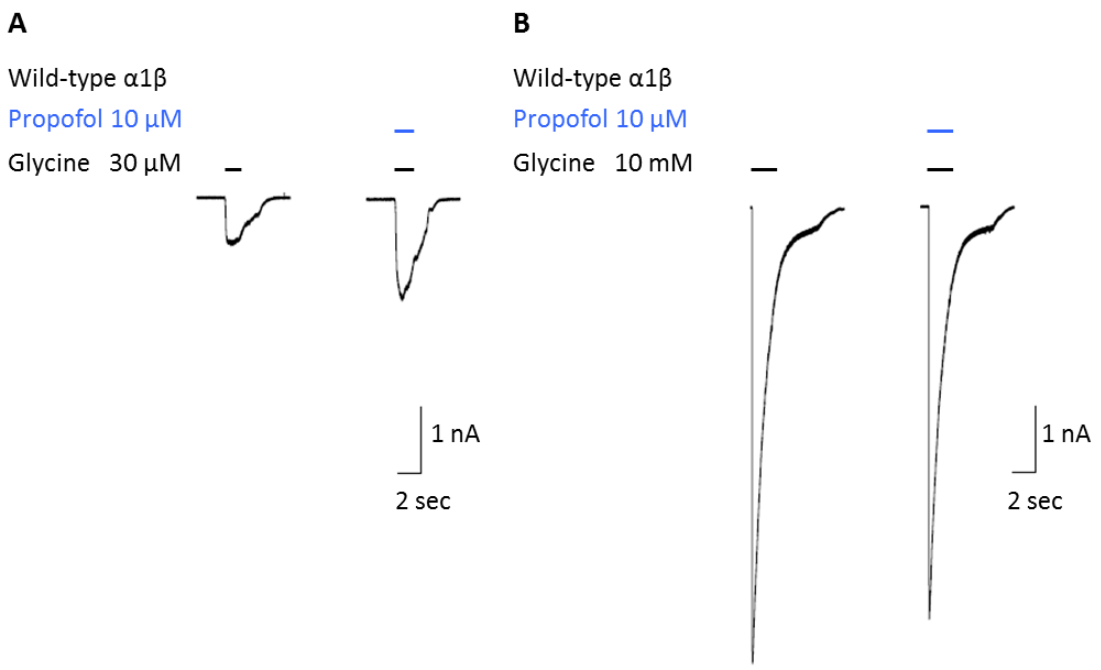


C

| Wild-type α1β | Fold change | *n* |
|---|---|---|
| $I_{20}$ modulation | 2.04 ± 0.13 | 4 |
| $I_{max}$ modulation | 0.87 ± 0.06 | 3 |

Fold change = Response to ligand + propofol / Response to ligand

**Figure 4.2 Propofol modulation of the wild-type α1β GlyR submaximal and maximal glycine responses.**

A) Traces show the effect of propofol co-application (10 µM) with $EC_{20}$ glycine (30 µM). Response to $EC_{20}$ glycine vs response to $EC_{20}$ glycine + propofol, $p < 0.001$, paired t-test. B) Co-Application of 10 µM propofol with maximal glycine concentration (10 mM). Response to $I_{max}$ glycine vs response to $I_{max}$ glycine + propofol, $p < 0.05$, paired t-test. The solid bars above the traces indicate the time of application. C) The calculated average modulation fold change by propofol for the submaximal and maximal glycine evoked currents are listed. Data are reported as fold change ± SEM.

### 4.2.2 Co-application of glycine with 10 μM propofol to α1(E103K)β GlyR

The effect of propofol on the α1(E103K)β GlyR whole-cell current was examined. As indicated earlier, the human hyperekplexia mutation shifted glycine $EC_{50}$ by 72.2 fold (Table 3.3) and reduced the maximum $P_{open}$ in response to saturating glycine concentration from 0.98 to 0.67 (Table 3.4). The aim was to find out if the response of the heteromeric E103K GlyR can be enhanced by propofol.

Co-application of 10 μM propofol with a glycine submaximal concentration (2 mM) produced a small increase in the glycine response (Figure 4.3.A). The glycine $I_{20}$ in the experiment shown was 0.57 nA before propofol application and increased to 0.84 nA with propofol application. The average fold change was 1.21 ± 0.11 ($n$ = 4; $p$ > 0.05, paired t-test, Figure 4.3.E). The enhancement of the glycine submaximal response was smaller than that obtained in the wild-type receptor (2.04 ± 0.13 fold change, Figure 4.2.A).

Glycine maximal response was similar in the presence, or absence, of 10 μM propofol. Figure 4.3.B shows the α1(E103K)β GlyR response to 100 mM glycine in the absence and in the presence of propofol. Glycine current was 1.99 nA and glycine with propofol response was 2.05 nA. The average $I_{Glycine + propofol}/ I_{Glycine}$ of the E103K receptor was 1.08 ± 0.03 at saturating glycine ($n$ = 4; $p$ > 0.05, paired t-test).

### 4.2.3 Co-application of β-alanine with 10 μM propofol to E103K GlyR

In order to verify if the effect of propofol was similar if a partial agonist was tested, β-alanine was selected. Application of 10 μM propofol to α1(E103K)β receptor increased the submaximal β-alanine response ($EC_{20;}$ note that the maximum response to β-alanine in this mutant is 103 % of the maximum response to glycine; Figure 4.3.C). Response to $EC_{20}$ β-alanine was 1.17 nA and the measured current response to β-alanine in the presence of propofol was 1.87 nA. Co-application of propofol to 3 mM β-alanine trends to potentiate the whole-cell submaximal response by 1.48 ± 0.11 fold but statistical significant is not achived ($n$ = 3; $p$ > 0.05, paired t-test, Figure 4.3.E).

Responses to saturating β-alanine concentrations were not affected by 10 μM propofol (Figure 4.3.D). In this example, the β-alanine $I_{max}$ response was 3.28 nA before propofol application and 3.02 nA with propofol. Co-application of 10 μM propofol with 100 mM β-

alanine did not change the response as the average ratio of $I_{\beta\text{-alanine + Propofol}}$ / $I_{\beta\text{-alanine}}$ was 1.01 ± 0.02 ($n$ = 5; $p$ > 0.05, paired t-test). Thus, propofol did not affect maximal glycine and β-alanine responses in the heteromeric α1(E103K)β mutant GlyRs, with average fold change for glycine and β-alanine 1.08 ± 0.03 and 1.01 ± 0.02, respectively (Figure 4.3.E).

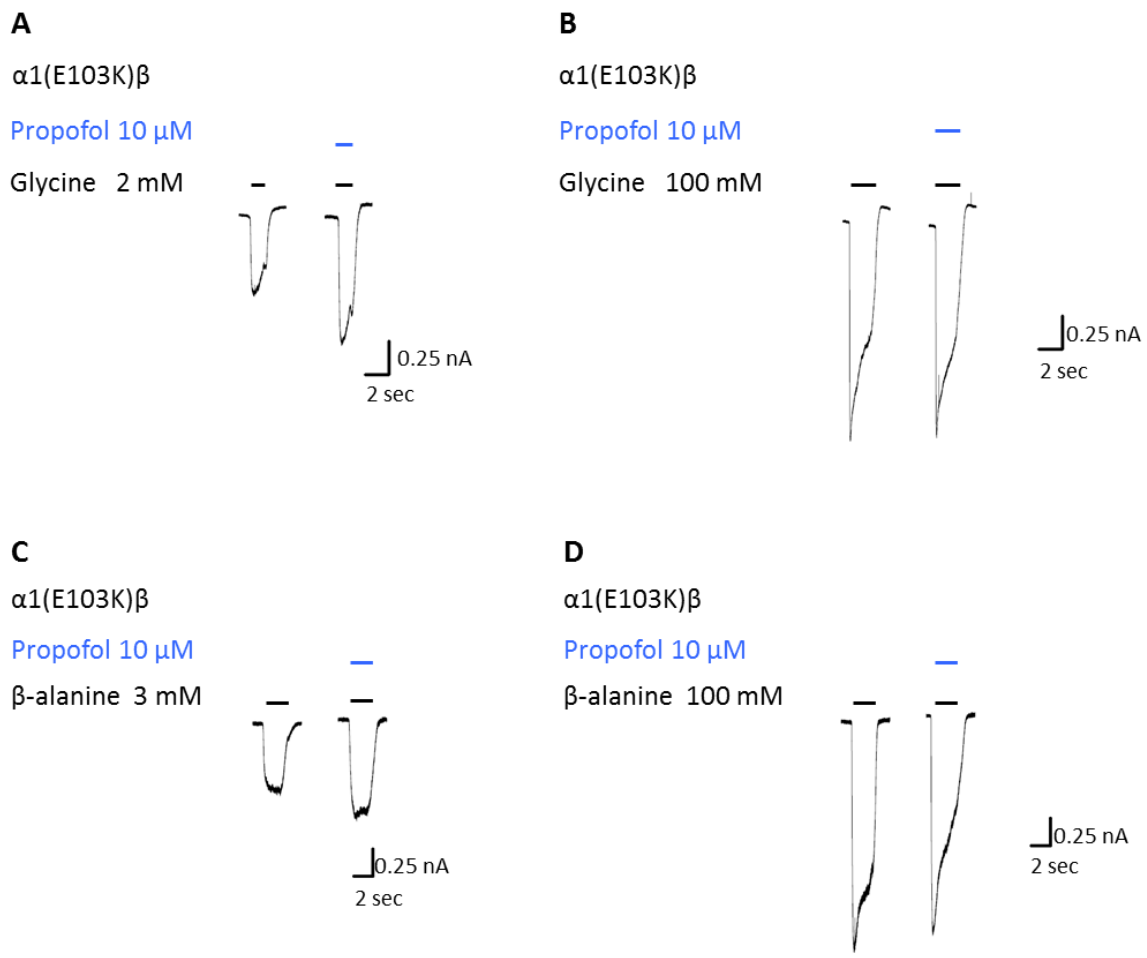


**E**

| Glycine | Fold change | *n* |
|---|---|---|
| $I_{20}$ modulation | 1.21 ± 0.11 | 4 |
| $I_{max}$ modulation | 1.08 ± 0.03 | 4 |

| β-alanine | Fold change | *n* |
|---|---|---|
| $I_{20}$ modulation | 1.48 ± 0.11 | 3 |
| $I_{max}$ modulation | 1.01 ± 0.02 | 5 |

Fold change = Response to ligand + propofol / Response to ligand

**Figure 4.3 Potentiation of agonist currents in α1(E103K)β mutant GlyR by 10 µM propofol.**

A) Whole-cell current traces evoked by U-tube application of glycine $EC_{20}$ to E103K receptors in the absence, or presence, of propofol. B) Glycine maximum responses in the absence, or presence, of 10 µM propofol. C) The same experiment for β-alanine. D) Response to $I_{max}$ β-alanine vs response to $EC_{max}$ β-alanine + propofol. E) Data is presented as fold change ± SEM.

### 4.2.4 Propofol (50 μM) co-application with glycine to wild-type GlyRs

As we did not observe an enhancement by 10 μM propofol of the maximal responses to glycine, or β-alanine, in α1 (E103K) β mutant GlyR, we proceeded to test the effect of higher concentration of propofol with the same application method. Co-application of 50 μM propofol with submaximal glycine concentration significantly increased glycine-gated currents in wild-type receptors. The average fold change was 2.97 ± 0.41 ($p < 0.01$, paired t-test; $n = 5$; Figure 4.4.A). In the example shown, the peak amplitude of glycine with propofol was higher (1.33 nA) than the value without the modulator (0.46 nA). This confirms that the higher propofol concentration of 50 μM had a greater effect than 10 μM propofol on submaximal glycine responses 2.97 ± 0.41 vs. 2.04 ± 0.13, however this was not significant ($p > 0.05$, unpaired t-test*;* $n = 5, 3$ respectively).

Co-application of 50 μM propofol with 10 mM glycine did not potentiate the glycine maximal response (Figure 4.4.B). In the example shown, the glycine response was similar in control (4.36 nA) and during propofol co-application (4.36 nA). The average $I_{Gly + Propofol} / I_{Gly}$ was 1.01 ± 0.02 for 5 cells ($p > 0.05$, paired t-test). Even at this higher concentration propofol did not potentiate maximum glycine-gated currents for the wild-type heteromeric GlyRs.

### 4.2.5 Pre-incubation of 50 μM propofol to wild-type GlyRs

Another step was added to the modulator application method. Pre-application of 50 μM propofol for about 30 seconds followed by co-application of glycine and propofol was tested. U-tube application of 50 μM propofol and glycine to the heteromeric wild-type GlyRs increased the glycine submaximal response (Figure 4.5.A). During the pre-application period of propofol no direct activation was observed. Glycine responses in propofol showed clearer and more extensive desensitisation than control responses. The magnitude of current potentiation induced by propofol to glycine $EC_{20}$ of 30 μM was around 5 fold change. (5.60 ± 1.4; $p < 0.05$, paired t-test; $n = 5$).

Adding pre-incubation of propofol did not change the results with saturating glycine concentration, which was not enhanced by propofol (Figure 4.5.B). The peak response to 10 mM glycine was similar in the presence (1.64 nA) or in the absence (1.99 nA) of 50 μM propofol with average of $I_{Gly + Propofol} / I_{Gly}$ 0.94 ± 0.05 for 4 cells ($p > 0.05$, paired t-test).

**Pre-application vs co-application**

The previous results showed that the average enhancement of glycine $I_{20}$ responses by propofol is larger for pre-application followed by co-application than for co-application alone (5.60 vs 2.97). However, for the $I_{max}$ , the lack of modulation was similar (0.94 vs 1.01). Pre-application of 50 μM propofol for around 30 seconds followed by co-application by the indicated concentration of the ligand with propofol was considered as the method of choice. In the following parts of the Chapter this method was used.

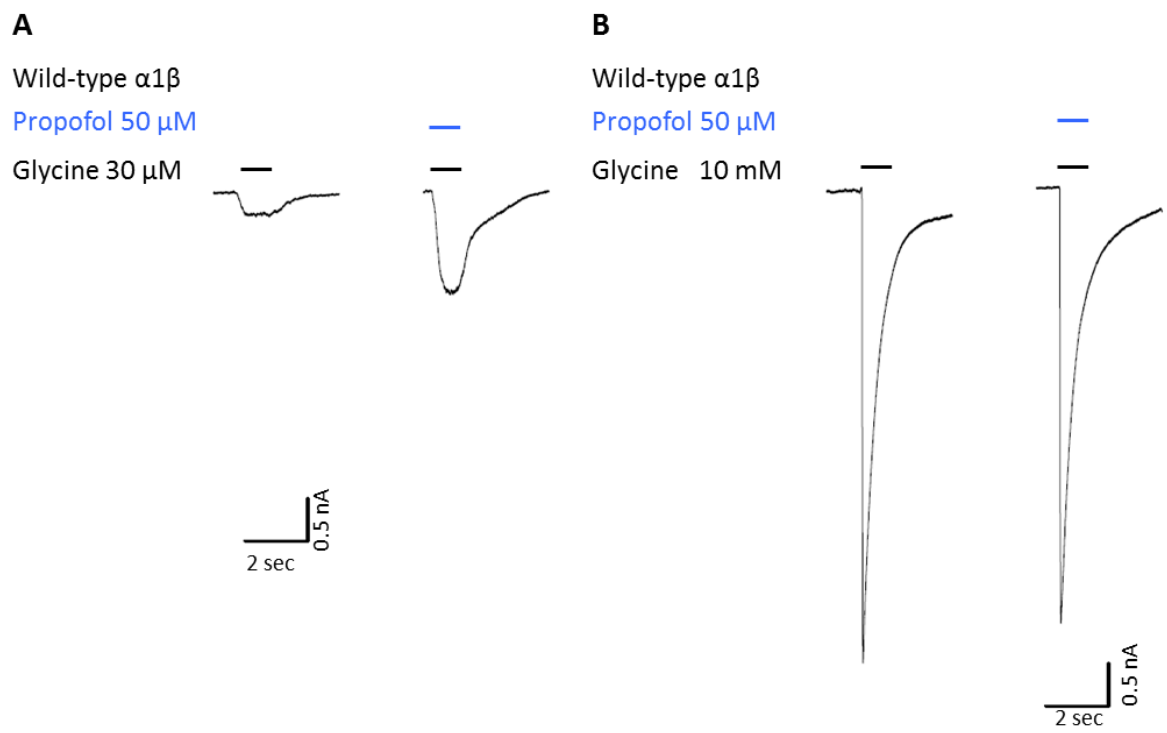


C

| Wild-type α1β | Fold change | *n* |
|---|---|---|
| $I_{20}$ modulation | 2.97 ± 0.41 | 5 |
| $I_{max}$ modulation | 1.01 ± 0.023 | 5 |

**Figure 4.4 Propofol (50 µM) modulation of α1β wild-type GlyRs; Co-application method.**

A) Sample glycine $EC_{20}$ current before and after propofol application. B) Whole-cell traces showing inward currents elicited by U-tube application of saturating glycine concentration with, or without, propofol. Solid lines above the traces indicate the time of application. C) Summary of the calculated modulation ratio.

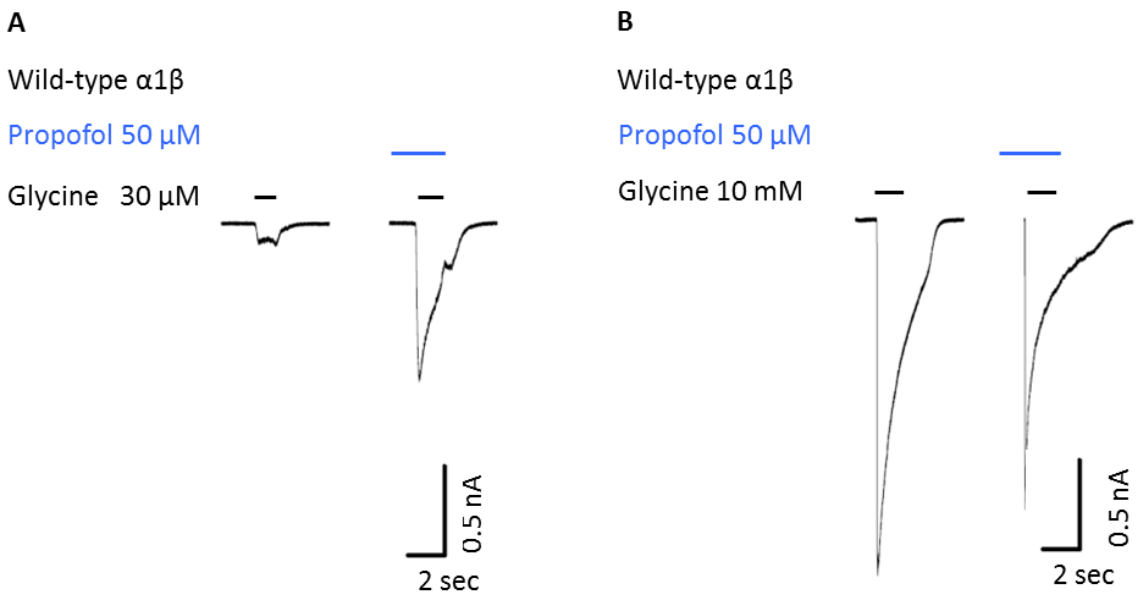


C

| Wild-type α1β | Fold change | *n* |
|---|---|---|
| $I_{20}$ modulation | 5.60 ± 1.4 | 5 |
| $I_{max}$ modulation | 0.94 ± 0.05 | 4 |

Fold change = Response to ligand + propofol / Response to ligand

**Figure 4.5 Propofol (50 µM) modulation of α1β wild-type GlyRs; Pre-application followed by co-application method.**

A) Representative macroscopic whole-cell traces showing inward currents elicited by U-tube application of $EC_{20}$ glycine to HEK293 cells expressing α1β human wild-type GlyRs with, or without, propofol. B) Current traces gated by saturating glycine concentration in the absence, or presence, of propofol. Propofol is pre-applied for 30s, and bars are not to scale. The effects of propofol on glycine submaximal, or maximal, response are summarized in (C).

### 4.2.6 The effect of propofol (50 μM) on the α1(E103K)β GlyR

The loop A hyperekplexia mutant reduced glycine potency and efficacy as demonstrated in the previous Chapters (Table 3.3, 3.4).

Propofol at 50 μM concentration enhanced glycine $I_{20}$ in HEK293 cells expressing the E103K mutation (Figure 4.6.A). Pre-application of propofol did not evoke a current. Application of propofol with 2 mM glycine to heteromeric E103K GlyR enhanced the submaximal glycine current by 5.35 fold for the illustrated example. The response to $EC_{20}$ glycine and propofol compared to that of glycine alone did not reach significance ($p > 0.05$, paired t-test). The average modulation was 3.18 ± 0.58 fold for α1(E103K)β GlyR ($n = 5$) compared to 5.60 ± 1.40 for wild-type ($p > 0.05$, unpaired t-test, $n = 4$).

Glycine maximal response in presence of propofol for the heteromeric α1 (E103K) β receptor is illustrated in Figure 4.6.B. During the application of propofol alone no current was found. Propofol appeared to speed up the channel desensitization. In this example glycine maximum current was 0.70 nA before propofol application and 0.60 nA after propofol application. The ratio of $I_{Gly+\ Propofol}$ / $I_{Gly}$ was 0.91, 0.54 ($n = 2$). Thus propofol did not potentiate maximum glycine responses in E103K mutants cf. 0.94 ± 0.05 fold in wild-type GlyR (Figure 4.6.C).

**Conclusion**

Propofol potentiated the submaximal glycine response of the α1 (E103K) β receptor but to lower extent than wild-type receptors. Propofol application was did not potentiate the glycine maximal response. Even that this mutation has reduced glycine gating efficacy as evaluated by single channel method, application of propofol to saturating glycine concentration was not enough to rescue the channel maximal response obtained by whole-cell experiments.

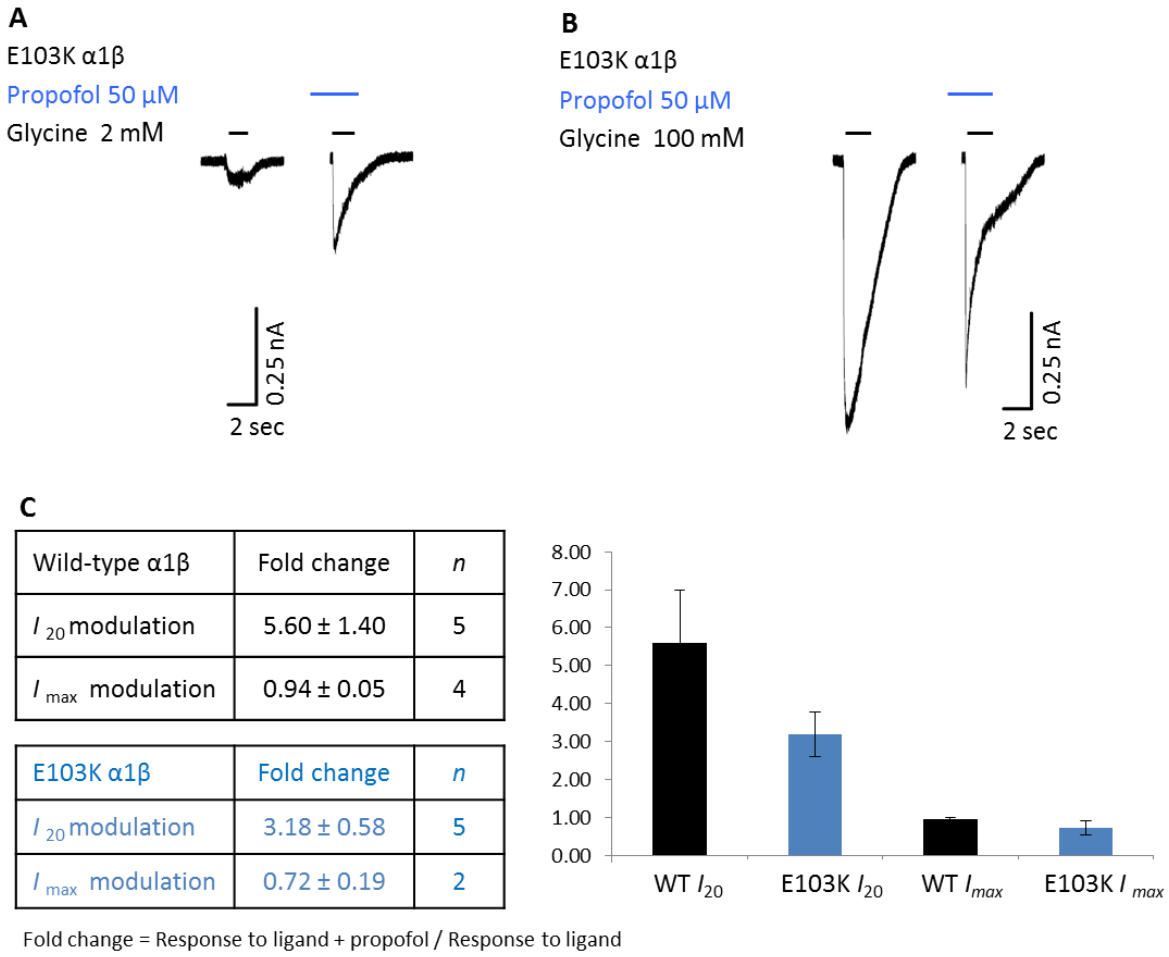


| Wild-type α1β | Fold change | *n* |
|---|---|---|
| $I_{20}$ modulation | 5.60 ± 1.40 | 5 |
| $I_{max}$ modulation | 0.94 ± 0.05 | 4 |

| E103K α1β | Fold change | *n* |
|---|---|---|
| $I_{20}$ modulation | 3.18 ± 0.58 | 5 |
| $I_{max}$ modulation | 0.72 ± 0.19 | 2 |

Fold change = Response to ligand + propofol / Response to ligand

**Figure 4.6 Propofol modulation of the α1(E103K)β GlyR mutant.**

A) Records of glycine current without or with propofol (50 μM) in HEK-293 cells expressing α1 (E103K) β GlyRs. B) Application of propofol to saturating glycine concentration. C) The average change in response ratio is listed. Lines above the traces show the time of application in case of propofol application was even earlier. Data are expressed as fold change ± SEM.

### 4.2.7 Propofol modulation of the α1(Q266H)β GlyR

The whole-cell concentration response curves from the previous chapter indicated a shift in glycine sensitivity by ~ 12 fold for the heteromeric Q266H GlyR mutation (Table 3.4). The maximum $P_{open}$ obtained from single-channel records indicated that this mutation reduces the channel open probability from 0.98 to 0.61 (Table 3.5). The aim was to examine if we are able to potentiate glycine $EC_{20}$, or maximal response, with propofol, and whether these effects were different than in wild type GlyRs.

Application of a submaximal concentration of glycine (200 μM, $EC_{20}$) produced inward current responses (Figure 4.7.A). During the pre-application of 50 μM propofol there was no observed direct activation effect. This finding is similar to the corresponding wild-type GlyRs results. Co-application of propofol following the pre-application period resulted in potentiation of the glycine-gated response. Propofol application increased the onset of desensitization. Measurement of the response before and after propofol application allowed fold change measurement for each individual cell. For the illustrated example the response to glycine was 1.32 nA but the response to glycine and propofol was increased to 3.35 nA. The α1(Q266H)β GlyR response to $EC_{20}$ glycine and propofol was significantly larger than response to $EC_{20}$ glycine, ($n$ = 4; $p < 0.05$, paired t-test,). The average fold change was 5.19 ± 1.35 for $n$ = 4 cells (Figure 4.7.C). This result is similar to propofol modulation of glycine submaximal response of wild-type GlyRs 5.60 ± 1.4 ($n$ = 5; $p > 0.05$, unpaired t-test; Figure 4.7.C).

Propofol potentiation of glycine maximal response was also tested. Application of saturating glycine concentration of 50 mM produced an inward current. In the example shown, this current was almost identical before and after application of 50 μM propofol (4.68, 4.56 nA; Figure 4.7.B). This result was consistent from one cell to another. There was no significant difference between the response to $I_{\max}$ glycine and the response to $I_{max}$ glycine + propofol ($n$ = 4; $p > 0.05$, paired t-test). The average fold change for the $I_{max}$ glycine response was 1.05 ± 0.06, $n$ = 4. These results are similar to those observed in wild-type glycine receptors (0.94 ± 0.05 fold change; $n$ = 5; $p > 0.05$) (Figure 4.7.C).

## Conclusion

Propofol potentiates the glycine $EC_{20}$ response of the heteromeric Q266H GlyR mutation but not the maximal response. Propofol effects (or lack thereof) for submaximal, or maximal, glycine concentrations were similar to the results obtained from wild-type GlyRs. So this GlyR mutation does not interfere with the normal potentiation effect of propofol.

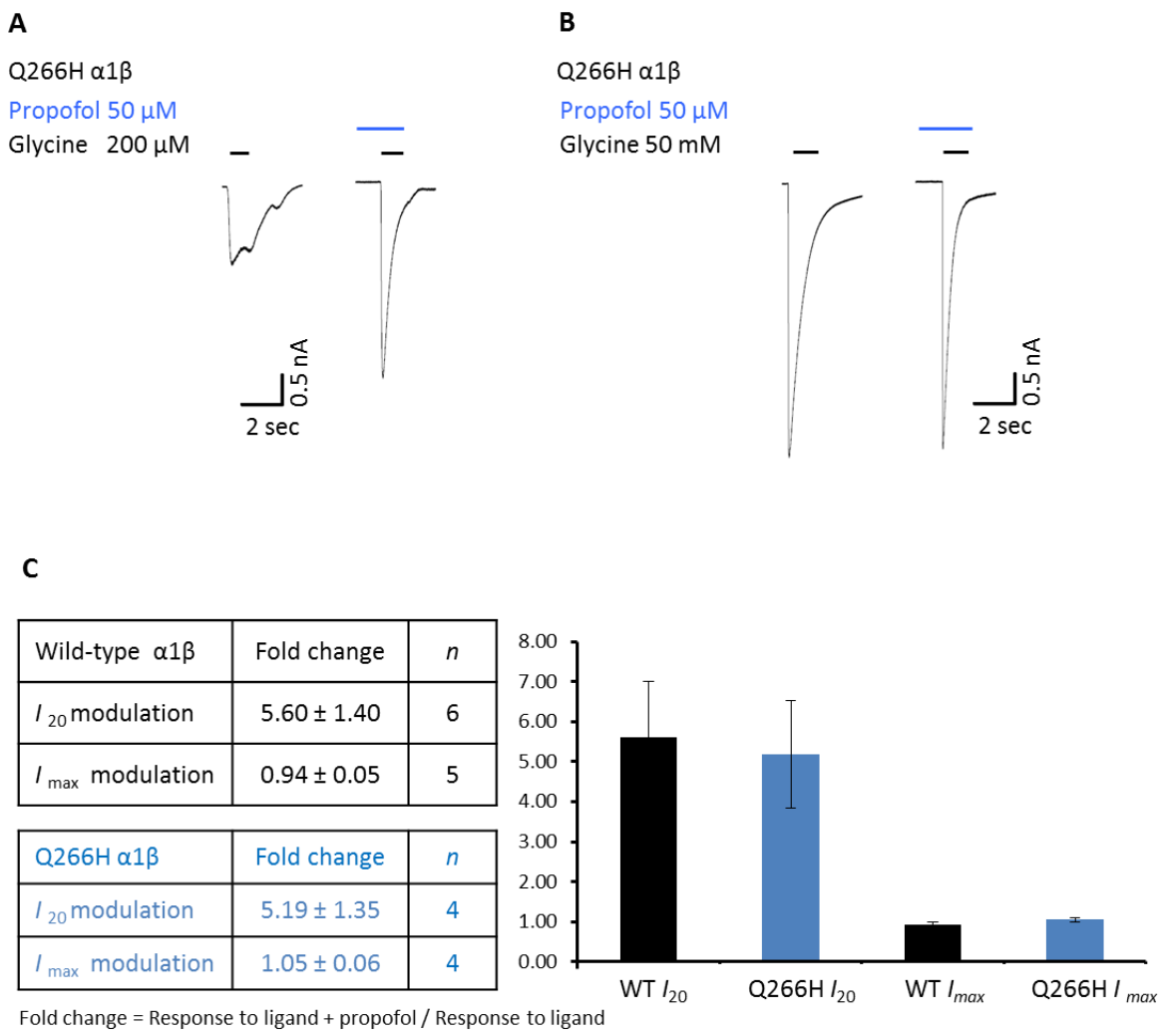


| Wild-type α1β | Fold change | *n* |
|---|---|---|
| $I_{20}$ modulation | 5.60 ± 1.40 | 6 |
| $I_{max}$ modulation | 0.94 ± 0.05 | 5 |

| Q266H α1β | Fold change | *n* |
|---|---|---|
| $I_{20}$ modulation | 5.19 ± 1.35 | 4 |
| $I_{max}$ modulation | 1.05 ± 0.06 | 4 |

Fold change = Response to ligand + propofol / Response to ligand

**Figure 4.7 Effect of propofol on α1(Q266H)β GlyR.**

A) Response to $EC_{20}$ glycine vs response to $EC_{20}$ glycine + propofol. B) Maximal glycine response before and after application of 50 μM propofol. The solid bars above the traces indicate the time of application (in case of propofol not to the scale). C) The calculated average modulation fold change by propofol for the submaximal and maximal glycine evoked currents are indicated. Data are represented as fold change ± SEM.

### 4.2.8 Potentiation of the glycine responses at the α1(S267N)β GlyRs

As I indicated earlier, this mutation (15' of TM2) increased glycine $EC_{50}$ by ~35 fold (Table 3.4) and also reduced the maximal channel $P_{open}$ from 0.99 to 0.37 (Table 3.5). For this mutation I tested whether propofol can enhance currents evoked by glycine $EC_{20}$ and by a maximal concentration of the agonist. A Glycine concentration of 1.5 mM was selected as $EC_{20}$ and 50 mM was selected as the saturating concentration (see Figure 3.21). Enhancement of the $EC_{20}$ glycine-gated currents in the presence of propofol is shown in Figure 4.8.A, where the submaximal glycine current was 2.55 nA vs 4.71 nA, in control and in propofol, respectively. Propofol significantly enhanced glycine submaximal response ($n$ = 6; $p < 0.05$, paired t-test,). The average potentiation of submaximal glycine response for α1(S267N)β GlyR was 2.71 ± 0.41 fold ($n$ = 6) compared to wild-type receptor response 5.60 ± 1.40 fold ($n$ = 6; $p > 0.05$, unpaired t-test; Figure 4.8.C). The effect of propofol varied considerbly across cells, and ranged between 2-5 fold change.

The response to maximal concentration of glycine (50 mM) showed a slight potentiation with propofol application (Figure 4.8.B). Peak currents measured at saturating glycine concentration were consistently larger in the presence of propofol ($n$ = 6, $p < 0.01$, paired t-test,). In the illustrated example, the peak measured current was 4.55 nA for glycine and 5.49 nA for glycine and propofol. The average modulation ratio was 1.29 ± 0.09 for 6 cells. Note that propofol did not increase the maximum response to glycine in wild-type receptors (0.94 ± 0.05; $n$ = 5; $p < 0.05$, unpaired t-test, Figure 4.8.C).

Work published by other groups is consistent with my results, and shows that the enhancement produced by allosteric modulators on submaximal glycine responses can be reduced by introducing mutations in S267 (Mihic *et al.*, 1997; Ahrens *et al.*, 2008).

In attempt to define the ethanol site Mihic *et al.,* investigated different TM2 and TM3 residues in glycine and $GABA_A$ receptors. They found that in oocytes expressing homomeric GlyR the S267I GlyR mutation abolished the potentiation effect of ethanol and reduced the potentiation effect of the anaesthetic enflurane. Potentiation effect was estimated at glycine $EC_{10}$ (Mihic *et al.,* 1997). From my results, it seems that propofol behaves in a manner similar to that of enflurane, in that their effects were reduced by the mutation.

Another study evaluated the modulating effect of propofol on HEK293 cells bearing S267I or S267M glycine receptor mutations using the whole-cell patch clamp technique (Ahrens *et al.,*

2008). They found that the heteromeric S267I and S267M GlyR mutations reduced glycine sensitivity by 2 and 3 fold respectively. They then co-applied glycine $EC_{20}$ with 3-300 μM propofol. They found that propofol potentiates the glycine submaximal response of the GlyR mutations S267M and S267I. However, the enhancing effect of propofol was smaller than that observed in the wild-type receptors. Thus, co-application of 50 uM propofol resulted in around 100 % potentiation of response in S267I compared to ~ 400% potentiation in wild-type receptors. Propofol modulation was reduced in the S267M GlyR mutation from ~400 to 200% (Ahrens *et al.,* 2008). The same Authors observed that propofol at concentrations equal to, or greater than, 100 μM directly activates the wild-type glycine receptor, but not the tested GlyR mutants (Ahrens *et al.,* 2008).

**Conclusion**

Glycine-gated submaximal currents at the heteromeric 15' α1(S267N)β GlyR are enhanced by propofol ($n$ = 6, $p < 0.05$, paired t-test). The maximum glycine response of the HEK293 cells bearing the heteromeric S267N mutation was significantly potentiated by propofol ($n$ = 6; $p < 0.01$, paired t-test,).

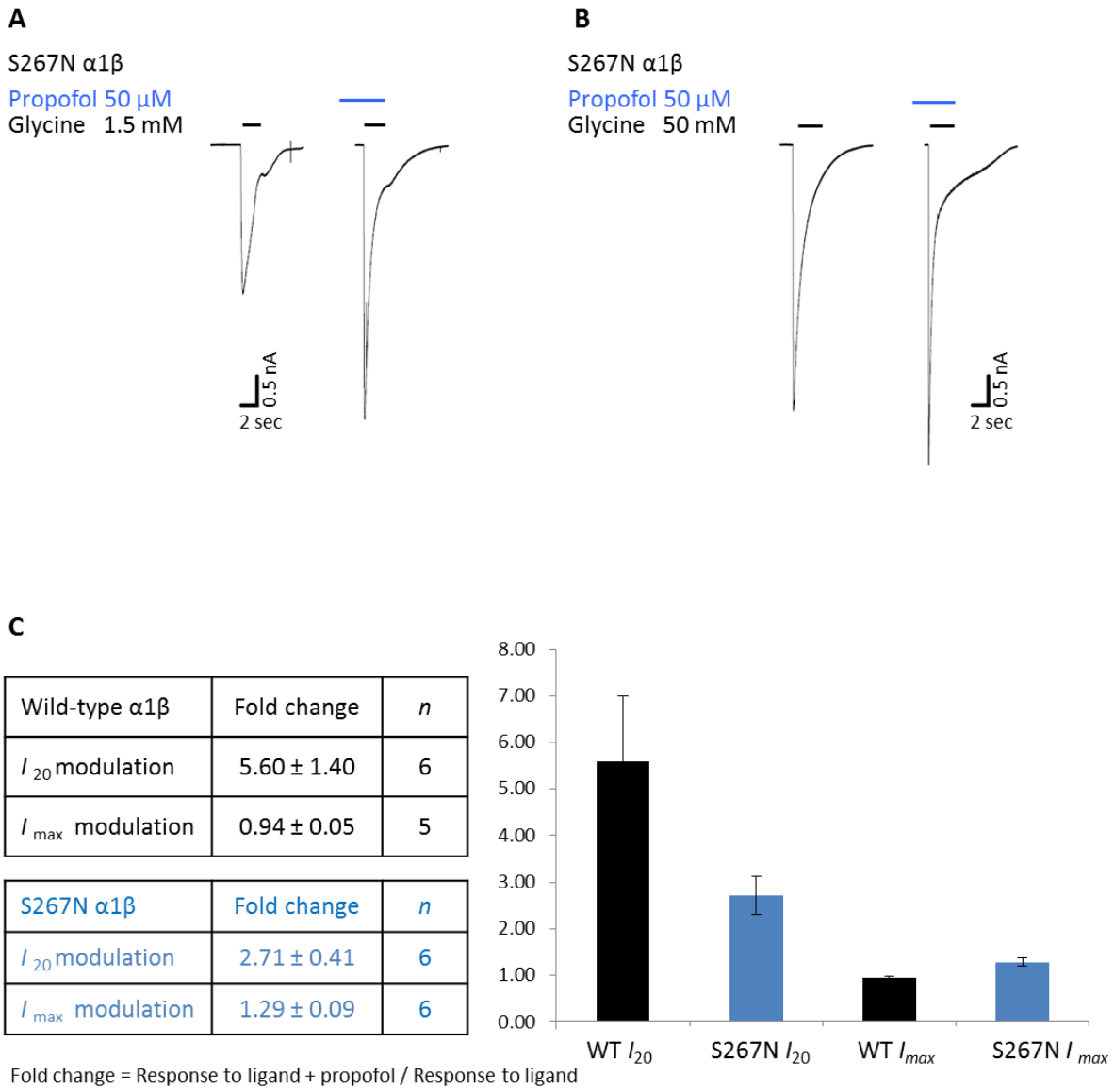


| Wild-type α1β | Fold change | *n* |
|---|---|---|
| $I_{20}$ modulation | 5.60 ± 1.40 | 6 |
| $I_{max}$ modulation | 0.94 ± 0.05 | 5 |

| S267N α1β | Fold change | *n* |
|---|---|---|
| $I_{20}$ modulation | 2.71 ± 0.41 | 6 |
| $I_{max}$ modulation | 1.29 ± 0.09 | 6 |

Fold change = Response to ligand + propofol / Response to ligand

**Figure 4.8 Propofol modulation of the α1(S267N)β GlyR mutant.**

A) Trace records shows the effect of 50 µM propofol application to $EC_{20}$ glycine induced current. Response to $EC_{20}$ glycine vs response to $EC_{20}$ glycine + propofol. B) Example traces showing inward chloride current responses to saturating glycine concentrations before and after propofol application. The solid bars above the traces indicate the time of application (not to the scale). C) Average calculated modulation ratio is indicated. Data are expressed as fold change ± SEM.

### 4.2.9 Propofol enhancement of the glycine current at the α1(S231N)β GlyRs

The $EC_{50}$ for glycine on the α1(S231N)β GlyRs shifted from 0.10 mM in the wild-type to 3.81 mM in the mutant (Table 3.4). This change in glycine potency was accompanied with a decrease in the maximum $P_{open}$ from 0.98 to 0.38 (Table 3.5). I proceeded to test whether the function of the mutant α1(S231N)β GlyRs can be rescued by propofol.

Application of 50 μM propofol was found to enhance the response to the current produced by submaximal glycine concentration in all of the tested cells (Figure 4.9.A). Glycine (1 mM) was used as the submaximal concentration according to our established protocol (Figure 3.13). At these low concentrations, responses to U-tube application of submaximal glycine concentration showed no apparent desensitisation, however, this became apparent in the presence of propofol. Also, propofol addition made the rise time of the current response faster. During the pre-application period of 50 μM propofol no direct activation was observed. The response to submaximal glycine concentration shown in the figure was 0.25 nA in control and 1.72 nA in the presence of propofol. Propofol significantly potentiated glycine submaximal response ($n = 6$; $p < 0.01$, paired t-test,). The average change of propofol modulation of the glycine submaximal response was 5.48 ± 1.38 fold ($n = 6$). The magnitude of average potentiation induced by 50 μM propofol was similar to that observed in wild type GlyRs (5.60 ± 1.40; $n = 5$; $p > 0.05$, unpaired t-test) (Figure 4.9.C).

A clear enhancement of the glycine maximal response by propofol was observed for this mutant (Figure 4.9.B). A glycine concentration of 50 mM was used with, or without, the presence of 50 μM propofol. No direct activation was noticed in the pre-application period of propofol. Desensitization was faster and reached a greater proportion of the peak response when propofol was co-applied with glycine. The ratio of the $I_{Glycine + Propofol} / I_{Glycine}$ was 1.97 for the illustrated example. Application of propofol was effective in potentiating the glycine maximal response ($n = 6$, $p < 0.05$, paired t-test). Unlike wild-type receptors which has average fold change of 0.94 ± 0.05, the response of α1(S231N)β GlyRs to an maximally effective concentration of glycine was markedly increased by propofol (1.98 ± 0.29; $p < 0.05$, unpaired t-test, $n = 6$ both).

### 4.2.10 Single-channel recordings of the α1(S231N)β GlyR in the presence of propofol

The pronounced effect of propofol on maximum glycine responses in this mutant warranted further investigation. To test whether propofol modulation affects channel gating, singlechannel recordings were done at saturating (100 mM) glycine concentration in the presence of 50 μM propofol (Figure 4.10). Propofol significantly increased the maximum $P_{open}$ of the α1(S231N)β GlyR mutant by 1.7 fold, from 0.38 ± 0.06 to 0.65 ± 0.04 ($n$ = 16, 28, respectively; $p < 0.0001$, unpaired t-test). There was no change in the single-channel current amplitude in the absence, or presence, of propofol (2.01 ± 0.05 vs 1.94 ± 0.04 pA; $n$ = 16, 28, respectively; $p > 0.05$, unpaired t-test). Similar to the single-channel records obtained for the S231N mutant without propofol (Figure 3.14), modes of openings within the cluster were detected. These single-channel results supported the results obtained from the whole-cell experiments.

In order to further characterize the effects of this mutation, I attempted to record responses to the partial agonist β-alanine, but was unsuccessful. It was impossible to obtain a full concentration-response curve for β-alanine with the α1(S231N)β mutation because U-tube application of 100 mM β-alanine to HEK293 cells expressing the mutant GlyR produced only a very small current (~ 300 pA).

**Conclusion**

In the α1(S231N)β GlyR mutant, propofol potentiates the whole-cell responses to both submaximal and maximal glycine concentrations. Propofol increases the maximal $P_{open}$ of the α1(S231N)β GlyR mutant.

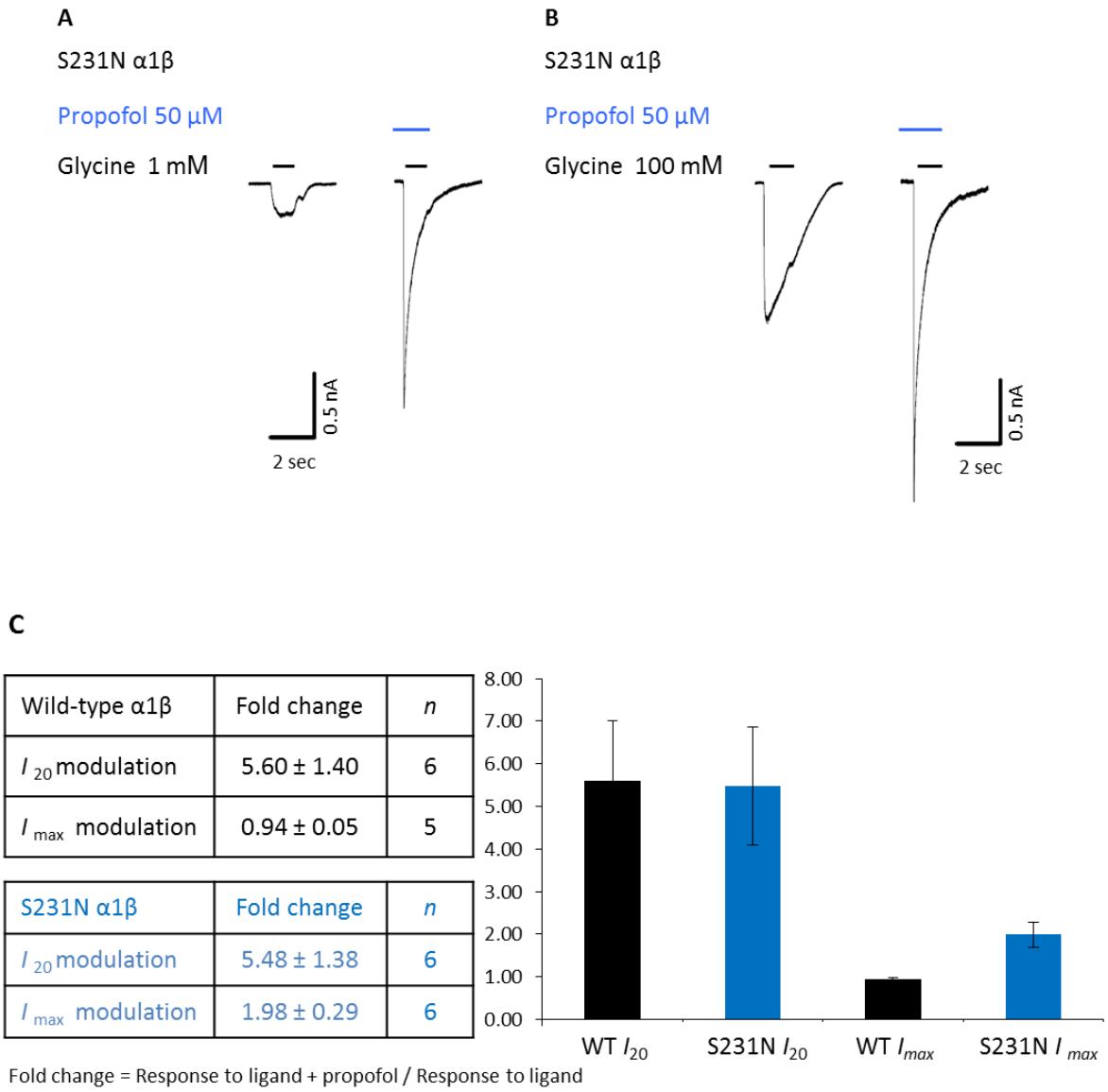


**Figure 4.9 Potentiation of the glycine submaximal and maximum responses of the α1(S231N)β GlyR mutation.**

A) Whole-cell traces showing inward currents elicited by U-tube application of $EC_{20}$ glycine concentration with, or without, propofol. B) Responses obtained by application of saturating glycine concentration in the absence, or presence, of propofol. The solid bars above the traces indicate the time of application (not to the scale). C) Summary of the effect of propofol. Data are expressed as fold change ± SEM.

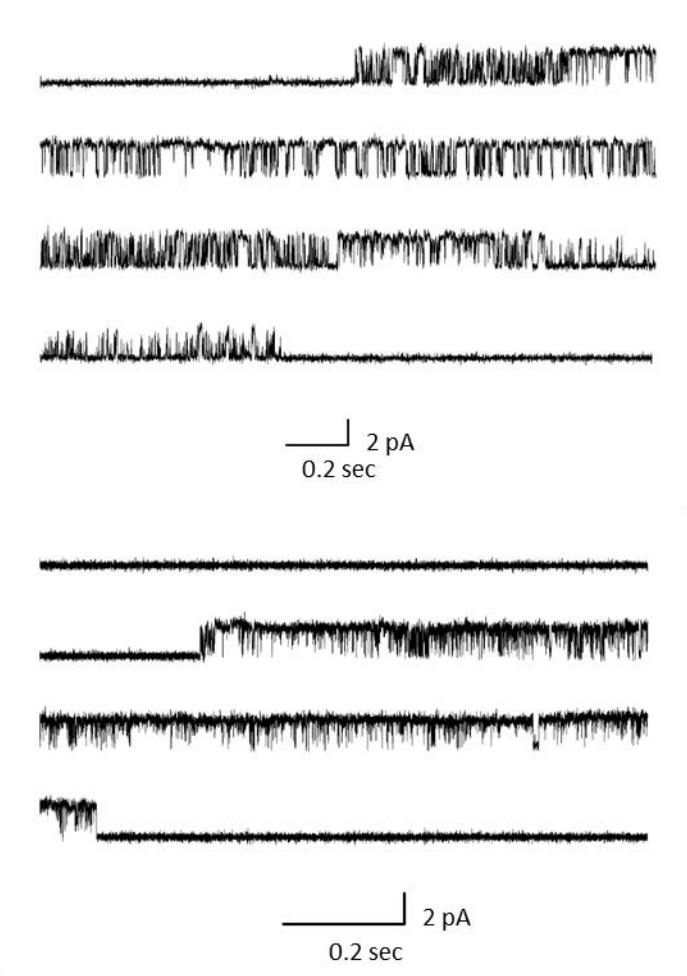


| Receptor | $I_{max}$ $P_{open}$ | Amplitude (pA) | *n clusters* |
|---|---|---|---|
| α1(S231N)β, $I_{max}$ glycine | 0.38 ± 0.06 | 2.01 ± 0.05 | 16 |
| α1(S231N)β, $I_{max}$ glycine and 50 μM propofol | 0.65 ± 0.04 | 1.94 ± 0.04 | 28 |

**Figure 4.10 Single-channel activity at saturating (100 mM) glycine concentration for HEK293 expressed α1(S231N)β GlyR in the presence of 50 μM propofol.**

Single-channel traces (cell-attached, pipette potential + 100 mV) show that the mutant receptor opens in clusters and propofol increased glycine maximum $P_{open}$.

**Summary of the effect of propofol on selected human hyperekplexia mutations**

Propofol (50 μM) was found effective in potentiating glycine submaximal response for α1(Q266H)β, α1(S267N)β, α1(S231N)β GlyRs mutants. The level of modulation varied from mutation to another and ranged from 2 to 5 fold change (Figure 4.11).

On the other hand, potentiation of the glycine maximal response was only found for the α1(S231N)β and α1(S267N)β GlyR mutations (Figure 4.11).

A

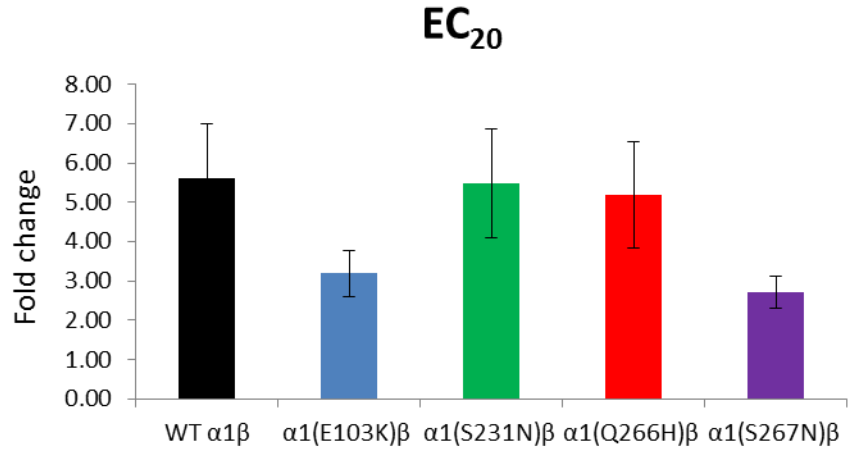


B

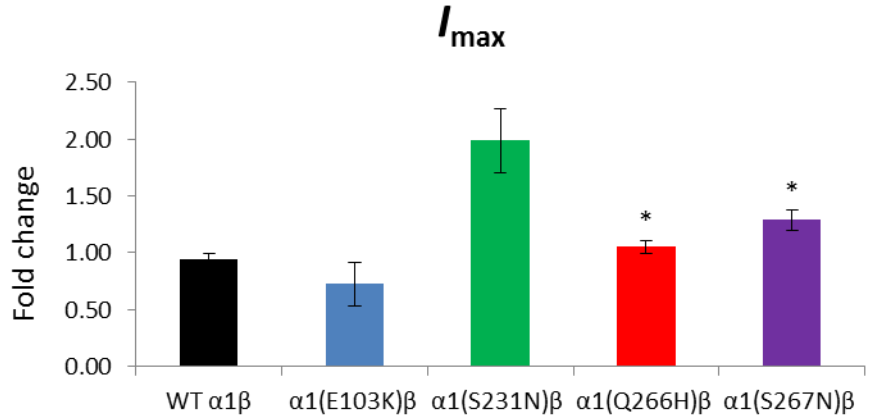


C

| Receptor | $I_{20}$ modulation (Fold change) | *n* | $I_{max}$ modulation (Fold change) | *n* |
|---|---|---|---|---|
| WT α1β | 5.60 ± 1.40 | 6 | 0.94 ± 0.05 | 5 |
| α1(E103K)β | 0.91, 0.54 | 5 | 0.72 ± 0.19 | 2 |
| α1(S231N)β | 5.48 ± 1.38 | 6 | 1.98 ± 0.29 | 6 |
| α1(Q266H)β | 5.19 ± 1.35 | 4 | 1.05 ± 0.06 | 4 |
| α1(S267N)β | 2.71 ± 0.41 | 6 | 1.29 ± 0.09 | 6 |

**Figure 4.11 Summary of propofol modulation of the heteromeric α1(Q266H) β, α1 (S267N) β, α1(S231N)β, and α1(E103K)β GlyRs mutations responses.**
A) Comparison of the effect of propofol on glycine $EC_{20}$ between wild-type receptors and the indicated mutations. B) Comparison of the effect of propofol on glycine $I_{max}$ and the indicated mutations. Fold change = response to ligand + propofol / response to ligand. * $p <$ 0.05, unpaired t-test. Data are presented as fold chnage ± SEM.

## 4.3 Discussion

While propofol is widely used as an intravenous anaesthetic, its mechanism of action is not fully understood. There is strong evidence that $GABA_A$ receptors are involved (Hales and Lambert, 1991; Jurd *et al.,* 2003), but it is unclear whether GlyRs contribute to the action of therapeutic concentrations of propofol.

As described in the introduction section of this Chapter, propofol potentiation of GlyR responses was reported by Mascia *et al.* (1996) for *Xenopus* oocytes expressed receptors and by Nguyen *et al.* (2009) for cultured rat neurons and *in vivo* receptor type.

In the literature, there is little about the effect of hyperekplexia mutations on propofol modulation of GlyR. Indeed only two mutations (R271Q and R271L in TM2) were evaluated. These mutant receptors are still sensitive to propofol, which rescued the glycine response, by enhancing glycine apparent affinity and efficacy. Treatment of transgenic mice carrying R271Q α1 GlyR mutation with propofol improved the hyperekplexia symptoms (O'Shea *et al.,* 2004).

More extensive studies have been done with other GlyR modulators, which have been assessed for their ability to improve the function of mutated GlyRs. For example, dehydroxylcannabidiol (DH-CBD), a nonpsychoactive synthetic cannabinoid, is effective in rescue the impaired glycine response (by lowering the glycine $EC_{50}$ in HEK293 expressed receptors) in several α1 GlyR hyperekplexia missense mutations, such as R218Q, P250T, V260M, R271Q, K276E, and M287L (Xiong *et al.,* 2014). Whereas DH-CBD enhanced the reduced maximal glycine-induced currents of R218Q, R271Q, and K276E α1 mutants GlyRs, the enhancement effect was absence in P250T, V260M, Q266I, S267Q, The restoration effect is seen also *in vivo,* where treatment with DH-CBD (50 mg/body weight) resolved the hyperekplexia exaggerated startle symptoms in heterozygous mice that carry α1R271Q or α1M287L GlyR mutations (Xiong *et al.,* 2014). The cannabinoid was not effective in rescuing the hyperekplexia symptoms in mice heterozygous for α1Q266I or α1S267Q GlyR mutations (which were also resistant to cannabinoid potentiation *in vitro*, Xiong *et al.*, 2014).

Zinc (100 nM), another GlyR modulator, was found to potentiate glycine submaximal response of the M287L and Q266I α1 GlyR mutations, in a manner similar that observed in wild-type receptors (Borghese *et al.,* 2012).

In my experiments I investigated whether propofol enhances responses of wild type and mutant α1β GlyRs expressed in HEK293 cells. Testing different protocols and concentrations of propofol on wild-type α1β GlyRs showed that propofol can enhance glycine submaximal responses, but not the maximal currents.

*E103K hyperekplexia mutant* In these GlyRs, a low concentration of propofol (10 μM) with glycine, or β-alanine, did not have any noticeable effects (Figure 4.3), whereas a higher concentration of 50 μM propofol resulted in a slight increase of glycine submaximal currents, but this failed to reach statistical significance (Figure 4.6). Despite the fact that gating is damaged in E103K receptors, no detectable increase of the maximal glycine current was observed by propofol. It is unlikely that this mutation is in the propofol binding site, so it is hard to explain why the maximum current is not rescued by propofol. A possible explanation is that if propofol in this case, affects only the early pre-open conformational changes (flip) and the increase in affinity with activation, the reduction in maximum glycine $P_{open}$ cannot be rescued if the mutation damages channel opening (E). Compensation cannot be achieved with increase in flip in this case.

*Q266H hyperekplexia mutant* Propofol (50 μM) significantly enhanced the glycine submaximal response of this mutant but it failed to do so for the maximum response (Figure 4.7). This result is in agreement with previous findings that the propofol effects (eg the enhancement of submaximal responses) are not changed (vs. wild type) by the Q266K, Q266E, and Q266F α1 GlyR mutations (Lynagh and Laube, 2014). Interestingly, the Q266I GlyR mutation made the receptor resistant to DH-CBD (Xiong *et al.,* 2014) and abolished ethanol potentiation of the glycine submaximal response (Borghese *et al.,* 2012). This argues that different modulators may bind to different sites and activate different transduction chains that are differentially sensitive to mutations.

*S267N hyperekplexia mutant* The S267 residue has been proposed to be one of the key residues involved in ethanol action (Mihic *et al.,* 1997). Ethanol potentiation was absent in the S267N mutant (Becker *et al.,* 2008) and S267Q GlyR was also found to be insensitive to cannabinoid modulation (DH-CBD; Xiong *et al.,* 2014). However, mutations at this positions did not affect some of the action of propofol and the submaximal glycine response of S267I and S267M mutant GlyR (note these are not hyperekplexia mutations) were potentiated by propofol (Ahrens *et al.,* 2008). Consistent with this observation, my results showed that both

the submaximal and the maximal responses of the heteromeric S267N GlyR are potentiated by propofol (Figure 4.8).

*S231N hyperekplexia mutant* Propofol restored the functional deficiency in the α1(S231N)β hyperekplexia mutant GlyRs. Importantly in this mutant both submaximal and maximal responses to glycine were enhanced by propofol (Figure 4.9).

Thus, we saw a different picture depending on the mutation considered. In the S267N and S231N mutants we saw that propofol enhanced both submaximal and maximal responses to glycine, whereas in the E103K and Q266H mutants only submaximal responses were potentiated. The enhancement of maximum responses was substantially larger for the S231N mutants. The reasons for these differences are not clear. It is unlikely that they are linked to greater, or smaller, effects of the mutations on overall gating, because the reduction in maximum $P_{open}$ is 0.38 and 0.37 for the S231N and S267N mutants, respectively and 0.67 0.61 for E103K and Q266H. It could be that we need to dissect the effects of the mutation into greater detail and establish whether some mutations affect preferentially the early pre-open conformational changes (flip) or the actual opening of the channel. It could be that propofol can rescue more fully one but not the other impairment.

More mutations need to be tested to have clear idea about propofol binding site in GlyRs. The homology model obtained recently from the GluCl structure by our collaborators at Oxford University, Biggin and Yu, proposed that propofol biding site involve residues from principal subunit: V280, I285, M287, A288, R271, L291 and I225, I229, P230 from the complementary subunit. Note that P230 is very close to the S231 position, whose mutation was the most sensitive to propofol.

# Chapter 5: Critical E103-R131 salt-bridge interaction that modifies channel gating

This chapter follows from work published as a paper and I am the first author (Safar *et al.*, 2017).

## 5.1 Introduction

Channels in the Cys-loop superfamily are activated by agonists and neurotransmitters with very different structures and sizes (from glycine to GABA, glutamate to 5-HT). How these channels achieve this agonist recognition is an area of intense investigation. In the present study we have investigated the role of residues at the back of the binding site, in loops A and E, E103 and R131, respectively, and established that they interact. This Chapter is part from work published as a paper of which I was a first author.

Little is known of how the hyperekplexia mutations in the receptor binding site might act. If such mutations do not abolish agonist binding, they might be interesting to investigate, as they are likely to interfere with the signal transduction that follows the agonist binding. Thus, these mutations could throw light on how the binding site contributes to agonist efficacy, a poorly understood phenomenon. One such mutation is E103K, whose effects on glycine response were discussed in detail in Chapter three. The E103 residue is conserved in all human and mouse glycine receptor subunits Figure (5.1) as described earlier in Chapter three. This suggests it has a vital role in channel function. Briefly, in homomeric GlyR, the mutation reduces glycine potency by 2.84 fold and reduces glycine efficacy from 0.992 ± 0.002 to 0.73 ± 0.07. In the heteromeric GlyR, the mutation has a much greater effect in reducing glycine potency by 72.7 fold and reducing glycine efficacy from 0.98 ± 0.01 to 0.67 ± 0.06. Further investigations of the effect of this mutation will be included in this Chapter. The initial experiments were conducted on the heteromeric receptor, but as the homology model of GlyR based on GluCl was established (Yu *et al.,* 2014), the later experiments were conducted on the homomeric expressed receptors that allowed comparison with the model.

The position of the E103 residue in a view taken from the GlyR homology model (Yu *et al.,* 2014) based on GluCl structure (Hibbs and Gouaux, 2011) is shown in Figure (5.2) E103 is located at (or just near) Loop A of the principal (+) subunit. The negatively charged side chain of the E103 is close to the positively charged side chain of R131 in Loop E on the complementary (-) side of the binding site. Arginine (R131) in this location is conserved in all subunits where E103 is conserved, and is conserved also in other receptors, such as, human $GABA_A$ β3 (where 103 is an Asp), *Gloeobacter violaceus* GLIC and *Dickeya chrysanthemi* ELIC, where E103 is not conserved.

(R131 part will be discussed in another PhD thesis by Elliot Hurdiss). The distances between the sidechain hydrogen atoms of R131 to the sidechain oxygen atoms of E103 are 2.5 ~ 2.8 Å. This range is compatible with the presence of a salt bridge, and it is worth investigating whether the charged side chains of E103 and R131 have an effect on channel gating. The side chains of both E103 and R131 are quite far from both the centre of the channel pore (distance of ~16 Å obtained from our model) and from the agonist (~8 Å from glycine). This suggests that it is unlikely that the side chains of these residues affect conductance directly and that any effects on agonist binding are likely to be indirect. However, we can not exclude that mutating either residues might affect conductance as the nearby K104 residue has been determined to affect the conductance in pLGIC (Hansen *et al.*, 2008; Moroni *et al.*, 2011a).

In order to test the hypothesis that a salt bridge between E103 and R131 stabilizes loops A and E, we decided to test the effects of the E103K hyperekplexia mutation on the GlyR responses to the partial agonist sarcosine (N-methyl glycine), as the effect to the full agonist glycine on E103K was established in Chapter three. Note that sarcosine is slightly bulkier than glycine.

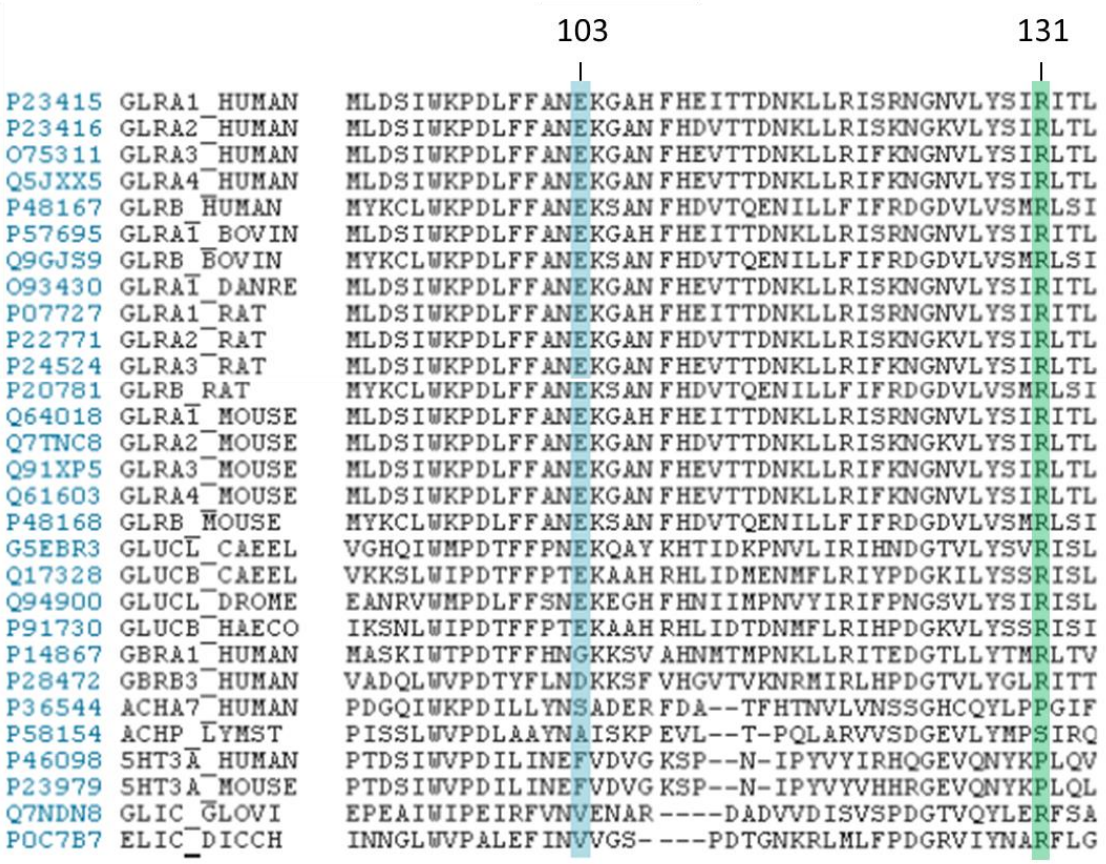


**Figure 5.1 Partial sequence alignment of α1(E103) GlyR and α1(R131) GlyR residues with other pLGICs and proteins.**

The E103 human hyperekplexia mutation residue in the ECD of the GlyR α1 is highlighted in blue and R131 highlighted in green. Glutamate is conserved in 21 receptors (see text). Uniprot accession numbers are indicated at the left side for each receptor, human glycine α1 (P23415), human glycine α2 (P23416), human glycine α3 (O75311), human glycine α4 (Q5JXX5), human glycine β (P48167), bovine glycine α1 (P57695), bovine glycine β (Q9GJS9), zebrafish glycine α1 (O93430), rat glycine α1 (P07727), rat glycine α2 (P22771), rat glycine α3 (P24524), rat glycine β (P20781), mouse glycine α1(Q64018), mouse glycine α2 (Q7TNC8), mouse glycine α3 (Q91XP5), mouse glycine α4 (Q61603), mouse glycine β (P48168), *C. elegans* GluCl α (G5EBR3), *C. elegans* GluCl β (Q17328), *D. melanogaster* GluCl α (Q94900), *H. contortus* GluCl β (P91730), human $GABA_A$ α1(P14867), human $GABA_A$ β3 (P28472), human α7 nAChR (P36544), *L. stagnalis* AChBP (P58154), human 5-HT3A (P46098), mouse 5-HT3A (P23979), *Gloeobacter violaceus* GLIC (Q7NDN8), and *Dickeya chrysanthemi* ELIC (P0C7B7).

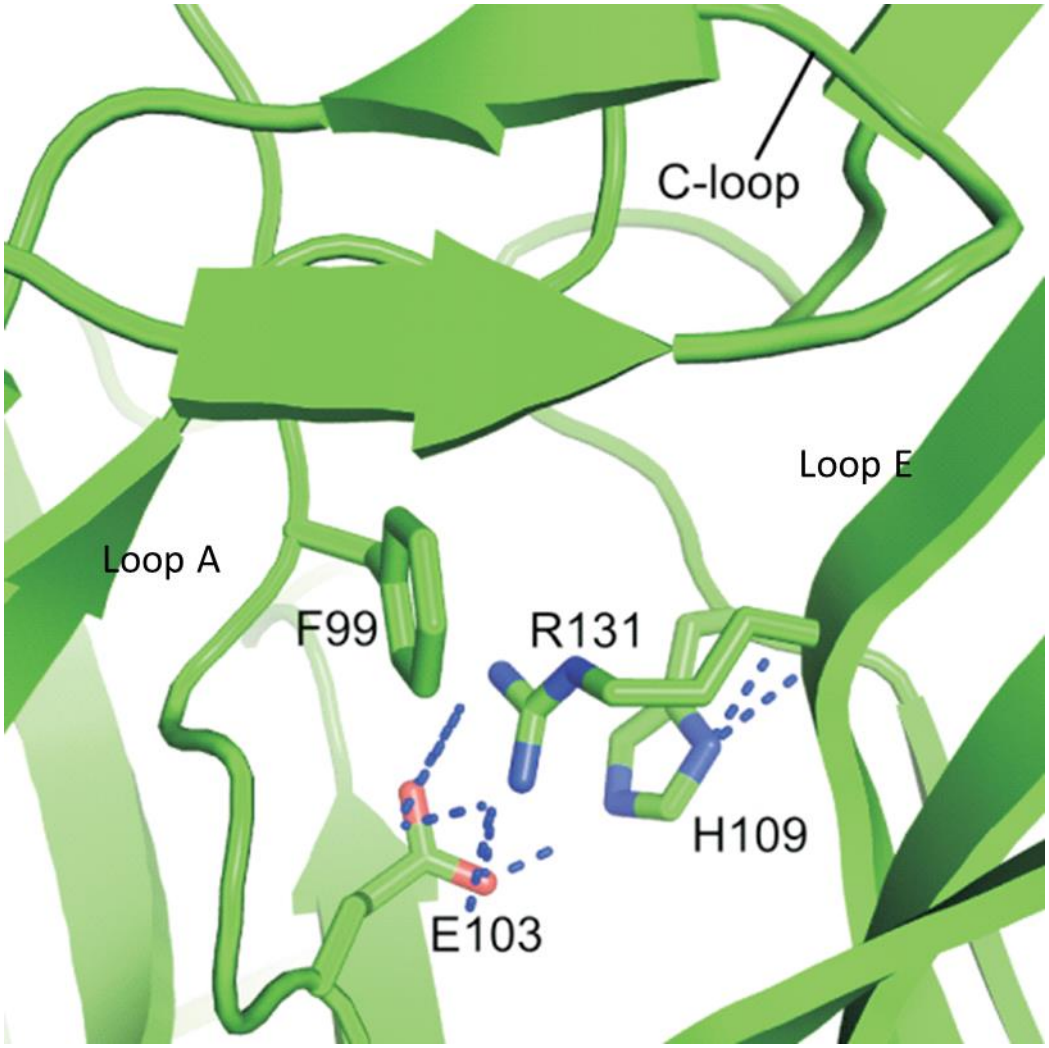


**Figure 5.2 Homology modelling indicates a possible salt-bridge between residues E103 and R131 of α1 GlyR.**

Homology model based upon the structure of GluCl showing the bottom of the binding site. The residues R131 and E103 are labeled. This model was first described in Yu *et al*. (2014).

## 5.2 Results

### 5.2.1 Whole-cell recordings of heteromeric wild-type GlyRs responses to β-alanine

Since in our lab we did not have established whole-cell concentration response curves for the wild-type GlyRs with β-alanine, I started with that, using 0.1 – 50 mM β-alanine and obtaining in each cell a response to saturating glycine concentration (10 mM) in order to normalise the β-alanine response. As it is shown in Figure 5.3, desensitization was clear with 1 mM (~ $EC_{80}$) β-alanine. $EC_{50}$, $I_{max}$ ,and $n_H$ were 0.45 ± 0.08 mM, 5.54 ± 0.856 nA, and 1.15 ± 0.10, respectively, $n$ = 4 cells. The maximum β-alanine response relative to glycine was 0.79 + 0.06.

### 5.2.2 Whole-cell recordings of α1(E103K)β GlyR responses to β-alanine

Whole-cell recordings of the heteromeric E103K GlyR with 1-200 mM β-alanine were obtained (Figure 5.4). Responses to a saturating glycine concentration of 100 mM were obtained in each cell to normalise the β-alanine responses. The β-alanine $EC_{50}$ was increased significantly by the mutation from 0.45 ± 0.08 mM to 11.17 ± 1.43 mM ($n$ = 6 cells; $p < 0.01$, unpaired t-test). The $I_{max}$ was 6.78 ± 1.40 nA and the $n_H$ was similar to wild-type 1.00 ± 0.10. The maximum β-alanine response relative to glycine was increased significantly from 0.79 ± 0.06 ($n$ = 4) to 1.03 ± 0.04 ($n$ = 6; $p < 0.05$, unpaired t-test). So although the mutation reduced β-alanine sensitivity, it increased the β-alanine efficacy relative to glycine. A change in relative maximum response to a partial agonist would indicate that the mutation alters channel gating.

To have a better evaluation of the effect of the heteromeric E103K mutation on the potency and the efficacy of glycine and β-alanine, concentration-response curves for the response of wild type and E103K GlyRs to both glycine and β-alanine, normalised to glycine are shown in Figure 5.5. As a result of the heteromeric α1(E103K)β GlyR mutation, the potency of glycine and β-alanine is reduced by 72.7 and 24.8 fold, respectively (Table 5.1). The fold change for glycine is almost three times the fold change for β-alanine. So the effect of the heteromeric GlyR mutation on the β-alanine response is less profound than for glycine. The β-alanine efficacy was also increased compared to wild-type receptors.

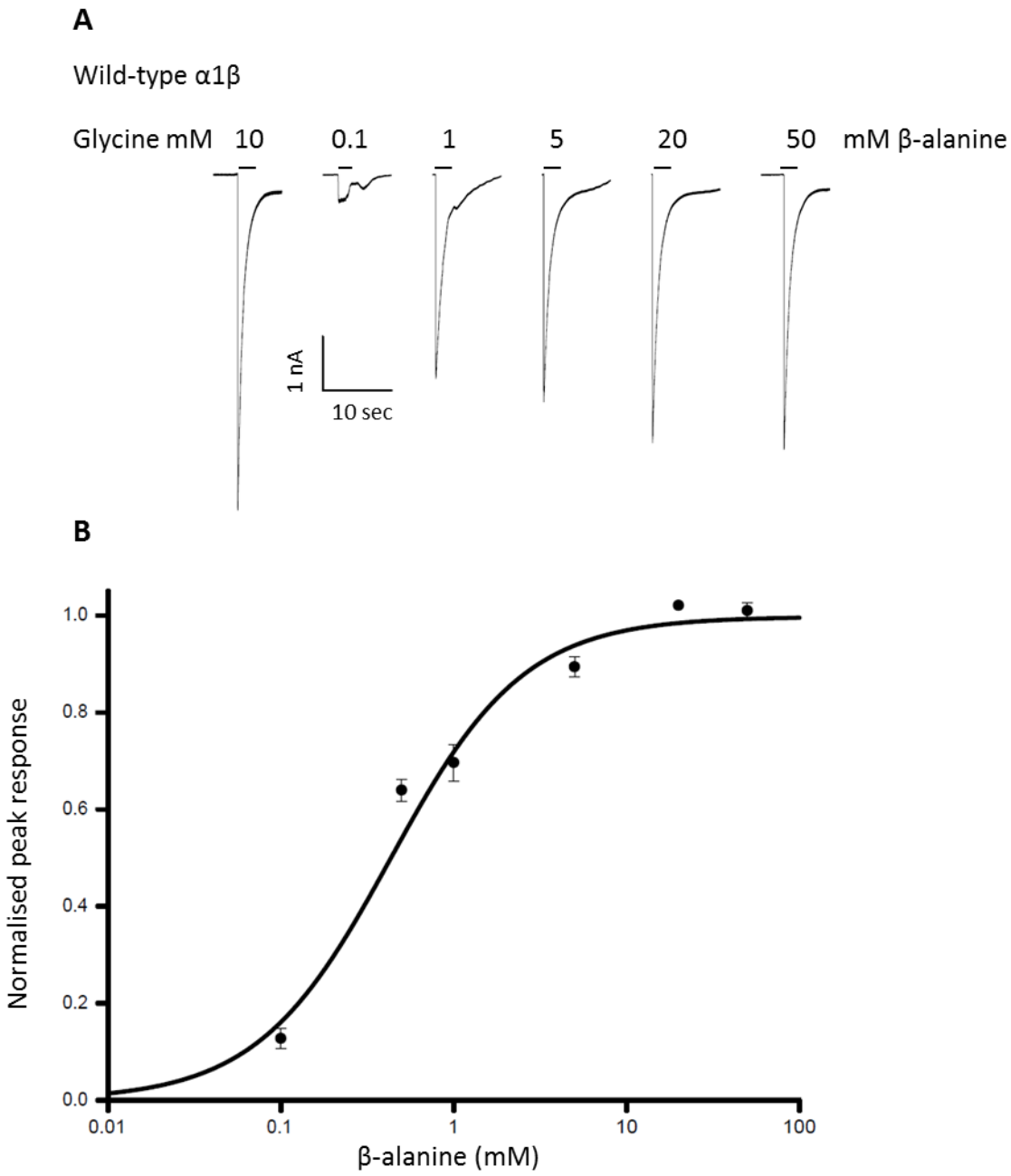


**Figure 5.3 Sensitivity of the human heteromeric wild-type GlyRs to β-alanine.**
Representative whole cell current traces evoked by U-tube application of β-alanine (black bars) to HEK293 cells expressing wild-type α1β GlyR (A). Cells were held at – 50 mV. B) Average β-alanine concentration-response curve obtained from α1 wild-type GlyR. The curve is a fit to the Hill equation. $EC_{50}$ = 0.45 ± 0.08 mM, $I_{max}$ = 5.54 ± 0.856 nA, $n_H$ = 1.15 ± 0.10, $n$ = 4 cells. The maximum β-alanine response relative to glycine was 0.79 + 0.06. Error bars indicate ± SEM.

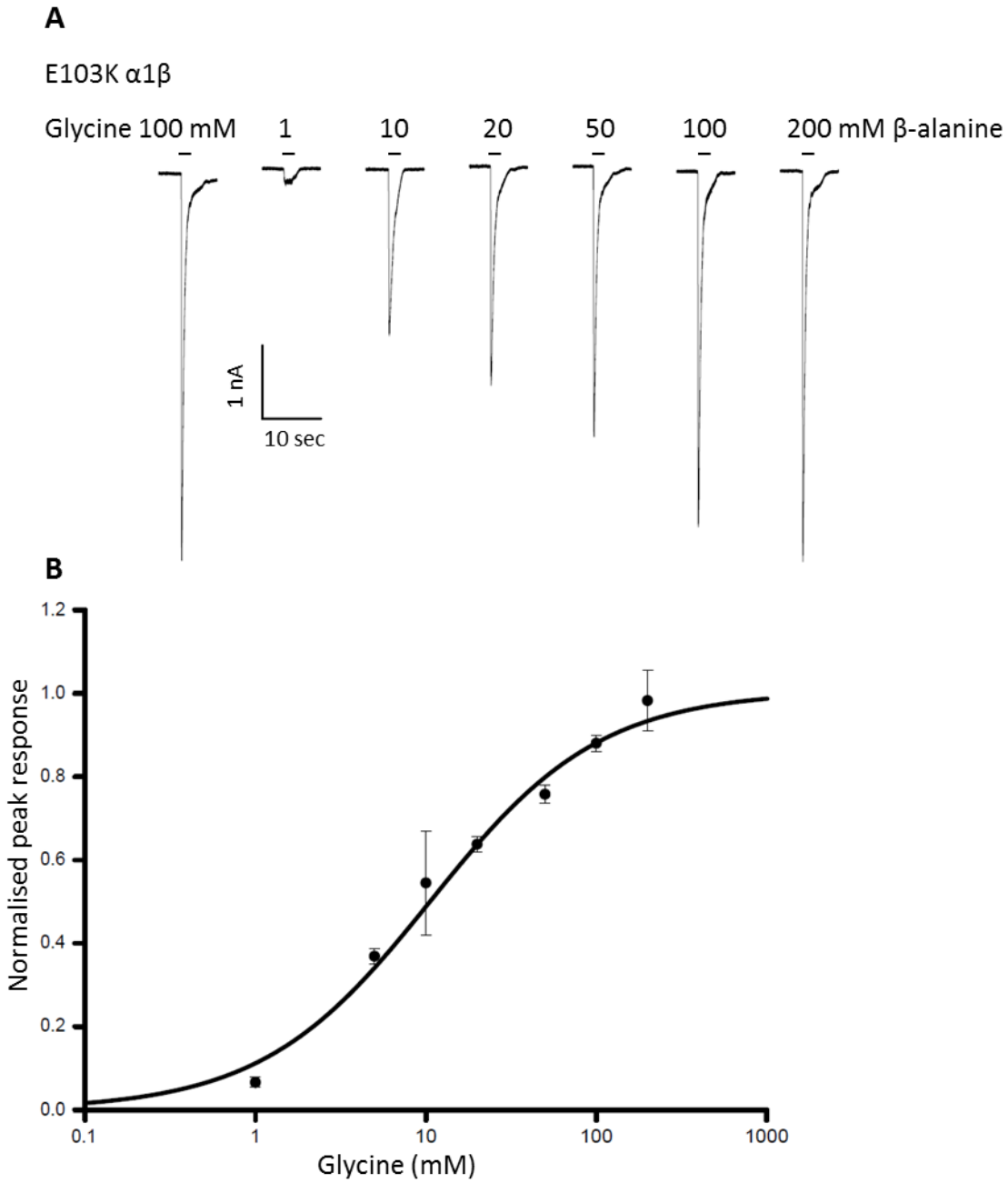


**Figure 5.4 The heteromeric α1(E103K)β hyperekplexia mutation reduces the sensitivity of GlyR to β-alanine.**

A) Representative whole-cell current responses evoked by U-tube β-alanine application to HEK293 cells expressing α1(E103K)β GlyR (upper panel). Black bars above the traces show the timing of the applications. The response to a saturating concentration of glycine obtained in the same cells (first trace) is also shown. B) Average β-alanine concentration-response curves obtained from α1(E103K)β GlyR. Solid curve is a fit to the Hill equation. $EC_{50}$ = 11.17 ± 1.43 mM, $I_{max}$ = 6.78 ± 1.40 nA, $n_H$ = 1.00 ± 0.10, $n$ = 6 cells. The maximum β-alanine response relative to glycine = 1.03 ± 0.04. Error bars indicate ± SEM.

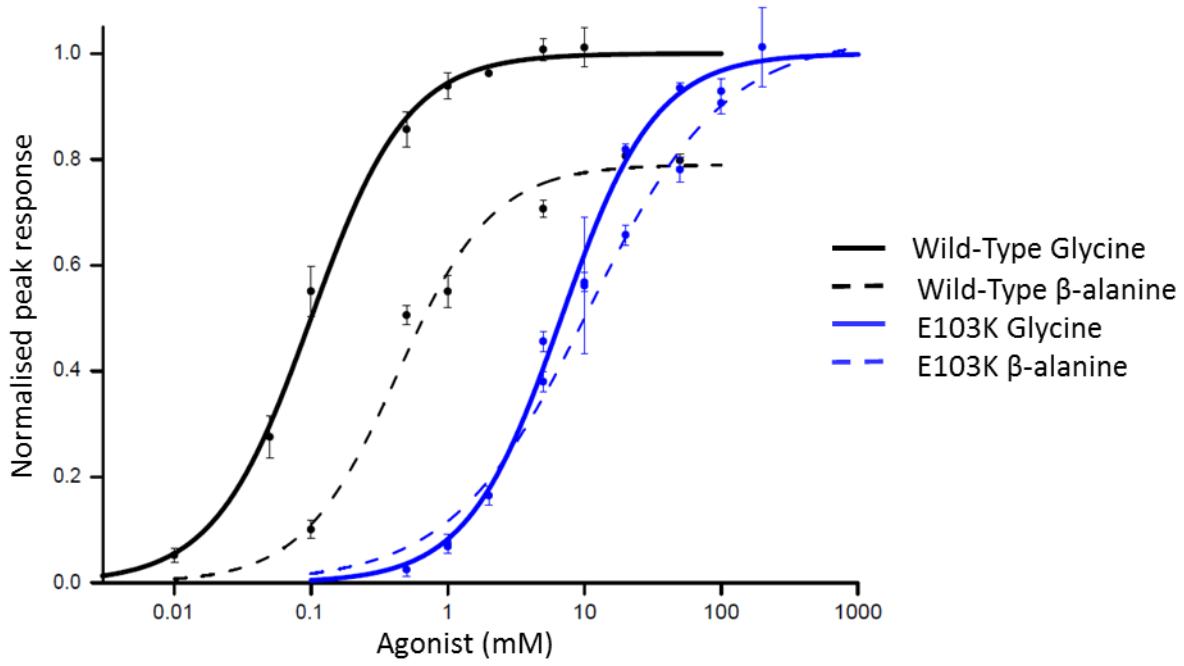


**Figure 5.5 The effect of α1(E103K)β GlyR on the potency and efficacy of glycine and β-alanine.**
Whole-cell concentration-response curves for the effect of α1(E103K)β mutant GlyR on glycine and β-alanine responses. β-alanine curves are normalized to the maximum glycine peak obtained from the same cell. For glycine wild-type α1β GlyR, $EC_{50}$ = 0.10 ± 0.03, $n_H$ = 1.48 ± 0.09, $I_{max}$ = 4.43 ± 1.08 nA, $n$ = 6. For β-alanine WT α1β GlyR, $EC_{50}$ = 0.45 ± 0.08, $n_H$ = 1.15 ± 0.10, $I_{max}$ = 5.54 ± 0.86 nA, $n$ = 4. For glycine α1(E103K)β, $EC_{50}$ = 7.27 ± 0.58, $n_H$ = 1.22 ± 0.08, $I_{max}$ = 3.62 ± 0.89 nA, $n$ = 6. For β-alanine α1(E103K)β, $EC_{50}$ = 11.17 ± 1.43, $n_H$ = 1.00 ± 0.10, $I_{max}$ = 6.78 ± 1.4 nA, $n$ = 6. Error bars indicate ± SEM.

**Table 5.1 Functional properties of heteromeric α1(E103K)β GlyR**

| | Glycine | | β-alanine | |
|---|---|---|---|---|
| Heteromeric Receptor | Wild-Type | E103K α1β | Wild-Type | E103K α1β |
| $EC_{50}$ (mM) | 0.10 ± 0.03 | 7.27 ± 0.58 | 0.45 ± 0.08 | 11.17 ± 1.43 |
| Fold change | 1 | 72.7 | 1 | 24.82 |
| $n_H$ | 1.48 ± 0.09 | 1.22 ± 0.08 | 1.15 ± 0.10 | 1.00 ± 0.10 |
| $I_{max}$ (nA) | 4.43 ± 1.08 | 3.62 ± 0.89 | 5.54 ± 0.86 | 6.78 ± 1.4 |
| *n* | 6 | 6 | 4 | 6 |
| Imax β-alanine/IGlycine | 1 | 1 | 0.79 ± 0.06 | 1.03 ± 0.04 |

### 5.2.3 Whole-cell recordings of GlyR bearing α1(E103K) hyperekplexia mutation

In order to test whether the effect of mutating E103 depends on the agonist, the response to the partial agonist sarcosine was examined. Whole-cell concentration response curves obtained from HEK293 cells expressing homomeric E103K GlyR were investigated. Figure 5.6 shows sample currents responses for the α1(E103K) GlyR to 10 – 300 mM sarcosine. Application of saturating concentration of glycine of 20 mM in the same cell was used to normalize the sarcosine current response relative to glycine.

In wild-type cells sarcosine is a partial agonist. Whole-cell recordings from our lab showed that sarcosine maximum current responses reached 80% of the maximum responses to glycine, when glycine was applied at the saturating concentration of 10 mM. The E103K mutation markedly reduced the channel sensitivity to sarcosine and prevented us from obtaining a full concentration-response curve as the response did not saturate even at 300 mM (Figure 5.6). We could not establish the whole-cell sarcosine maximum response in the mutant. $EC_{50}$ > 80 mM, $n_H$ = 1.37 ± 0.03, $I_{max}$ = 1.5 ± 0.4 nA, $n$ = 4 cells.

The clearest way to assess whether a mutation has an effect on gating is to measure the channel maximum $P_{open}$ in single channel records. The wild-type trace shown previously in Chapter three (Figure 3.3), shows a cluster of single channel activity in a cell-attached patch at saturating glycine concentrations with very high $P_{open}$. The channel exposed to 10 mM glycine is practically either desensitized, or open, almost all the time, with a maximum $P_{open}$ of 0.992 ± 0.002 ($n$ = 30 clusters; measured as cluster open time/total cluster time). The measurement of cluster open probability has the advantage that it measures only changes in receptor activation and is not affected by desensitization (as the desensitized intervals are not included in the analysis). This is why we decided to display some concentration-response curves as whole cell responses *scaled* to the maximum open probability measured by single-channel analysis.

Single-channel clusters activated by a saturating sarcosine concentration (100 mM, not shown Hurdiss personal communication) confirmed that sarcosine is a partial agonist in wild-type receptors, with a maximum $P_{open}$ of 0.70 ± 0.03 ($n$ = 22 clusters from 4 records). As shown previously in Figure 3.9, the E103K mutation clearly decreased the cluster $P_{open}$ elicited by

saturating glycine to 0.73 ± 0.07 ($n$ =13 clusters from 3 records). This effect strongly suggests that the E103K mutation must impair channel gating.

In order to test the hypothesis that there is a salt bridge between E103 and R131, we mutated both residues individually to alanine. Also, the charge was inverted to arginine and glutamate, respectively. The effects of mutating E103, or R131, residue or both on the channel response to the full agonist glycine were evaluated. In my Thesis I will focus on the effect of mutating the E103 residue.

### 5.2.4 Whole-cell and single channel recordings of GlyR bearing α1(E103A) mutation

Whole-cell recordings of the homomeric E103A responses to glycine are were obtained by U-tube application of 0.1-100 mM glycine. The concentration-response curve is shown in Figure 5.7. Desensitization was clear starting from 0.5 mM (~ $EC_{50}$). Glycine $EC_{50}$ was increased by 1.72 fold to 0.43 ± 0.05 mM ($p < 0.05$ , unpaired t-test; Table 5. 2). The $I_{max}$ was 5.91 ± 0.26 nA and $n_H$ was 1.24 ± 0.06, $n$ = 3 cells (Table 5.2).

Single-channel recordings using saturating concentration of 100 mM glycine were examined. Sample cell-attached trace is shown in Figure 5.8. There were clear channel openings and the cluster pattern was similar to wild-type GlyR channels shown previously in Chapter three (Figure 3.3.3). The maximum $P_{open}$ was measured for each cluster. The efficacy of glycine was unchanged and the maximum $P_{open}$ was high (0.97 ± 0.01, $n$ = 11 clusters from 3 patches). The current amplitude was 5.64 ± 0.23 pA. There was a change in glycine sensitivity but not the efficacy a result of the E103A GlyR mutation. The effect of inverting the charge in the side chain of E103 was then evaluated.

### 5.2.5 Whole-cell and single channel recordings of GlyR bearing α1(E103R) mutation

Whole-cell recordings of homomeric E103R were obtained. Sample current responses to 0.1 – 100 mM glycine are shown in Figure 5.9. Desensitization was detectable from 0.1 mM ($EC_{10}$) glycine. Glycine sensitivity was reduced by ~ 15 fold as $EC_{50}$ was shifted from 0.25 ±

0.03 to 3.68 ± 1.18 mM ($p$ < 0.01, unpaired t-test, $n$ = 6, 4, respectively). The reduction in glycine sensitivity to glycine is accompanied with increase in the slope of its concentration-response curve from 1.87 ± 0.37 ($n$ = 6) to 0.71 ± .07 (p < 0.05, unpaired t-test; $n$ = 4; Table 5. 2). The $I_{max}$ was 9.03 ± 3.86 nA comparable with wild-type GlyR (p > 0.05, unpaired t-test; $n$ = 4). Thus charge inversion had a very noticeable effect on the potency of glycine and on the slope of its concentration-response curve.

The effect of charge inversion mutations on the maximum $P_{open}$ was then evaluated. Single-channel clusters activated by a saturating glycine concentration (100 mM; Figure 5.10) were examined for the α1(E103R) GlyR. It was noticed that the mutation affected the maximum $P_{open}$. The maximum $P_{open}$ was reduced significantly from 0.992 ± 0.002 to 0.87 ± 0.02 ($n$ = 30 and 42, respectively; $p$ < 0.001, unpaired t-test; Table 5.2). The current amplitude was similar to wild-type with value of 5.75 ± 0.10 nA ($p$ > 0.05, unpaired t-test).

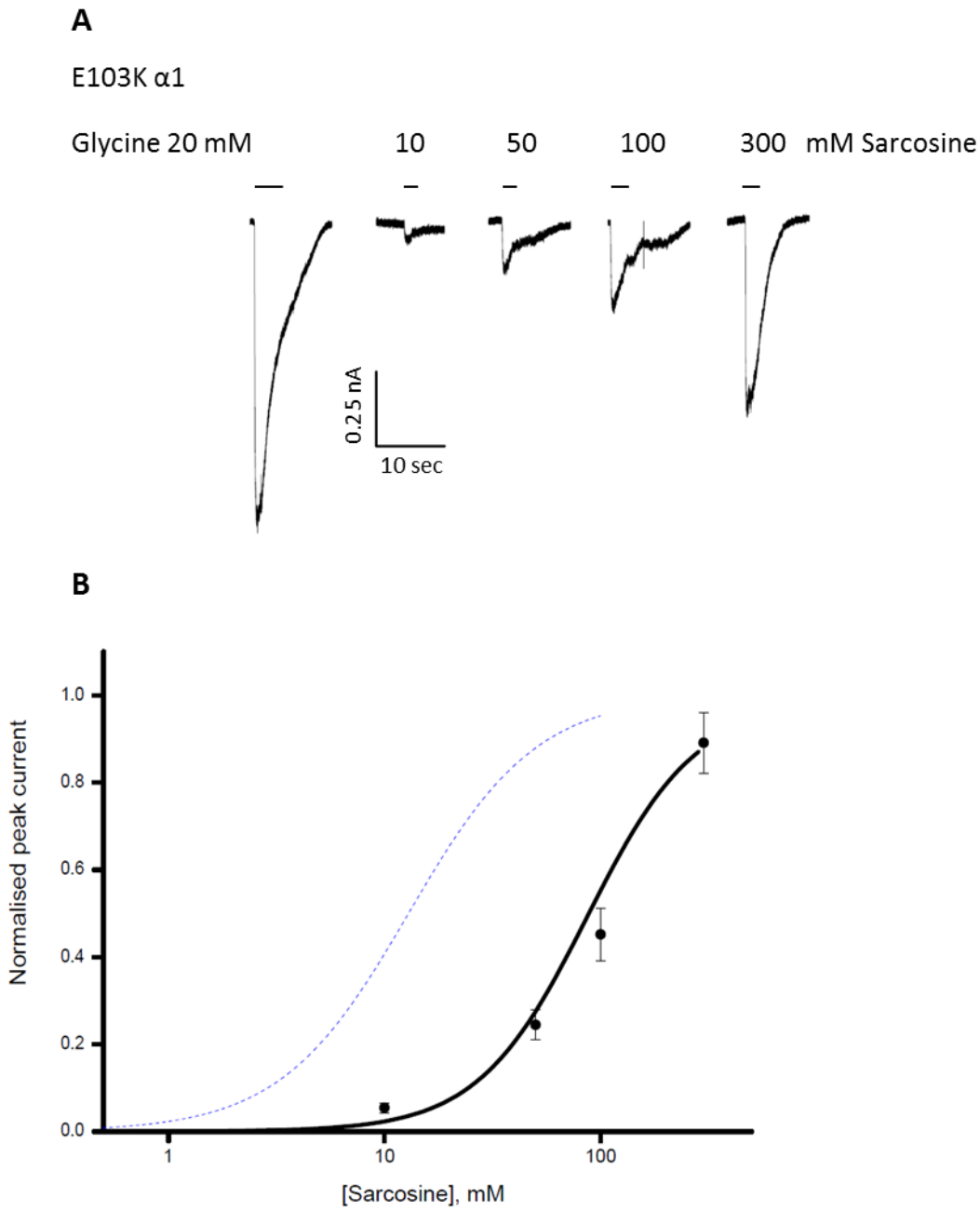


**Figure 5.6 The α1(E103K) startle mutation reduces the sensitivity of α1 GlyR to sarcosine.**
A) Representative whole-cell current responses evoked by U-tube sarcosine application to HEK293 cells expressing E103K α1 GlyR (upper panel). Black bars above the traces show the timing of the applications. The response to a saturating concentration of glycine obtained in the same cell is also shown. B) Incomplete concentration-response curve. The dashed blue curve is sarcosine wild-type concentration-response curve not scaled to glycine. $EC_{50}$ > 80 mM, $n_H$ = 1.37 ± 0.03, $I_{max}$ = 1.5 ± 0.4 nA, $n$ = 4 cells. Error bars indicate ± SEM.

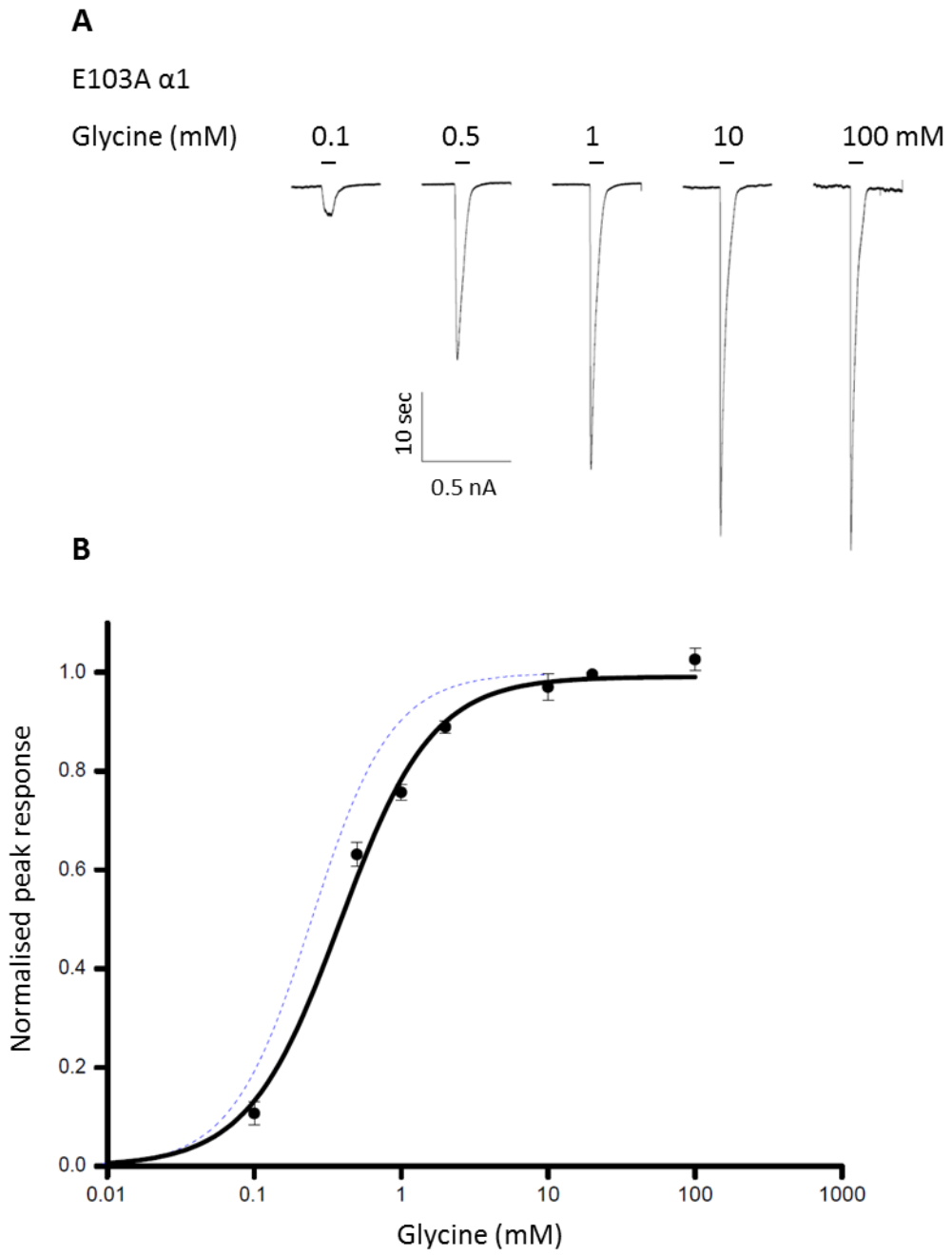


**Figure 5.7 The effect of α1(E103A) GlyR on the potency of glycine.**
A) Representative whole cell current responses to glycine applied to homomeric E103A. Black bars above the traces show the timing of the applications. B) Whole-cell concentration-response curves for the effect of glycine on E103A GlyR. $EC_{50}$ = 0.43 ± 0.05 mM, $n_H$ = 1.24 ± 0.06, $I_{max}$ = 5.91 ± 0.26 nA, $n$ = 3 cells. Error bars indicate ± SEM.

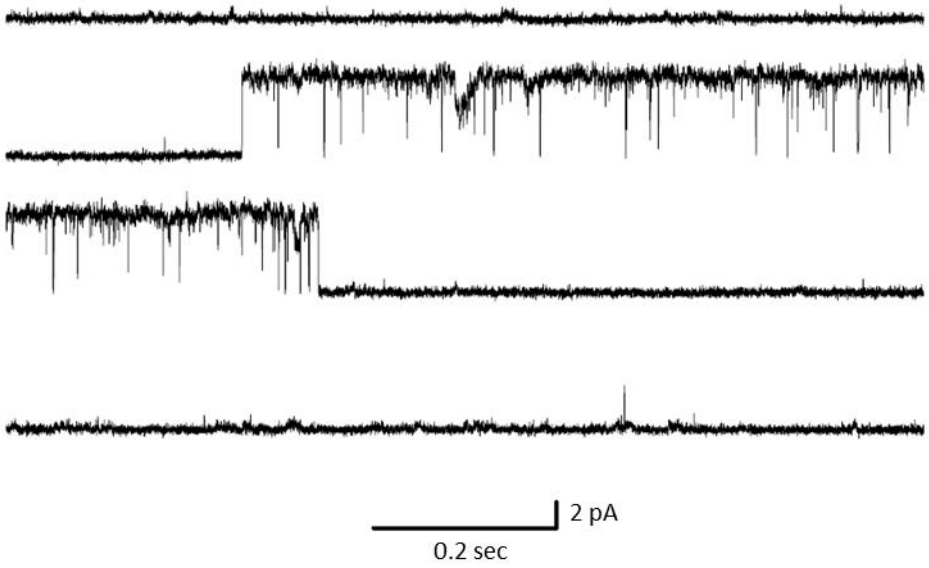


**Figure 5.8 The effect of α1(E103A) GlyR on the efficacy of glycine.**

Cluster of single channel activity elicited by saturating concentrations of glycine (100 mM) on homomeric E103A GlyR. Cell-attached configuration (pipette potential +100 mV), Channel openings are upward. $P_{open}$ = 0.97 ± 0.01, Amplitude = 5.64 ± 0.23 pA.

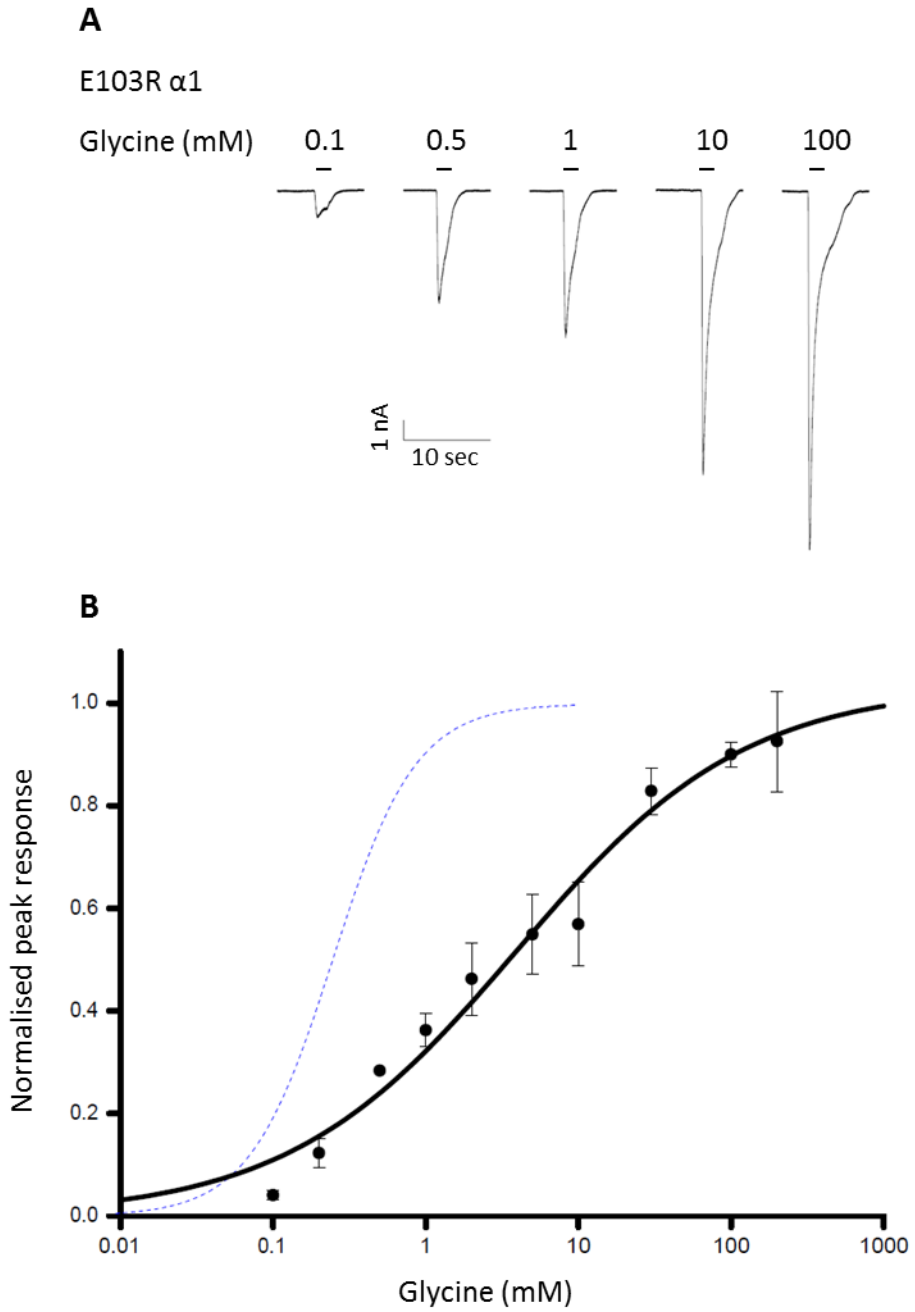


**Figure 5.9 The effect of α1(E103R) GlyR on the potency of glycine.**

A) Representative whole-cell current responses to glycine applied to homomeric E103R. B) Whole-cell concentration-response curves for the effect of glycine on α1(E103R) GlyR. The lines above the tracing refer to application of glycine (in mM). B) Average glycine concentration-response curve fitted with the Hill equation. $EC_{50}$ = 3.68 ± 1.18 mM, $I_{max}$ = 9.03 ± 3.86, $n_H$ = 0.71 ± 0.07, $n$ = 4 cells. Error bars represent SEM.

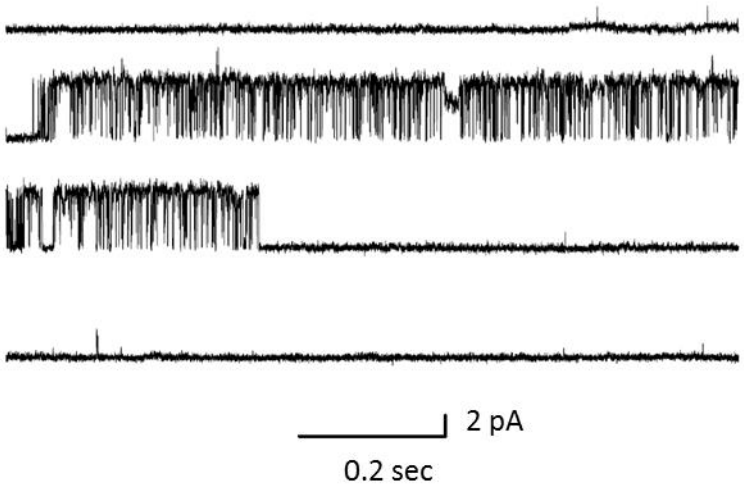


**Figure 5.10 Single channel recordings of homomeric α1(E103R) GlyR with glycine.**

Single channel cluster elicited by saturating concentrations of glycine (100 mM) on homomeric E103R GlyR. Cell-attached configuration (pipette potential +100 mV), Channel openings are upward. $P_{open}$= 0.87 ± 0.02, Amplitude = 5.75 ± 0.10 pA.

### 5.2.6 Whole-cell and single channel recordings of GlyR bearing the α1(E103A) mutation elicited by sarcosine

The effect of the E103 residue on the response to the partial agonist sarcosine was examined. Whole-cell concentration-response curves from HEK293 cells expressing homomeric E103A GlyR were obtained. Typical current responses to 5 - 200 mM sarcosine are shown in Figure 5.11. Desensitization was observed at 10 mM (~ $EC_{20}$) sarcosine. In the same cell glycine was applied at the saturating concentration of 100 mM. Sarcosine elicited maximum current responses that reached 56 % of those to glycine in the illustrated example. Sarcosine sensitivity was reduced by 1.71 fold, as the average $EC_{50}$ increased significantly from 13.63 ± 1.06 mM to 23.31 ± 2.81 mM ($p < 0.05$, unpaired t-test, $n = 3, 4$ respectively). The sacosine $I_{max}$ for α1(E103A) was comparable to the one obtained from wild-type receptors (5.11 ± 1.69 nA and 1.46 ± 0.06 nA; $p > 0.05$, unpaired t-test; $n = 4$ and 3, respectively) Also, the $n_H$ was similar to that of wild-type receptors ($n_H$ = 1.84 ± 0.17 for α1(E103A) and 1.46 ± 0.06 for wild-type GlyR; $p > 0.05$, unpaired t-test; $n = 4$ and 3, respectively) The average sarcosine maximum response relative to glycine was 0.76 ± 0.03 (Table 5.3).

Single-channel recordings of GlyR expressing α1(E103A) were obtained (Figure 5.12) at saturating sarcosine concentration of 100 mM. The average maximum $P_{open}$ elicited by sarcosine was similar to that of wild-type GlyR (0.67 ± 0.08 and 0.70 ± 0.03; $p > 0.05$, $n$ clusters = 8, 22, respectively (4 records each). The current amplitude was 4.55 ± 0.41 pA ($n$ = 8 clusters from 4 records) similar to the wild-type receptor amplitude (5.64 ± 0.30 pA; $p >$ 0.05, unpaired t-test, $n = 22$ from 4 records; Table 5.3).

### 5.2.7 Whole-cell and single-channel recordings of GlyR bearing α1(E103R) mutation using sarcosine

Whole-cell recordings of GlyRs expressing α1 E103R were obtained. Sample current traces elicited by U-tube applications of 1 – 200 mM sarcosine are shown in Figure 5.13. Desensitization was apparent at 1 mM (~ $EC_5$) for sarcosine. The average sarcosine $EC_{50}$ was 12.72 ± 0.85 mM ($n = 3$) similar to sarcosine $EC_{50}$ obtained from wild-type GlyR (13.63 ± 1.06 mM; $p > 0.05$, unpaired t-test, $n = 3$). The effect of the E103R mutation was small with 0.93 fold shifts in the macroscopic $EC_{50}$. The $n_H$ for α1(E103R) was similar to that of wild-type GlyR ($n_H$ = 1.46 ± 0.06, 1.30 ± 0.03; $p > 0.05$, unpaired t-test; $n = 3$ for both). The $I_{max}$

was also similar between α1(E103R) GlyR and wild-type GlyR (2.72 ± 1.03 nA, 4.40 ± 0.9 nA, respectively; $p > 0.05$, unpaired t-test; $n = 3$ for both; Table 5.3). A saturating concentration of 300 mM glycine was used in the same cell to determine the ratio of $I_{max\ sarcosine}/I_{max\ Glycine}$. The $I_{max\ sarcosine}/I_{max\ Glycine}$ ratio was higher than the one measured in wild-type cells 0.80 ± 0.03 vs 0.95 ± 0.004, $n = 3$ for both (Table 5.3).

Single-channel recordings using a saturating sarcosine concentration of 200 mM were obtained in cell-attached configuration (Figure 5.14). The average maximum $P_{open}$ for α1(E103R) was 0.79 ± 0.03 ($n = 31$ clusters obtained from four records) similar to that of wild-type 0.70 ± 0.03 ($p > 0.05$, unpaired t-test; $n = 22$ clusters obtained from four records). The current amplitude was comparable to its wild type value (4.96 ± 0.05 pA, 5.64 ± 0.30 pA; $p < 0.05$, unpaired t-test, $n = 31$, 22 clusters, from four records each, respectively; Table 5.3).

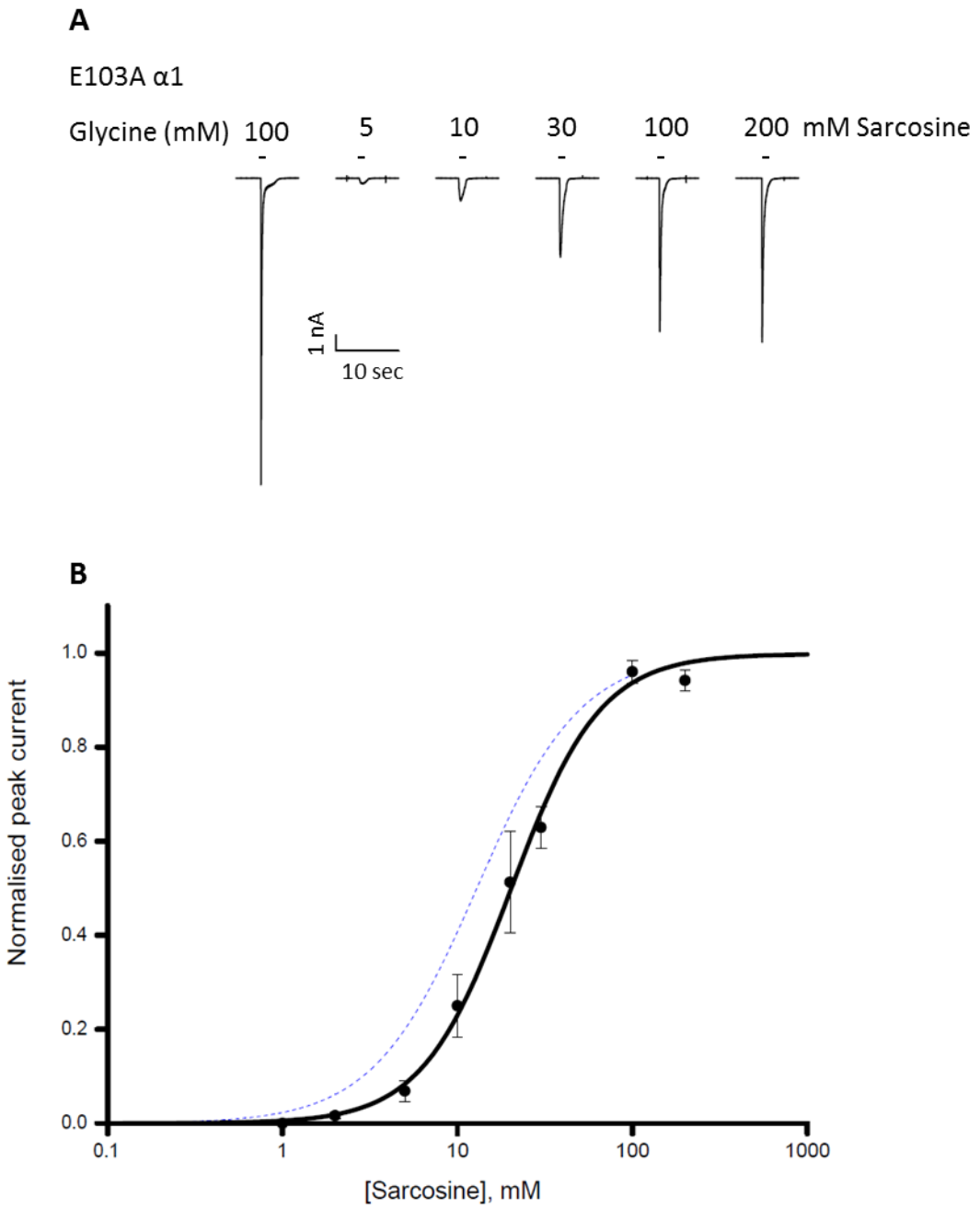


**Figure 5.11 Whole-cell recordings of α1(E103A) GlyR using sarcosine.**
A) Representative whole-cell current responses to sarcosine in homomeric E103R GlyR. Black bars above the traces show the timing of the applications. B) Sarcosine whole-cell concentration-response curves in mutant α1(E103R) GlyR. $EC_{50}$ = 23.31 ± 2.81, $n_H$ = 1.84 ± 0.17, $I_{max}$ = 5.11 ± 1.69 nA, $n$ = 4. The dashed blue curve is sarcosine wild-type GlyR concentration-response curve not scaled to glycine. Error bars represent SEM.

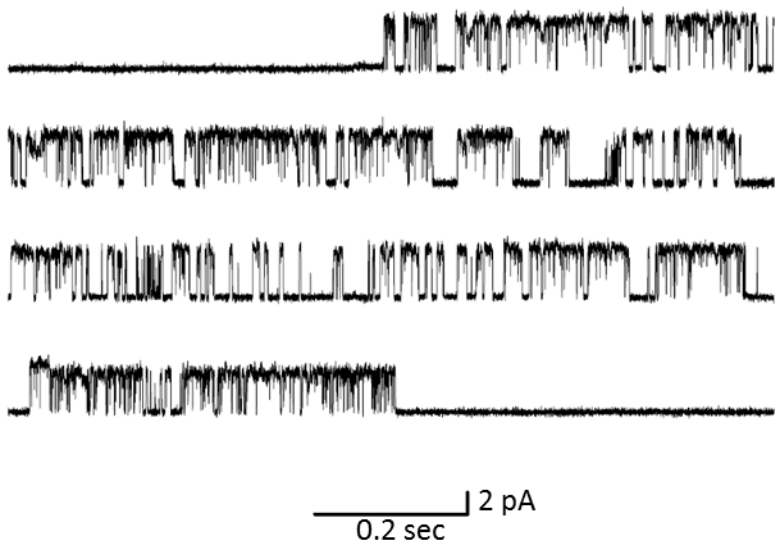


**Figure 5.12 Single-channel recordings of α1(E103A) GlyR using sarcosine.**

Cluster of single-channel E103A GlyR activity elicited in cell-attached patches by 100 mM concentration of sarcosine. The average maximum $P_{open}$ = 0.67 ± 0.08, *n* clusters = 8 obtained from 4 records. Amplitude = 4.55 ± 0.41 pA.

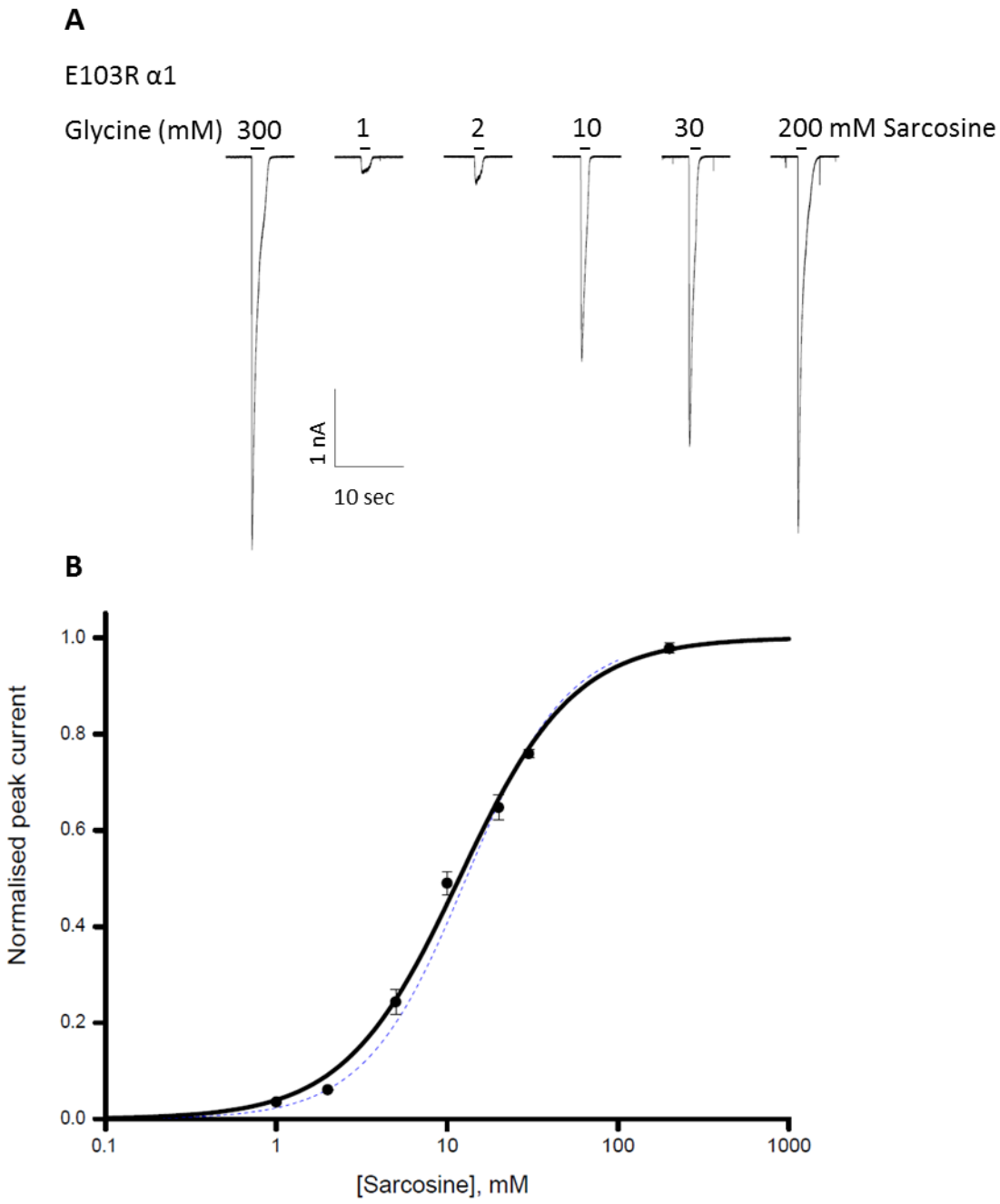


**Figure 5.13 Whole-cell recordings of currents evoked by sarcosine from α1(E103R) GlyR.**

A) Representative current traces evoked by U-tube application of sarcosine (1 – 200 mM) to HEK293 cells bearing homomeric E103R GlyR. The response to saturating concentration of glycine in the same cell (300 mM) is also shown. The timing of application is illustrated by black bars. B) Sarcosine concentration-response curve. $EC_{50}$ = 12.72 ± 0.85 mM. , $n_H$ = 1.30 ± 0.03, $I_{max}$ = 2.72 ± 1.03 nA. The $I_{max}$ sarcosine /$I_{max}$ Glycine ratio = 0.95 ± 0.004. Error bars represent SEM.

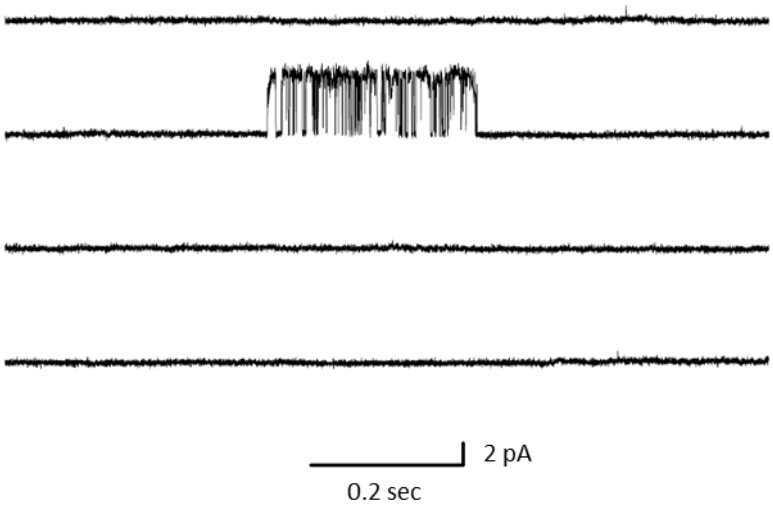


**Figure 5.14 Single-channel recordings of α1(E103R) GlyR using sarcosine.**

Cluster of single-channel activity elicited by saturating concentration (200 mM) of sarcosine on homomeric E103R GlyR. Cell-attached configuration, channel openings are upwards. Single-channel $P_{open}$ = 0.79 ± 0.03, amplitude = 4.96 ± 0.05 pA, $n$ = 31 clusters from 4 records.

### 5.2.8 Whole-cell and single channel currents elicited by glycine in GlyR bearing α1(E103R/R131E) mutation

In order to investigate whether the E103 and R131 form a salt bridge, we reversed the charges on both residues and made an E103R/R131E double mutant. Whole-cell recordings of responses to 0.1 - 50 mM glycine of the double mutant α1(E103R/R131E) GlyR are shown in Figure 5.15. Desensitization was observed from 1 mM (~ $EC_{20}$). The average glycine $EC_{50}$ for the E103R/R131E mutant was 0.43 ± 0.04 mM ($n$ = 5) close to the wild-type value of 0.25 ± 0.03 mM, but significnt ($p$ > 0.05; unpaired t-test; $n$ = 6; Table 5.2). This indicates that the GlyR E103R/R131E mutation rescued the receptor function with respect to either of the single charge reversal mutants. Results regarding the R131 residue and its mutants are shown for comparison in Table 5.2 (courtesy of E. Hurdiss).

The $I_{max}$ was reduced in comparsion to wild type 3.74 ± 0.40 nA and 10.34 ± 2.47 nA, respectively, ($p$ > 0.05; unpaired t-test; $n$ = 5, 6, respectively). The slope of the concentration curve was lower than in wild-type 0.95 ± 0.02 and 1.87 ± 0.37 ($p$ > 0.05; unpaired t-test; $n$ = 5, 6, respectively).

Single-channel recordings using a saturating concentration of 100 mM glycine were examined (Figure 5.16). The traces in the five records looked similar to that of wild-type ($P_{open}$ = 0.992 ± 0.002, $n$ = 30 clusters) as both had long openings clusters with high maximum $P_{open}$ 0.996 ± 0.001 ($p$ > 0.05; unpaired t-test; $n$ = 9 clusters). The current amplitude was lower than  amplitude in wild-type 4.81 ± 0.12 pA ($n$ = 30 clusters from 4 records) and 5.77 ± 0.06 pA ($p$ <0.05; unpaired t-test; $n$ = 9 clusters from 5 records).

### 5.2.9 Whole-cell and single channel currents elicited by sarcosine in GlyR bearing α1(E103R/R131E) mutation using sarcosine

We further investigated the effect of the double mutant on GlyR with the partial agonist sarcosine. Whole-cell recordings of homomeric E103R/R131E using 1 - 100 mM sarcosine are shown in Figure (5.17). Desensitization was observed at 10 mM sarcosine ($EC_{50}$). Sarcosine sensitivity was similar to that of wild-type receptors 12.64 ± 0.33 mM and 13.63 ± 1.06 mM for the double mutant and wild type, respectively ($p$ > 0.05, unpaired t-test; $n$ = 3 each). The $I_{max}$ was lower for α1(E103R/R131E) 1.32 ± 0.03 nA than for wild-type 4.4 ± 0.9

nA ($p < 0.05$, unpaired t-test; $n = 3$ each). The slope of the concentration curve for α1(E103R/R131E) was similar to wild-type 1.20 ± 0.15 and 1.46 ± 0.06 ($p > 0.05$, unpaired t-test; $n = 3$ each; Table 5.3). In each cell, responses to saturating glycine (50 mM) were obtained. The maximum sarcosine current response relative to glycine was similar to wild-type 0.86 ± 0.19 for the double mutant GlyR and 0.80 ± 0.03 for wild-type GlyR.

Single-channel recordings of GlyR bearing the E103R/R131E mutation using 100 mM sarcosine are shown in Figure 5.18. Clusters had very high open probability. The maximum $P_{open}$ elicited by sarcosine in the double mutant was significantly higher than the wild-type 0.97 ± 0.01 vs 0.70 ± 0.03 ($p < 0.01$, unpaired t-test; $n = 23$ clusters from 8 records, $n = 22$ clusters from 4 records, respectively). It resembles the R131E GlyR mutation (0.91 ± 0.04). The current amplitude was 4.51 ± 0.12 pA ($n = 23$ clusters obtained from eight records) similar to that of wild-type 5.64 ± 0.30 pA ($p > 0.05$, unpaired t-test, $n = 22$ clusters from 4 records).

The overall effects of the α1(E103R), α1(R131E) and the double mutant α1(E103R/R131E) on glycine and sarcosine responses are illustrated in Figure 5.19. The concentration-response curves in Figure 5.19 are displayed as whole cell responses *scaled* to the maximum open probability measured by single channel analysis. In this way the desensitized intervals are not included in the analysis and only the changes in receptor activation are included. It clearly shows how the double mutant rescued the glycine response (Figure 5.19.A). The figure shows how the double charge reversal mutant $EC_{50}$ of 0.43 ± 0.04 mM (black circles; $n = 5$) was close to the wild-type $EC_{50}$ value of 0.25 mM. It is much lower in either of the single mutants E103R or R131E (3.68 ± 1.18 mM and 1.60 ± 0.15 mM, respectively; shown as dashed and dotted curves in Figure 5.19; Table 5.2). For sarcosine the picture is slightly different. While the double mutant has a sarcosine $EC_{50}$ similar to that of wild-type receptors (12.64 ± 0.33 and 13.63 ± 1.06), sarcosine efficacy resemble more the reverse charge mutant R131E (0.91 ± 0.04) than it does the wild-type (0.70 ± 0.03) Table (5.3).

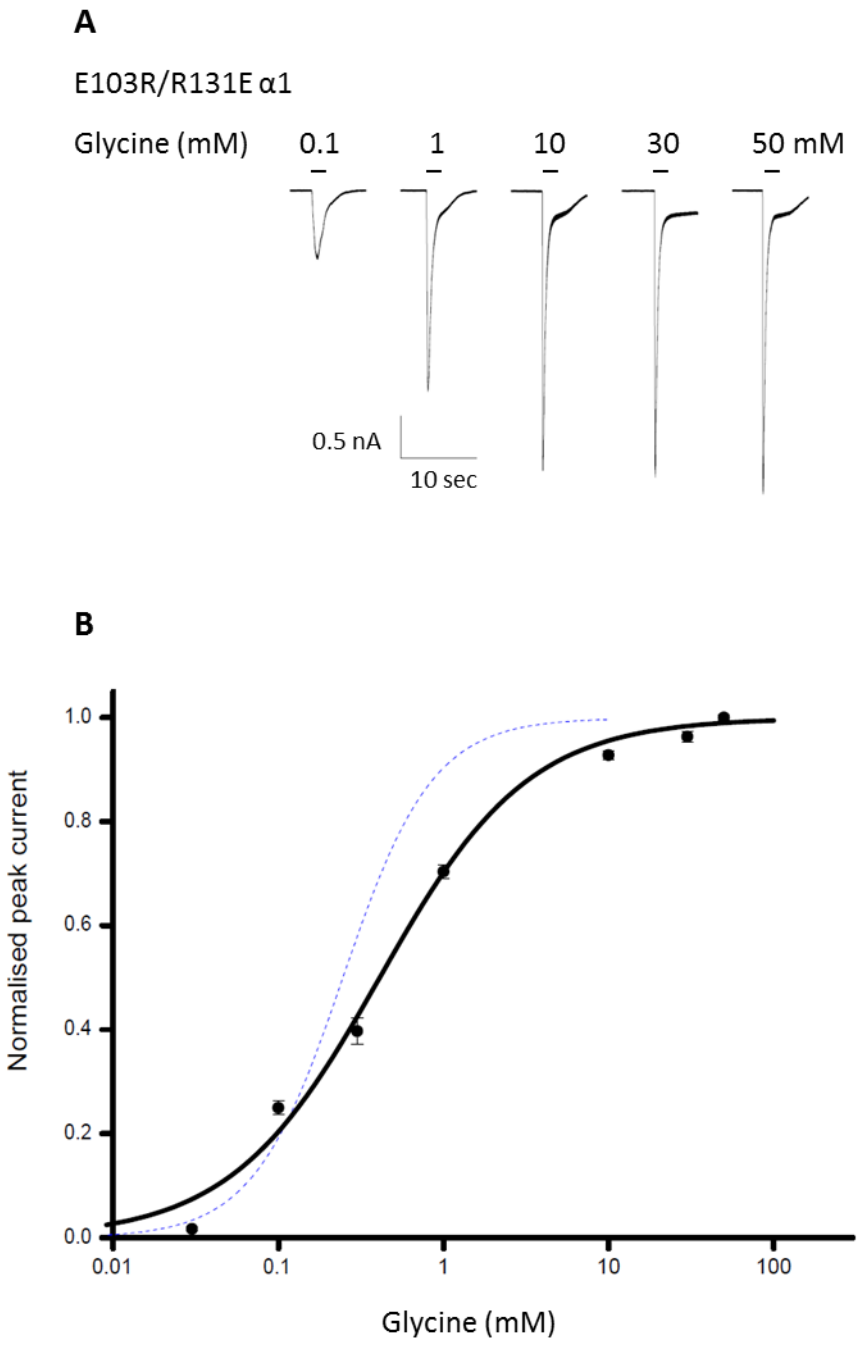


**Figure 5.15 Whole-cell recordings of α1(E103R/R131E) GlyR using glycine.**

A) Representative double mutant GlyR responses to glycine (0.1 – 50 mM). Black bars above the traces show the timing of the applications. B) Whole-cell concentration-response curves to glycine in homomeric E103R/R131E GlyR. $EC_{50}$ = 0.43 ± 0.04 mM, $n_H$ = 0.95 ± 0.02. $I_{max}$ = 3.74 ± 0.40 nA, $n$ = 5. Error bars represent SEM.

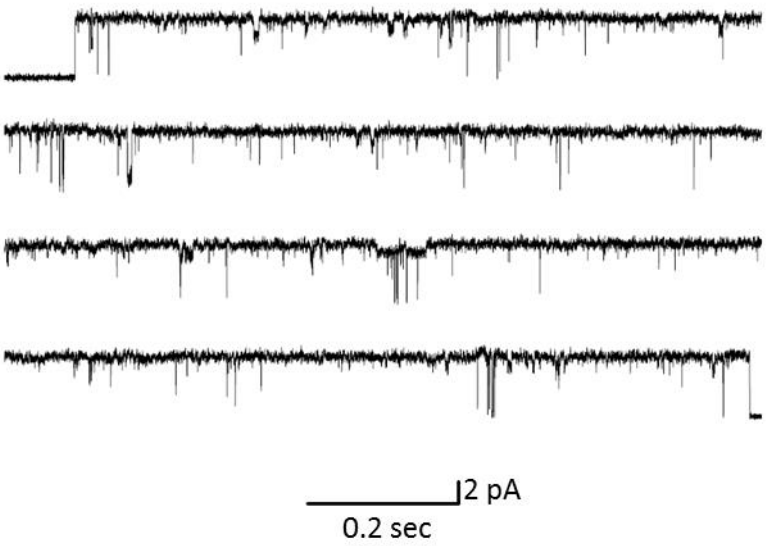


**Figure 5.16 Single-channel recordings of α1(E103R/R131E) GlyR using saturating concentration of glycine**

Cluster of single-channel activity elicited by 100 mM glycine in the homomeric E103R/R131E mutant. Cell-attached configuration, channel openings are upwards. Single-channel $P_{open}$ = 0.996 ± 0.001, current amplitude = 4.81 ± 0.12 pA, $n$ = 9 clusters from 5 records.

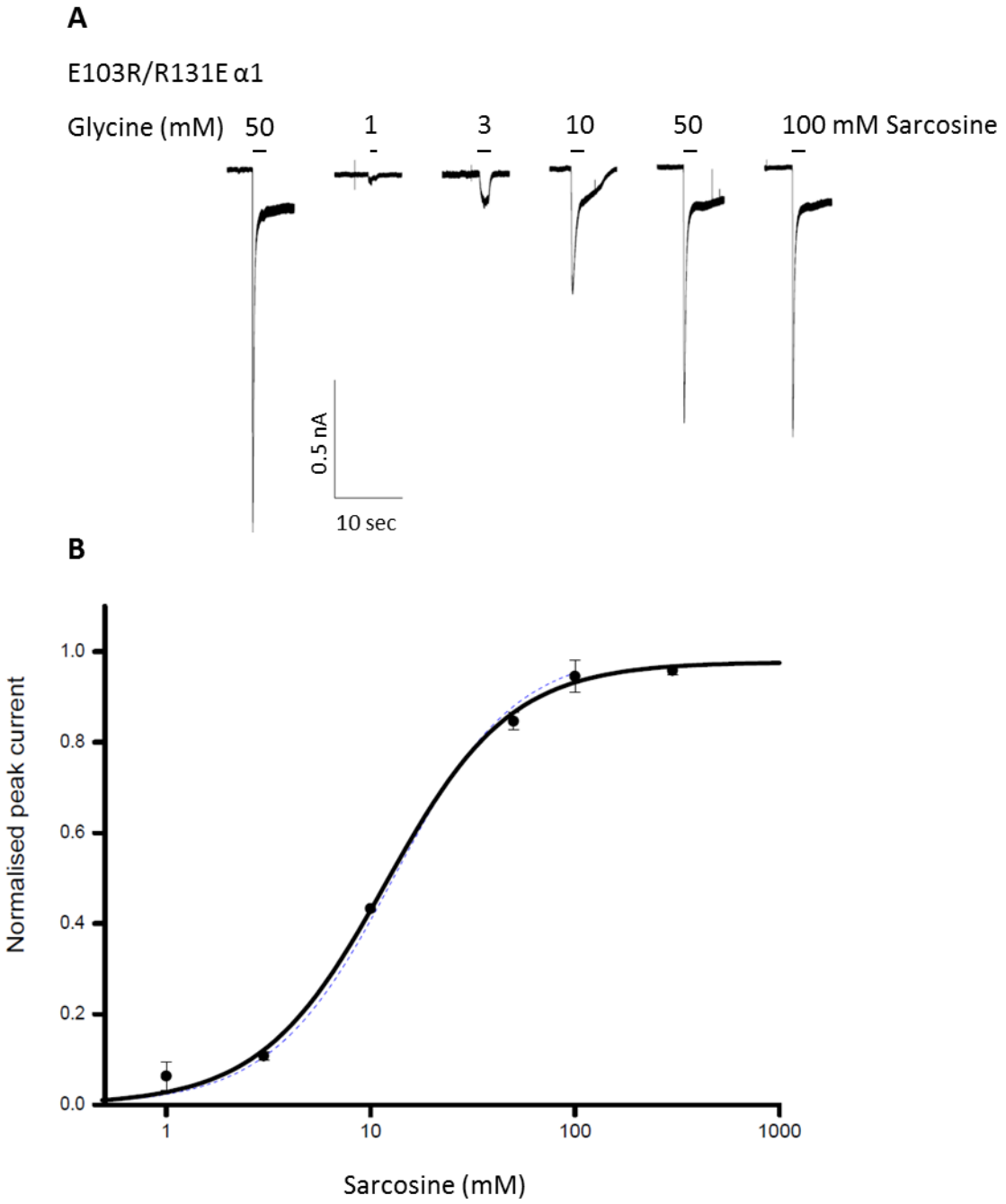


**Figure 5.17 Whole-cell recordings of α1(E103R/R131E) GlyR using sarcosine.**
A) Representative whole-cell current responses to sarcosine (1-100 mM) in the double charge reversal mutant α1(E103R/R131E) GlyR. Black bars above the traces show the timing of the applications. B) Sarcosine whole-cell concentration-response curves in the double mutant GlyR. $EC_{50}$ = 12.64 ± 0.33 mM, $I_{max}$ = 1.32 ± 0.03 nA, the $n_H$ = 1.20 ± 0.15, $n$ = 3 cells. Saturating concentration of 50 mM glycine was used in the same cell. The $I_{max\ sarcosine}$ /$I_{max\ Glycine}$ ratio = 0.86 ± 0.19. Error bars represent SEM.

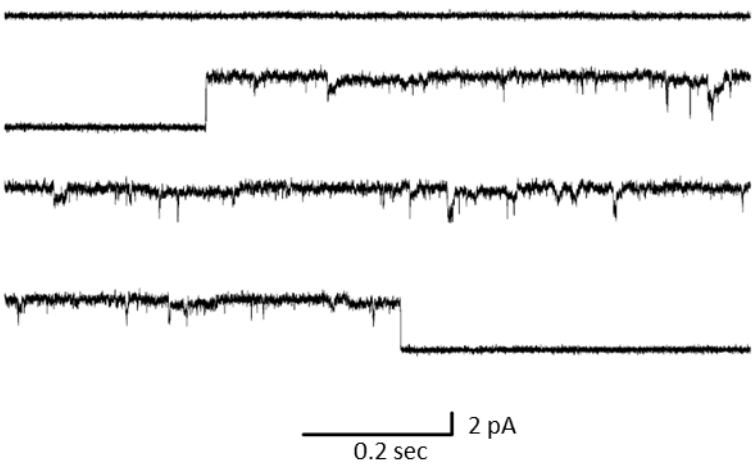


**Figure 5.18 Single-channel recordings of GlyR bearing α1( E103R/R131E) using sarcosine.**

Cluster of single-channel mutant GlyR activity elicited in cell-attached record by saturating concentrations of sarcosine (100 mM). Cell-attached configuration, channel openings are upwards. The maximum $P_{open}$ elicited by sarcosine in the double mutant = 0.97 ± 0.01. The current amplitude = 4.51 ± 0.12 pA, $n$ = 23 clusters obtained from eight records.

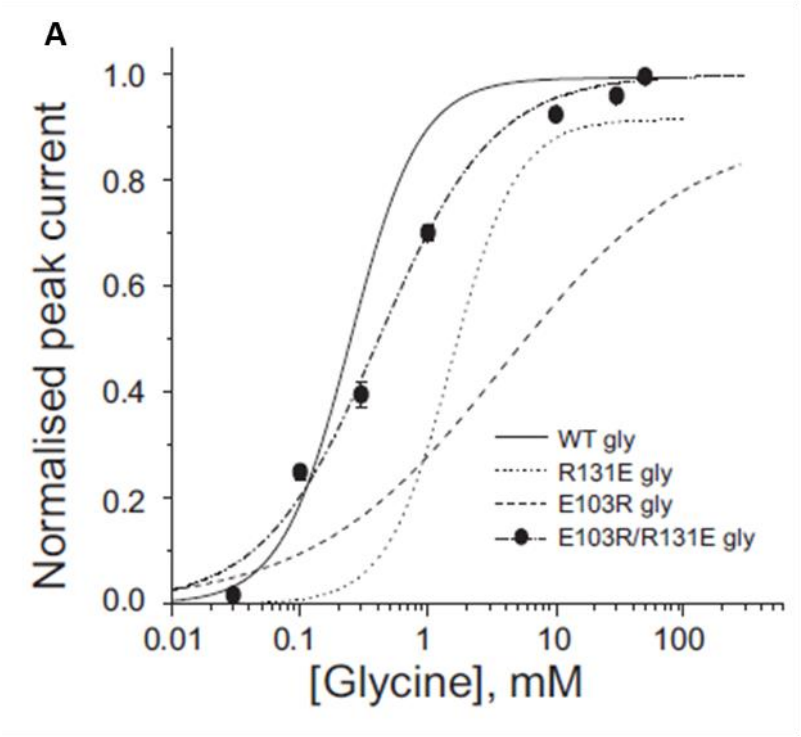


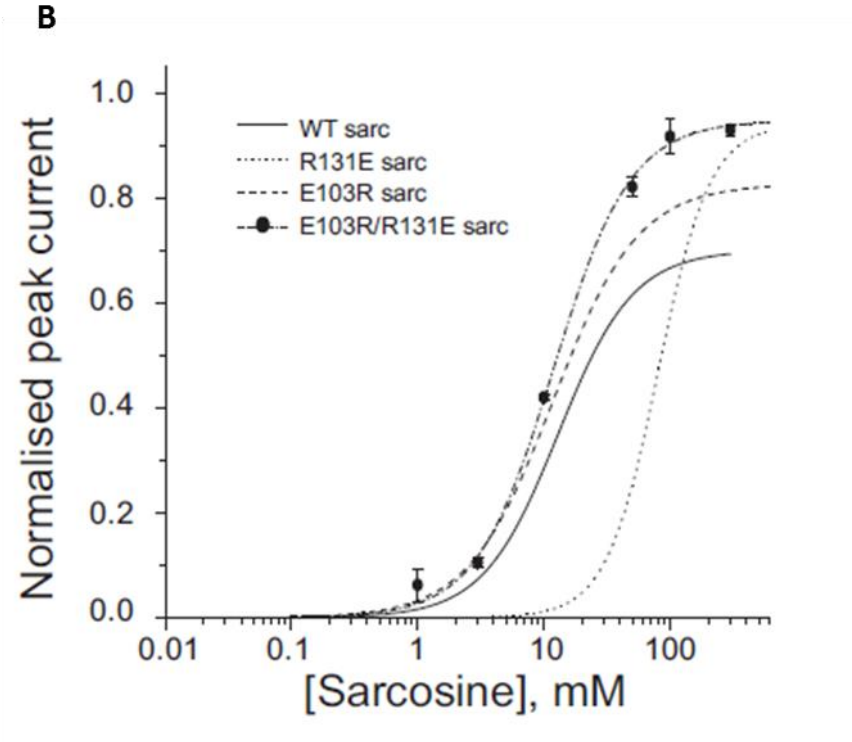


**Figure 5.19 E103R/R131E mutation rescues GlyR α1 response to glycine and sarcosine.** Glycine and sarcosine whole-cell concentration-response curves in wild-type and double mutant GlyR. Curves are scaled to the appropriate maximum $P_{open}$ measured by single-channel recordings.

**Table 5.2 E103R/R131E mutation rescues GlyR α1 response to glycine**

| Glycine | | | | | | | | | |
|---|---|---|---|---|---|---|---|---|---|
| | Max $P_{open}$ (# clusters) | Amplitude (pA) | Concentration (mM) | *n* | $I_{max}$ (nA) | $EC_{50}$ (mM) | $EC_{50}$ fold change | $n_H$ | *n* |
| α1Wild-type | 0.992 ± 0.002 (30) | 5.77 ± 0.06 | 10 | 4 | 10.34 ± 2.47 | 0.25 ± 0.03 | - | 1.87 ± 0.37 | 6 |
| α1(R131A) | 0.95 ± 0.01 (16) | 4.58 ± 0.04 | 30 | 2 | 7.24 ± 0.86 | 0.33 ± 0.02 | 1.32 | 2.15 ± 0.21 | 3 |
| α1(R131E) | 0.93 ± 0.02 (28) | 3.90 ± 0.03 | 50 | 2 | 1.52 ± 0.34 * | 1.60 ± 0.15 ‡ | 6.4 | 1.64 ± 0.13 | 4 |
| α1(E103K) | 0.73 ± 0.07 (13) | 5.24 ± 0.12 | 50 | 3 | 2.73 ± 1.41 | 0.71 ± 0.11 ‡ | 2.84 | 1.32 ± 0.07 | 3 |
| α1(E103R) | 0.87 ± 0.02 ‡ (42) | 5.75 ± 0.10 | 100 | 3 | 9.03 ± 3.86 | 3.68 ± 1.18 ‡ | 14.72 | 0.71 ± 0.07* | 4 |
| α1(E103A) | 0.97 ± 0.01 (11) | 5.64 ± 0.23 | 100 | 3 | 5.91 ± 0.26 | 0.43 ± 0.05 * | 1.72 | 1.24 ± 0.06 | 3 |
| α1(R131E/E103R) | 0.998± 0.0005 (9) | 4.81 ± 0.12 * | 100 | 5 | 3.74 ± 0.40 * | 0.43 ± 0.04 * | 1.72 | 0.95 ± 0.02 * | 5 |

**Table 5.3 E103R/R131E mutation rescues GlyR α1 response to sarcosine**

| Sarcosine | | | | | | | | | |
|---|---|---|---|---|---|---|---|---|---|
| | Max $P_{open}$ (# clusters) | Amplitude (pA) | Concentration (mM) | *n* | $I_{max}$ (nA) | $EC_{50}$ (mM) | $EC_{50}$ fold change | $n_H$ | *n* |
| α1Wild-type | 0.70 ± 0.03 (22) | 5.64 ± 0.30 | 100 | 4 | 4.4 ± 0.9 | 13.63 ± 1.06 | - | 1.46 ± 0.06 | 3 |
| α1(R131A) | 0.95 ± 0.01 ‡ (37) | 5.42 ± 0.12 | 100 | 3 | 7.08 ± 0.18 * | 4.09 ± 0.22 ‡ | 0.30 | 1.56 ± 0.04 | 3 |
| α1(R131E) | 0.91 ± 0.04 ‡ (21) | 4.7 ± 0.10 | 300 | 2 | 4.32 ± 0.97 | 87.30 ± 12.94 ‡ | 6.40 | 1.97 ± 0.02 * | 3 |
| α1(E103K) | - | - | - | - | - | - | - | - | - |
| α1(E103R) | 0.79 ± 0.03 (31) | 4.96 ± 0.05 | 200 | 4 | 2.72 ± 1.03 | 12.72 ± 0.85 | 0.93 | 1.30 ± 0.03 | 3 |
| α1(E103A) | 0.67 ± 0.08 (8) | 4.55 ± 0.41 | 100 | 4 | 5.11 ± 1.69 | 23.31 ± 2.81 | 1.71 | 1.84 ± 0.17 | 4 |
| α1(R131E/E103R) | 0.97 ± 0.01 ‡ (23) | 4.51 ± 0.12 | 100 | 8 | 1.32 ± 0.03 * | 12.64 ± 0.33 | 0.93 | 1.20 ± 0.15 | 3 |

## 5.3 Discussion

How a dominant mutation affects glycine transmission by substitutions of a single amino acid in hyperekplexia causing mutation (E103K) is unknown. Mutating a negative to a positive residue in the ECD just near to the binding site has an influence on channel gating as observed in chapter three (Figure 3.9, Table 3.5) but how E103K has a role in channel gating is not known. Here we identified key residues in the ECD that can influence channel gating of the homomeric α1 GlyRs. This is based on site-directed mutagenesis combined with homology modeling based on the crystal structure of GluCl. Since GluCl displays up to 42% amino acid identity to human α1 GlyR it has been used as a template for the modeling (Yu *et al.*, 2014). The oppositely charged E103 and R131 are conserved in all human GlyR subunits (Figure 5.1). E103 and R131 residues were predicted to form a salt bridge interaction. E103 and R131 were mutated to explore the validity of the prediction and to identify the role of key residues in the transduction of channel binding to channel gating. The predicted salt-bridge between E103 and R131 might be essential in maintaining the correct conformation of Loop A, which in turn influences the direct bonds of other residues with the agonist such as F99 of loop A which forms interactions with glycine. E103 and R131 residues were exchanged to alanine. Also the influence of E103R/R131E on glycine and sarcosine responses was investigated. Our results as highly suggestive of a salt-bridge interaction between α1E103 located on the positive side and α1R131 located on the negative side.

The effect of the E103 and R131 mutations is different for glycine vs. sarcosine. The glycine response seems indifferent to alanine substitutions as E103A glycine sensitivity shifted by 1.72 fold and the maximum $P_{open}$ was similar to wild type 0.97 ± 0.01, 0.9992 ± 0.002 ($n$ = 11, 30, Table 5.2). R131A shifted glycine sensitivity by 1.32 only and the maximum $P_{open}$ was similar to wild-type GlyRs 0.95 ± 0.01 (n = 16, Table 5.2).

For sarcosine homomeric E103K $EC_{50}$ could not be established as the sarcosine response did not saturate up to 300 mM (Figure 5.6), however, it is worth to mention that the relative efficacy of the partial agonist β-alanine to glycine was increased as a result of the heteromeric E103K mutation (Figure 5.4). This indicates that this position has effect on gating that depends on the agonist and maybe the β subunit has an influence. E103R and E103A did not do much as glycine sensitivity changed by 0.93, 1.71 fold respectively. Glycine efficacy also did not change much as it was 0.79 ± 0.03, 0.67 ± 0.08 for E103R and E103A, respectively

(Table 5.2). On the other hand, R131 mutations R131A and R131E increase efficacy from 0.70 ± 0.03 to 0.95 ± 0.01 in R131A and to 0.91 ± 0.04 in R131E but their $EC_{50}$ effects were not similar. R131A shifted sarcosine sensitivity by 0.30 and R131E decreased sarcosine sensitivity by 6.40 fold. An earlier study using the *Xenopus laevis* oocyte expression system found that R131A homomeric α1 GlyR did not affect glycine sensitivity as it increased glycine sensitivity by 0.58 fold only (this was not significant). On the other hand taurine sensitivity significantly changed from 3.6 ± 1.6 to 0.42 ± 0.16 mM and its efficacy relative to glycine was increased by double (Grudzinska *et al.*, 2005). Also, R131A homomeric α1 GlyR can be activated by zinc alone (Grudzinska 2008).

The substantial rescue with charge reversal double mutant suggests that there is a salt bridge that matters. Reversal is good for glycine as it improved glycine response. However, the double mutant fails to make sarcosine partial as in the wild-type GlyRs (Figure 5. 17). This could mean that the salt bridge may have the right length, but the position of the interacting charged moieties (guanidinium in Arg and carboxylate in glutamate) might be different.

Here we show interaction between E103 and R131 is crucial for gating function of the glycine receptor. Our results show a role of salt bridge interaction between E103 and R131 by demonstrating rescue of glycine response to homomeric mutant GlyRs. This might be a good explanation for the deterioration of glycine receptor function in the hyperekplexia causing mutation E103K.

# Chapter 6: General Conclusions

GlyRs are ligand gated ion channels that are vital for synaptic inhibitory neurotransmission in the mammalian CNS. The understanding of the structure-function relation of GlyR is enhanced by the availability of human hyperekplexia mutations that highlight residues essential for channel function. The α1 GlyR human hyperekplexia mutations are found in different parts of the GlyR, from the ECD to the TM4. Each region might provide us with valuable information about the function of the receptor.

To characterize α1 GlyR mutations that contribute to human hyperekplexia pathogenesis, functional measurements of the effect of GlyR mutations on glycine potency and efficacy were determined by whole-cell and single-channel recordings. The effect of homomeric α1(E103K), α1(S231N), α1(Q266H), α1(S267N) and heteromeric α1(E103K)β, α1(S231N)β, α1(Q266H)β, α1(S267N)β GlyR mutations expressed in HEK293 cells was studied. This was done after establishing data for homomeric and heteromeric wild-type human GlyRs, as for previous controls rat GlyR had been used in our lab (Lape *et al.,* 2012).

E103K is located at the ECD (loop A of the principal side of the binding site). It causes a marked reduction in glycine potency that is more marked in the heteromeric than the homomeric channel (2.8 cf ~ 72 fold change in $EC_{50}$). This reduction is associated with a significant reduction in glycine maximum $P_{open}$ from 0.99 ± 0.002 to 0.73 ± 0.07 (homomeric α1(E103K) and 0.98 ± 0.01 to 0.67 ± 0.06 (heteromeric α1(E103K)β).

The S231N hyperekplexia mutation which is found in the TM1 also reduced glycine sensitivity. Glycine $EC_{50}$ increased significantly from its wild-type value of 0.25 ± 0.03 mM ($n$ = 6) to 1.16 ± 0.13 mM ($n$ = 4) for α1(S231N) GlyR and from 0.10 ± 0.03 mM ($n$ = 6) to 3.81 ± 0.42 mM ($n$ = 4) for α1(S231N)β GlyR. The reduction in glycine potency is more marked in the heteromeric than the homomeric receptors (5 vs 38; $EC_{50}$ fold change). This reduction is related to a significant reduction in glycine maximum $P_{open}$ from 0.98 ± 0.01 (α1β wild-type GlyR) to 0.38 ± 0.06 (α1(S231N)β GlyR).

The Q266H GlyR mutation located on the TM2 reduced glycine potency significantly and the effect is more marked in the heteromeric channel (2.7 vs. ~ 12 fold change). This reduction is associated with a significant reduction in maximum glycine $P_{open}$ from 0.98 ± 0.01 ($n$ = 29) to 0.61 ± 0.06 in heteromeric α1(Q266H)β GlyR ($n$ = 20).

The S267N GlyR hyperekplexia mutation produced a significant reduction in glycine potency. This effect is more noticeable in the heteromeric channel (18 cf ~ 35 fold change). The reduction in glycine sensitivity is associated with a channel-gating disturbance. The maximum glycine $P_{open}$ for the heteromeric α1(S267N)β was significantly reduced from 0.98 ± 0.01 ($n$ = 29) to 0.37 ± 0.06 ($n$ = 6) suggesting improper channel gating.

The main finding in Chapter Three of the thesis is that the E103K, S231N, Q266H and S267N human hyperekplexia mutations within the α1 subunit of GlyR reduce the channel sensitivity to glycine. The change in glycine potency was more marked in the heteromeric than in the homomeric receptors. The data suggests that the gating efficacy is interrupted by those mutations as glycine maximum $P_{open}$ was reduced (Table 3.5).

It would be of interest to screen all α1 human hyperekplexia mutations that are documented in the literature. By comparing the effect of mutations on glycine $EC_{50}$ it would be possible to know which residues are most important for glycine sensitivity. Also, it might be useful to correlate the location of the mutation with the severity of the hyperekplexia symptoms. Testing α1 mutations in both homomeric and heteromeric GlyR helps in understanding whether incorporation of the β-subunit improves the function of human hyperekplexia mutations or not. Exploring this within a single lab will expand our knowledge despite there being some difficulty in working with these mutations knowing that the function of the GlyR is disturbed.

**Can the reduced glycine response of the hyperekplexia mutant GlyRs be rescued?**

Given the importance of the proper function of GlyR, the intravenous anaesthetic propofol was used to study the possibility of improving the function of the hyperekplexia mutant α1β GlyR. In the present study, I described how the application of propofol can improve glycine-gated currents of α1(E103K)β, α1(S231N)β, α1(Q266H)β, and α1(S267N)β hyperekplexia GlyR mutations expressed in HEK293 cells.

The function of GlyR can be modulated by a variety of allosteric modulators such as $Zn^{2+}$, ethanol and anaesthetics (Harvey *et al.*, 1999; Mihic *et al.*, 1997; Miller *et al.*, 2005a; Yevenes and Zeilhofer, 2011). Most of the enhancement effects of these modulators are observed when the submaximal concentrations of glycine are tested. However, application of these allosteric modulators with saturating concentrations of glycine has minimal modulation effects. Therefore, both saturating and subsaturating concentrations of glycine were used in

this study. The aim was to examine whether propofol can potentiate glycine $EC_{20}$ and/or maximal response and whether these effects were different than in wild-type GlyRs.

Propofol-potentiated glycine submaximal current of α1(E103K)β GlyR (3.18 ± 0.58 fold change; although not significant, $n$ = 5). Propofol failed to potentiate glycine maximal responses for the same mutation in whole-cell experiments (0.72 ± 0.19 fold change; $n$ = 2).

Propofol potentiation of glycine submaximal and maximal responses of the α1(Q266H)β were investigated. This study suggests that propofol can significantly enhance submaximal glycine-gated currents for the α1(Q266H)β (5.19 ± 1.35 fold change; $n$ = 4), however, glycine maximal response could not be restored (1.05 ± 0.06 fold change; $n$ = 4). Similar effects were observed for the wild-type GlyRs.

α1(S267N) GlyR hyperekplexia mutation, which reduced ethanol modulation, was also tested (Becker *et al.,* 2008). The submaximal glycine response of HEK293 cells bearing α1(S267N)β hyperekplexia GlyR mutation was significantly potentiated by propofol (2.71 ± 0.41 fold change; $n$ = 6). At the same residue other non-hyperekplexia mutations S267I and S267M were tested for propofol modulation. Their results were consistent with my study, as propofol modulation of glycine sub-maximal response was not affected by the mutations (Ahrens *et al.,* 2008). Enhancement of glycine-gated maximal currents by propofol were observed (1.29 ± 0.09 fold change, $n$ = 6). Therefore, both submaximal and maximal responses to glycine were significantly potentiated for this mutation. The results are consistent with role of the S267 residue in mediating allosteric modulation.

Propofol enhancement of the glycine current at the α1(S231N)β GlyR mutation was also found. Similar to wild-type GlyR, glycine-gated submaximal currents at the heteromeric α1(S231N)β GlyR are enhanced by propofol (5.48 ± 1.38 fold change; $n$ = 6). Unlike in wild-type receptors, propofol potentiates glycine-gated maximal currents (1.98 ± 0.29 fold change). This residue might be essential for propofol sensitivity in GlyR. Indeed, single-channel recordings of α1(S231N)β GlyR at saturating glycine concentration in the presence of 50 μl propofol showed that the maximum glycine $P_{open}$ was increased significantly from 0.38 ± 0.06 to 0.65 ± 0.04 ($n$ = 16, 38 clusters, respectively) without affecting single channel current amplitude (2.01 ± 0.05 pA vs 1.94 ± 0.04 pA). In the α1(S231N)β GlyR mutation the functional deficiency was restored by propofol as both the submaximal and maximal response to glycine were potentiated by propofol. Allosteric modulators such as zinc have minimal

effects when applied with maximal glycine concentration (Farley and Mihic, 2015). Here we observed enhancement of currents elicited by saturating concentration of glycine. This effect might be explained by increasing gating of the channel ($P_{open}$) as it cannot be explained by increasing glycine affinity as glycine is already at saturating concentration.

Altogether, propofol (50 μM) was effective in potentiating glycine submaximal and maximal response in α1(S231N)β and α1(S267N)β hyperekplexia mutations; however, only the submaximal responses were potentiated in the α1(E103K)β and α1(Q266H)β hyperekplexia mutations. Why S231 was most sensitive to propofol is not clear. According to the GlyR homology model based on GluCl structure, the proposed propofol binding site involves P230 which is close to S231. The reason behind the lack of propofol potentiation of glycine maximal current for α1(E103K)β and α1(Q266H)β hyperekplexia mutations is not clear. If we assume that propofol affects only flip and the increase in affinity with activation. It could not reverse the decrease in maximum $P_{open}$ if this is produced by a mutation that damages channel opening (E), as per E103K. No increase in flip can compensate. If a mutation affects both flip and channel opening, its effects on maximum $P_{open}$ could be partially reversed by propofol, if flip has become rate limiting for the maximum $P_{open}$ (as it is for a partial agonist).

In summary, my results indicate that propofol can partially rescue the reduced maximal glycine response of α1(S231N)β and α1(S267N)β GlyR (in a recombinant system). However, the modulation property of propofol cannot be generalized to all hyperekplexia mutations as the response varied from one residue to other. Testing different mutations will allow a better understanding of the mechanism behind propofol modulation of glycine in GlyR.

**The startle disease mutation E103K impairs activation of human homomeric α1 glycine receptors by disrupting an intersubunit salt bridge across the agonist binding site**

Results from our lab demonstrated that hyperekplexia mutation located at the TM2 (where most of the α1 GlyR mutations are expressed) exerts its effect by interfering with channel gating. This was based on characterization of K276E (Lewis *et al.,* 1998; Lape et *al.,* 2012). Little is known about how mutations near the binding site disrupt the normal glycinergic synaptic transmission. As a possible explanation, it has been recently suggested that the α1(N46K) GlyR, which is a lethal hyperekplexia in mice, speeds up the deactivation of GlyR (Wilkins *et al.,* 2016). Exploring hyperekplexia mutations that are located at the binding site

but do not suppress agonist binding might provide valuable information about signal transduction to the gate once the agonist has bound.

A salt bridge at the back of the binding site between the charged side chain of E103 in loop A to that of R131 in loop E is suggested by homology modeling of α1GlyR (Yu *et al.,* 2014) based on GluCl (Hibbs and Gouaux, 2011) and the recent structure of the zebrafish α1(GlyR) (Du *et al.,* 2015). Interaction between these two residues is confirmed by our study using site-directed mutagenesis, whole-cell and single-channel recordings (Safar *et al.,* 2017). This was based on investigating the effect of different mutations in which the side-chain charge was either eliminated (by Ala mutations) or reversed. The effect of the double mutation E103R/R131E was also tested. We concluded that despite the α1(E103K) hyperekplexia mutation being located in the ECD it impairs the efficacy of glycine. The effect of E103 and R131 mutations on GlyR response to the full agonist glycine was different from the partial agonist sarcosine. Since sarcosine is a partial agonist its maximum $P_{open}$ should change clearly due to gain or loss of function mutations (in this case). For sarcosine, the effect of mutating E103 residue was minimal for α1(E103A) or α1(E103R) GlyR mutations. On the other hand, both α1(R131A) and α1(R131E) enhanced sarcosine efficacy. Whereas α1(R131A) increased sarcosine potency, α1(R131E) decreased it. This suggests that α1(R131E) causes a reduction in sarcosine binding affinity. A small loss of affinity and efficacy for glycine was caused by α1(R131E) GlyR mutation. These findings indicate that the efficacy determinants for glycine are different from those of sarcosine, being the first time that such findings have been reported at the single-channel level. An alanine scan of other residues within loop A of GlyR such as K104, F108 and T112 suggested a gain of function in response to a range of agonists. The maximum whole-cell response of taurine (partial agonist) relative to glycine was increased for those mutations (Schmieden *et al.,* 1999). The R131E/E103R experiments provide strong evidence for the existence of the salt bridge, as swapping the side chains of E103 and R131 residues rescued most of the effects of the single point mutations. The increased efficacy of the α1(R131) GlyR mutation in response to sarcosine, however, persisted in the double mutation. The reason behind this is unknown. It might be that in the R131/E103 mutation the salt bridge is of a correct length but the interaction between the charged moieties is in a different position. Our results show that even with the availability of a validated homology model and measurements of efficacy by single-channel recordings, it is difficult to fully understand the network of interactions at the ECD of GlyR.

**In conclusion**, this study provides insight into the role of different residues of α1GlyR using human hyperekplexia mutations. It demonstrates the molecular explanation behind E103K, S231N, Q266H, and S267N α1 GlyR mutations. The study also indicates that the human hyperekplexia mutations tested here affect the channel gating of GlyR. This might interrupt the normal glycinergic synaptic inhibition of GlyRs leading to hyperekplexia. It also shows that the function of some of the hyperekplexia mutations can be rescued using propofol. Furthermore, improper salt-bridge interaction at the binding site influences the normal function of GlyR.

# Bibliography


Ahrens, J., Leuwer, M., Stachura, S., Krampfl, K., Belelli, D., Lambert, J., and Haeseler, G. (2008). A transmembrane residue influences the interaction of propofol with the strychnine-sensitive glycine α1 and α1β receptor. *Anesthesia & Analgesia*, 107(6), 1875-1883.

Akabas, M.H., and Karlin, A. (1995). Identification of acetylcholine receptor channel-lining residues in the M1 segment of the alpha-subunit. *Biochemistry*, 34(39), 12496-12500.

Al-Futaisi, A.M., Al-Kindi, M.N., Al-Mawali, A.M, Koul, R.L, Al-Adawi, S., and Al-Yahyaee, S.A. (2012). Novel mutation of GLRA1 in Omani families with hyperekplexia and mild mental retardation. *Pediatric Neurology*, 46(2), 89-93.

Ali, D.W., Drapeau, P., and Legendre, P. (2000). Development of spontaneous glycinergic currents in the mauthner neuron of the zebrafish embryo. *Journal of Neurophysiology*, 84, 1726-1736.

Althoff, T., Hibbs, R.E., Banerjee, S., and Gouaux, E. (2014). X-ray structures of GluCl in apo states reveal a gating mechanism of Cys-loop receptors. *Nature*, 512(7514), 333-337.

Araki, T., Yamano, M., Murakami, T., Wanaka, A., Betz, H., and Tohyama, M. (1988). Localization of glycine receptors in the rat central nervous system: an immunocytochemical analysis using a monoclonal antibody. *Neuroscience Research Supplements*, 7, S161.

Awatramani, G.B, Turecek, R., and Trussell, L.O. (2005). Staggered development of GABAergic and glycinergic transmission in the MNTB. *Journal of Neurophysiology*, 93(2), 819-828.

Absalom, N.L., Lewis, T.M., Kaplan, W., Pierce, K.D., and Schofield, P.R. (2003). Role of charged residues in coupling ligand binding and channel activation in the extracellular domain of the glycine receptor. *Journal of Biological Chemistry*, 278(50), 50151-50157.

Ahmadi, S., Lippross, S., Neuhuber, W.L., and Zeilhofer, H.U. (2002). $PGE_2$ selectively blocks inhibitory glycinergic neurotransmission onto rat superficial dorsal horn neurons. *Nature Neuroscience*, 5(1), 34-40.

Alexander, S.P., Peters, J.A., Kelly, E., Marrion, N.V., Faccenda, E., Harding, S.D, Pawson, A.J., Sharman, J.L., Southan, C., Davies, J. A., and CGTP Collaborators. (2017). The concise guide to pharmacology 2017/18: ligand-gated ion channels. *British Journal of Pharmacology*, 174 Suppl 1, S130-S159.

Aprison, M.H., and Werman, R. (1965). The distribution of glycine in cat spinal cord and roots. *Life Sciences*, 4(21), 2075-83.

Assaf, S.Y., and Chung, S.H. (1984). Release of endogenous $Zn^{2+}$ from brain tissue during activity. *Nature*, 308(5961), 734-736.

Baccei, M.L., and Fitzgerlad, M. (2004). Development of GABAergic and glycinergic transmission in the neonatal rat dorsal horn. *Journal of Neuroscience*, 24(20), 4749-4757.

Bakker, M.J, van Dijk, J.G, van den Maagdenberg, A.M, and Tijssen, M.A. (2006). Startle syndromes. *The Lancet Neurology*, 5(6), 513-524.

Bali, M., and Akabas, M.H. (2004). Defining the propofol binding site location on the $GABA_A$ receptor. *Molecular Pharmacology*, 65(1), 68-76.

Balling, R. (2001). ENU mutagenesis: analyzing gene function in mice. *Annual Review of Genomics and Human Genetics*, 2(1), 463-492.

Baptista-Hon, D.T., Deeb, T.Z., Lambert, J.J., Peters, J.A., and Hales, T.G. (2013). The minimum M3-M4 loop length of neurotransmitter-activated pentameric receptors is critical for the structural integrity of cytoplasmic portals. *Journal of Biological Chemistry*, 288(30), 21558-21568.

Basak, S., Gicheru, Y., Samanta, A., Molugu, S.K., Huang, W., Fuente, M., Hughes, T., Taylor D.J., Nieman, M.T., Moiseenkova-Bell, V., and Chakrapani, S. Cryo-EM structure of $5\text{-}HT_{3A}$ receptor in its resting conformation. *Nature Communication*. 2018 Feb 6;9(1):514.

Beato, M. (2008). The time course of transmitter at glycinergic synapses onto motoneurons. *Journal of Neuroscience*, 28(29), 7412-7425.

Beato, M., and Sivilotti, L.G. (2007). Single-channel properties of glycine receptors of juvenile rat spinal motoneurones *in vitro*. *The Journal of Physiology*, 580(2), 497-506.

Beato, M., Groot-Kormelink, P.J., Colquhoun, D., and Sivilotti, L.G. (2002). Openings of the rat recombinant α1 homomeric glycine receptor as a function of the number of agonist molecules bound. *The Journal of General Physiology*, 119(5), 443-466.

Beato, M., Groot-Kormelink, P.J, Colquhoun, D., and Sivilotti, L.G. (2004). The activation mechanism of α1 homomeric glycine receptors. *Journal of Neuroscience*, 24(4), 895-906.

Becker, C.M., Hoch, W., and Betz, H. (1988). Glycine receptor heterogeneity in rat spinal cord during postnatal development. *The EMBO Journal*, **7**, 3717-3726.

Becker, K., Breitinger, H., Humeny, A., Meinck, H.M, Dietz, B., Aksu, F., and Becker, C.M (2007). The novel hyperekplexia allele *GLRA1*(S267N) affects the ethanol site of the glycine receptor. *European Journal of Human Genetics*, 16(2), 223-228.

Becker, L., Hartenstein, B., Schenkel, J., Kuhse, J., Betz, H., and Weiher, H. (2000). Transient neuromotor phenotype in transgenic spastic mice expressing low levels of glycine receptor β-subunit: an animal model of startle disease. *The European Journal of Neuroscience*, 12, 27-32.

Becker, L., von Wegerer, J., Schenkel, J., Zeilhofer, H.U, Swandulla, D., and Weiher, H. (2002). Disease-specific human glycine receptor α1 subunit causes hyperekplexia phenotype and impaired glycine- and $GABA_A$-receptor transmission in transgenic mice. *The Journal of Neuroscience*, 22(7), 2505-2512.

Beene, D., Brandt, G.S, Zhong, W., Zacharias, N.M, Lester, H.A., and Dougherty, D.A. (2002). Cation−π interactions in ligand recognition by serotonergic (5-$HT_{3A}$) and nicotinic acetylcholine receptors: the anomalous binding properties of nicotine. *Biochemistry*, 41(32), 10262-10269.

Belelli, D., Pistis, M., Peters, J.A, and Lambert, J.J. (1999). The interaction of general anaesthetics and neurosteroids with $GABA_A$ and glycine receptors. *Neurochemistry International*, 34(5), 447-452.

Bellini, G., Miceli, F., Mangano, S., Miraglia del Giudice, E., Coppola, G., Barbagallo, A., Taglialatela, M., and Pascotto, A. (2007). Hyperekplexia caused by dominant-negative suppression of glyra1 function. *Neurology*, 68(22), 1947-1953.

Betz, H., Gomeza, J., Armsen, W., Scholze, P., and Eulenburg, V. (2006). Glycine transporters: essential regulators of synaptic transmission. *Biochemical Society Transactions*, 34(Pt 1), 55-58.

Betz, H., and Laube, B. (2006). Glycine receptors: recent insights into their structural organization and functional diversity. *Journal of Neurochemistry*, 97(6), 1600-1610.

Birinyi, A., Parker, D., Antal, M., and Shupliakov, O. (2001). Zinc co-localizes with GABA and glycine in synapses in the lamprey spinal cord. *The Journal of Comparative Neurology*, 433(2), 208-221.

Blednov, Y., Benavidez, J., Homanics, G., and Harris, R. (2011). Behavioral characterization of knockin mice with mutations M287L and Q266I in the glycine receptor α1 Subunit. *Journal of Pharmacology and Experimental Therapeutics*, 340(2), 317-329.

Bocquet, N., Nury, H., Baaden, M., Le Poupon, C., Changeux, J., Delarue, M., and Corringer, P. (2008). X-ray structure of a pentameric ligand-gated ion channel in an apparently open conformation. *Nature*, 457(7225), 111-114.

Bocquet, N., Prado de Carvalho, L., Cartaud, J., Neyton, J., Le Poupon, C., Taly, A., Grutter, T., Changeux, J., and Corringer, P. (2006). A prokaryotic proton-gated ion channel from the nicotinic acetylcholine receptor family. *Nature*, 445(7123), 116-119.

Bode, A., and Lynch, J.W. (2014). The impact of human hyperekplexia mutations on glycine receptor structure and function. *Molecular Brain*, 7(1), 2.

Bode, A., Wood, S-E, Mullins, J.G.L., Keramidas, A., Cushion, T.D., Thomas, R.H., Pickrell, W.O., Drew, C.J.G., Masri, A., Jones, E.A., Vassallo, G., Born, A.P., Alehan, F., Aharoni, S., Bannasch, G., Bartsch, M., Kara, B., Krause, A., Karam, E.G., Matta, S., Jain, V., Mandel, H., Freilinger, M., Graham, G.E, Hobson, E., Chatfield, S., Vincent-Delorme, C., Rahme, J.E., Afawi, Z., Berkovic, S.F., Howell, O.W., Vanbellinghen, J-F, Rees, M.I., Chung, S-K, and Lynch, J.W. (2013). New hyperekplexia mutations provide insight into glycine receptor assembly, trafficking, and activation mechanisms. *Journal of Biological Chemistry*, 288(47), 33745-33759.

Borghese, C., Blednov, Y., Quan, Y., Iyer, S., Xiong, W., Mihic, S., Zhang, L., Lovinger, D., Trudell, J., Homanics, G., and Harris, R. (2011). Characterization of two mutations, M287L and Q266I, in the α1 glycine receptor subunit that modify sensitivity to alcohols. *Journal of Pharmacology and Experimental Therapeutics*, 340(2), 304-316.

Bormann, J., Hamill, O., and Sakmann, B. (1987). Mechanism of anion permeation through channels gated by glycine and gamma-aminobutyric acid in mouse cultured spinal neurones. *The Journal of Physiology*, 385(1), 243-286.

Bormann, J., Rundström, N., Betz, H., and Langosch, D. (1993). Residues within transmembrane segment M2 determine chloride conductance of glycine receptor homo- and hetero-oligomers. *The EMBO Journal*, 12(10), 3729-3737.

Bourne, Y., Talley, T., Hansen, S., Taylor, P., and Marchot, P. (2005). Crystal structure of a Cbtx–AChBP complex reveals essential interactions between snake α-neurotoxins and nicotinic receptors. *The EMBO Journal*, 24(8), 1512-1522.

Bowery, N.G., and Smart, T.G. (2006). GABA and glycine as neurotransmitters: A brief history. *British Journal of Pharmacology*, 147 Suppl 1, S109-S119.

Brejc, K., van Dijk, W., Klaassen, R., Schuurmans, M., van Der Oost, J., Smit, A., and Sixma, T. (2001). Crystal structure of an ACh-binding protein reveals the ligand-binding domain of nicotinic receptors. *Nature*, 411(6835), 269-276.

Bristow, D., Bowery, N., and Woodruff, G. (1986). Light microscopic autoradiographic localisation of [$^3$H]glycine and [$^3$H]strychnine binding sites in rat brain. *European Journal of Pharmacology*, 126(3), 303-307.

Brune, W., Weber, R. G., Saul, B., von Knebel Doeberitz, M., Grond-Ginsbach, C., Kellerman, K., Meinck, H. M., and Becker, C. M. (1996). A *GLRA1* null mutation in recessive hyperekplexia challenges the functional role of glycine receptors. *American Journal of Human Genetics*, 58(5), 989–997.

Buckwalter, M.S., Cook, S.A., Davisson, M.T., White, W.F., and Camper, S.A. (1994). A frameshift mutation in the mouse α1 glycine receptor gene (*Gira1*) results in progressive neurological symptoms and juvenile death. *Human Molecular Genetics*, 3(11), 2025-2030.

Burzomato, V., Beato, M., Groot-Kormelink, P.J, Colquhoun, D., and Sivilotti, L.G. (2004). Single-channel behavior of heteromeric alpha1beta glycine receptors: an Attempt to detect a conformational change before the channel opens. *Journal of Neuroscience*, 24(48), 10924-10940.

Burzomato, V., Groot-Kormelink, P.J, Sivilotti, L.G., and Beato, M. (2003). Stoichiometry of recombinant heteromeric glycine receptors revealed by a pore-lining region point mutation. *Receptors and Channels*, 9(6), 353-361.

Brown, C.E., and Dyck, R.H. (2002). Rapid, experience-dependent changes in levels of synaptic zinc in primary somatosensory cortex of the adult mouse. *The Journal of Neuroscience*, 22(7), 2617-25.

Carland, J.E, Cooper, M.A, Sugiharto, S., Jeong, H., Lewis, T.M, Barry, P.H, Peters, J.A, Lambert, J.J, and Moorhouse, A.J. (2009). Characterization of the effects of charged residues in the intracellular loop on ion permeation in α1 Glycine receptor channels. *Journal of Biological Chemistry*, 284(4), 2023-2030.

Castaldo, P., Stefanoni, P., Miceli, F., Coppola, G., del Giudice, E., Bellini, G., Pascotto, A., Trudell, J., Harrison, N., Annunziato, L. , and Taglialatela, M. (2004). A novel hyperekplexia-causing mutation in the pre-transmembrane segment 1 of the human

glycine receptor α1 subunit reduces membrane expression and impairs gating by agonists. *Journal of Biological Chemistry*, 279(24), 25598-25604.

Castillo, J. , and Katz, B. (1957). Interaction at End-Plate Receptors between Different Choline Derivatives. *Proceedings of the Royal Society B: Biological Sciences*, 146(924), 369-381.

Cecchini, M., and Changeux, J.P. (2015). The nicotinic acetylcholine receptor and its prokaryotic homologues: Structure, conformational transitions & allosteric modulation. *Neuropharmacology*, 96, 137-149.

Celie, P., van Rossum-Fikkert, S., van Dijk, W., Brejc, K., Smit, A. , and Sixma, T. (2004). Nicotine and carbamylcholine binding to nicotinic acetylcholine receptors as studied in AChBP crystal structures. *Neuron*, 41(6), 907-914.

Chalphin, A., and Saha, M. (2010). The specification of glycinergic neurons and the role of glycinergic transmission in development. *Frontiers in molecular neuroscience*, 3,1-13.

Chau, P.L. (2010). New insights into the molecular mechanisms of general anaesthetics. *British Journal of Pharmacology*, 161(2), 288-307.

Chung, S., Vanbellinghen, J., Mullins, J., Robinson, A., Hantke, J., Hammond, C., Gilbert, D., Freilinger, M., Ryan, M., Kruer, M., Masri, A., Gurses, C., Ferrie, C., Harvey, K., Shiang, R., Christodoulou, J., Andermann, F., Andermann, E., Thomas, R., Harvey, R., Lynch, J. , and Rees, M. (2010). Pathophysiological mechanisms of dominant and recessive *GLRA1* mutations in hyperekplexia. *Journal of Neuroscience*, 30(28), 9612-9620.

Cohen, B., Labarca, C., Czyzyk, L., Davidson, N., and Lester, H. (1992). Tris+/Na+ permeability ratios of nicotinic acetylcholine receptors are reduced by mutations near the intracellular end of the M2 region. *The Journal of General Physiology*, 99(4), 545-572.

Colquhoun, D. (1998). Binding, gating, affinity and efficacy: The interpretation of structure-activity relationships for agonists and of the effects of mutating receptors. *British Journal of Pharmacology*, 125(5), 923-947.

Corringer, P., Bertrand, S., Galzi, J., Devillers-Thiéry, A., Changeux, J. , and Bertrand, D. (1999). Mutational analysis of the charge selectivity filter of the α7 nicotinic acetylcholine receptor. *Neuron*, 22(4), 831-843.

Corringer, P., Novère, N. , and Changeux, J. (2000). Nicotinic receptors at the amino acid level. *Annual Review of Pharmacology and Toxicology*, 40(1), 431-458.

Coto, E., Armenta, D., Espinosa, R., Argente, J., Castro, M. , and Alvarez, V. (2005). Recessive hyperekplexia due to a new mutation (R100H) in the *GLRA1* gene. *Movement Disorders*, 20(12), 1626-1629.

Cymes, G. , and Grosman, C. (2008). Pore-opening mechanism of the nicotinic acetylcholine receptor evinced by proton transfer. *Nature Structural & Molecular Biology*, 15(4), 389-396.

Cymes, G., Ni, Y. , and Grosman, C. (2005). Probing ion-channel pores one proton at a time. *Nature*, 438(7070), 975-980.

Czajkowski, C. (2005). Neurobiology: triggers for channel opening. *Nature*, 438(7065), 167-168.

Callister, R.J., and Graham, B.A. (2010). Early history of glycine receptor biology in mammalian spinal cord circuits. *Frontiers in Molecular Neuroscience*, 3, 13.

Chatterton, J.E., Awobuluyi, M., Premkumar, L.S., Takahashi, H., Talantova, M., Shin, Y., Cui, J., Tu, S., Sevarino, K.A., Nakanishi, N., Tong, G., Lipton, S.A., and Zhang, D. (2002). Excitatory glycine receptors containing the NR3 family of NMDA receptor subunits. *Nature*, 415(6873), 793-8.

Curtis, D.R. , and Watkins, J.C. (1960). The excitation and depression of spinal neurones by structurally related amino acids. *Journal of Neurochemistry*, 6, 117-741.

Curtis, D.R., Hösli, L., and Johnston, G.A. (1968). A pharmacological study of the depression of spinal neurones by glycine and related amino acids. *Experimental Brain Research*, 1968;6(1):1-18.

Curtis, D.R., Hösli, L., and Johnston, G.A. (1967). Inhibition of spinal neurons by glycine. *Nature*, 215(5109), 1502-1503.

Curtis, D.R. , and Malik R. (1985). Glycine antagonism by RU 5135. *European Journal of Pharmacology*, 110(3), 383-384.

daCosta, C., and Baenziger, J. (2013). Gating of pentameric ligand-gated ion channels: structural insights and ambiguities. *Structure*, 21(8), 1271-1283.

Dang, H., England, P., Farivar, S., Dougherty, D. , and Lester, H. (2000). Probing the role of a conserved M1 proline residue in 5-hydroxytryptamine (3) receptor gating. *Molecular Pharmacology*, 57, 1114-1122.

Davies, J.S., Chung, S-K, Thomas, R.H., Robinson, A., Hammond, C.L., Mullins, J.G., Carta, E., Pearce, B.R., Harvey, K., Harvey, R.J., and Rees, M.I. (2010). The glycinergic system in human startle disease: a genetic screening approach. *Frontiers in Molecular Neuroscience*, 3, 1-10.

Deleuze, C., Runquist, M., Orcel, H., Rabié, A., Dayanithi, G., Alonso, G., and Hussy, N. (2005). Structural difference between heteromeric somatic and homomeric axonal glycine receptors in the hypothalamo-neurohypophysial system. *Neuroscience*, 135(2), 475-483.

del Giudice, E., Coppola, G., Bellini, G., Cirillo, G., Scuccimarra, G. , and Pascotto, A. (2001). A mutation (V260M) in the middle of the M2 pore-lining domain of the glycine receptor causes hereditary hyperekplexia. *European Journal of Human Genetics*, 9(11), 873-876.

Dellisanti, C.D., Yao, Y., Stroud, J.C., Wang, Z., and Chen, L. (2007). Erratum: crystal structure of the extracellular domain of nAChR α1 bound to α-bungarotoxin at 1.94 Å resolution. *Nature Neuroscience*, 10(9), 1222-1222.

Delpy, A., Allain, A.E., Meyrand, P., and Branchereau, P. (2008). NKCC1 cotransporter inactivation underlies embryonic development of chloride-mediated inhibition in mouse spinal motoneuron. *The Journal of Physiology*, 586(4):1059-1075.

Dibas, M., Gonzales, E., Das, P., Bell-Horner, C., and Dillon, G. (2002). Identification of a novel residue within the second transmembrane domain that confers use-facilitated block by picrotoxin in glycine α1 receptors. *Biological Chemistry*, 277, 9112-9117.

Donato, R., and Nistri, A. (2000). Relative contribution by GABA or glycine to Cl(-)-mediated synaptic transmission on rat hypoglossal motoneurons in vitro. *Journal of Neurophysiology*, 84(6), 2715-24.

Dong, X., and Xu, T. (2002). The Actions of propofol on gamma-aminobutyric acid-A and glycine receptors in acutely dissociated spinal dorsal horn neurons of the rat. *Anesthesia & Analgesia*, 95(4), 907-914.

Doria Lamba, L., Giribaldi, G., De Negri, E., Follo, R., De Grandis, E., Pintaudi, M. , and Veneselli, E. (2007). A case of major form familial hyperekplexia: prenatal diagnosis and effective treatment with clonazepam. *Journal of Child Neurology*, 22(6), 769-772.

Downie, D., Hall, A., Lieb, W. , and Franks, N. (1996). Effects of inhalational general anaesthetics on native glycine receptors in rat medullary neurones and recombinant glycine receptors in Xenopus oocytes. *British Journal of Pharmacology*, 118(3), 493-502.

Dreissen, Y., Bakker, M., Koelman, J., and Tijssen, M. (2012). Exaggerated startle reactions. *Clinical Neurophysiology*, 123(1), 34-44.

Du, J., Lü, W., Wu, S., Cheng, Y. , and Gouaux, E. (2015). Glycine receptor mechanism elucidated by electron cryo-microscopy. *Nature*, 526(7572), 224-229.

Dumoulin, A., Triller, A., and Dieudonne, S. (2001). IPSC kinetics at identified GABAergic and mixed GABAergic and glycinergic synapses onto cerebellar Golgi cells. *Journal of Neuroscience*, 21, 6045-6057.

Duret, G., Van Renterghem, C., Weng, Y., Prevost, M., Moraga-Cid, G., Huon, C., Sonner, J.M., and Corringer, P.J. Functional prokaryotic-eukaryotic chimera from the pentameric ligand-gated ion channel family. *Proceedings of the National Academy of Sciences of the United States of America.* 2011 Jul 19;108(29):12143-8.

Durisic, N., Godin, A., Wever, C., Heyes, C., Lakadamyali, M., and Dent, J. (2012). Stoichiometry of the human glycine receptor revealed by direct subunit counting. *Journal of Neuroscience*, 32(37), 12915-12920.

Dutertre, S., Becker, C.M., and Betz, H. (2012). Inhibitory glycine receptors: an update. *Journal of Biological Chemistry*, 287(48), 40216-40223.

Eaton, M.M, Cao, L.Q, Chen, Z., Franks, N.P, Evers, A.S, and Akk, G. (2015). Mutational analysis of the putative high-affinity propofol binding site in human *β*3 homomeric $GABA_A$ receptors. *Molecular Pharmacology*, 88(4), 736-745.

Elmslie, F.V, Hutchings, S.M, Spencer, V., Curtis, A., Covanis, T., Gardiner, R.M, and Rees, M. (1996). Analysis of *GLRA1* in hereditary and sporadic hyperekplexia: a novel mutation in a family cosegregating for hyperekplexia and spastic paraparesis. *Journal of Medical Genetics*, 33(5), 435-436.

Eulenburg, V., Armsen, W., Betz, H., and Gomeza, J. (2005). Glycine transporters: essential regulators of neurotransmission. *Trends in Biochemical Sciences*, 30(6), 325-33.

Fatima-Shad, K., and Barry, P.H. (1993). Anion permeation in GABA-and glycine-gated channels of mammalian cultured hippocampal neurons. *Proceedings of the Royal Society of London B: Biological Sciences*, 253(1336), 69-75.

Filippova, N., Wotring, V. , and Weiss, D. (2004). Evidence that the TM1-TM2 Loop Contributes to the ρ1 GABA Receptor Pore. *Journal of Biological Chemistry*, 279(20), 20906-20914.

Findlay, G.S., Wick, M.J., Mascia, M.P., Wallace, D., Miller, G.W., Harris, R.A. , and Blednov, Y.A. (2002). Transgenic expression of a mutant glycine receptor decreases alcohol sensitivity of mice. *Journal of Pharmacology and Experimental Therapeutics*, 300(2), 526-534.

Findlay, G.S., Phelan, R., Roberts, M.T., Homanics, G.E., Bergeson, S.E., Lopreato, G.F., Mihic, S.J., Blednov, Y.A. , and Harris, R.A. (2003). Glycine receptor knock-in mice and hyperekplexia-like phenotypes: comparisons with the null mutant. *The Journal of Neuroscience*, 23(22), 8051-8059.

Flint, A., Liu, X. , and Kriegstein, A. (1998). Nonsynaptic glycine receptor activation during early neocortical development. *Neuron*, 20(1), 43-53.

Flood, P., Ramirez-Latorre, J., and Role, L. (1997). α4β2 neuronal nicotinic acetylcholine receptors in the central nervous system are inhibited by isoflurane and propofol, but α7-type nicotinic acetylcholine receptors are unaffected. *Anesthesiology*, 86(4), 859-865.

Forsyth, R.J., Gika, A.D., Ginjaar, I., and Tijssen, M.A. (2007). A novel *GLRA1* mutation in a recessive hyperekplexia pedigree. *Movement Disorders*, 22(11), 1643-1645.

Franks, N. (2008). General anaesthesia: From molecular targets to neuronal pathways of sleep and arousal. *Nature Reviews Neuroscience*, 9(5), 370-386.

Franks, N. (2015). Structural comparisons of ligand-gated ion channels in open, closed, and desensitized states identify a novel propofol-binding site on mammalian γ-aminobutyric acid type A receptors. *Anesthesiology*, 122(4), 787-794.

Franks, N. , and Lieb, W. (1994). Molecular and cellular mechanisms of general anaesthesia. *Nature*, 367(6464), 607-614.

Fucile, S., de Saint Jan, D., David-Watine, B., Korn, H., and Bregestovski, P. (1999). Comparison of glycine and GABA actions on the zebrafish homomeric glycine receptor. *The Journal of Physiology*, 517(2), 369-383.

Farley, N.M. , and Mihic, S.J. (2015). Allosteric modulation of the glycine receptor activated by agonists differing in efficacy. *Brain Research*, 1606, 95-101.

Frederickson, C.J., and Danscher, G. (1990). Zinc-containing neurons in hippocampus and related CNS structures. *Progress in Brain Research*, 83, 71-84.

Fritschy, J.M., Harvey, R.J., Schwarz, G. (2008). Gephyrin: where do we stand, where do we go? *Trends in Neurosciences*, 31(5), 257-64.

Galzi, J., and Changeux, J. (1995). Neuronal nicotinic receptors: Molecular organization and regulations. *Neuropharmacology*, 34(6), 563-582.

Galzi, J., Devillers-Thiery, A., Hussy, N., Bertrand, S., Changeux, J., and Bertrand, D. (1992). Mutations in the channel domain of a neuronal nicotinic receptor convert ion selectivity from cationic to anionic. *Nature*, 359(6395), 500-505.

Gasnier, B. (2004). The SLC32 transporter, a key protein for the synaptic release of inhibitory amino acids. *Pflügers Archiv - European Journal of Physiology*, 447(5), 756-759.

Gao, B.X., Stricker, C., and Ziskind-Conhaim, L. (2001). Transition from GABAergic to glycinergic synaptic transmission in newly formed spinal networks. *Journal of Neurophysiology*, 86(1), 492-502.

Gao, B.X., and Ziskind-Conhaim, L. (1995). Development of glycine-and GABA-gated currents in rat spinal motoneurons. *Journal of Neurophysiology*, 74(1), 113-121.

Garcia, P., Kolesky, S., and Jenkins, A. (2010). General anesthetic actions on $GABA_A$ receptors. *Current Neuropharmacology*, 8(1), 2-9.

García-Alcocer, G., Mejía, C., Berumen, L., Miledi, R., and Martínez-Torres, A. (2008). Developmental expression of glycine receptor subunits in rat cerebellum. *International Journal of Developmental Neuroscience*, 26(3-4), 319-322.

Ghosh, B., Satyshur, K. , and Czajkowski, C. (2013). Propofol binding to the resting state of the gloeobacter violaceus ligand-gated ion channel (GLIC) induces structural changes in the inter- and intrasubunit transmembrane domain (TMD) cavities. *Journal of Biological Chemistry*, 288(24), 17420-17431.

Gilbert, S.L., Ozdag, F., Ulas, U.H., Dobyns, W.B., and Lahn, B.T. (2004). Hereditary hyperekplexia caused by novel mutations of *GLRA1* in Turkish families. *Molecular Diagnosis*, 8(3), 151-155.

Gordon, N. (1993). Startle disease of hyperekplexia. *Developmental Medicine & Child Neurology*, 35(11), 1015-1018.

Graham, D., Pfeiffer, F., and Betz, H. (1983). Photoaffinity-labelling of the glycine receptor of rat spinal cord. *European Journal of Biochemistry*, 131(3), 519-525.

Graham, D., Pfeiffer, F., Simler, R., and Betz, H. (1985). Purification and characterization of the glycine receptor of pig spinal cord. *Biochemistry*, 24(4), 990-994.

Gregory, M.L., Guzauskas, G.F., Edgar, T.S., Clarkson, K.B., Srivastava, A.K., and Holden, K.R. (2008). A novel *GLRA1* mutation associated with an atypical hyperekplexia phenotype. *Journal of Child Neurology*, 23(12), 1433-1438.

Grenningloh, G., Schmieden, V., Schofield, P.R., Seeburg, P.H., Siddique, T., Mohandas, T.K., Becker, C.M. , and Betz, H., (1990). Alpha subunit variants of the human glycine receptor: primary structures, functional expression and chromosomal localization of the corresponding genes. *The EMBO Journal*, 9(3), 771.

Groot-Kormelink, P.J., Beato, M., Finotti, C., Harvey, R.J., and Sivilotti, L.G. (2002). Achieving optimal expression for single channel recording: a plasmid ratio approach to the expression of α1 glycine receptors in HEK293 cells. *Journal of Neuroscience Methods*, 113(2), 207-214.

Grosman, C., Zhou, M., and Auerbach, A. (2000). Mapping the conformational wave of acetylcholine receptor channel gating. *Nature*, 403(6771), 773-776.

Grudzinska, J., Schemm, R., Haeger, S., Nicke, A., Schmalzing, G., Betz, H., and Laube, B. (2005). The β Subunit determines the ligand binding properties of synaptic glycine receptors. *Neuron*, 45(5), 727-739.

Grudzinska, J., Schumann, T., Schemm, R., Betz, H., and Laube, B. (2008). Mutations within the agonist-binding site convert the homomeric α1 glycine receptor into a $Zn^{2+}$ -activated chloride channel. *Channels*, 2(1), 13-18.

Gunthorpe, M.J, and Lummis, S.C. (2001). Conversion of the ion selectivity of the $5\text{-}HT_{3A}$ receptor from cationic to anionic reveals a conserved feature of the ligand-gated ion channel superfamily. *Journal of Biological Chemistry*, 276(14), 10977-10983.

Haeger, S., Kuzmin, D., Detro-Dassen, S., Lang, N., Kilb, M., Tsetlin, V., Betz, H., Laube, B., and Schmalzing, G. (2010). An intramembrane aromatic network determines pentameric assembly of Cys-loop receptors. *Nature Structural & Molecular Biology*, 17(1), 90-98.

Hales, T.G., Dunlop, J.I., Deeb, T.Z., Carland, J.E., Kelley, S.P., Lambert, J.J. , and Peters, J.A. (2006). Common determinants of single channel conductance within the large cytoplasmic loop of 5-hydroxytryptamine type 3 and $\alpha_4\beta_2$ nicotinic acetylcholine receptors. *Journal of Biological Chemistry*, 281(12), 8062-8071.

Hales, T.G., and Lambert, J.J. (1991). The actions of propofol on inhibitory amino acid receptors of bovine adrenomedullary chromaffin cells and rodent central neurones. *British Journal of Pharmacology*, 104(3), 619-628.

Han, N.L., Haddrill, J.L. , and Lynch, J.W. (2001). Characterization of a glycine receptor domain that controls the binding and gating mechanisms of the β-amino acid agonist, taurine. *Journal of Neurochemistry*, 79(3), 636-647.

Hansen, S.B., Sulzenbacher, G., Huxford, T., Marchot, P., Taylor, P., and Bourne, Y. (2005). Structures of *Aplysia* AChBP complexes with nicotinic agonists and antagonists reveal distinctive binding interfaces and conformations. *The EMBO Journal*, 24(20), 3635-3646.

Hansen, S.B., Wang, H.L., Taylor, P., and Sine, S.M. (2008). An ion selectivity filter in the extracellular domain of Cys-loop receptors reveals determinants for ion conductance. *Journal of Biological Chemistry*, *283*(52), 36066-36070.

Harris, R.A., Trudell, J.R., and Mihic, S.J. (2008). Ethanol's molecular targets. *Science Signaling*, 1(28), re7.

Hartenstein, B., Schenkel, J., Kuhse, J., Besenbeck, B., Kling, C., Becker, C.M., Betz, H., and Weiher, H. (1996). Low level expression of glycine receptor beta subunit transgene is sufficient for phenotype correction in spastic mice. *The EMBO Journal*, *15*(6), 1275.

Harvey, R.J., Depner, U.B., Wässle, H., Ahmadi, S., Heindl, C., Reinold, H., Smart, T.G., Harvey, K., Schütz, B., Abo-Salem, O.M. and Zimmer, A. Poisbeau, P., Welzl. H., Wolfer, D.P., Betz, H., Zeilhofer, H.U., Müller, U. (2004). GlyR α3: an essential target for spinal PGE2-mediated inflammatory pain sensitization. *Science*, 304(5672), 884-887.

Harvey, R.J., Thomas, P., James, C.H., Wilderspin, A., and Smart, T.G. (1999). Identification of an inhibitory $Zn^{2+}$ binding site on the human glycine receptor α1 subunit. *The Journal of Physiology*, 520(1), 53-64.

Harvey, R.J., Topf, M., Harvey, K., and Rees, M.I. (2008). The genetics of hyperekplexia: more than startle! *Trends in Genetics*, 24(9), 439-447.

Hassaine, G., Deluz, C., Grasso, L., Wyss, R., Tol, M.B., Hovius, R., Graff, A., Stahlberg, H., Tomizaki, T., Desmyter, A. , and Moreau, C. (2014). X-ray structure of the mouse serotonin 5-HT3 receptor. *Nature*, 512(7514), 276-281.

Herdon, H.J., Godfrey, F.M., Brown, A.M., Coulton, S., Evans, J.R. , and Cairns, W.J. (2001). Pharmacological assessment of the role of the glycine transporter GlyT-1 in mediating high-affinity glycine uptake by rat cerebral cortex and cerebellum synaptosomes. *Neuropharmacology*, 41, 88-96.

Hibbs, R.E., and Gouaux, E. (2011). Principles of activation and permeation in an anion-selective Cys-loop receptor. *Nature*, 474(7349), 54-60.

Hilf, R.J., and Dutzler, R. (2008). X-ray structure of a prokaryotic pentameric ligand-gated ion channel. *Nature*, 452(7185), 375-379.

Holland, K.D., Fleming, M.T., Cheek, S., Moran, J.L., Beier, D.R., and Meisler, M.H. (2006). *De novo* exon duplication in a new allele of mouse *Glra1* (spasmodic). *Genetics*, 174(4), 2245-2247.

Hruskova, B., Trojanova, J., Kulik, A., Kralikova, M., Pysanenko, K., Bures, Z., Syka, J., Trussell, L.O., and Turecek, R. (2012). Differential distribution of glycine receptor subtypes at the rat calyx of held synapse. *The Journal of Neuroscience*, 32(47), 17012-17024.

Humeny, A., Bonk, T., Becker, K., Jafara-Boroujerdi, M., Stephani, U., Reuter, K., and Becker, C.M. (2002). A novel recessive hyperekplexia allele GLRA1 (S231R): genotyping by MALDI-TOF mass spectrometry and functional characterisation as a determinant of cellular glycine receptor trafficking. *European Journal of Human Genetics*, 10(3), 188-196.

Hussain, S., Prasad, M., Rittey, C., and Desurkar, A. (2013). A startling case of neonatal hyperekplexia responsive to levetiracetam a new alternative in management? *Journal of Child Neurology*, *28*(11), 1513-1516.

Hirzel, K., Müller, U., Latal, A.T., Hülsmann, S., Grudzinska, J., Seeliger, M.W., Betz, H., Laube, B. (2006). Hyperekplexia phenotype of glycine receptor α1 subunit mutant mice identifies $Zn^{2+}$ as an essential endogenous modulator of glycinergic neurotransmission. *Neuron*, 52(4), 679-90.

Hopkin, J.M. , and Neal, M.J. (1970). The release of $^{14}$C-glycine from electrically stimulated rat spinal cord slices. *British Journal of Pharmacology*, 40(1), 136P-138P.

Horváth, E., Farkas K, Herczegfalvi A, Nagy N, Széll M. (2014). Identification of a novel missense *GLRA1* gene mutation in hyperekplexia: A case report. *Journal of Medical Case Reports*, 8, 233.

Howard, R.J., Murail, S., Ondricek, K.E., Corringer, P.J., Lindahl, E., Trudell, J.R., Harris, R.A. (2011). Structural basis for alcohol modulation of a pentameric ligand-gated ion channel. *Proceedings of the National Academy of Sciences of the United States of America*, 108(29), 12149-54.

Howell, G.A., Welch, M.G., and, Frederickson, C.J. (1984). Stimulation-induced uptake and release of zinc in hippocampal slices. *Nature*, 308(5961), 736-738.

Huang, X., Chen, H., Michelsen, K., Schneider, S., Shaffer, P.L. (2015). Crystal structure of human glycine receptor-α3 bound to antagonist strychnine. *Nature*, 526(7572), 277-280.

Huang X, Chen H, Shaffer PL. (2017). Crystal structures of human GlyRα3 bound to ivermectin. *Structure*, 25(6), 945-950.e2.

Imoto, K., Busch, C., Sakmann, B., Mishina, M., Konno, T., Nakai, J., Bujo, H., Mori, Y., Fukuda, K., and Numa, S. (1988). Rings of negatively charged amino acids determine the acetylcholine receptor channel conductance. *Nature*, 335(6191), 645-648.

Imoto, K. (1993). Molecular aspects of ion permeation through channels. *Annals of the New York Academy of Sciences*, 707(1), 38-50.

Imoto, K., Konno, T., Nakai, J., Wang, F., Mishina, M., and Numa, S. (1991). A ring of uncharged polar amino acids as a component of channel constriction in the nicotinic acetylcholine receptor. *FEBS Letters*, 289(2), 193-200.

Jadey, S., and Auerbach, A. (2012). An integrated catch-and-hold mechanism activates nicotinic acetylcholine receptors. *The Journal of General Physiology*, 140(1), pp.17-28.

Jan, D., David-Watine, B., Korn, H., and Bregestovski, P. (2001). Activation of human α1 and α2 homomeric glycine receptors by taurine and GABA. *The Journal of Physiology*, 535(3), 741-755.

Jayakar, S., Zhou, X., Chiara, D., Dostalova, Z., Savechenkov, P., Bruzik, K., Dailey, W., Miller, K., Eckenhoff, R. , and Cohen, J. (2014). Multiple propofol-binding sites in a γ-aminobutyric acid type A receptor ($GABA_AR$) identified using a photoreactive propofol analog. *Journal of Biological Chemistry*, 289(40), 27456-27468.

Jonas, P. (1998). Corelease of two fast neurotransmitters at a central synapse. *Science*, 281(5375), 419-424.

Johnson, J.W. , and Ascher, P. (1987). Glycine potentiates the NMDA response in cultured mouse brain neurons. Nature, 325(6104), 529-31.

Jungbluth, H., Rees, M.I., Manzur, A.Y., Sewry, C.A., Gobbi, P., and Muntoni, F., 2000. An unusual case of hyperekplexia. *European Journal of Paediatric Neurology*, 4(2), 77-80.

Jurd, R. (2002). General anesthetic actions in vivo strongly attenuated by a point mutation in the $GABA_A$ receptor β3 subunit. *The FASEB Journal*, 17(2), 250-252.

Kang, H., Jeong Y.S., Jae C.M., Sam B. J., Kim, J.W., and Ki, C.S. (2008).Identification of a *de novo* Lys304Gln mutation in the glycine receptor α-1 subunit gene in a Korean infant with hyperekplexia. *Movement Disorders*, 23(4), 610-613.

Karlin, A. (2002). Emerging structure of the nicotinic acetylcholine receptors. *Nature Reviews Neuroscience*, 3, 102-114.

Kelley, S.P., Dunlop, J.I., Kirkness, E.F., Lambert, J.J., and Peters, J.A. (2003). A cytoplasmic region determines single-channel conductance in 5-$HT_3$ receptors. *Nature*, 424(6946), 321-324.

Keramidas, A., Moorhouse, A.J., French, C.R., Schofield, P.R., and Barry, P.H. (2000). M2 pore mutations convert the glycine receptor channel from being anion- to cation-selective. *Biophysical Journal*, 79(1), 247-259.

Keramidas, A., Moorhouse, A.J., Pierce, K.D., Schofield, P.R., and Barry, P.H. (2002). Cation-selective mutations in the M2 domain of the inhibitory glycine receptor channel reveal determinants of ion-charge selectivity. *The Journal of General Physiology*, 119(5), 393-410.

Keramidas, A., Moorhouse, A.J., Schofield, P.R., and Barry, P.H. (2004). Ligand-gated ion channels: mechanisms underlying ion selectivity. *Progress in Biophysics and Molecular Biology*, 86(2), 161-204.

Kingsmore, S.F., Giros, B., Suh, D., Bieniarz, M., Caron, M.G., and Seldin, M.F. (1994). Glycine receptor β–subunit gene mutation in spastic mouse associated with LINE–1 element insertion. *Nature Genetics*, 7(2), 136-142.

Kirstein, L., and Silfverskiöld, B. (1958). A Family with Emotionally precipitated "drop seizures". *Acta Psychiatrica Scandinavica*, 33(4), 471-476.

Kling, C., Koch, M., Saul, B., and Beckera, C.M. (1997). The frameshift mutation *oscillator* (*Glra1*$^{spd\text{-}ot}$) produces a complete loss of glycine receptor α1-polypeptide in mouse central nervous system. *Neuroscience*, 78(2), 411-417.

Kneussel, M., and Betz, H. (2000). Receptors, gephyrin and gephyrin-associated proteins: novel insights into the assembly of inhibitory postsynaptic membrane specializations. *The Journal of Physiology*, 525(1), 1-9.

Kneussel, M., and Loebrich, S. (2007). Trafficking and synaptic anchoring of ionotropic inhibitory neurotransmitter receptors. *Biology of the Cell*, 99(6), 297-309.

Konno, T., Busch, C., Kitzing, E., Imoto, K., Wang, F., Nakai, J., Mishina, M., Numa, S. , and Sakmann, B. (1991). Rings of Anionic Amino Acids as Structural Determinants of Ion Selectivity in the Acetylcholine Receptor Channel. *Proceedings of the Royal Society B: Biological Sciences*, 244(1310), 69-79.

Kotak, V.C., Korada, S., Schwartz, I.R., and Sanes, D.H. (1998). A developmental shift from GABAergic to glycinergic transmission in the central auditory system. *The Journal of Neuroscience*, 18(12), 4646-4655.

Krashia, P., Lape, R., Lodesani, F., Colquhoun, D., and Sivilotti, L.G. (2011). The long activations of α2 glycine channels can be described by a mechanism with reaction intermediates ("flip"). *The Journal of General Physiology*, 137(2), 197-216.

Krasowski, M.D., and Harrison, N.L. (1999). General anaesthetic actions on ligand-gated ion channels. *Cellular and Molecular Life Sciences*, 55(10), 1278-1303.

Krasowski, M.D., Nishikawa, K., Nikolaeva, N., Lin, A., and Harrison, N.L. (2001). Methionine 286 in transmembrane domain 3 of the $GABA_A$ receptor β subunit controls a binding cavity for propofol and other alkylphenol general anesthetics. *Neuropharmacology*, 41(8), 952-964.

Krishtal, O.A., and Pidoplichko, V.I. (1980). A receptor for protons in the nerve cell membrane. *Neuroscience*, 5(12), 2325-2327.

Kuhse, J., Kuryatov, A., Maulet, Y., Malosio, M., Schmieden, V., and Betz, H. (1991). Alternative splicing generates two isoforms of the α2 subunit of the inhibitory glycine receptor. *FEBS Letters*, 283(1), 73-77.

Kuhse, J., Laube, B., Magalei, D., and Betz, H. (1993). Assembly of the inhibitory glycine receptor: Identification of amino acid sequence motifs governing subunit stoichiometry. *Neuron*, 11(6), 1049-1056.

Kuhse, J., Schmieden, V. , and Betz, H. (1990). Identification and functional expression of a novel ligand-binding subunit of the inhibitory glycine receptor. *Journal of Biological Chemistry*, 265, 22317-22320.

Kwok, J., Raskin, S., Morgan, G., Antoniuk, S.A., Bruk, I., and Schofield, P. (2001). Mutations in the glycine receptor α1 subunit (*GLRA1*) gene in hereditary hyperekplexia pedigrees: evidence for non-penetrance of mutation Y279C. *Journal of Medical Genetics*, 38(6), e17.

Kondratskaya, E.L., Betz, H., Krishtal, O.A., and Laube, B. (2005). The beta subunit increases the ginkgolide B sensitivity of inhibitory glycine receptors. Neuropharmacology, 49(6), 945-51.

Kondratskaya, E.L., Lishko, P.V., Chatterjee, S.S. , and Krishtal, O.A. (2002). BN52021, a platelet activating factor antagonist, is a selective blocker of glycine-gated chloride channel. *Neurochemistry International*, 40(7), 647-53.

Kuryatov, A., Laube, B., Betz, H. , and Kuhse, J. (1994). Mutational analysis of the glycine-binding site of the NMDA receptor: structural similarity with bacterial amino acid-binding proteins. *Neuron*, 12(6), 1291-300.

Labarca, C., Nowak, M. W., Zhang, H., Tang, L., Deshpande, P., and Lester, H. A. (1995). Channel gating governed symmetrically by conserved leucine residues in the M2 domain of nicotinic receptors. *Nature*, 376, 514-516.

Langosch, D., Thomas, L., and Betz, H. (1988). Conserved quaternary structure of ligand-gated ion channels: the postsynaptic glycine receptor is a pentamer. *Proceedings of the National Academy of Sciences*, 85(19), 7394-7398.

Langosch, D., Laube, B., Rundström, N., Schmieden, V., Bormann, J., and Betz, H. (1994). Decreased agonist affinity and chloride conductance of mutant glycine receptors associated with human hereditary hyperekplexia. The EMBO Journal, 13(18), 4223.

Lape, R., Colquhoun, D., and Sivilotti, L.G. (2008). On the nature of partial agonism in the nicotinic receptor superfamily. *Nature*, 454, 722-727.

Lape, R., Plested, A.J., Moroni, M., Colquhoun, D., and Sivilotti, L.G. (2012). The α1K276E startle disease mutation reveals multiple intermediate states in the gating of glycine receptors. *The Journal of Neuroscience*, 32(4), 1336-1352.

Lapunzina, P., Sánchez, J.M., Cabrera, M., Moreno, A., Delicado, A., Torres, M.L., Mori, A.M., Quero, J., and Pajares, I.L. (2003). Hyperekplexia (Startle Disease). *Molecular Diagnosis*, 7(2), 125-128.

Laube, B., Hirai, H., Sturgess M., Betz, H., and Kuhse, J. (1997). Molecular determinants of agonist discrimination by NMDA receptor subunits: analysis of the glutamate binding site on the NR2B subunit. *Neuron*, 18(3), 493-503.

Laube, B., Kuhse, J., and Betz, H. (2000). Kinetic and mutational analysis of $Zn^{2+}$ modulation of recombinant human inhibitory glycine receptors. *The Journal of Physiology*, 522(2), 215-230.

Laube, B., Maksay, G., Schemm, R., and Betz, H. (2002). Modulation of glycine receptor function: a novel approach for therapeutic intervention at inhibitory synapses? *Trends in Pharmacological Sciences*, 23(11), 519-27.

Lee, C.G., Kwon, M.J., Yu, H.J., Nam, S.H., Lee, J., Ki, C.S., and Lee, M. (2013). Clinical features and genetic analysis of children with hyperekplexia in Korea. *Journal of Child Neurology*, *28*(1), 90-94.

Legendre, P. (2001). The glycinergic inhibitory synapse. *Cellular and Molecular Life Sciences*, 58, 760-793.

Legendre, P., and Korn, H. (1995). Voltage dependence of conductance changes evoked by glycine release in the zebrafish brain. *Journal of Neurophysiology*, 73, 2404-2412.

Lewis, C.A., Ahmed, Z., and Faber, D.S. (1991). A characterization of glycinergic receptors present in cultured rat medullary neurons. *Journal of Neurophysiology*, 66, pp.1291-1303.

Lewis, T.M., Sivilotti, L.G., Colquhoun, D., Gardiner, R.M., Schoepfer, R., and Rees, M. (1998). Properties of human glycine receptors containing the hyperekplexia mutation α1 (K276E), expressed in *Xenopus* oocytes. *The Journal of Physiology*, 507(1), 25-40.

Lobo, I.A., and Harris, R.A. (2005). Sites of alcohol and volatile anesthetic action on glycine receptors. *International Review of Neurobiology*, 65, 53-87.

Lobo, I.A., Trudell, J.R., and Harris, R.A. (2004). Cross-linking of glycine receptor transmembrane segments two and three alters coupling of ligand binding with channel opening. *Journal of Neurochemistry*, 90(4), 962-969.

Lu, T., Rubio, M.E., and Trussell, L.O. (2008). Glycinergic transmission shaped by the corelease of GABA in a mammalian auditory synapse. *Neuron*, 57(4), 524-535.

Lynagh, T., and Lynch, J.W. (2010). A glycine residue essential for high ivermectin sensitivity in Cys-loop ion channel receptors. *International Journal for Parasitology*, 40(13), 1477-1481.

Lynagh, T., and Lynch, J.W. (2012). Molecular mechanisms of Cys-loop ion channel receptor modulation by ivermectin. *Frontiers in Molecular Neuroscience*, (5), 60.

Lynagh, T., and Laube, B. (2014). Opposing effects of the anesthetic propofol at pentameric ligand-gated ion channels mediated by a common site. *The Journal of Neuroscience*, 34(6), 2155-2159.

Lynagh, T., Webb, T.I., Dixon, C.L., Cromer, B.A., and Lynch, J.W. (2011). Molecular determinants of ivermectin sensitivity at the glycine receptor chloride channel. *Journal of Biological Chemistry*, *286*(51), 43913-43924.

Lynch, J.W. (2004). Molecular structure and function of the glycine receptor chloride channel. *Physiological Reviews*, 84(4), 1051-1095.

Lynch, J.W. (2009). Native glycine receptor subtypes and their physiological roles. *Neuropharmacology*, 56(1), 303-309.

Lynch, J.W., Rajendra, S., Pierce, K.D., Handford, C.A., Barry, P.H., and Schofield, P.R. (1997). Identification of intracellular and extracellular domains mediating signal transduction in the inhibitory glycine receptor chloride channel. *The EMBO Journal*, 16(1), 110-120.

Lynch, J.W., Rajendra, S., Barry, P.H., and Schofield, P.R. (1995). Mutations affecting the glycine receptor agonist transduction mechanism convert the competitive antagonist, picrotoxin, into an allosteric potentiator. *Journal of Biological Chemistry*, 270(23), 13799-806.

Lynch, J.W., Jacques, P., Pierce, K.D., and Schofield, P.R. (1998). Zinc potentiation of the glycine receptor chloride channel is mediated by allosteric pathways. *Journal of Neurochemistry*, 71(5), 2159-68.

Mallorga, P.J., Williams, J.B., Jacobson, M., Marques, R., Chaudhary, A., Conn, P.J., Pettibone, D.J., and Sur, C. (2003). Pharmacology and expression analysis of glycine transporter GlyT1 with [$^3$H]-(N-[3-(4′-fluorophenyl)-3-(4′phenylphenoxy)propyl]) sarcosine. *Neuropharmacology*, 45(5), 585-593.

Malosio, M.L., Marqueze-Pouey, B., Kuhse, J., and Betz, H. (1991). Widespread expression of glycine receptor subunit mRNAs in the adult and developing rat brain. *The EMBO Journal*, 10(9), 2401.

Madry, C., Mesic, I., Bartholomäus, I., Nicke, A., Betz, H., and Laube, B. (2007). Principal role of NR3 subunits in NR1/NR3 excitatory glycine receptor function. *Biochemical and Biophysical Research Communications*, 354(1), 102-108.

Marabelli, A., Moroni, M., Lape, R., and Sivilotti, L. (2013). The kinetic properties of the α3 rat glycine receptor make it suitable for mediating fast synaptic inhibition. *The Journal of Physiology*, 591(13), 3289-3308.

Marchais, D., and Marty, A. (1979). Interaction of permeant ions with channels activated by acetylcholine in Aplysia neurones. *The Journal of Physiology*, 297(1), 9-45.

Mascia, M.P, Machu, T.K, and Harris, R.A. (1996). Enhancement of homomeric glycine receptor function by long chain alcohols and anaesthetics. *British Journal of Pharmacology*, 119(7), 1331-1336.

Melzer, N., Villmann, C., Becker, K., Harvey, K., Harvey, R., Vogel, N., Kluck, C., Kneussel, M., and Becker, C. (2010). Multifunctional Basic Motif in the Glycine Receptor Intracellular Domain Induces Subunit-specific Sorting. *Journal of Biological Chemistry*, 285(6), 3730-3739.

Meyer, G., Kirsch, J., Betz, H., and Langosch, D. (1995). Identification of a gephyrin binding motif on the glycine receptor β subunit. *Neuron*, 15(3), 563-572.

Milani, N., Dalprá, L., Del Prete, A., Zanini, R. , and Larizza, L., 1996. A novel mutation (Gln266→ His) in the alpha 1 subunit of the inhibitory glycine-receptor gene (*GLRA1*) in hereditary hyperekplexia. *American Journal of Human Genetics*, *58*(2), 420-422.

Mihic, S.J., Ye, Q., Wick, M.J., Koltchine, V.V., Krasowski, M.D., Finn, S.E., Mascia, M.P., Valenzuela, C.F., Hanson, K.K., Greenblatt, E.P. , and Harris, R.A., 1997. Sites of alcohol and volatile anaesthetic action on GABAA and glycine receptors. *Nature*, 389(6649), 385-389.

Miller, P.S, Beato, M., Harvey, R.J., and Smart, T.G. (2005a). Molecular determinants of glycine receptor αβ subunit sensitivities to $Zn^{2+}$ -mediated inhibition. *The Journal of Physiology*, 566(3), 657-670.

Miller, P.S., Da Silva, H.M, and Smart, T.G (2005b). Molecular Basis for Zinc Potentiation at Strychnine-sensitive Glycine Receptors. *Journal of Biological Chemistry*, 280(45), 37877-37884.

Mine, J., Taketani, T., Yoshida, K., Yokochi, F., Kobayashi, J., Maruyama, K., Nanishi, E., Ono, M., Yokoyama, A., Arai, H., Tamaura, S., Suzuki, Y., Otsubo, S., Hayashi, T., Kimura, M., Kishi, K. , and Yamaguchi, S. (2014). Clinical and genetic investigation of 17 Japanese patients with hyperekplexia. *Developmental Medicine & Child Neurology*, 57(4), 372-377.

Miraglia, D., Coppola, G., Bellini, G., Ledaal, P., Hertz, J., and Pascotto, A. (2003). A novel mutation (R218Q) at the boundary between the N-terminal and the first transmembrane domain of the glycine receptor in a case of sporadic hyperekplexia. *Journal of Medical Genetics*, 40(5), e71-e71.

Miyazawa, A., Fujiyoshi, Y. , and Unwin, N. (2003). Structure and gating mechanism of the acetylcholine receptor pore. *Nature*, 423(6943), 949-955.

Moorhouse, A.J., Jacques, P., Barry, P.H., and Schofield, P.R., 1999. The startle disease mutation Q266H, in the second transmembrane domain of the human glycine receptor, impairs channel gating. *Molecular Pharmacology*,*55*(2), 386-395.

Moorhouse, A., Keramidas, A., Zaykin, A., Schofield, P., and Barry, P. (2002). Single Channel Analysis of Conductance and Rectification in Cation-selective, Mutant Glycine Receptor Channels. *The Journal of General Physiology*, 119(5), 411-425.

Moraga-Cid, G., Sauguet, L., Huon, C., Malherbe, L., Girard-Blanc, C., Petres, S., Murail, S., Taly, A., Baaden, M., Delarue, M. , and Corringer, P. (2015). Allosteric and hyperekplexic mutant phenotypes investigated on an α 1 glycine receptor transmembrane structure. *Proceedings of the National Academy of Sciences*, 112(9), 2865-2870.

Moraga-Cid, G., Yevenes, G., Schmalzing, G., Peoples, R., and Aguayo, L. (2011). A Single phenylalanine residue in the main intracellular loop of α1 γ-aminobutyric acid type A and glycine receptors influences their sensitivity to propofol. *Anesthesiology*, 115(3), 464-473.

Moroni, M., Meyer, J.M, Lahmann, C., and Sivilotti, L.G. (2011a). In glycine and $GABA_A$ channels, different subunits contribute asymmetrically to channel conductance *via* residues in the extracellular domain. *Journal of Biological Chemistry*, 286(15), 13414-13422.

Moroni, M., Biro, I., Giugliano, M., Vijayan, R., Biggin, P.C., Beato, M., and Sivilotti, L.G. (2011b). Chloride ions in the pore of glycine and GABA channels shape the time course and voltage dependence of agonist currents. *Journal of Neuroscience*, 31(40), 14095-14106.

Mowrey, D., Cui, T., Jia, Y., Ma, D., Makhov, A.M., Zhang, P., Tang, P., and Xu, Y. (2013). Open-channel structures of the human glycine receptor α1 full-length transmembrane domain. *Structure*, 21(10), 1897-1904.

Mukhtasimova, N., Lee, W., Wang, H., and Sine, S. (2009). Detection and trapping of intermediate states priming nicotinic receptor channel opening. *Nature*, 459(7245), 451-454.

Mülhardt, C., Fischer, M., Gass, P., Simon-Chazottes, D., Guenet, J., Kuhse, J., Betz, H., and Becker, C. (1994). The spastic mouse: aberrant splicing of glycine receptor β subunit mRNA caused by intronic insertion of Ll element. *Neuron*, 13(4), 1003-1015.

Muller, E., Le Corronc, H., Triller, A., and Legendre, P. (2006). Developmental dissociation of presynaptic inhibitory neurotransmitter and postsynaptic receptor clustering in the hypoglossal nucleus. *Molecular and Cellular Neuroscience*, 32(3), 254-273.

Nabekura, J., Katsurabayashi, S., Kakazu, Y., Shibata, S., Matsubara, A., Jinno, S., Mizoguchi, Y., Sasaki, A., and Ishibashi, H. (2004). Developmental switch from GABA to glycine release in single central synaptic terminals. *Nature Neuroscience*, 7(1), 17-23.

Nguyen, H.T., Li, K.Y., daGraca, R.L., Delphin, E., Xiong, M., and Ye, J.H. (2009). Behavior and cellular evidence for propofol-induced hypnosis involving brain glycine receptors. *Anesthesiology*, 110(2), 326-332.

Nikolic, Z., Laube, B., Weber, R., Lichter, P., Kioschis, P., Poustka, A., Mulhardt, C., and Becker, C. (1998). The human glycine receptor subunit alpha3. Glra3 gene structure, chromosomal localization, and functional characterization of alternative transcripts. *Journal of Biological Chemistry*, 273(31), 19708-19714.

Nishikawa, K., and Harrison, N. (2003). The Actions of Sevoflurane and Desflurane on the γ-Aminobutyric Acid Receptor Type A. *Anesthesiology*, 99(3), 678-684.

Nury, H., Van Renterghem, C., Weng, Y., Tran, A., Baaden, M., Dufresne, V., Changeux, J., Sonner, J., Delarue, M., and Corringer, P.J. (2011). X-ray structures of general anaesthetics bound to a pentameric ligand-gated ion channel. *Nature*, 469(7330), 428-431.

O'Brien, J.A., and Berger, A.J. (1999). Cotransmission of GABA and glycine to brain stem motoneurons. *Journal of Neurophysiology*, 82(3), 1638-1641.

O'Shea, S.M., Becker, L., Weiher, H., Betz, H., and Laube, B. (2004). Propofol restores the function of "hyperekplexic" mutant glycine receptors in *Xenopus* oocytes and mice. *Journal of Neuroscience*, 24(9), 2322-2327.

O'Shea, S.M., Wong, L.C., and Harrison, N.L. (2000). Propofol increases agonist efficacy at the $GABA_A$ receptor. *Brain Research*, 852(2), 344-348.

Pribilla, I., Takagi, T., Langosch, D., Bormann, J., and Betz, H. (1992). The atypical M2 segment of the beta subunit confers picrotoxinin resistance to inhibitory glycine receptor channels. *The EMBO Journal*, 11(12), 4305.

Peters, J.A., Cooper, M.A, Carland, J.E, Livesey, M.R, Hales, T.G., and Lambert, J.J. (2010). Novel structural determinants of single channel conductance and ion selectivity in 5-hydroxytryptamine type 3 and nicotinic acetylcholine receptors. *The Journal of Physiology*, 588(4), 587-596.

Peters, J.A., Hales, T.G, and Lambert, J.J. (2005). Molecular determinants of single-channel conductance and ion selectivity in the Cys-loop family: insights from the 5-$HT_3$ receptor. *Trends in Pharmacological Sciences*, 26(11), 587-594.

Peters, J.A., Kelley, S.P., Dunlop, J.I., Kirkness, E.F., Hales, T.G., and Lambert, J.J. (2004). The 5-hydroxytryptamine type 3 (5-$HT_3$) receptor reveals a novel determinant of single-channel conductance. *Biochemical Society Transactions*, 32(3), 547-552.

Piomelli, D. (2003). The molecular logic of endocannabinoid signalling. *Nature Reviews Neuroscience*, 4(11), 873-884.

Pilorge, M., Fassier, C., Le Corronc, H., Potey, A., Bai, J., De Gois, S., Delaby, E., Assouline, B., Guinchat, V., Devillard, F., Delorme, R., Nygren, G., Råstam, M., Meier, J.C., Otani, S., Cheval, H., James, V., Topf , M., Dear, N., Gillberg, C., Leboyer, M., Giros, B., Gautron, S., Hazan, J., Harvey, R., Legendre, and P., Betancur, C. (2016). Genetic and functional analyses demonstrate a role for abnormal glycinergic signaling in autism. *Molecular Psychiatry*, 21(7), 936-45.

Pistis, M., Belelli, D., Peters, J.A., and Lambert, J.J. (1997). The interaction of general anaesthetics with recombinant $GABA_A$ and glycine receptors expressed in *Xenopus laevis* oocytes: a comparative study. *British Journal of Pharmacology*, 122(8), 1707-1719.

Pitt, S.J., Sivilotti, L.G., and Beato, M. (2008). High Intracellular chloride slows the decay of glycinergic currents. *Journal of Neuroscience*, 28(45), 11454-11467.

Pless, S.A., Hanek, A.P., Price, K.L., Lynch, J.W., Lester, H.A., Dougherty, D.A., and Lummis, S.C. (2011). A cation-π interaction at a phenylalanine residue in the glycine receptor binding site is conserved for different agonists. *Molecular Pharmacology*, 79(4), 742-748.

Pless, S.A., Millen, K.S., Hanek, A.P., Lynch, J.W., Lester, H.A., Lummis, S.C., and Dougherty, D.A. (2008). A cation-π interaction in the binding site of the glycine receptor is mediated by a phenylalanine residue. *Journal of Neuroscience*, 28(43), 10937-10942.

Poon, W.T., Chan, K.Y., Au, K.M., Tong, S.F., Chan, Y.W., Lam, C.W., and Chow, C.B. (2006). Novel missense mutation (Y279S) in the *GLRA1* gene causing hyperekplexia. *Clinica Chimica Acta*, 364(1-2), 361-362.

Probst, A., Cortés, R. , and Palacios, J. (1986). The distribution of glycine receptors in the human brain. A light microscopic autoradiographic study using [3H]strychnine. *Neuroscience*, 17(1), 11-35.

Purohit, P., Mitra, A. , and Auerbach, A. (2007). A stepwise mechanism for acetylcholine receptor channel gating. *Nature*, 446(7138), 930-933.

Rajendra, S., Lynch, J.W., Pierce, K.D., French, C.R., Barry, P.H. , and Schofield, P.R. (1994). Startle disease mutations reduce the agonist sensitivity of the human inhibitory glycine receptor. *Journal of Biological Chemistry*, 269(29), 18739-18742.

Rea, R., Tijssen, M., Herd, C., Frants, R. , and Kullmann, D. (2002). Functional characterization of compound heterozygosity for GlyRα1 mutations in the startle disease hyperekplexia. *European Journal of Neuroscience*, 16(2), 186-196.

Rees, M., Andrew, M., Jawad, S. , and Owen, M. (1994). Evidence for recessive as well as dominant forms of startle disease (hyperekplexia) caused by mutations in the α 1 subunit of the inhibitory glycine receptor. *Human Molecular Genetics*, 3(12), 2175-2179.

Rees, M.I., Harvey, K., Ward, H., White, J.H., Evans, L., Duguid, I.C., Hsu, C., Coleman, S., Miller, J., Baer, K., Waldvogel, H.J., Gibbon, F., Smart, T.G, Owen, M., Harvey, R.J, and Snell, R.G. (2003). Isoform heterogeneity of the human gephyrin gene (GPHN), binding domains to the glycine receptor, and mutation analysis in hyperekplexia. *Journal of Biological Chemistry*, 278(27), 24688-24696.

Rees, M.I, Lewis, T.M, Vafa, B., Ferrie, C., Corry, P., Muntoni, F., Jungbluth, H., Stephenson, J.B., Kerr, M., Snell, R.G., Schofield, P.R., and Owen, M.J. (2001). Compound heterozygosity and nonsense mutations in the α1-subunit of the inhibitory glycine receptor in hyperekplexia. *Human Genetics*, 109(3), 267-270.

Richardson, J.E., Garcia, P.S., O'Toole, K."K., Derry, J.M., Bell, S.V., and Jenkins, A. (2007). A conserved tyrosine in the $\beta_2$ sbunit M4 segment is a determinant of γ-aminobutyric acid type A receptor sensitivity to propofol. *The Journal of the American Society of Anesthesiologists*, 107(3), 412-418.

Rovira, J., Vicente-Agulló, F., Campos-Caro, A., Criado, M., Sala, F., Sala, S., and Ballesta, J. (1999). Gating of α3β4 neuronal nicotinic receptor can be controlled by the loop M2-M3 of both α3 and β4 subunits.*Pflügers Archiv - European Journal of Physiology*, 439(1), 86-92.

Rundstrom, N., Schmieden, V., Betz, H., Bormann, J., and Langosch, D. (1994). Cyanotriphenylborate: Subtype-specific blocker of glycine receptor chloride channels. *Proceedings of the National Academy of Sciences*, 91(19), 8950-8954.

Rüsch, D., Braun, H.A., Wulf, H., Schuster, A., and Raines, D.E. (2007). Inhibition of human 5-$HT_{3A}$ and 5-$HT_{3AB}$ receptors by etomidate, propofol and pentobarbital. *European Journal of Pharmacology*, 573(1-3), 60-64.

Russier, M., Kopysova, I., Ankri, N., Ferrand, N., and Debanne, D. (2002). GABA and glycine co-release optimizes functional inhibition in rat brainstem motoneurons *in vitro*. *The Journal of Physiology*, 541(1), 123-137.

Ryan, S.G., Buckwalter, M.S., Lynch, J.W., Handford, C.A., Segura, L., Shiang, R., Wasmuth, J.J., Camper, S.A., Schofield, P., and O'Connell, P. (1994). A missense mutation in the gene encoding the α1 subunit of the inhibitory glycine receptor in the spasmodic mouse. *Nature Genetics*, 7(2), 131-135.

Sauguet, L., Howard, R.J., Malherbe, L., Lee, U.S., Corringer, P.J., Harris, R.A., and Delarue, M. (2013). Structural basis for potentiation by alcohols and anaesthetics in a ligand-gated ion channel. *Nature Communications*, *4*, 1697.

Sauguet, L., Shahsavar, A., Poitevin, F., Huon, C., Menny, A., Nemecz, A., Haouz, A., Changeux, J., Corringer, P. , and Delarue, M. (2014). Crystal structures of a pentameric ligand-gated ion channel provide a mechanism for activation. *Proceedings of the National Academy of Sciences*, 111(3), 966-971.

Saul, B., Kuner, T., Sobetzko, D., Brune, W., Hanefeld, F., Meinck, H.M., and Becker, C.M. (1999). Novel *GLRA1* missense mutation (P250T) in dominant hyperekplexia defines an intracellular determinant of glycine receptor channel gating. *Journal of Neuroscience*, 19(3), 869-877.

Schaefer, N., Kluck, C., Price, K., Meiselbach, H., Vornberger, N., Schwarzinger, S., Hartmann, S., Langlhofer, G., Schulz, S., Schlegel, N., Brockmann, K., Lynch, B., Becker, C., Lummis, S. , and Villmann, C. (2015). Disturbed Neuronal ER-Golgi Sorting of Unassembled Glycine Receptors Suggests Altered Subcellular Processing is a Cause of Human Hyperekplexia. *Journal of Neuroscience*, 35(1), 422-437.

Schmieden, V., and Betz, H. (1995). Pharmacology of the inhibitory glycine receptor: agonist and antagonist actions of amino acids and piperidine carboxylic acid compounds. *Molecular Pharmacology*, 48(5), 919-927.

Schmieden, V., Kuhse, J., and Betz, H. (1992). Agonist pharmacology of neonatal and adult glycine receptor α subunits: identification of amino acid residues involved in taurine activation. *The EMBO Journal*, 11, 2025-2032.

Schmieden, V., Kuhse, J., and Betz, H. (1999). A novel domain of the inhibitory glycine receptor determining antagonist efficacies: further evidence for partial agonism resulting from self-inhibition. *Molecular Pharmacology*, 56(3), 464-472.

Schmitt, B., Knaus, P., Becker, C., and Betz, H. (1987). The Mr 93,000 polypeptide of the postsynaptic glycine receptor complex is a peripheral membrane protein. *Biochemistry*, 26(3), 805-811.

Seidahmed, M.Z., Salih, M.A., Abdulbasit, O.B., Shaheed, M., Al Hussein, K., Miqdad, A.M., Al Rasheed, A.K., Alazami, A.M., Alorainy, I.A., and Alkuraya, F.S. (2012). A novel syndrome of lethal familial hyperekplexia associated with brain malformation. *BMC Neurology*, 12(125).

Seri, M., Bolino, A., Galietta, L., Lerone, M., Silengo, M., and Romeo, G. (1997). Startle disease in an Italian family by mutation (K276E): The α-subunit of the inhibiting glycine receptor. *Human Mutation*, 9(2), 185-187.

Shan, Q. (2001). Ivermectin, an Unconventional Agonist of the Glycine Receptor Chloride Channel. *Journal of Biological Chemistry*, 276(16), 12556-12564.

Shiang, R., Ryan, S., Zhu, Y., Fielder, T., Allen, R., Fryer, A., Yamashita, S., O'Connell, P., and Wasmuth, J. (1995). Mutational analysis of familial and sporadic hyperekplexia. *Annals of Neurology*, 38(1), 85-91.

Shiang, R., Ryan, S., Zhu, Y., Hahn, A., O'Connell, P., and Wasmuth, J. (1993). Mutations in the α1 subunit of the inhibitory glycine receptor cause the dominant neurologic disorder, hyperekplexia. *Nature Genetics*, 5(4), 351-358.

Singer, J.H. (2008). GABA is an endogenous ligand for synaptic glycine receptors. *Neuron*, 57(4), 475-477.

Singer, J.H., and Berger, A.J. (1999). Contribution of single-channel properties to the time course and amplitude variance of quantal glycine currents recorded in rat motoneurons. *Journal of Neurophysiology*, 81, 1608-1616.

Singer, J.H., and Berger, A.J. (2000). Development of inhibitory synaptic transmission to motoneurons. *Brain Research Bulletin*, 53, 553-560.

Singer, J.H., Talley, E.M., Bayliss, D.A., and Berger, A.J., 1998. Development of glycinergic synaptic transmission to rat brain stem motoneurons. *Journal of Neurophysiology*, 80(5), 2608-2620.

Sixma, T.K. (2007). Nicotinic receptor structure emerging slowly. *Nature Neuroscience*, 10(8), 937-938.

Sixma, T.K., and Smit, A.B. (2003). Acetylcholine binding protein (AChBP): a secreted glial protein that provides a high-resolution model for the extracellular domain of pentameric ligand-gated ion channels. *Annual Review of Biophysics and Biomolecular Structure*, 32(1), 311-334.

Smart, T.G., Hosie, A.M., and Miller, P.S. (2004). $Zn^{2+}$ Ions: Modulators of excitatory and inhibitory synaptic activity. *The Neuroscientist*, 10(5), 432-442.

Smith, K., Borden, L., Hartig, P., Branchek, T., and Weinshank, R. (1992). Cloning and expression of a glycine transporter reveal colocalization with NMDA receptors. *Neuron*, 8(5), 927-935.

Sola, M., Bavro, V., Timmins, J., Franz, T., Ricard-Blum, S., Schoehn, G., Ruigrok, R., Paarmann, I., Saiyed, T., O'Sullivan, G., Schmitt, B., Betz, H., and Weissenhorn, W. (2004). Structural basis of dynamic glycine receptor clustering by gephyrin. *The EMBO Journal*, 23(13), 2510-2519.

Song, X.X., and Yu, B.W. (2014). Anesthetic effects of propofol in the healthy human brain: functional imaging evidence. *Journal of Anesthesia*, 29(2), 279-288.

Sunesen, M., de Carvalho, L.P, Dufresne, V., Grailhe, R., Savatier-Duclert, N., Gibor, G., Peretz, A., Attali, B., Changeux, J.P, and Paas, Y. (2006). Mechanism of $Cl^-$ selection by a glutamate-gated chloride (GluCl) receptor revealed through mutations in the selectivity filter. *Journal of Biological Chemistry*, 281(21), 14875-14881.

Safar, F., Hurdiss, E., Erotocritou, M., Greiner, T., Lape, R., Irvine, M.W., Fang, G., Jane, D., Yu, R., Dämgen, M.A., Biggin, P.C., and Sivilotti, L.G. (2017). The Startle Disease Mutation E103K Impairs Activation of Human Homomeric α1 Glycine Receptors by Disrupting an Intersubunit Salt Bridge across the Agonist Binding Site. *Journal of Biological Chemistry*, 292(12), 5031-5042.

Scott, S., Lynch, J.W., and Keramidas A. (2015). Correlating structural and energetic changes in glycine receptor activation. *Journal of Biological Chemistry*, 290(9), 5621-5634.

Shank, R.P., and Aprison, M.H. (1970). The metabolism in vivo of glycine and serine in eight areas of the rat central nervous system. *Journal of Neurochemistry*. 17(10),1461-1475.

Simmonds, M.A., and Turner, J.P. (1985). Antagonism of inhibitory amino acids by the steroid derivative RU5135. *British Journal of Pharmacology*, 84(3):631-5.

Spurny, R., Ramerstorfer, J., Price, K., Brams, M., Ernst, M., Nury, H., Verheij, M., Legrand, P., Bertrand, D., Bertrand, S., Dougherty, D.A., de Esch, I.J., Corringer, P.J., Sieghart, W., Lummis, S.C., and Ulens, C. (2012). Pentameric ligand-gated ion channel ELIC is activated by GABA and modulated by benzodiazepines. *Proceedings of the National Academy of Sciences of the United States of America*, 109(44), E3028-3034.

Takahashi, T., and Momiyama, A. (1991). Single-channel currents underlying glycinergic inhibitory postsynaptic responses in spinal neurons. *Neuron*, 7(6), 965-969.

Takahashi, T., Momiyama, A., Hirai, K., Hishinuma, F., and Akagi, H. (1992). Functional correlation of fetal and adult forms of glycine receptors with developmental changes in inhibitory synaptic receptor channels. *Neuron*, 9(6), 1155-1161.

Tang, P., Mandal, P., and Xu, Y. (2002). NMR Structures of the Second Transmembrane Domain of the Human Glycine Receptor α1 Subunit: Model of Pore Architecture and Channel Gating. *Biophysical Journal*, 83(1), 252-262.

Thomas, R., Chung, S., Wood, S., Cushion, T., Drew, C., Hammond, C., Vanbellinghen, J., Mullins, J. , and Rees, M. (2013). Genotype-phenotype correlations in hyperekplexia: apnoeas, learning difficulties and speech delay. *Brain*, 136(10), 3085-3095.

Thomas, R.H., Stephenson, J.B., Harvey, R.J., and Rees, M.I. (2010). Hyperekplexia: Stiffness, startle and syncope. *Journal of Pediatric Neurology, 8*(1), 11.

Thompson, A., Lester, H. , and Lummis, S. (2010). The structural basis of function in Cys-loop receptors. *Quarterly Reviews of Biophysics*, 43(04), 449-499.

Todd, A.J., Watt, C., Spike, R.C., and Sieghart, W. (1996). Colocalization of GABA, glycine, and their receptors at synapses in the rat spinal cord. *Journal of Neuroscience*, 16(3), 974-982.

Traka, M., Seburn, K.L., and Popko, B. (2006). Nmf11 is a novel ENU-induced mutation in the mouse glycine receptor alpha 1 subunit. *Mammalian Genome*, 17(9), 950-955.

Triller, A., Cluzeaud, F., and Korn, H. (1987). Gamma-aminobutyric acid-containing terminals can be opposed to glycine receptors at central synapses. *The Journal of Cell Biology*, 104(4), 947-956.

Tsai, C., Chang, F., Su, Y., Tsai, F., Lu, M., Lee, C., Kuo, C., Yang, Y., and Lu, C. (2004). Two novel mutations of the glycine receptor gene in a Taiwanese hyperekplexia family. *Neurology*, 63(5), 893-896.

Turecek, R., and Trussell, L.O. (2001). Presynaptic glycine receptors enhance transmitter release at a mammalian central synapse. *Nature*, 411(6837), 587-590.

Twyman, R.E, and Macdonald, R.L. (1991). Kinetic properties of the glycine receptor main- and sub-conductance states of mouse spinal cord neurones in culture. *The Journal of Physiology*, 435(1), 303-331.

Ulens, C., Hogg, R.C., Celie, P.H., Bertrand, D., Tsetlin, V., Smit, A.B., and Sixma, T.K. (2006). Structural determinants of selective α-conotoxin binding to a nicotinic

acetylcholine receptor homolog AChBP. *Proceedings of the National Academy of Sciences of the United States of America*, 103(10), 3615-3620.

Unwin, N. (2005). Refined structure of the nicotinic acetylcholine receptor at 4 Å resolution. *Journal of Molecular Biology*, 346(4), 967-989.

Unwin, N., Miyazawa, A., Li, J., and Fujiyoshi, Y. (2002). Activation of the nicotinic acetylcholine receptor involves a switch in conformation of the α subunits. *Journal of Molecular Biology*, 319(5), 1165-1176.

Vafa, B., Lewis, T.M., Cunningham, A.M., Jacques, P., Lynch, J.W., and Schofield, P.R. (1999). Identification of a new ligand binding domain in the alpha1 subunit of the inhibitory glycine receptor. *Journal of Neurochemistry*, 73, 2158-2166.

Vergouwe, M.N., Tijssen, M.A., Peters, A.C., Wielaard, R., and Frants, R.R. (1999). Hyperekplexia phenotype due to compound heterozygosity for *GLRA1* gene mutations. *Annals of Neurology*, 46(4), 634-638.

Villmann, C., Oertel, J., Melzer, N., and Becker, C.M. (2009). Recessive hyperekplexia mutations of the glycine receptor α1 subunit affect cell surface integration and stability. *Journal of Neurochemistry*, 111(3), 837-847.

Wang, D.S., Xu, T.L., and Li, J.S. (1999). Modulation of glycine-activated chloride currents by substance P in rat sacral dorsal commissural neurons. *Sheng li xue bao:[Acta Physiologica Sinica]*, 51(4), 361-370.

Watanabe, E., and Akagi, H. (1995). Distribution patterns of mRNAs encoding glycine receptor channels in the developing rat spinal cord. *Neuroscience Research*, 23(4), 377-382.

Wang, C.H., Hernandez, C.C., Wu, J., Zhou, N., Hsu, H.Y., Shen, M.L., Wang, Y.C., Macdonald, R.L., Wu, D.C. (2018). A Missense Mutation A384P Associated with Human Hyperekplexia Reveals a Desensitization Site of Glycine Receptors. *Journal of Neuroscience*, 38(11), 2818-2831.

Werman, R. (1966). Criteria for identification of a central nervous system transmitter. *Comparative Biochemistry and Physiology*, 18(4):745-66.

Werman, R., Davidoff, R.A., Aprison, M.H. (1967). Inhibition of motoneurones by iontophoresis of glycine. *Nature*, 214(5089), 681-3.

Xie, X., and Smart, T.G. (1991). A physiological role for endogenous zinc in rat hippocampal synaptic neurotransmission. *Nature*, 349(6309), 521-524.

Xiong, W., Chen, S.R, He, L., Cheng, K., Zhao, Y.L, Chen, H., Li, D.P, Homanics, G.E, Peever, J., Rice, K.C, Wu, L.G, Pan, H.L., and Zhang, L. (2014). Presynaptic glycine receptors as a potential therapeutic target for hyperekplexia disease. *Nature Neuroscience*, 17(2), 232-239.

Xiong, W., Cheng, K., Cui, T., Godlewski, G., Rice, K.C, Xu, Y. , and Zhang, L. (2011). Cannabinoid potentiation of glycine receptors contributes to cannabis-induced analgesia. *Nature Chemical Biology*, 7(5), 296-303.

Xiu, X., Puskar, N.L, Shanata, J.A, Lester, H.A., and Dougherty, D.A, (2009). Nicotine binding to brain receptors requires a strong cation–π interaction. *Nature*, 458(7237), 534-537.

Yamakura, T., Bertaccini, E., Trudell, J.R., and Harris, R.A. (2001). Anesthetics and ion channels: molecular models and sites of action. *Annual Review of Pharmacology and Toxicology*, 41, 23-51.

Yang, Z., Cromer, B.A., Harvey, R.J., Parker, M.W., and Lynch, J.W. (2007). A proposed structural basis for picrotoxinin and picrotin binding in the glycine receptor pore. *Journal of Neurochemistry*, 103(2), 580-589.

Yang, Z., Taran, E., Webb, T.I., and Lynch, J.W. (2012). Stoichiometry and Subunit Arrangement of α1β Glycine Receptors as Determined by Atomic Force Microscopy. *Biochemistry*, 51(26), 5229-5231.

Yang, Z., Sun, G., Yao, F., Tao, D., and Zhu, B. (2017). A novel compound mutation in GLRA1 cause hyperekplexia in a Chinese boy- a case report and review of the literature. *BMC Medical Genetics*, 18(1), 110.

Yevenes, G.E , and Zeilhofer, H.U. (2011). Allosteric modulation of glycine receptors. *British Journal of Pharmacology*, 164(2), 224-236.

Ye, J.H. (2008). Regulation of excitation by glycine receptors. *Results and Problems in Cell Differentiation*, 44, 123-43.

Yip, G.M, Chen, Z.M, Edge, C.J, Smith, E.H, Dickinson, R., Hohenester, E., Townsend, R.R, Fuchs, K., Sieghart, W., Evers, A.S , and Franks, N.P. (2013). A propofol binding site on mammalian $GABA_A$ receptors identified by photolabeling. *Nature Chemical Biology*, 9(11), 715-720.

Young, A.B. , and Snyder, S.H., (1973). Strychnine binding associated with glycine receptors of the central nervous system. *Proceedings of the National Academy of Sciences*, 70(10), 2832-2836.

Yu, R., Hurdiss, E., Greiner, T., Lape, R., Sivilotti, L., and Biggin, P.C. (2014). Agonist and antagonist binding in human glycine receptors. *Biochemistry*, 53(38), 6041-6051.

Zafra F, Gomeza J, Olivares L, Aragón C, Giménez C. (1995). Regional distribution and developmental variation of the glycine transporters GLYT1 and GLYT2 in the rat CNS. *European Journal of Neuroscience*, 7(6), 1342-52.

Zarbin, M.A, Wamsley, J.K , and Kuhar, M.J (1981). Glycine receptor: light microscopic autoradiographic localization with [$^3$H]strychnine. *Journal of Neuroscience*, 1(5), 532-547.

Zeller, A., Jurd, R., Lambert, S., Arras, M., Drexler, B., Grashoff, C., Antkowiak, B. , and Rudolph, U. (2008). Inhibitory ligand-gated ion channels as substrates for general anesthetic actions. In: Schüttler J., Schwilden H. (eds) Modern Anesthetics. *Handbook of Experimental Pharmacology*, vol 182. Springer, Berlin, Heidelberg

Zhang, H.X., Lyons-Warren, A., and Thio, L.L. (2009). The glycine transport inhibitor sarcosine is an inhibitory glycine receptor agonist. *Neuropharmacology*, 57(5-6), 551-555.

Zhang, Y., Bode, A., Nguyen, B., Keramidas, A. , and Lynch, J.W. (2016). Investigating the mechanism by which gain-of-function mutations to the α1 glycine receptor cause hyperekplexia. *Journal of Biological Chemistry*, 291(29), 15332-15341.

Zhou, L., Chillag, K.L., and Nigro, M.A. (2002). Hyperekplexia: a treatable neurogenetic disease. *Brain and Development*, 24(7), 669-674.

Zhou, N., Wang, C.H., Zhang, S., and Wu, D.C. (2013). The *GLRA1* Missense Mutation W170S Associates Lack of $Zn^{2+}$ Potentiation with Human Hyperekplexia. *Journal of Neuroscience*, 33(45), 17675-17681.

Zimmermann, I., and Dutzler, R. (2011). Ligand activation of the prokaryotic pentameric ligand-gated ion channel ELIC. *PLoS Biology*, 9(6), e1001101.

Zoons, E., Ginjaar, I.B., Bouma, P.A., Carpay, J.A., and Tijssen, M.A. (2012). A new hyperekplexia family with a recessive frameshift mutation in the *GLRA1* gene. *Movement Disorders*, 27(6), 795-796.

# Acknowledgements

I would like to express my sincere gratitude towards my supervisor, Professor Lucia Sivilotti for her leadership, advice, and valuable guidance at various stages of my PhD.

I am grateful to Dr. Remi Lape and Dr.Timo Greiner for sharing their exceptional skills with me and for all support and valuable comments they have given me.

I also thank my fellow PhD students Dr.Alesandro Marabelli and Elliot Hurdiss for the stimulating discussions. They each helped make my time in the PhD program more interesting.

I am grateful to Kuwait University for providing me with the scholarship.

Finally, I would like to thank the most important people in my world, my family. I thank my parents for their great support and my husband for his love, patience and faith in me. I dedicate this Thesis to my sweet little angels Zainab, Noor and Mariam.